Genetic Engineering of Uridyl Peptide Antibiotic Biosynthetic Gene Clusters for Improved Production

Dissertation

der Mathematisch-Naturwissenschaftlichen Fakultät

der Eberhard Karls Universität Tübingen

zur Erlangung des Grades eines

Doktors der Naturwissenschaften

(Dr. rer. nat.)

vorgelegt von

Panagiota-Hanna Koutsandrea

aus Sparta/Griechenland

Tübingen

2023

Gedruckt mit Genehmigung der Mathematisch-Naturwissenschaftlichen Fakultät der Eberhard Karls Universität Tübingen.

Tag der mündlichen Qualifikation:	06.11.2023
Dekan:	Prof. Dr. Thilo Stehle
1. Berichterstatter/-in:	PD Dr. Bertolt Gust
2. Berichterstatter/-in:	Prof. Dr. Harald Groß

Table of Contents

List of Abbreviations vii

Summary xi

Zusammenfassung xiii

1. Introduction 1

1.1 **Nucleoside antibiotics** 1

1.1.1 Cytidine-derived nucleosides 1

1.1.2 Uridine-derived nucleosides 2

1.1.2.1 Uridyl peptide antibiotics (UPAs) 3

1.2 **Biosynthesis of UPAs** 6

1.3 **Mode of action of UPAs** 9

1.3.1 Peptidoglycan Biosynthesis 9

1.3.2 MraY-Translocase 11

1.4 **Structure-activity relationships (SARs)** 12

1.5 **Previous work** 14

1.6 **Aims of this study** 16

2. Materials and Methods 18

2.1 Materials 18

2.1.1 Devices 18

2.1.2 Equipment and Consumables 19

2.1.3 Chemicals 20

2.1.4 Enzymes and Kits 23

2.1.5 Size markers for gel electrophoresis 24

2.1.6 Antibiotics 24

2.1.7 Primers 24

2.1.8 gBlocks® 29

2.1.9 Plasmids and Cosmids 29

2.1.10 Buffers and Solutions 33

2.1.10.1 Solutions for DNA Isolation (plasmids and cosmids) 33
2.1.10.2 Buffers and Solutions for Agarose Gel Electrophoresis 34
2.1.10.3 Solutions for Blue/White Selection of *E. coli* 34
2.1.10.4 Further Solutions 35
2.1.11 Culture Media 35
2.1.11.1 Media for Cultivation of *Escherichia coli* 35
2.1.11.2 Media for Cultivation of *Streptomyces* 36
2.1.12 Bacterial Strains 37
2.1.12.1 *Escherichia coli* strains 37
2.1.12.2 *Streptomyces* strains 38
2.1.13 Software 44
2.2 Methods 45
2.2.1 Methods of molecular biology 45
2.2.1.1 Isolation of cosmid/plasmid DNA of *E. coli* 45
2.2.1.2 Purification/Extraction of DNA with phenol/chloroform/isoamyl alcohol 45
2.2.1.3 Precipitation of DNA 45
2.2.1.4 DNA restriction 46
2.2.1.5 DNA ligation 46
2.2.1.6 Agarose gel electrophoresis 47
2.2.1.6.1 Analytical gel electrophoresis 47
2.2.1.6.2 Preparative gel electrophoresis 47
2.2.1.7 Polymerase chain reaction (PCR) 48
A) Amplification of DNA by Taq/Pfu - polymerase 48
B) Amplification of DNA by Q5 - polymerase 49
C) Colony PCR of *E. coli* 49
D) PCR - mediated verification of *Streptomyces* exconjugants 50
2.2.1.8 Spin column - based DNA purification 50
2.2.1.9 DNA sequencing 51

2.2.1.10 λRed/ET- mediated homologous recombination 51
2.2.1.11 Golden Gate Assembly 52
2.2.1.12 Gibson Assembly 53
2.2.1.13 Blue-White-Screening 53
2.2.1.14 FLP-mediated excision of resistance genes 54
2.2.1.15 Cre-mediated excision of resistance genes 54
2.2.2 Methods of horizontal gene transfer in bacteria 55
2.2.2.1 Preparation of electrocompetent cells 55
2.2.2.2 Transformation of *E. coli* 55
2.2.2.3 Heat shock transformation 56
2.2.2.4 Intergenic conjugation of *E. coli* with *Streptomyces* 56
2.2.3 Microbiological Methods 57
2.2.3.1 Growth conditions and maintenance of *E. coli* strains 57
2.2.3.2 Growth conditions and maintenance of *Streptomyces* 58
2.2.3.3 Preparation of *Streptomyces* spore suspension stocks 58
2.2.3.4 Cultivation of *Streptomyces* strains 59
2.2.4 Analytical Methods 59
2.2.4.1 Determination of cell dry weight 59
2.2.4.2 LC-MS analysis of UPA production 60
3. Results 61
3.1 Pacidamycin biosynthetic gene cluster 61
3.1.1 Increased production by promoter replacements 61
3.1.1.1 Introduction of bidirectional promoter cassettes *P15_aac(3)IV_P16* and *P03_aac(3)IV_P04* into modified pacidamycin biosynthetic gene clusters 61
3.1.1.2 Introduction of bidirectional promoter cassettes *ermE*p_aac(3)IV_ermE*p* (PC3) and *ermE*p_aac(3)IV_kasOp*-SP44* (PC4) into modified pacidamycin biosynthetic gene clusters 79
3.1.2 Investigation of operon structure by RNA-sequencing 84
3.1.3 Increased production by optimized heterologous hosts 102

3.1.4 Genetic reorganization of the pacidamycin BGC by operon inversion 104
3.1.5 Comparison of constructed UPA producer strains 109
3.2 Napsamycin biosynthetic gene cluster 110
3.2.1. Increased production by promoter replacements and an NRPS knockout 110
3.2.2. Increased production and compound specificity by knockouts 118
3.2.3. Combination of promoter replacements and knockout 126
3.2.4. Comparison of constructed UPA producer strains 128
3.3 Optimized mutant strain for mureidomycin A production 129
4. Discussion 132
4.1 Increased production by expression of the pacidamycin gene cluster 132
4.2 Increased production by expression of the napsamycin gene cluster 141
4.3 Increased production by engineered heterologous hosts 145
4.4 Outlook 149
5. Bibliography 150
6. List of Tables 169
7. List of Figures 170
8. Appendix 174

List of Abbreviations

$(NH_4)_6Mo_7O_{24}$	Ammonium molybdate tetrahydrate
°C	Degrees Celcius
µ	Micro
aac(3)IV	Apramycin resistance gene
Ac	Acetate
A-domain	Adenylation domain
Ala	Alanine
AMP	Adenosine monophosphate
Apra	Apramycin
B	Boron
BGC	Biosynthetic gene cluster
Bidest./ddH_2O	Double-distilled water
BLAST	Basic local alignment search tool
bp	Base pair
BPC	Base peak chromatogram
C_{55}-P	Undecaprenyl phosphate
C_{55}-PP	Undecaprenyl pyrophosphate
Ca	Calcium
CA	California
Carb	Carbenicillin
C-domain	Condensation domain
Cl	Chloride
cm	Centimeter
Cml	Chloramphenicol
CO	Colorado
CoA	Coenzyme A
Cu	Copper
d	Day
Da	Dalton
ddH_2O	Double-distilled water
DMSO	Dimethyl sulfoxide
DNA	Deoxyribonucleic acid
dNTP	Deoxyribonucleoside 5’ - triphosphate
E. coli	*Escherichia coli*
EDTA	Ethylenediaminetetraacetic acid
EIC	Extracted ion chromatogram
et al.	*et alii* (and others)
EtOH	Ethanol
Fe	Iron
Fig.	Figure

FW	Forward
g	Gram
GC content	Guanine and cytosine content
GGA	Golden Gate Assembly
GlcNAc	*N*-acetylglucosamine
Gly	Glycine
h	Hour
HCl	Hydrochloric acid
HH	Heterologous Host
HPLC	High Performance Liquid Chromatography
HR	High resolution
IC_{50}	Half-maximal inhibitory concentration
IGR	Intergenic region
IPTG	Isopropyl β-D-1-thiogalactopyranoside
k	Kilo
K	Potassium
Kan	Kanamycin
kb	Kilo-base pair
KH_2PO_4/K_2HPO_4	Potassium phosphate buffer
L	Liter
LB	Luria Bertani
Li	Lithium
m	Milli
M	Molarity
m/z	Mass-to-charge ratio
MA	Massachusetts
mAU	Milli-absorbance unit
MCS	Multiple cloning site
Met	Methionine
Mg	Magnesium
$MgCl_2$	Magnesium chloride
MIC	Minimum inhibitory concentration
min	Minute
Mn	Manganese
MO	Missouri
ms	Millisecond
MS	Mannitol soya or Mass spectometry
***m*-Tyr**	*m*-Tyrosine
MurNAc	*N*-acetylmuramic acid
MW	Molecular weight
n	Nano
Na	Sodium
NaCl	Sodium chloride

NaOH	Sodium hydroxide
Ndx	Nalidixic acid
NEB	New England BioLabs
neo	Kanamycin resistance gene
nm	Nanometer
No.	Number
NRPS	Nonribosomal peptide synthetase
OD_{600}	Optical density at 600 nm
oriT	Origin of transfer
PA	Pennsylvania
PCR	Polymerase chain reaction
pH	Potential of hydrogen
Phe	Phenylalanine
PKS	Polyketide synthase
PLP	Pyridoxal phosphate
pmol	Picomole
RBS	Ribosomal binding site
RNA	Ribonucleic acid
RNase	Ribonuclease
RP	Reverse phase
rpm	Revolutions per minute
RT	Room temperature
RV	Reverse
S, sec	Second
S.	*Streptomyces*
SDS	Sodium dodecyl sulfate
SOB	Super Optimal Broth
Sol	Solution
SOP	Standard operating procedure
sp.	Species
T-domain	Thiolation domain
TE-domain	Thioesterase domain
Tet	Tetracycline
Trp	Tryptophan
TSB	Tryptic soy broth
Tyr	Tyrosine
UDP	Uridine diphosphate
UPA	Uridyl Peptide Antibiotic
USA	United States of America
UV	Ultraviolet
V	Volt
Vol.	Volume
WI	Wisconsin

WT	Wild type
X-Gal	5-bromo-4-chloro-3-indolyl-β-D-galactopyranoside
Zn	Zinc

Summary

Mureidomycins are a subclass of uridyl peptide antibiotics (UPAs), which were originally isolated from *Streptomyces flavidovirens*[1,2] and display potent and selective activity against the WHO priority pathogen[3] *Pseudomonas aeruginosa*[4]. Other UPA subclasses consist of pacidamycins[5–7], napsamycins[8], and sansanmycins[9], which mainly differ in the respective pseudo tetra - or pentapeptide moiety. UPAs target bacterial cell wall biosynthesis by inhibiting phospho-MurNAc-pentapeptide translocase (MraY). This enzyme constitutes a promising and underexplored target, since it is not currently being addressed by antibiotics on the market[10–12]. Furthermore, the respective biosynthetic gene clusters have been identified for all subclasses[13–17]. As mureidomycins A and C were identified as the most bioactive UPAs against *P. aeruginosa*, exhibiting the lowest MIC and IC_{50} values[4,18], this study aimed to establish a selective and strong biosynthetic production platform of these compounds.

The first part of this thesis covers genetic manipulations of the pacidamycin biosynthetic gene cluster. This strongly expressed gene cluster had previously been genetically modified to direct biosynthesis toward mureidomycins. However, since a significant decrease in production yield was detected subsequent to these alterations, the goal emerged to improve production further. For this purpose, four bidirectional promoter cassettes were inserted into modified pacidamycin gene clusters in different combinations into the two sites, where bidirectional promoters have to be situated in order for most genes to be transcribed. Out of all combinations, UPA production was solely elevated after the knock-in of promoter cassette PC1 containing promoters P15 and P16 into the intergenic region between *pac3* and *pac4*, which led to a 4.10-fold increase in mureidomycin A yield. Contrastingly, mureidomycin C production was not detected. RNA-sequencing of mutant strains was conducted and, thus, an operon structure consisting of seven operons was postulated and operons displaying lesser transcription rates were identified. Moreover, the increased mureidomycin A production rate detected after the investigated promoter replacement was found to correlate with elevated transcription rates. With the intention to enhance production rates further, the modified cluster was conjugated with several optimized heterologous hosts. While all tested strains elevated yield significantly, the highest increase was detected for *S. albus* Del14, which improved mureidomycin A production 11.58-fold. Lastly, a reorganization of the operon structure was attempted through the inversion of operon 4 consisting of genes *npsP4*, *pac13* and *npsP3*. This strategy aimed to enhance production rates by forming a continuous operon of genes *pac4* - *pac22*, however, UPA biosynthesis was significantly reduced in the resulting mutant strains.

In the second part of this work, efforts were commenced to improve UPA production encoded by the napsamycin biosynthetic gene cluster, to enhance the originally low yield, whilst simultaneously narrowing the spectrum of produced compounds. The low production rate was firstly addressed with

knock-ins of the bidirectional promoter cassette PC1 upstream of the cluster-specific positive regulator *npsM* of the napsamycin gene cluster, and then upstream of the major facilitator transporter *npsO*. The former promoter replacement was performed with a simultaneous knockout of an NRPS A-domain, to narrow down the spectrum of synthetized compounds. While mureidomycin A production levels were not affected, production of other UPAs was decreased. Contrastingly, after the knock-in of a promoter upstream of *npsO*, a 4.58-fold increase in mureidomycin A production was detected. For the purpose of narrowing the plethora of produced UPAs, oxidoreductases *npsE* and *npsU* were knocked out. The knockout of *npsE* led to significant reduction in the produced mureidomycin E/napsamycin A and napsamycin C levels, without affecting mureidomycin A and B yields. Furthermore, knocking out *npsU* increased mureidomycin A levels 3.49-fold in comparison with the promoter swap mutant, which had already elevated production. This knockout also eliminated compound production of the less bioactive dihydrouracil-containing UPAs. Subsequent conjugation of the *npsU* knockout cluster with *S. albus* Del14 generated mutants in which a 1.92-fold increase in mureidomycin A yield was detected. Although neither the attempted combination of knockouts, nor the combination of promoter replacement and *npsU* knockout further elevated compound yields, modifications on both biosynthetic gene clusters in combination with the expression in different heterologous hosts led to a significant improvement of production yields and finally allowed the establishment of a robust production platform for mureidomycin A and its derivatives.

Zusammenfassung

Mureidomycine sind eine Unterklasse der Uridylpeptid-Antibiotika (UPA), welche erstmalig aus *Streptomyces flavidovirens*[1,2] isoliert wurden und eine starke und selektive Aktivität gegen den von der WHO als Problemkeim[3] eingestuften Erreger *Pseudomonas aeruginosa* aufweisen[4]. Andere UPA-Unterklassen sind die Pacidamycine[5–7], Napsamycine[8] und Sansanmycine[9], welche sich hauptsächlich durch den jeweiligen Pseudotetra- oder Pseudopentapeptidanteil unterscheiden. UPA greifen in die bakterielle Zellwandbiosynthese ein, indem sie die Phospho-MurNAc-Pentapeptid-Translokase (MraY) inhibieren. Dieses Enzym stellt eine vielversprechende und wenig erforschte Zielstruktur für Antibiotika dar, da es bislang nicht von auf dem Markt befindlichen Antiinfektiva adressiert wird[10–12]. Des Weiteren wurden die entsprechenden biosynthetischen Gencluster für alle Unterklassen identifiziert[13–16]. Da die Mureidomycine A und C als die bioaktivsten UPA (niedrigste MHK- und IC_{50}-Werte) identifiziert wurden[4,18], zielte diese Studie darauf ab, eine selektive und robuste biosynthetische Produktionsplattform für diese Verbindungen aufzubauen.

Der erste Teil dieser Arbeit befasst sich mit der genetischen Manipulation des Pacidamycin-Biosynthese-Genclusters. Dieses stark exprimierte Gencluster ist zuvor so modifiziert worden, dass die Biosynthese auf Mureidomycine ausgerichtet wurde. Da jedoch nach diesen Veränderungen ein signifikanter Rückgang der Produktionsmenge festgestellt wurde, ergab sich hieraus das Ziel, die Produktion weiter zu steigern. Zu diesem Zweck wurden vier bidirektionale Promotorkassetten in die modifizierten Pacidamycin-Gencluster in verschiedenen Kombinationen an den beiden intergenischen Loci eingefügt, an denen sich bidirektionale Promotoren befinden müssen, damit die meisten Gene transkribiert werden können. Von allen Kombinationen war die UPA-Produktion nur nach dem Einbringen der Promotorkassette PC1 mit den Promotoren P15 und P16 in die Region zwischen *pac3* und *pac4* erhöht, welches eine 4,10-fache Steigerung der Mureidomycin A-Ausbeute herbeiführte. Im Gegensatz dazu wurde keine Mureidomycin C-Produktion nachgewiesen. Anschließend wurde eine RNA-Sequenzierung der mutierten Stämme durchgeführt und dadurch eine Operonstruktur aus 7 Operonen postuliert, sowie Operone mit geringeren Transkriptionsraten identifiziert. Darüber hinaus wurde festgestellt, dass die erhöhte Mureidomycin A-Produktion, die nach dem untersuchten Promotoraustausch beobachtet wurde, in der Tat mit einer erhöhten Transkriptionsrate korreliert. Um die Produktionsraten weiter zu steigern, wurde das modifizierte Gencluster mit mehreren optimierten heterologen Wirtsorganismen konjugiert. Während alle getesteten Stämme den Ertrag signifikant steigerten, wurde die höchste Steigerung bei *S. albus* Del14 festgestellt, welcher die Mureidomycin A-Produktion um das 11,58-Fache steigerte. Schließlich wurde versucht, die Operonstruktur durch Inversion des Operons 4, bestehend aus den Genen *npsP4*, *pac13* und *npsP3*, zu reorganisieren. Diese Strategie zielte darauf ab, die Produktionsraten durch die Bildung eines kontinuierlichen Operons der

Gene *pac4* - *pac22* zu erhöhen, aber die UPA-Biosynthese war in den resultierenden Mutantenstämmen deutlich reduziert.

Im zweiten Teil dieser Arbeit wurde versucht, die UPA-Produktion durch erhöhte Expression des Napsamycin-Biosynthese-Genclusters zu verbessern und hierbei Produktionsraten zu steigern und gleichzeitig das Spektrum der produzierten Verbindungen zu verringern. Die geringe Produktion wurde zunächst mit dem Einbringen der bidirektionalen Promotorkassette mit den Promotoren P15 und P16 strangaufwärts des clusterspezifischen positiven Regulators des Napsamycin-Genclusters *npsM* und dann strangaufwärts des Major-Facilitator-Transporters *npsO* in Angriff genommen. Der erste Promotoraustausch wurde bei gleichzeitiger Deletion einer NRPS A-Domäne durchgeführt, um das Spektrum der synthetisierten Verbindungen einzuschränken. Die Produktion von Mureidomycin A wurde zwar nicht beeinflusst, dafür gelang es, die Produktion von biologisch weniger aktiven UPA zu reduzieren. Im Gegensatz dazu wurde nach der Insertion eines Promotors strangaufwärts von *npsO* ein 4,58-facher Anstieg der Mureidomycin-A-Produktion festgestellt. Um die Vielzahl der produzierten UPAs einzuschränken, wurden als Nächstes die Oxidoreduktasen *npsE* und *npsU* deletiert. Die Deletion von *npsE* führte zu einer signifikanten Verringerung der Mureidomycin E/Napsamycin A- und Napsamycin C-Ausbeute, ohne den Ertrag von Mureidomycin A und B zu beeinträchtigen. Darüber hinaus erhöhte die Deletion von *npsU* den Mureidomycin A-Gehalt um das 3,49-Fache im Vergleich zu den Promotoraustausch Mutanten, welche bereits eine erhöhte Produktion aufwiesen. Durch diese Deletion wurde auch die Produktion von biologisch wenig aktiven Dihydrouracil-haltigen UPA eliminiert. Die anschließende Konjugation dieses Genclusters mit *S. albus* Del14 verbesserte die Mureidomycin A-Ausbeute weiterhin um das 1,92-Fache. Obwohl weder die angestrebte Kombination der Gendeletionen noch die Kombination von Promotoraustausch und *npsU*-Deletion zu einer weiteren Steigerung der Ausbeute führten, zeigte sich in der vorliegenden Arbeit, dass eine Kombination aus genetisch veränderten Genclustern und optimalen heterologen Produktionsstämmen in der Tat die Etablierung einer stabilen Produktionsplattform erlauben und somit Mureidomycin A und dessen Derivate mit deutlich erhöhter Produktivität gebildet werden können.

1. Introduction

Pseudomonas aeruginosa constitutes a gram-negative pathogen, which has been classified by the World Health Organization to be of critical priority in the endeavor of developing novel antibiotics and combating widespread resistance to commonly administered medicines[19]. This biofilm-building bacterium causes severe nosocomial infections like pneumonia or bacteremia, especially in vulnerable patients (e.g., exacerbation of cystic fibrosis and ventilator-associated pneumonia in mechanically ventilated patients)[20–24]. Due to the plethora of resistance mechanisms often present simultaneously in this pathogen, efforts to develop novel antipseudomonal agents are of urgent necessity[25–27]. The present study aims to contribute to this process by enhancing production levels of a subclass of nucleoside antibiotics, displaying potent antipseudomonal activity.

1.1 Nucleoside antibiotics

A myriad of different natural products containing nucleoside moieties have been discovered, ranging from derivatives of purines to pyrimidines, some of which are highly modified, and display a variety of biological activities (antiviral, antibacterial, pesticidal, herbicidal or antitumor)[28–30]. Herein, the pyrimidine nucleoside antibiotics, derived from cytidine and uridine, will be highlighted.

1.1.1 Cytidine-derived nucleosides

One class of cytidine-derived nucleosides consists of the broad-spectrum antibiotics albomycins, active for example against *Streptococcus* sp. and *Yersinia* sp., which were isolated from several *Streptomyces* species[31,32]. The respective gene cluster was isolated from *Streptomyces* sp. ATCC 700974, which encodes for these ‘‘Trojan horse’’ antibiotics, consisting of a nucleoside core linked to a peptide-based siderophore moiety[33,34]. These moieties are synthesized separately and then linked via *N*-acylation, with the peptide-based siderophore being synthesized by a multidomain nonribosomal peptide synthetase (NRPS)[33,35]. Albomycin is actively imported into the cells due to its siderophore moiety, which is then cleaved from the nucleoside. The latter causes cell death by inhibiting the seryl-tRNA synthetase[33,36].

Another member of this class constitutes the amicetin family of cytidine-derived nucleosides, including, inter alia, oxamicetin, bamicetin and streptcytosine, which have been isolated from a variety of *Actinomycetes*[30]. This family harbors an acylated or alkylated cytosine base linked to an amicetose

(deoxy saccharide), which is often linked via an α-(1 →4)-glycoside bond to an amosamine forming a disaccharide nucleoside[37–39]. The broad-spectrum antibiotic amicetin inhibits translation and, more specifically, peptide bond formation by binding the 23S rRNA[40,41]. Moreover, the biosynthetic gene cluster of amicetin was isolated from *Streptomyces vinaceusdrappus* NRRL 2363[42].

A final example of cytidine-derived nucleosides is found in the gougerotin family, consisting of gougerotin and its structural variants ningnanmycin and bagougeramine, which all possess a broad spectrum of biological activity (antibacterial, antiviral and antitumor)[43–48]. Gougerotin belongs to the group of peptidyl nucleoside antibiotics and was isolated from different *Streptomyces*, including *Streptomyces gougerotii*[49]. A cytosine base coupled with a 4-amino-4-deoxyglucuronamide form the nucleoside core in this compound family, which is linked to a 4'-*N*-appended sarcosyl-serine dipeptide[50,51]. As described for amicetin, its mode of action consists of binding the 23S rRNA, leading to an alteration in the positioning of the P site-bound tRNA and, thus, inhibiting protein biosynthesis[52]. The BGC of gougerotin was isolated from *Streptomyces graminearus* AS4.506[49].

1.1.2 Uridine-derived nucleosides

One group of nucleoside antibiotics encompasses the lipouridines liposidomycins, caprazamycins, A-90289s and muraminomicins[30]. The common structural elements in this family consist of a diazepanone ring attached to a fatty acyl moiety and a disaccharide core formed of a ribose-modified uridine and an aminoribose[53–56]. The biosynthetic gene clusters of all subclasses have been identified[57–60]. All compounds inhibit bacterial peptidoglycan biosynthesis by targeting phospho-MurNAc pentapeptide translocase (MraY)[54–56,61] and possess antibacterial activity against gram-positive bacteria, like *Staphylococcus aureus*, *Streptococcus pyogenes* and especially against the genus *Mycobacterium*, including *M. tuberculosis*[30,55,56,62,63].

Another class of uridine-containing, MraY-inhibiting antibiotics are muraymycins, which were isolated from *Streptomyces* sp. LL-AA896[64]. Muraymycins closely resemble the aforementioned lipouridine family, since they harbor the same disaccharide core. However, the diazepanone is replaced by a pseudo-tripeptide in these compounds[64]. Muraymycins display modest antibacterial activity (against *Staphylococci*, *Enterococci* and Gram-negatives)[64]. Niro *et al.* (2020)[65] synthesized a muraymycin hybrid with the uridyl peptide antibiotic sansanmycin B, however no significant antibacterial activity against *P. aeruginosa*, *S. aureus* or *E. coli* was detected.

Additional uridine-derived nucleosides constitute:

- The antifungal jawsamycin (FR-900848) from *Streptomyces roseoverticillatus* HP-891[66]
- The MraY inhibitor capuramycin from *S. griseus* 446-S3 (activity against *Streptococcus pneumoniae*, *Mycobacterium tuberculosis* and *Mycobacterium smegmatis*)[67,68]

- The MraY inhibitor A-94964 from *Streptomyces* sp. SANK 60404 (activity against *Staphylococcus aureus* and *Enterococcus faecalis*)[69,70]
- The selective chitin synthase inhibitors nikkomycin and polyoxin from *Streptomyces tendae* Tü 901 and *S. cacaoi*, respectively (fungicidal and insecticidal)[71–74]
- The MraY inhibitors belonging to the tunicamycin-type family, isolated from several *Streptomyces* strains (broad antibiotic spectrum, including Gram-positive bacteria and fungi)[75–78]. Contrasting to other MraY inhibitors, this class displays toxicity against mammalian cells by inhibiting eukaryotic glycoprotein formation[79].

1.1.2.1 Uridyl peptide antibiotics (UPAs)

The class of uridine-derived nucleosides, which was investigated in the present study, consists of uridyl peptide antibiotics (UPAs). Hitherto, four subclasses have been described, encompassing the mureidomycins, napsamycins, pacidamycins, and sansanmycins. UPAs selectively inhibit phospho-N-acetylmuramyl-pentapeptide translocase (MraY), which constitutes a promising, underexplored antibiotic target, since it is not currently addressed by antibiotics on the market[10,12,78,80]. The benefit, which UPAs display in contrast with other MraY inhibitors, consists of the narrow spectrum of potent antibiotic activity, which is mostly specific against the problematic, Gram-negative pathogen *P. aeruginosa*[6,8,81]. Sansanmycins, however, have been shown to possess activity against *P. aeruginosa* and *Mycobacterium tuberculosis*[9]. Mureidomycins were firstly isolated from *Streptomyces flavidovirens* SANK 60486, pacidamycins from *S. coeruleorubidus* AB 1183F-64, napsamycins from *S*. sp. HIL Y-82,11372 (DSM accession No. 5940) and sansanmycins from *S*. sp. SS[1,7–9,82].

UPAs share a common structural scaffold (Fig. 1), consisting of an atypical 3'-deoxyuridine moiety attached to a central (*2S*, *3S*)-*N*-methyl-2,3-diaminobutyric acid (*N*-methyl-DABA) moiety via a unique 4',5'-enamide linkage. The *N*-methyl-DABA forms the core of a pseudotetra- or pseudopentapeptide residue. The peptide chain direction is reversed twice, once at the DABA residue and once at the ureido moiety, present in the C-terminus[2,5,8,9,83].

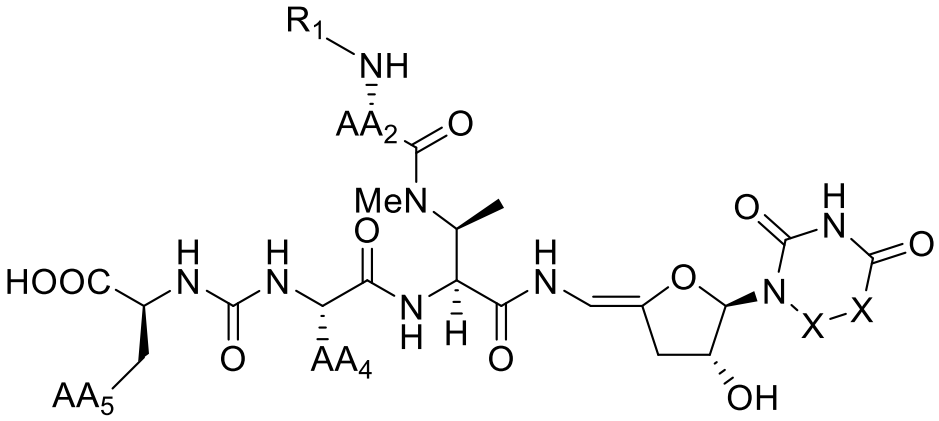


Fig. 1: Uridyl peptide antibiotic structure scaffold.

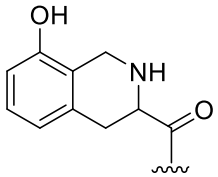
Depending on the combination of amino acids incorporated in this scaffold, the four different compound subclasses can be distinguished (Table 1). Notably, all pacidamycins harbor an L-Ala at position four (AA4) of the scaffold, while mureidomycins and napsamycins contain an L-Met at AA4 and an L-*m*-Tyr at position five (AA5). Napsamycins, furthermore, carry a bicyclic amino acid at position two (AA2), containing a 6-hydroxy-tetrahydro-isoquinoline carboxylic acid moiety. Contrastingly, mureidomycins harbor an L-*m*-Tyr or a bicyclic residue at the same site. Regarding AA5 of the scaffold, one of three different aromatic amino acids can be incorporated in UPAs (L-*m*-Tyr, L-Trp and L-Phe). Moreover, in pacidamycins and mureidomycins the incorporation of an additional amino acid at position one (R1) has been noted (L-Ala or L-Gly). Additionally, a structural variation occurs within the uridine residue, since for mureidomycins and napsamycins the respective dihydrouracil derivatives have been detected[2,5,8,9,14,83].

Table 1: Structures of representative uridyl peptide antibiotics

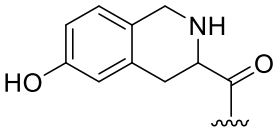
Name	R1	AA2	AA4	AA5	Other	MW
Pacidamycin 1	Ala	*m*-Tyr	Ala	Trp	Uracil	874.4
Pacidamycin 2	Ala	*m*-Tyr	Ala	Phe	Uracil	835.4
Pacidamycin 3	Ala	*m*-Tyr	Ala	*m*-Tyr	Uracil	851.4
Pacidamycin 4	H	*m*-Tyr	Ala	Trp	Uracil	803.3
Pacidamycin 4N	H	Bicyclic a	Ala	Trp	Uracil	815.3
Pacidamycin 5	H	*m*-Tyr	Ala	Phe	Uracil	764.3
Pacidamycin 5T	H	*m*-Tyr	Ala	*m*-Tyr	Uracil	780.3
Pacidamycin 6	Gly	*m*-Tyr	Ala	Trp	Uracil	860.4
Pacidamycin 7	Gly	*m*-Tyr	Ala	Phe	Uracil	821.3
Pacidamycin D	H	Ala	Ala	Trp	Uracil	711.3

Name	R1	AA2	AA4	AA5	Other	MW
Pacidamycin S	H	Ala	Ala	Phe	Uracil	672.3
Pacidamycin T	H	Ala	Ala	*m*-Tyr	Uracil	688.3
Met-pacidamycin D	H	Ala	Met	Trp	Uracil	771.3
Met-pacidamycin S	H	Ala	Met	Phe	Uracil	732.3
Met-pacidamycin 4	H	*m*-Tyr	Met	Trp	Uracil	863.4
Met-pacidamycin 5	H	*m*-Tyr	Met	Phe	Uracil	825.3
Mureidomycin A	H	*m*-Tyr	Met	*m*-Tyr	Uracil	840.3
Mureidomycin B	H	*m*-Tyr	Met	*m*-Tyr	Dihydrouracil	842.3
Mureidomycin C	Gly	*m*-Tyr	Met	*m*-Tyr	Uracil	897.3
Mureidomycin D	Gly	*m*-Tyr	Met	*m*-Tyr	Dihydrouracil	899.3
Mureidomycin E	H	Bicyclic a	Met	*m*-Tyr	Uracil	852.3
Napsamycin A	H	Bicyclic b	Met	*m*-Tyr	Uracil	852.3
Napsamycin B	H	Bicyclic c	Met	*m*-Tyr	Uracil	866.3
Napsamycin C	H	Bicyclic b	Met	*m*-Tyr	Dihydrouracil	854.3
Napsamycin D	H	Bicyclic c	Met	*m*-Tyr	Dihydrouracil	868.3
Sansanmycin A (= met-pacidamycin 4)	H	*m*-Tyr	Met	Trp	Uracil	863.4
Sansanmycin B	H	*m*-Tyr	Leu	Trp	Uracil	845.4
Sansanmycin C	H	*m*-Tyr	Met^{SO}	Trp	Uracil	879.4
Sansanmycin D (= mureidomycin A)	H	*m*-Tyr	Met	*m*-Tyr	Uracil	840.3
Sansanmycin E	H	*m*-Tyr	Met^{SO}	*m*-Tyr	Uracil	856.3
Sansanmycin F	H	Bicyclic d	Met	Trp	Uracil	903.4
Sansanmycin G	H	Bicyclic d	Leu	Trp	Uracil	885.4

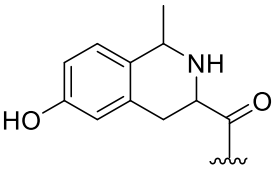
Met^{SO}: methionine sulfoxide



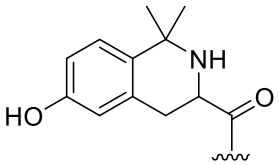
Bicyclic a



Bicyclic b



Bicyclic c



Bicyclic d

1.2 Biosynthesis of UPAs

The biosynthetic gene clusters of pacidamycins, napsamycins, sansanmycins and a cryptic mureidomycin gene cluster have been identified. The pacidamycin BGC from *S. coeruleorubidus* NRRL 18370 and AB1183F-64 was reported from two independent working groups in 2010[13,17] and consists of 22 open reading frames (ORFs), spanning over approximately 30.3 kb (Fig. 2). The napsamycin BGC was identified in *S*. sp. DSM5940 and described to span approximately 34.5 kb, distributed over 29 ORFS, and to produce napsamycins and mureidomycins (Fig. 2)[14]. Moreover, the sansanmycin BGC was discovered in *S*. sp. SS and consists of 25 ORFs with a length of approximately 33 kb[84]. Lastly, a cryptic mureidomycin gene cluster from *S. roseosporus* NRRL 15998 was activated by the constitutive expression of *ssaA*, the cluster-specific, positive regulator of sansanmycin biosynthesis, which led to the production of *N*-acetylated mureidomycin analogs[15].

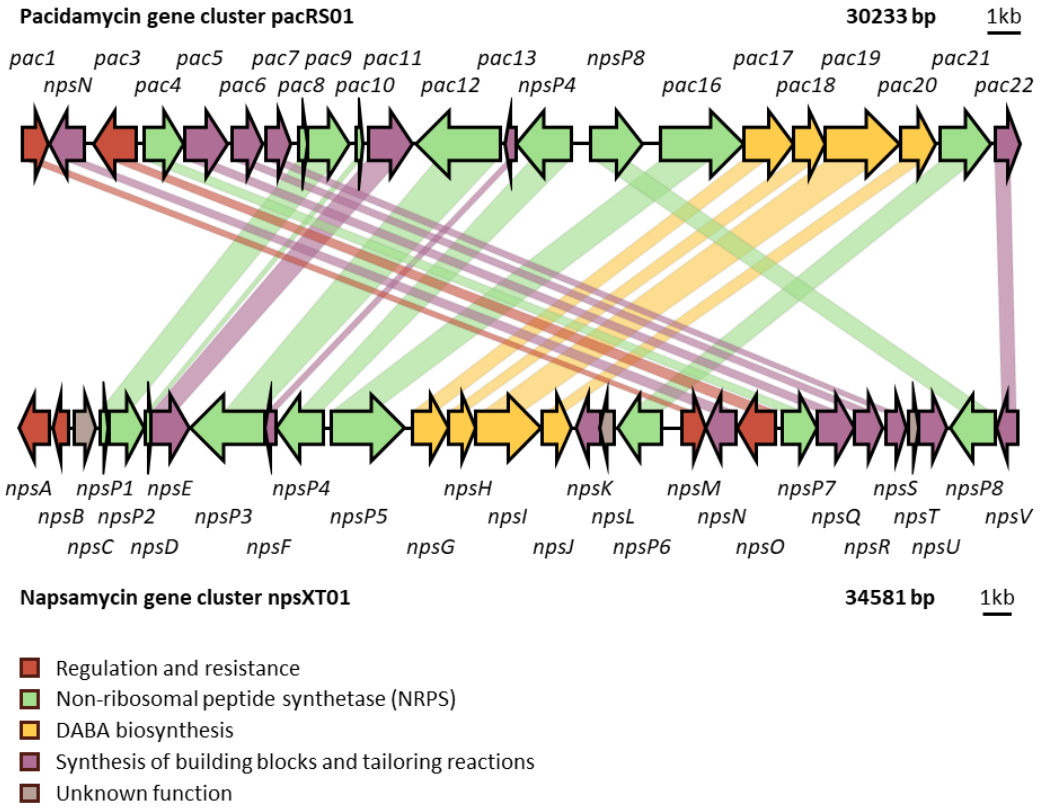


Fig. 2: Pacidamycin and napsamycin biosynthetic gene clusters, the orthologous genes have been connected.

While operon organization differs between the clusters, all genes of the pacidamycin BGC possess orthologs in the other BGCs with high levels of similarity on protein level (68 - 88 %, Table 2, where gene names in brackets correspond to the nomenclature with letters of Zhang *et al*.[17]). Moreover,

similar compounds are produced by the gene clusters. Thus, it was proposed that the biosynthetic pathways of other UPAs closely resemble pacidamycin biosynthesis[14,17,84].

Table 2: Orthologous genes of the pacidamycin and napsamycin gene clusters and deduced roles, generated by BLAST analysis [13,17]

Gene	Postulated function	Napsamycin ortholog	Identity (%)	Similarity (%)
pac1 (*A*)	Transcriptional regulator	*npsM*	81	87
pac2 (*B*)	tRNA-dependent aminoacyl transferase (R1: N-terminal L-Ala)	*npsN*	67	82
pac3 (*C*)	Putative major facilitator transporter (UPA export)	*npsO*	84	93
pac4 (*D*)	NRPS condensation (C) domain (condensation of DABA with Pac14-tethered thioester of C-terminal ureido peptide)	*npsP7*	68	77
pac5 (*E*)	PLP-dependent aminotransferase (uridine modification: 5'-transamination)	*npsQ*	87	93
pac6 (*F*)	Fe(II)/α-oxoglutarate oxygenase (postulated uridine modification)	*npsR*	72	82
pac7 (*G*)	Oxidoreductase	*npsS*	85	94
pac8 (*H*)	NRPS thiolation (T) domain (key carrier domain of biosynthesis)	*npsP1*	77	87
pac9 (*I*)	NRPS C-domain (condensation of peptide chain with nucleoside substrate)	*npsP2*	78	86
pac10 (*J*)	MbtH domain (interaction with adenylation domains, specifically A-domain Pac12)	*npsD*	66	80
pac11 (K)	FAD-dependent oxidoreductase (glycolate oxidase, uridine modification: 5'-OH → 5'-aldehyde)	(*npsE*)	81	88
pac12 (*L*)	NRPS ($C_{truncated}$-A-T, activation of aromatic amino acids for position five of the UPA scaffold)	*npsP3*	67	77
pac13 (M)	Homodimeric, metal-free cupin dehydratase (uridine modification: 3',4'-dehydration)	*npsF*	77	90
pac14 (*N*)	NRPS C-T didomain (Cognate loading partner of Pac15, catalyzation of ureido bond formation)	*npsP4*	68	79
pac15 (*O*)	NRPS A-domain (preferred activation of L-Ala for position four of the UPA scaffold)	*npsP8*	73	84
pac16 (P)	NRPS A-T-TE tridomain (DABA activation)	*npsP5*	84	90
pac17 (Q)	Argininosuccinate lyase (DABA biosynthesis)	*npsG*	87	91
pac18 (*R*)	Homoserine kinase (DABA biosynthesis, putative threonine kinase might provide improved leaving group for β-elimination)	*npsH*	86	92

Gene	Postulated function	Napsamycin ortholog	Identity (%)	Similarity (%)
pac19 (S)	DABA synthase (Didomain protein containing a PLP-dependent cysteine synthase and an argininosuccinate lyase, catalyzes the β-replacement of the threonine hydroxyl by the α-amino of aspartate)	*npsI*	85	91
pac20 (*T*)	PLP-dependent threonine aldolase (responsible for 3S configuration of DABA)	*npsJ*	87	92
pac21 (*U*)	NRPS A-domain (dual function: specific activation of N-terminal alanine and condensation with DABA)	*npsP6*	74	83
pac22 (V)	SAM-dependent *N*-methyltransferase (*N*-methylation of DABA)	*npsV*	74	84
pac21h (*W*)	NRPS A-domain (specific activation of N-terminal *meta*-tyrosine)	*npsP6*	77	86
phhA (*X*)	Phenylalanine-3-hydroxylase (formation of *meta*-tyrosine from phenylalanine)	*npsK*	78	85
-	Transcriptional regulator	*npsA*	-	-
-	*N*-acetyltransferase	*npsB*	-	-
-	Phosphatase	*npsC*	-	-
-	Hypothetical protein	*npsL*	-	-
-	Hypothetical protein	*npsT*	-	-
-	FMN-dependent oxidoreductase (formation of dihydrouracil)	*npsU*	-	-

As previously mentioned, a common biosynthetic pathway has been postulated for UPAs[14]. Thus, the pacidamycin biosynthesis will be described herein, since it has been investigated thoroughly. The peptide scaffold is synthesized by highly dissociated nonribosomal peptide synthetase (NRPS) modules. Regarding the biosynthesis of the core DABA moiety, Lam *et al.* (2008)[85] identified a novel ammonia-dependent β-replacement reaction, by which DABA is synthesized from L-Thr. This was postulated to be catalyzed by Pac19, while Pac17, Pac18 and Pac20 (3S configuration of DABA) also contribute to DABA biosynthesis. Then, DABA is recognized and activated by the A-T-TE tridomain Pac16 and methylation carried out by the SAM-dependent *N*-methyltransferase Pac22. Subsequently DABA is transferred onto the key carrier Pac8 (T-domain). Moreover, the peptide backbone is constructed in a nonmodular NRPS assembly, by discrete single-, di- or tridomain proteins. *In vitro* assays by Zhang *et al.* (2010)[17] found the C-terminus, containing the atypical ureido linkage, to be produced by Pac10 (MbtH interacting with Pac12), Pac12, Pac14 and Pac15. The condensation domain Pac4 then transfers the C-terminus onto the DABA moiety, tethered to the key carrier Pac8. Simultaneously, the N-terminal amino acid is recognized, activated as Ala-AMP and then condensed to the core DABA-S-Pac8 complex by Pac21 or Pac21h. Interestingly, instead of utilizing the respective

nucleotide, the nucleoside moiety is synthesized from uridine by Pac5, Pac11 and Pac13[86]. Lastly, the freestanding C-domain Pac9 loads the peptide chain onto the nucleoside moiety, thus releasing the compound from Pac8. This constitutes the first identified C-domain capable of condensing peptide and nucleoside substrates[13,17,87–89].

In 2001, the chemical synthesis of dihydropacidamycin D was reported. The first total chemical synthesis of pacidamycin D, including the chemically labile *Z*-oxyenamide, was conducted in 2011. Moreover, semisynthetic approaches have been utilized to diversify the UPA scaffold and obtain novel derivatives, as the halogenated derivative bromo-pacidamycin, or the aforementioned muraymycin-sansanmycin B hybrid. However, biosynthesis and semisynthesis remain desirable strategies, due to the complexity of the total synthesis[65,90–92].

1.3 Mode of action of UPAs

1.3.1 Peptidoglycan Biosynthesis

The bacterial cell wall constitutes a crucial element for bacterial survival, since it segregates the bacterium from its perilous environment, while only allowing passage to nutrients from the outside and the export of waste products, provides protection from osmotic lysis and confers cell shape[93,94]. Therefore, the inhibition of cell wall biosynthesis by UPAs leads to disruptive effects and, eventually, cell lysis. Since no corresponding cell wall exists in mammalian cells, selective toxicity is conferred[95].

More specifically, the Gram-negative bacterial cell wall consists of a thin peptidoglycan layer, surrounded by the outer and the inner (cytoplasmic) membrane, while the Gram-positive counterpart harbors a peptidoglycan layer around the cytoplasmic membrane. In Gram-positives, additional protection due to lack of the outer membrane is conferred by the peptidoglycan wall, which is many layers thicker than the Gram-negative one[94]. Peptidoglycan constitutes a polymer of alternating saccharide units of β-1,4-linked *N*-acetylglucosamine (GlcNAc) and *N*-acetylmuramic acid (MurNAc), which are cross-linked via peptide chains, attached to the MurNAc residues. Therein, the third (*meso*-diaminopimelic acid or L-lysine) and fourth (D-alanine) amino acid of adjacent peptides are cross-linked by DD-transpeptidases via pentaglycine bridges, which, therefore, stabilize the developing cell wall (Fig. 3)[93,94,96].

Peptidoglycan biosynthesis is commenced in the cytoplasm, where the nucleotide-activated saccharides UDP-MurNAc-pentapeptide (UDP: uridine diphosphate) and UDP-GlcNAc are synthesized by enzymes GlmS, GlmM, GlmU and MurA to MurF (Fig. 3). Simultaneously, the lipid carrier

undecaprenyl pyrophosphate is synthesized and dephosphorylated in the cytoplasm and, subsequently, anchored to the cytoplasmic membrane as undecaprenyl phosphate (C_{55}-P). The key enzyme MraY (Phospho-MurNAc-pentapeptide translocase/ translocase I), which is also membrane-bound, then catalyzes the formation of lipid I, by transferring MurNAc-pentapeptide onto the lipid carrier C_{55}-P. Subsequently, the membrane-bound glycosyl transferase MurG catalyzes the formation of lipid II by attaching one molecule of GlcNAc to lipid I. Thus, lipid II is exported over the cytoplasmic membrane by the flippase MurJ, polymerized by transglycosylases (TGases), released from the lipid carrier into the periplasm and cross-linked by transpeptidases (TPases), constructing the newly-synthesized peptidoglycan[97–101].

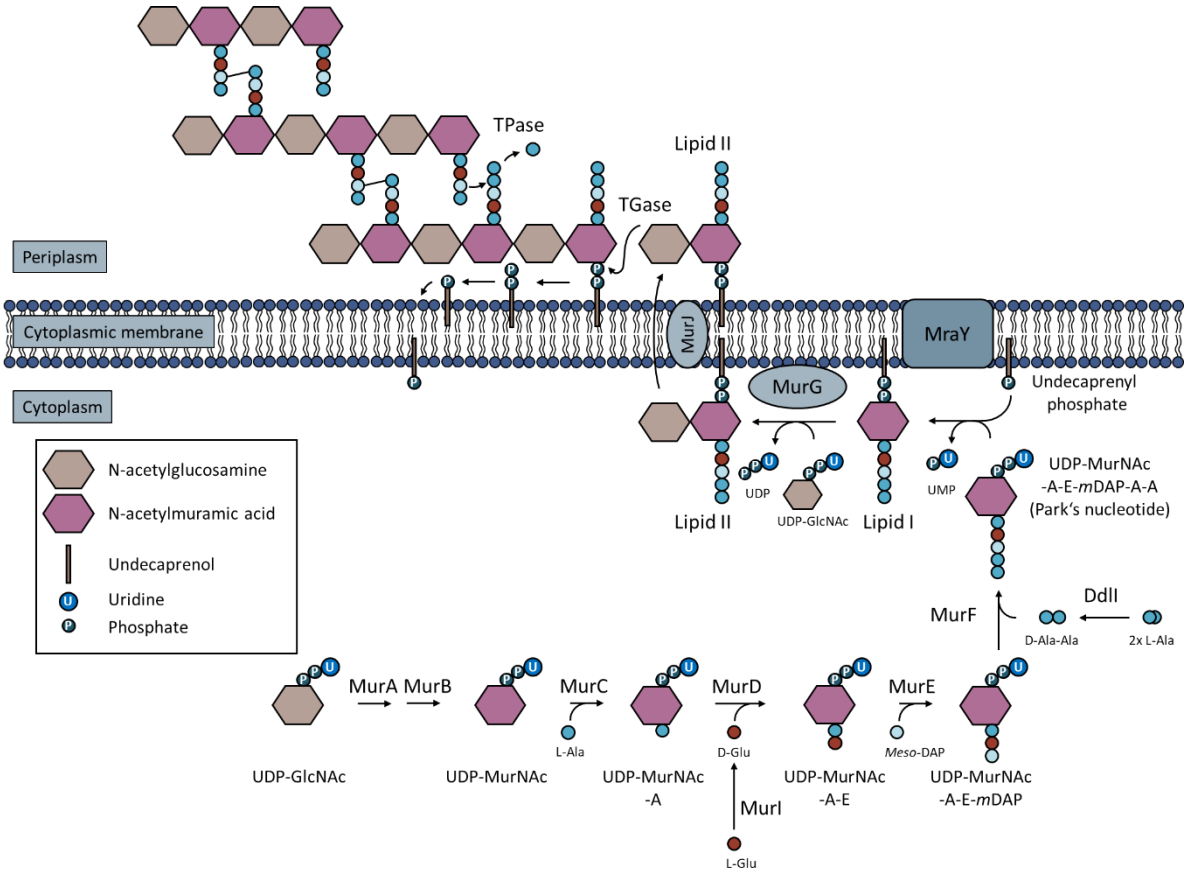


Fig. 3: Schematic representation of peptidoglycan biosynthesis, adapted from Egan *et al.* (2020)[102].

Many commercially available antibiotics target peptidoglycan biosynthesis. For example, β-lactam antibiotics target transpeptidases (penicillin-binding proteins)[99], while vancomycin binds to the D-Ala-D-Ala terminus of lipid II[103] and bacitracin inhibits the dephosphorylation of C_{55}-PP[104].

1.3.2 MraY-Translocase

MraY (UDP-MurNAc-pentapeptide translocase) constitutes a key enzyme in peptidoglycan biosynthesis, crucial for bacterial survival, and is, thus, a promising target for novel antibiotics[105]. The first crystal structure was crystallized from *Aquifex aeolicus* in a dimer configuration, harboring a tunnel in the center of the interface[106]. Each unit was detected to contain ten transmembrane helices (TM), five cytoplasmic loops (A - E), an interfacial helix (IH), a periplasmic β hairpin (PB) and a periplasmic helix (PH), while the N- and C-termini are both located on the periplasmic site (Fig. 4). Essential amino acids of the active binding site for MraY function were discovered to be the highly conserved aspartic acid residues Asp115, Asp116 and Asp267, located on TM3 and TM4, and the HHH motif (326 - 328, especially His326), situated on loop E (based on numbering of *P. aeruginosa* MraY)[106,107].

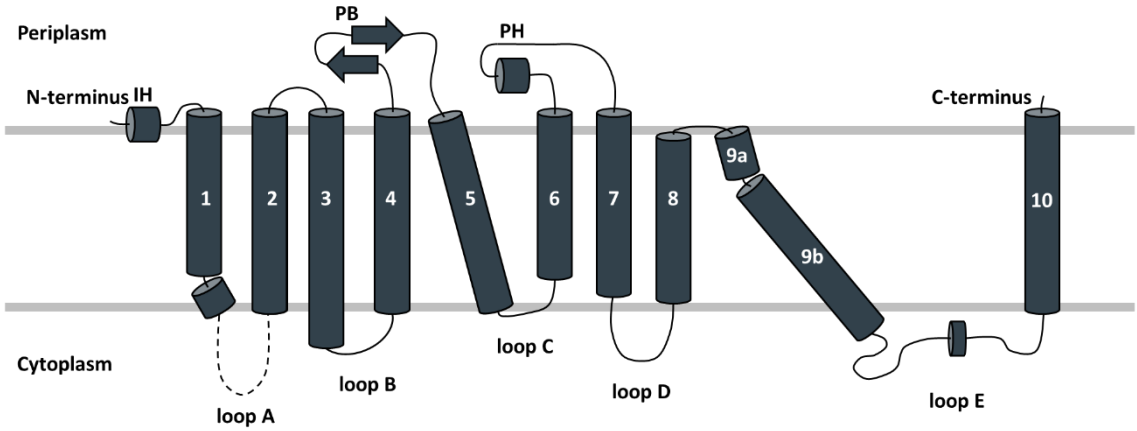


Fig. 4: Data from crystal structure of *A. aeolicus* MraY, figure adapted from Chung *et al.* (2013)[106]: Topology diagram of MraY protomer. TMs are numbered, while cytoplasmic loops (A - E), the interfacial helix (IH), the periplasmic β hairpin (PB) and the periplasmic helix (PH) are labeled.

As previously described, MraY catalyzes the formation of lipid I on the cytoplasmic side of the inner membrane, by binding UDP-MurNAc-pentapeptide and transferring Phospho-MurNAc-pentapeptide to the lipid carrier C_{55}-P with Mg^{2+} as a cofactor[101,106]. The mechanism of action of UPAs consists of the inhibition of MraY. While tunicamycins were detected to exhibit reversible inhibition of MraY (Ki = 0.55 +/- 0.1 µM), which was non-competitive regarding the lipid acceptor substrate and competitive for UDP-MurNAc-pentapeptide, liposidomycins were found to exhibit slow-binding inhibition (Ki = 80 +/- 15 nM), competitive solely for the lipid acceptor substrate[78]. Additionally, mureidomycin A exhibits slow-binding inhibition of MraY with Ki = 36 nM and Ki* = 2 nM, which is competitive to both the undecaprenyl phosphate moiety and UDP-MurNAc-pentapeptide[78]. Thus, mureidomycin A is regarded a potent MraY inhibitor, since its Ki value is 500-fold lower than the respective value for the substrate analog dansyl-UDP-MurNAc-pentapeptide, utilized in the study[108].

The half-maximal inhibitory concentration (IC_{50}) of mureidomycin A regarding MraY was detected to be IC_{50} = 0.05 µg/mL, while no significant inhibition of teichoic acid synthesis in *Bacillus subtilis* or of glycoprotein biosynthesis in a mammalian system were observed[80]. Moreover, the respective minimal inhibitory concentrations (MICs) of mureidomycins against many *Pseudomonas aeruginosa* strains were detected to be 0.1 - 3.13 µg/mL[4], for pacidamycins 8 - 64 µg/mL[6], for napsamycins 12.5 - 25 µg/mL[8] and for sansanmycins 10 - 12.5 µg/mL[9]. Furthermore, mureidomycins displayed low toxicity in mice, while being effective in a mouse model of infection with *P. aeruginosa*[4]. The combined activity of sansanmycins and the macrolide antibiotic roxithromycin was also investigated and detected to inhibit the generation of biofilms and proliferation of *P. aeruginosa* PA1 and PA27853 at sub-MIC levels[109]. Thus, mureidomycins comprise the most potent drug candidates.

Additionally, the lysis protein E of bacteriophage *φ*X174 was found to cause lysis of the bacterial cell by inhibiting MraY and thus disruption of cell wall biosynthesis[110]. This protein consists of 91 amino acids and contains an N-terminal transmembrane domain[111]. More recently, a novel, periplasmic target site was identified in MraY via a helical wheel model of transmembrane domain 9 of MraY and the transmembrane domain of lysis protein E. More specifically, a motif in protein E was identified, which consists of Arg-Trp-x-x-Trp and interacts with Phe288 and Glu287 of MraY. Mutations in these amino acids led to reduced or no detectable MraY inhibition[112]. Regarding other MraY inhibitors, pacidamycins were affected by mutations of the outer binding site as well, displaying up to 10-fold decreased activity, while activity of the liponucleoside derivatives hydroxyacylcaprazoles was not altered[112] (supporting information of the respective work). In a further investigation, Rodolis *et al.* (2014)[112] hypothesized that UPAs might bind to the periplasmic interaction site of lysis protein E and thus trigger a conformational change in MraY, which allows for their uptake into the cytoplasm by the hydrophobic channel present in the protein. This would explain the slow-binding inhibition of some UPAs. Thus, compound optimization regarding binding to the second site might lead to optimized drug candidates in the future.

1.4 Structure-activity relationships (SARs)

The structure of UPAs and compound modifications have been investigated in-depth regarding their biological activity, thus posing structural requirements for MraY inhibition. The stereochemistry was elucidated in combination with the total synthesis of 4*R*-dihydropacidamycin D and a series of analogs. Therein, the C(4') exocyclic olefin was hydrogenated leading to products, which retained similar bioactivity to the parental compound but possessed slightly elevated MICs. This suggests the enamide to not be essential for UPA activity[90]. However, some analogs displayed an enhanced antimicrobial

spectrum. More specifically, a derivative, containing 4-fluorophenylalanine at position four of the UPA scaffold, was detected to be active against clinical *E. coli* (MIC 4 - 8 µg/mL) and *M. tuberculosis* strains (MIC 4 - 10 µg/mL)[113]. Furthermore, a series of 5'-uridinyl dipeptide analogs of UPAs was synthesized, in order to investigate the activity of the UPA N-terminus[114]. This led to the hypothesis that the primary amino terminus acts competitively with the cofactor Mg^{2+}, binding in the respective pocket via positioning by the essential *cis*-*N*-methyl amide linkage. Moreover, in structure-activity studies of mureidomycin A the uridine moiety was detected to be crucial for activity[115]. In 2011, the total synthesis of pacidamycin D was published, which prompted the synthesis of analogs differing in the N-terminus. Therein, an N-terminal *m*-tyrosine was observed to convey enhanced activity in comparison with L-tyrosine, while the (*2S*, *3S*)-stereochemistry of DABA was concluded to be essential for enzyme inhibition and antibacterial activity[91,116].

Immense progress for the comprehension of MraY inhibition and structure-activity studies regarding UPAs and other MraY inhibitors was accomplished by Mashalidis *et al.* (2019)[117], who published the crystal structure of MraY (*Aquifex aeolicus*) in complex with several inhibitors (carbacaprazamycin, capuramycin and 3'-hydroxymureidomycin A; muraymycin D2 in previous study)[106]. Therein, 3'-hydroxymureidomycin A was identified to bind the uridine (residues Gly194, Leu195, Asp196, Asn255 and Phe262), uridine-adjacent (residues Thr75, Asn190 and Asp193), TM9b/loop E (residues Gln305, Ala321 and His325) and Mg^{2+} (residue Asp265) pockets of MraY. As observed for all MraY inhibitors, the uridine moiety of 3'-hydroxymureidomycin A binds to the uridine pocket, mimicking the natural substrate, which also contains an uracil moiety. Additional stabilization is derived from a hydrogen bond with Asp193. Hence, the uracil moiety was assumed to be essential for inhibition, while the ribosyl residue might provide the necessary directionality. Moreover, the *m*-tyrosine incorporated at position two of the UPA scaffold occupies the uridine adjacent pocket by forming a hydrogen bond with Thr75 via its hydroxyl group, while its N-terminal amino group is bound by Asn190. Since this pocket displays high degrees of flexibility, the bicyclic residue of napsamycins or the alanine of pacidamycins were postulated to be accommodated as well. As postulated in previously described studies, the same primary amino group of *m*-tyrosine occupies the Mg^{2+} pocket through a hydrogen bond with the essential aspartate residue Asp265 (Asp267 in *P. aeruginosa* numbering), which typically coordinates the cofactor Mg^{2+}. Interestingly, this pocket is solely occupied by 3'-hydroxymureidomycin A and tunicamycin, out of all MraY inhibitors. Lastly, the TM9b/loop E pocket is substantially occupied by the urea-dipeptide motif of the UPA C-terminus, by interactions with Gln305 and Ala321 via hydrogen bonds with the carboxylate and urea moieties (TM9b), respectively, and with His325 of loop E. The extensive knowledge on binding motifs of the aforementioned MraY inhibitors forms a crucial tool for drug development and inhibitor optimization.

In an even more recent study, 3'-hydroxymureidomycin A was synthesized and structure activity studies conducted regarding *P. aeruginosa* MraY, which was found to display high similarity to its counterpart of *A. aeolicus* and to possess almost identical amino acid residues, regarding their interactions (Fig. 5)[118]. Firstly, the *m*-tyrosine incorporated at position two of the mureidomycin scaffold was proposed to be responsible for the improved inhibitory activity against MraY, since this amino acid engages several MraY residues in contrast with the L-alanine typically found in pacidamycins. Secondly, the urea-dipeptide motif was confirmed to play a crucial role in MraY interaction. Contrastingly, the amino acids of the C-terminus were concluded to not be essential for MraY inhibition, since none of the side chains were found to interact with it. However, these side chains were essential for antibacterial activity against *P. aeruginosa* PAO1. More specifically, more hydrophobic or aromatic amino acids located at the C-terminus were postulated to improve cellular uptake by the *P. aeruginosa* ABC-type transporter NppA1A2BCD. This transporter had previously been suggested to be involved in UPA uptake in *P. aeruginosa*[119]. Thus, UPAs need to be optimized toward interaction with MraY and NppA1A2BCD, since their amino acid composition presumably affects the selectivity for uptake by the latter[118].

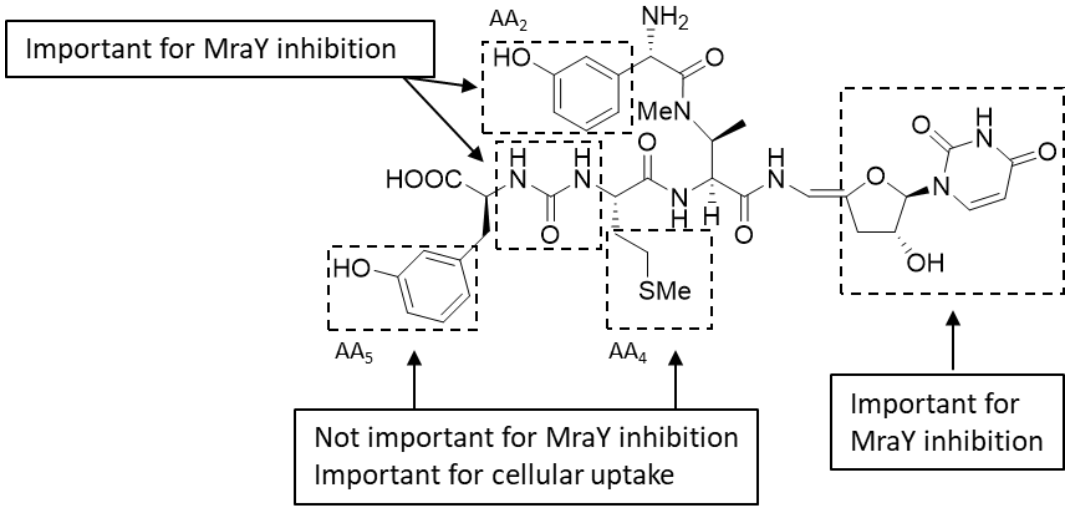


Fig. 5: SARs of UPAs, adapted from Terasawa *et al.* (2020)[118].

1.5 Previous work

In his PhD thesis[18], Dr. Nils Hauck heterologously expressed the pacidamycin biosynthetic gene cluster. For this purpose, several heterologous host strains were tested, alongside with different media and precursor feeding. It was concluded that expression of the biosynthetic gene cluster in *S. albus* J1074 with cultivation in P-medium and optional feeding of amino acids led to the most beneficial compound yield of the major compounds pacidamycin D and pacidamycin S. Thus, these conditions were

implemented at the beginning of the present study. Additionally, compound isolation and the subsequent determination of IC_{50} and MIC values were conducted for several UPAs (of all four subclasses) in the same PhD thesis. Thus, mureidomycins harboring an uracil instead of a dihydrouracil were concluded to be the most promising candidates for further development, which was attempted in this study. Thus, Dr. Nils Hauck commenced the engineering process of the pacidamycin BGC by replacing two NRPS domains (A-domain *pac15* and C-domain *pac14*) with the respective orthologous genes of the napsamycin BGC[18]. This led to the production of met-pacidamycin D and met-pacidamycin S, which harbor a methionine at position four of the UPA scaffold, which was desirable based on the previously mentioned bioactivity data.

Additionally, Grueschow *et al.* (2011)[120] directed pacidamycin biosynthesis toward production of compounds harboring *m*-tyrosine at position two of the UPA scaffold, which is considered important for MraY inhibition, as previously mentioned. This was accomplished by enhancing precursor availability with the expression of the 3-phenylalanine hydroxylase *phhA* (synthesis of *m*-tyrosine from phenylalanine) and the NRPS A-domain *pac21h*, which displays a preference for the activation of *m*-tyrosine and its incorporation specifically at the desired position. These adjacent genes were discovered in the genome of the original pacidamycin producer *S. coeruleorubidus* outside the pacidamycin BGC, where *pac21h* has arisen from a gene duplication event. Since the incorporation of *m*-tyrosine is desirable, the two genes were cloned into an integrative vector by Richard Sonnengruen (pRS02, unpublished data) and utilized in this study to direct UPA biosynthesis toward the most promising compounds (Fig. 6A). Moreover, the cluster-specific positive regulator of the napsamycin BGC was cloned into this plasmid by Richard Sonnengruen (unpublished data), resulting in pRS04 (Fig. 6B). This was decided based on data of Dr. Nils Hauck[18], in which the orthologous regulators SsaA, Pac1 and NpsM of the sansanmycin, pacidamycin and napsamycin BGC, respectively, were overexpressed in strains harboring the pacidamycin or the napsamycin gene cluster. Solely NpsM led to yield enhancement in both cases. Hence, both plasmids were utilized in the present study, in order to improve production rates and to influence the major compounds produced by the mutant strains.

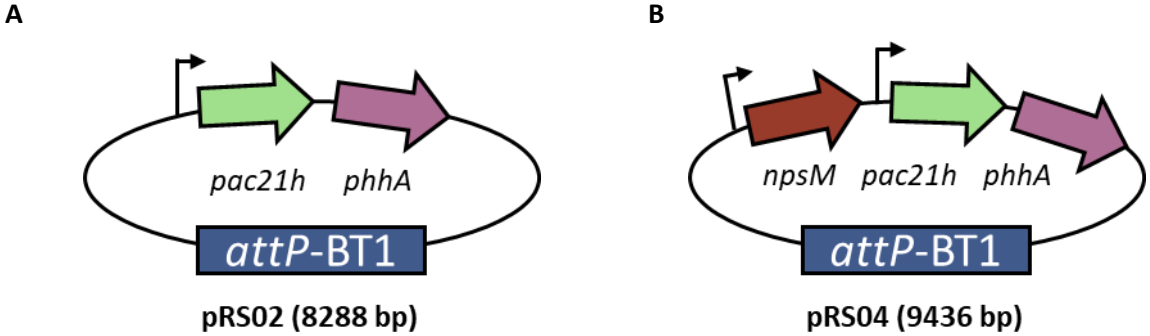


Fig. 6: Integrative plasmids harboring genes beneficial for mureidomycin biosynthesis, constructed by Richard Sonnengruen. A) Plasmid pRS02, containing the A-domain *pac21h* and the 3-phenylalanine hydroxylase *phhA* and B) Plasmid pRS04, containing the A-domain pac21h, 3-phenylalanine hydroxylase phhA and the cluster-specific positive regulator *npsM* of the napsamycin BGC.

Regarding the napsamycin BGC, cloning and heterologous expression were performed by Kaysser *et al.* (2011)[14] in *S. coelicolor* M1154 and by Dr. Nils Hauck in his PhD thesis in *S. albus* J1074[18], where mureidomycin B was identified as the major compound of all produced mureidomycins/napsamycins. Furthermore, the gene encoding for the ArsR family regulator NpsA was separately knocked out on the napsamycin BGC and overexpressed in a study by Dr. Nils Hauck[18], however UPA biosynthesis was abolished in both cases. Thus, the manipulation of this regulator was excluded from the present work. Additionally, in the aforementioned study by Kaysser *et al.* (2011)[14], the FMN-dependent oxidoreductase *npsU* was inactivated. Thus, production of compounds harboring a dihydrouracil moiety was abolished, while the uracil-containing counterparts were significantly increased. This prompted the knockout of the same gene in the present study, in order to narrow the spectrum of produced compounds and enhance mureidomycin A production.

Concerning the present work, LC-MS measurements were kindly conducted by Dipl. Ing. Andreas Kulik (Interfaculty Institute of Microbiology and Infection Medicine, University of Tuebingen). Moreover, data processing and alignment, regarding the RNA-sequencing, was performed by Theresa Harbig (PhD student, working group of Prof. Dr. Kay Nieselt, Interfaculty Institute for Bioinformatics and Medical Informatics, University of Tuebingen).

1.6 Aims of this study

The overarching aim of this study is the enhancement of mureidomycin production to facilitate compound isolation and, thus, the advancement toward pharmacokinetic/pharmacodynamic and preclinical studies. This is approached through a double strategy. In the first part of this thesis, experiments on the pacidamycin biosynthetic gene cluster are conducted and in the second part the napsamycin BGC is investigated.

Regarding the pacidamycin biosynthetic gene cluster, the first objective is the refactoring of the BGC by the insertion of strong, constitutive promoters into selected sites of the cluster. For this purpose, four bidirectional promoters, out of which two should be constructed in the present study by Golden Gate assembly, are knocked into the two bidirectional promoter sites of the BGC in several combinations. The effects on UPA production should be investigated by cultivation of the obtained mutant strains and a subsequent LC-MS analysis of culture extracts. Subsequently, the data regarding compound production should be correlated with a transcriptional analysis of the gene cluster. This is accomplished via the RNA-sequencing of cultures of the promoter swap mutant strains. In the RNA-sequencing, the operon structure of the BGC is also investigated. Furthermore, several optimized heterologous host strains are examined for improved production rates, which consist of *S. albus* Del14,

S. albus B2P1 and *S. griseus* CS065. Herein, the pacidamycin BGC is conjugated with the respective strains and UPA production levels are analyzed. Lastly, a reorganization of operon structure is attempted, in order to optimize transcription and, hence, production rates. This strategy includes the construction of an inversion cassette, containing the genes to be inverted, by Gibson assembly. The respective genes are knocked out on the BGC to be modified and then the inversion cassette is knocked in at the same site. Once more, the influence on production rates is investigated by LC-MS.

With regard to the second part of this study, refactoring of the napsamycin gene cluster should be conducted. For this purpose, several knock-ins of bidirectional promoter cassettes are attempted into two sites of the BGC. At one of the sites, a simultaneous knockout of the A-domain *npsP6* (activates bicyclic moieties and *m*-tyrosine) is performed, in order to limit the spectrum of produced compounds to mureidomycins. The promoter knock-ins are conducted upstream of the cluster-specific positive regulator *npsM* and the UPA exporter *npsO*, to improve yield by regulator and exporter overexpression. Subsequently, two oxidoreductases are knocked out, at first separately and then simultaneously, to further enhance production and limit the synthesis of undesired compounds. The first is the FAD-dependent oxidoreductase *npsE*, which was postulated in earlier studies[14] to catalyze the generation of the bicyclic moiety contained in napsamycins and some mureidomycins. Then, the FMN-dependent oxidoreductase *npsU*, which leads to the production of dihydro-derivatives of mureidomycins, is knocked out. Moreover, the most promising promoter knock-in is combined with knockout of *npsU* and the influence on compound yield investigated by LC-MS in each case.

Lastly, the most promising candidates of both gene clusters are compared regarding mureidomycin A yield and the variety of detected compounds in each mutant strain. Thus, the most beneficial host, constituting a selective and potent UPA production platform will be identified.

2. Materials and Methods

2.1 Materials

2.1.1 Devices

Table 3: Devices used in this study

Device	Specification	Manufacturer
(Micro-) Scales	Sartorius MC210 P ISO9001	Sartorius AG, Göttingen, Germany
Autoclave	Systec VX-150	Systec GmbH, Linden, Germany
Autoclave	Systec DE-23	Systec GmbH, Linden, Germany
Centrifuge	Micro Star 17R	VWR International, Radnor, PA, USA
Centrifuge	Multifuge 1 S-R 75002005 G Sorvall Heraeus	Thermo Fisher Scientific, Waltham, MA, USA
Clean bench	Heraeus Herasafe	Thermo Fisher Scientific, Waltham, MA, USA
Electrophoresis power supply	EPS 300	Pharmacia Biotech, Uppsala, Sweden
Electroporation apparatus	Micro Pulser™	Bio-Rad Laboratories, Inc., Hercules, CA, USA
Gel documentation system	Vilber E-Box VX5	Vilber Lourmat, Collégien, France
Incubator	Heraeus Function Line B12	Thermo Fisher Scientific, Waltham, MA, USA
Incubator	Innova®44 Incubator Shaker Series	New Brunswick Scientific, Eppendorf, Hamburg, Germany
Incubator	Certomat HK	Sartorius AG, Göttingen, Germany
Laboratory Shaker	TS 100 Thermo Shaker	VWR International, Radnor, PA, USA (Previously PEQLAB Biotechnologie GmbH)
LC-MS System	LC/MSD Ultra Trap System XCT 6330	Agilent Technologies, Santa Clara, CA, United States
Magnetic stirrer	Heidolph MR Hei-Standard	Heidolph Instruments GmbH & Co. KG, Schwabach, Germany
Microwave	Sharp Inverter	SHARP, Sakai, Japan

Device	Specification	Manufacturer
NanoDrop	NanoDrop 1000	VWR International, Radnor, PA, USA (Previously PEQLAB Biotechnologie GmbH)
PCR cycler	iCycler BioRad	Bio-Rad Laboratories, Inc., Hercules, CA, USA
PCR cycler	peqSTAR	VWR International, Radnor, PA, USA (Previously PEQLAB Biotechnologie GmbH)
pH meter	HANNA Instruments pH 211 Microprocessor pH-Meter	Sigma-Aldrich®, St. Louis, MO, USA
Rotary evaporator	Rotavapor R-210, Vacuum Controller V-855, Vacuum Pump V-700, Recirculating Chiller F-108, Heating Bath B-491	Büchi Deutschland, Essen, Germany
Spectrophotometer	Novaspec II	Pharmacia Biotech, Uppsala, Sweden
SpeedVac Vacuum Concentrator	Concentrator plus	Eppendorf, Hamburg, Germany
Vortex mixer	Vortex Genie 2, VF2	Scientific Industries, Inc., Bohemia, New York, USA

2.1.2 Equipment and Consumables

Table 4**:** Equipment and consumables used in this study

Equipment/Consumable	Specification	Manufacturer
Centrifuge tubes	50 mL, 15 mL	greiner bio-one, Kremsmünster, Austria
Culture dishes	94 mm x 16 mm	greiner bio-one, Kremsmünster, Austria
DNA Gel Loading Dye	6x concentrated	Thermo Fisher Scientific, Waltham, MA, USA
Electroporation cuvettes	Peqlab, 2 mm gap	VWR International, Radnor, PA, USA (Previously PEQLAB Biotechnologie GmbH)
Eppendorf® Safe-Lock microcentrifuge tubes	2 mL, 1.5 mL	Eppendorf, Hamburg, Germany
LC-MS caps	11 mm Aluminum Crimp Caps with septum	WICOM, Heppenheim, Germany
LC-MS column	Nucleosil-100 C18, 3µm, 100 mm x 2 mm	Macherey-Nagel, Düren, Germany

Equipment/Consumable	Specification	Manufacturer
LC-MS vials	11 mm CRIMPSNAP-Vial, polypropene, 500 µL, conical bottom	WICOM, Heppenheim, Germany
Parafilm		Bemis®, Neenah, Wisconsin, USA
Pipette tips	10000 µL, 1000 µL, 200 µL, 20 µL, 2 µL	Eppendorf, Hamburg, Germany
Pipettes	10000 µL, 1000 µL, 200 µL, 20 µL, 2 µL Discovery	Eppendorf, Hamburg, Germany
Single tubes for PCR	Multiply®-µStrip Pro 8-strip	SARSTEDT AG & Co. KG, Nümbrecht, Germany
Sterile filters	0.2 µm	Sartorius AG, Göttingen, Germany
Syringes	20 mL, 10 mL	Becton, Dickinson and Company, Franklin Lanes, New Jersey, USA

2.1.3 Chemicals

Table 5: Chemicals used in this study

Chemical/Media component	Manufacturer
Acetic acid	Sigma-Aldrich®, St. Louis, MO, USA
Acetonitrile	Carl Roth GmbH & Co. KG, Karlsruhe, Germany
Agar	Becton, Dickinson and Company, Franklin Lanes, New Jersey, USA
Agarose	Genaxxon bioscience GmbH, Ulm, Germany
Ammonium molybdate tetrahydrate $(NH_4)_6Mo_7O_{24}\cdot 4H_2O$	Sigma-Aldrich®, St. Louis, MO, USA
Apramycin	Sigma-Aldrich®, St. Louis, MO, USA
Betaine	Sigma-Aldrich®, St. Louis, MO, USA
Bromophenol blue	Carl Roth GmbH & Co. KG, Karlsruhe, Germany
Butan-1-ol	Thermo Fisher Scientific, Waltham, MA, USA
Carbenicillin	Carl Roth GmbH & Co. KG, Karlsruhe, Germany

Chemical/Media component	Manufacturer
Chloramphenicol	Sigma-Aldrich®, St. Louis, MO, USA
Copper(II) chloride dehydrate ($CuCl_2 \cdot 2H_2O$)	Sigma-Aldrich®, St. Louis, MO, USA
Dimethyl sulfoxide (DMSO)	Sigma-Aldrich®, St. Louis, MO, USA
DL-*meta*-tyrosine	Sigma-Aldrich®, St. Louis, MO, USA
D-Maltose monohydrate	Carl Roth GmbH & Co. KG, Karlsruhe, Germany
dNTPs	Genaxxon bioscience GmbH, Ulm, Germany
Ethanol	Honeywell, Thermo Fisher Scientific, Waltham, MA, USA
Ethyl acetate HPLC-grade	Honeywell, Thermo Fisher Scientific, Waltham, MA, USA
Ethylene-diamine-tetra acetic acid (EDTA)	Carl Roth GmbH & Co. KG, Karlsruhe, Germany
Glucose	Carl Roth GmbH & Co. KG, Karlsruhe, Germany
Glycerol	Carl Roth GmbH & Co. KG, Karlsruhe, Germany
Glycine	Carl Roth GmbH & Co. KG, Karlsruhe, Germany
Hydrochloric acid	Sigma-Aldrich®, St. Louis, MO, USA
IPTG	Carl Roth GmbH & Co. KG, Karlsruhe, Germany
Iron(III) chloride hexahydrate ($FeCl_3 \cdot 6H_2O$)	Carl Roth GmbH & Co. KG, Karlsruhe, Germany
Isopropanol	Thermo Fisher Scientific, Waltham, MA, USA
Kanamycin	Carl Roth GmbH & Co. KG, Karlsruhe, Germany
L-arabinose	Sigma-Aldrich®, St. Louis, MO, USA
Lithium chloride	Sigma-Aldrich®, St. Louis, MO, USA
Magnesium chloride hexahydrate	Carl Roth GmbH & Co. KG, Karlsruhe, Germany
Malt extract	Becton, Dickinson and Company, Franklin Lanes, New Jersey, USA
Manganese(II) chloride tetrahydrate ($MnCl_2 \cdot 4H_2O$)	Sigma-Aldrich®, St. Louis, MO, USA
Mannitol	Carl Roth GmbH & Co. KG, Karlsruhe, Germany

Chemical/Media component	Manufacturer
Methanol HPLC-grade	Honeywell, Thermo Fisher Scientific, Waltham, MA, USA
Nalidixic acid	Carl Roth GmbH & Co. KG, Karlsruhe, Germany
peqGREEN	VWR International, Radnor, PA, USA (Previously PEQLAB Biotechnologie GmbH)
Phenol/Chloroform/Isoamyl alcohol 25:24:1 *(v/v)*	Carl Roth GmbH & Co. KG, Karlsruhe, Germany
Potassium acetate	Sigma-Aldrich®, St. Louis, MO, USA
Sodium acetate	Sigma-Aldrich®, St. Louis, MO, USA
Sodium chloride	Sigma-Aldrich®, St. Louis, MO, USA
Sodium dodecyl sulphate (SDS)	Carl Roth GmbH & Co. KG, Karlsruhe, Germany
Sodium hydroxide	Sigma-Aldrich®, St. Louis, MO, USA
Sodium tetraborate decahydrate ($Na_2B_4O_7 \cdot 10H_2O$)	Sigma-Aldrich®, St. Louis, MO, USA
Soluble starch	Becton, Dickinson and Company, Franklin Lanes, New Jersey, USA
Soy flour	SOBO Naturkost, Köln, Germany
Soytone	Becton, Dickinson and Company, Franklin Lanes, New Jersey, USA
Trizma base	Sigma-Aldrich®, St. Louis, MO, USA
Trypticase soy broth	Becton, Dickinson and Company, Franklin Lanes, New Jersey, USA
Tryptone	Becton, Dickinson and Company, Franklin Lanes, New Jersey, USA
X-β-Gal	Carl Roth GmbH & Co. KG, Karlsruhe, Germany
Yeast extract	Becton, Dickinson and Company, Franklin Lanes, New Jersey, USA
Zinc chloride ($ZnCl_2$)	Carl Roth GmbH & Co. KG, Karlsruhe, Germany

2.1.4 Enzymes and Kits

Table 6: Enzymes and kits used in this study

Enzyme/Kit	Specification	Manufacturer
BamHI-HF	CutSmart® Buffer, 37 °C	NEB, Ipswich, MA, USA
Cre Recombinase	Cre Recombinase Reaction Buffer, 30 min, 37 °C	NEB, Ipswich, MA, USA
EcoRI-HF	CutSmart® Buffer, 37 °C	NEB, Ipswich, MA, USA
EcoRV-HF	CutSmart® Buffer, 37 °C	NEB, Ipswich, MA, USA
Gibson Assembly® Master Mix	1 h, 50 °C	NEB, Ipswich, MA, USA
HindIII-HF	CutSmart® Buffer, 37 °C	NEB, Ipswich, MA, USA
I-SceI	CutSmart® Buffer, 37 °C	NEB, Ipswich, MA, USA
KpnI-HF	CutSmart® Buffer, 37 °C	NEB, Ipswich, MA, USA
NEBridge® Golden Gate Assembly Kit (BsaI-HF® v2)	See 2.2.1.11	NEB, Ipswich, MA, USA
NEBuilder® HiFi DNA Assembly Master Mix	1 h, 50 °C	NEB, Ipswich, MA, USA
Q5® High-Fidelity DNA Polymerase	See 2.2.1.7.B	NEB, Ipswich, MA, USA
QIAquick Gel Extraction Kit	Purification of DNA from agarose gels	Qiagen, Hilden, Germany
QIAquick PCR Purification Kit	Purification of PCR products	Qiagen, Hilden, Germany
RNase A	Stock solution: 100 mg/mL Working concentration: 0.1 mg/mL	Macherey-Nagel, Düren, Germany
ScaI-HF	CutSmart® Buffer, 37 °C	NEB, Ipswich, MA, USA
SpeI-HF	CutSmart® Buffer, 37 °C	NEB, Ipswich, MA, USA
SwaI	NEBuffer™ r3.1, 25 °C	NEB, Ipswich, MA, USA
T4 DNA Ligase	T4 DNA ligase buffer, 4 °C, overnight	NEB, Ipswich, MA, USA
Taq:Pfu (9:1) Polymerase Mix	See 2.2.1.7.A	In-house production
XhoI	CutSmart® Buffer, 37 °C	NEB, Ipswich, MA, USA

All enzymes were stored at - 20 °C. The sole exception consists of I-SceI, which was stored at - 80 °C.

2.1.5 Size markers for gel electrophoresis

Table 7**:** Gel electrophoresis supplies used in this study

Gel electrophoresis supply	Specification	Manufacturer
Gene Ruler High Range DNA Ladder	6x concentrated, 10171 – 48502 bp	Thermo Fisher Scientific, Waltham, MA, USA
GeneRuler 1 kb DNA Ladder	6x concentrated, 250 – 10000 bp	Thermo Fisher Scientific, Waltham, MA, USA

2.1.6 Antibiotics

Antibiotic stock solutions were dissolved in the stated solvent and sterilized by filtration through a 0.2 µm filter.

Table 8: Antibiotics used in this study

Antibiotic	Stock solution (mg/mL)	Working concentration (µg/mL)	Solvent
Apramycin	50	50	ddH_2O
Carbenicillin	50 - 100	50 - 100	ddH_2O
Chloramphenicol	25	25	EtOH 100%
Kanamycin	50	50	ddH_2O
Nalidixic acid	25	25	0.3 M NaOH

All antibiotics were stored at - 20 °C.

2.1.7 Primers

Table 9: Primers designed in this study

No.	Primer	Sequence (5’ → 3’)
1	BidPrCas1_FW	CGCGTGGAGCGAGACGACCGCGACCAGCGGCAAAGCCAC TGAGGACCACCTCTCATAAC
2	BidPrCas1_RV	GGTCAGTTGTGCGCTCAACAAGGGAAGCCTGTCGGTCAT AGCGGACCTCTATGGCTTG
3	BidPrCas2_FW	GAGCCAGACGATTTGCTGTGCGGCGCTGAGCGGAAACAC CCGCGACTCCTTGCACATTAG

No.	Primer	Sequence (5’ → 3’)
4	BidPrCas2_RV	GGCCGTGTCGAGCAGAGACCGCTGCTCTGCGGCGGTCAT CCAGCTCCTCCTATCCGCTAC
5	BidPrCas1_FW_vol2	TACTTCAGTCACGGCGCCAACGTAGCAGGATGGGTTCAA TGAGGACCACCTCTCATAAC
6	pac3_test_FW	CCATCAGTCTTCGACTCTAC
7	neu_pac3_test_FW	CAATCATGATGGAGCGCTTG
8	pac4_test_RV	ATGCACGGAACATCAAGGTG
9	npsP8_test_FW	CAACAGCGCGGAAGAGATC
10	npsP4_test_RV	CACCATGAAATTCGACCACC
11	pac4_test_FW	CGAGATGACGGTGTTCATG
12	IGR_pac3_4_PC1_RV	GCTTCACTCTCAACGTCAAG
13	pacP8_test_FW	TCGGTCCGTAGATGTTGAC
14	IGR_P4P8_PC2_RV	GAGTTGACTGTGTTCTCGTC
15	HB_FW	GGCCGTGTCGAGCAGAGACCGCTGCTCTGCGGCGGTCAT AGCGGACCTCTATGGCTTG
16	HB_ RV	GAGCCAGACGATTTGCTGTGCGGCGCTGAGCGGAAACAC TGAGGACCACCTCTCATAAC
17	PromB_ISce_FW	GGCCGTGTCGAGCAGAGACCGCTGCTCTGCGGCGGTCAT ATTCCGGGGATCCGTCGACC
18	PromB_ISce_RV	GAGCCAGACGATTTGCTGTGCGGCGCTGAGCGGAAACA CTGTAGGCTGGAGCTGCTTC
19	PC1B_Amp_FW	GGAGGTGTAGATCACGTACG
20	PC1B_Amp_RV	GTACTGGTCGAGCACGTCG
21	pacHK08_test_FW	GGACCCGTCGAAGATGAACG
22	pacHK08_test_RV	TCGATGCTGAACCGGGCAC
23	ISceI_pacRS03_PS1_FW	GGTCAGTTGTGCGCTCAACAAGGGAAGCCTGTCGGTCATATTCCGGG GAT CCGTCGACC
24	ISceI_pacRS03_PS1_RV	TACTTCAGTCACGGCGCCAACGTAGCAGGATGGGTTCAATGTAGGCT GGA GCTGCTTC
25	PC1_on_RS03_Amp_FW	ATGAGCAGCATCGACTGTTC
26	PC1_on_RS03_Amp_RV	CAGGTAGCTCTGGTAAGCG

No.	Primer	Sequence (5’ → 3’)
27	RS03_PC1_test_FW	ATGACGCGGGTGTCCTTCC
28	RS03_PC1_test_RV	GGCGTACGACAGCGCGTC
29	GGA_774_FW	AAAAAAGGTCTCTATTCCGGGGATCCGTCGAC
30	GGA_774_RV	AAAAAAGGTCTCTTGTAGGCTGGAGCTGCTTCG
31	GGA_test_FW	GAACTTGGCCGTAACCTGC
32	GGA_test_RV	AAACAAATAGGGGTTCCGCC
33	PC3-4_npsP8P4_FW	GGCCGTGTCGAGCAGAGACCGCTGCTCTGCGGCGGTCAT GTCAACGCATCTCCCGGG
34	PC3_npsP8P4_RV	GAGCCAGACGATTTGCTGTGCGGCGCTGAGCGGAAACAC ATCCTACCAACCGGCACG
35	PC4_npsP8P4_RV	GAGCCAGACGATTTGCTGTGCGGCGCTGAGCGGAAACAC ACACCAGACTTTACAACACC
36	PC3-4_pac4_FW	GGTCAGTTGTGCGCTCAACAAGGGAAGCCTGTCGGTCAT GTCAACGCATCTCCCGGG
37	PC3_pac3_RV	TACTTCAGTCACGGCGCCAACGTAGCAGGATGGGTTCAA ATCCTACCAACCGGCACG
38	PC4_pac3_RV	TACTTCAGTCACGGCGCCAACGTAGCAGGATGGGTTCAA ACACCAGACTTTACAACACC
39	npsP4Frag_FW	ATGGAGCGCCGTAGGCAGC
40	npsP4Frag_RV	GTGTTTCCGCTCAGCGCCG
41	npsP3_Frag_FW	TCAGAGCAGCCGCGCGAGCTC
42	npsP3_Frag_RV	GCTGCCTACGGCGCTCCATG
43	300P8_FW	ACGGTATCGATAAGCTTGATATTTAAATAGCGGGACATAGGCGGCTC C
44	300P8_RV	AGCTCGCGCGGCTGCTCTGAATGACCGCCGCAGAGCAGCG
45	ISceI_Del_3gen_FW	GGCCGTGTCGAGCAGAGACCGCTGCTCTGCGGCGGTCATA TTCCGGGGATCCGTCGACC
46	ISceI_Del_3gen_RV	GGCCGCTTCCCCGGCTACCTCGGCACCCCCGTGCAGTAATG TAGGCTGGAGCTGCTTC
47	Seq_Anfang_npsP3_Fa	CCGTCTGTTCCGATCCGCAG
48	Seq_Anfang_npsP3_Fb	TCGTCGACGACGAGCACG
49	Seq_Anfang_npsP3_Ra	TGCCGCACGAACTCGCCCTG

No.	Primer	Sequence (5’ → 3’)
50	Seq_Anfang_npsP3_Rb	AGTCGATGACCACGGACCAC
51	Seq_Ende_npsP4_F	CCGAACTCCTCGTCCTTGTC
52	Seq_Ende_npsP4_R	ATGTTCGCCATGCACGACGC
53	Seq_last_npsP3_F	CGCATGCTCGGTTCCACTG
54	Seq_last_npsP3b_F	TCGTCGTCGGAGAACAGCTC
55	npsP3_NW_F	ACGAGCAGGTCAAGGTACG
56	npsP3_NW_R	TGGTCGAAGTTCCAGCAGAT
57	npsP3_SeqPrimer_F	AGCTTCTCGTACGGGCTC
58	npsP3_SeqPrimer_R	TCCAGGACATAGACGTGCC
59	pBluescript_FW	CGCTTACAATTTCCATTCGC
60	pBluescript_RV	CACAGGAAACAGCTATGACC
61	ISceI_npsP8_3_P15_FW	GGCCGTGTCGAGCAGAGACCGCTGCTCTGCGGCGGTCATA TTCCGGGGATCCGTCGACC
62	ISceI_npsP8_3_P15_RV	CGGCACCCGACCGTCGCCGAGCTCGCGCGGCTGCTCTGATG TAGGCTGGAGCTGCTTC
63	Test_Inv_P15_FW	GACACGGACATCCTTGAGCC
64	Test_Inv_P15_RV	TGACGCCGAACGGGAAGAC
65	pRS02_TF1	CTAGTAACGCTCACTGGGTAC
66	pRS02_TR1	CACCGTTTGTCAAGCTGCTC
67	KOnpsP6_FW	CAGAATCACTTCTGCATCACGCTCGAAAAGGTTGTCCAT TGAGGACCACCTCTCATAAC
68	KOnpsP6_RV	CTCGGCGTCGGAAAAGATTCTCGGTGGCAGTGCGGGCAT AGCGGACCTCTATGGCTTG
69	Test_KOnpsP6_FW	ATGTGAAGACGGTGAGTTCG
70	Test_KOnpsP6_RV	CGGAAGGCATGTCGACAAC
71	ISceI_O_P7_FW	AGCCAGTTGGGCACTCGACAAGGGAAGCCTGTCGATCAT ATTCCGGGGATCCGTCGACC
72	ISceI_O_P7_RV	TGTTTCGACACCCTGAGAATCGTTCGCCACTTCCGTCAT TGTAGGCTGGAGCTGCTTC

No.	Primer	Sequence (5’ → 3’)
73	Test_npsPK02_FW	TCGAGAACCAGTAGCAGATG
74	Test_npsPK02_RV	ATCGTCAGCACGTCGAAGG
75	npsP7_PC1_FW	AGCCAGTTGGGCACTCGACAAGGGAAGCCTGTCGATCAT AGCGGACCTCTATGGCTTG
76	npsP7_PC1_RV	TGTTTCGACACCCTGAGAATCGTTCGCCACTTCCGTCAT TGAGGACCACCTCTCATAAC
77	Amp_npsXT01_PS2_FW	CGGTCGAAAACGGCGTTCC
78	Amp_npsXT01_PS2_RV	ATCAGCGAGGGCAGGTAGC
79	KO_npsE_FW	CTCTGACCGCGCGCAGTAGTCCGGGGACCACCCGGACTA ATTCCGGGGATCCGTCGACC
80	KO_npsE_RV	TCCGTCCGGCGACGAGGACGGGGCCACCCGAGGATGAAC TGTAGGCTGGAGCTGCTTC
81	npsE_test_FW	CGTGGACGAGGGATTCTTCG
82	npsE_test_RV	GTGGAACAGCTCCTGGAAGC
83	npsU_KO_FW	AGCGGTCTCAGGCTTTCGGGGGAGTCCCGTGCTGAATCA ATTCCGGGGATCCGTCGACC
84	npsU_KO_RV	GTGCATCTGGCCGTTCACACGGGACGGGGCGGCGTGAGC TGTAGGCTGGAGCTGCTTC
85	npsUKO_test_FW	CACATGCTCGCTTCCCTTC
86	npsUKO_test_RV	ATCAGTTCGGCTGCTCGAAG
87	npsU_KO_test_FW	CTATCAGTTCGTCCCTGAG
88	npsU_KO_test_RV	AGACGAGTGTTCCCTTCTAC
89	Test_PC1_P7_O_FW	GTTCGGTGACATGACACTCGG
90	Test_PC1_P7_O_RV	ATCAGCAGGCGCAGCAGATC

All primers were dissolved in ddH_2O to a final concentration of 100 pmol/µL and stored at - 20 °C.

2.1.8 gBlocks®

Table 10: gBlocks® designed in this study

gBlock	Sequence (5' → 3')
ermE_Mon	AAATAAAAAAGGTCTCTGGAGGGTACCGTCAACGCATCTCCCGGGTCGGTCC CGAAGAGTCAGATCCTCCCCGCACCTCTCGCCAGCCGTCAAGATCGACCGCAT TCAGAGACCAAAAAATAAAA
ermE_pUWL	AATAAAGGTCTCTTACAGCGGTCGATCTTGACGGCTGGCGAGAGGTGCGGGG AGGATCTGACCGACGCGGTCCACACGTGGCACCGCGATGCTGTTGTGGGCAC AATCGTGCCGGTTGGTAGGATGATATCCCATAGAGACCAAAATA
kasOP*_SP44	ATAATAAAAAAAATAAAAAGGTCTCTTACATGTTCACATTCGAACCGTCTCTGC TTTGACAACATGCTGTGCGGTGTTGTAAAGTCTGGTGTGATATCCCATAGAGA CCAAAATAAATAAAAATAA
Inv_R3pac11ermE	TGCGGCGCTGAGCGGAAACACGTCAACGCATCTCCCGGGTCGGTCCCGAAGA GTCAGATCCTCCCCGCACCTCTCGCCAGCCGTCAAGATCGACCGCTTACTGCAC GGGGGTGCCGAGGTAGCCGGGGAAGCGGCCTTCGGGGTCACGGACGGTGCG GATCTGCTGGAACTTCGACCAGGCCGCGTCGGACATGATCCGGTCGGGGCGG ACGGTGAAGTCGCTGTCGCCCAGGTAGCAGCCGGCCGAGTACGGTGCCGCGC GCTCCATGGTCCCGTCCAGCCAGGAGCGGCACCGGGCGTCCTCTTCCGGGGTT TCGCCGATCACGTACGCGGCGAAGTACAGGTCGGTCTGCACCGACAGGGCCAT GTCCGGCGGGCGGCGGGACAGCAGGGGGGTATTTAAATATCGAATTCCTGCA GCCCGGGGGAT
P15_Inversion	AAAAAACGCCAGGCGTGCGGCGATCCGGTCCGTCAGGTCGTCGAGCTCGCGGT AGCTGAGGGTCCGCTCGCCGTCTCGGAGGGCCGGGGCGGCACCACGGGCCGCA GCAACAGCGCGGAAGAGATCGGGCAGGGAAACGGCCGTGTCGAGCAGAGACC GCTGCTCTGCGGCGGTCATTGAGGACCACCTCTCATAACGAACACGTGGCAGGT TAACCTATATTGCTTCACTCTCAACGTCAAGTGGGCAATTTCAGAGCAGCCGCGC GAGCTCGGCGACGGTCGGGTGCCGGAACAGCACTCGCGCCCTGAGGTCGACAC CGAGCGCGCTCCGAATCCTGGTCCTCAGCCGGGTCGCCAACAGCGAGTCCCCGC CCAGGGCGAAGAATCCCTCGTCCACGCCGACCCGTTCCACCCCCAGGACCTCGG CGAACAGAGCGCACAGACGCTCCTCGTCGGCCGTGCGGGGGCCTTGGCCCGCG CCGCCGCCGTAGTAAAAAA

All gBlocks® were dissolved in ddH_2O to a final concentration of 10 ng/µL and stored at - 20 °C.

2.1.9 Plasmids and Cosmids

Table 11: Plasmids and cosmids used and designed in this study

Plasmid/Cosmid	Description	Reference
npsHK01	npsXT01 derivative, *npsE* knocked out; Kan^R, Tet^R	Present work

Plasmid/Cosmid	Description	Reference
npsHK02	npsXT01 derivative, *npsU* knocked out; Kan^R, Tet^R	Present work
npsHK03	npsHK02 derivative, intergenic region between *npsO* und *npsP7* replaced by bidirectional promoter cassette P15-P16 (PC1); Kan^R, Tet^R	Present work
npsHK04	npsHK02 derivative, *npsE* knocked out; Kan^R, Tet^R	Present work
npsPK01	npsXT01 derivative, intergenic region between *npsL* und *npsM* replaced by bidirectional promoter cassette P15-P16 (PC1), *npsP6* knocked out; Kan^R, Tet^R	Present work - Philipp Konrad
npsPK02	npsXT01 derivative, intergenic region between *npsO* und *npsP7* replaced by bidirectional promoter cassette P15-P16 (PC1); Kan^R, Tet^R	Present work - Philipp Konrad
npsPK03	npsPK01 derivative, intergenic region between *npsO* und *npsP7* replaced by bidirectional promoter cassette P15-P16 (PC1); Kan^R, Tet^R	Present work - Philipp Konrad
npsXT01	Derivative of integrative cosmid SuperCos1 containing the napsamycin biosynthetic gene cluster cloned into the BamHI/XbaI restriction sites, *bla* gene replaced by cassette from pIJ787 (*oriT, tet, attP, int* of phage ϕC31); Kan^R, Tet^R	Kaysser *et al.* (2011)[14]
pacHK01	pacRS01 derivative, intergenic region between *pac3* and *pac4* based on annotation of the pacidamycin BGC by Zhang *et al.*[17] replaced by bidirectional promoter cassette P15-P16 (PC1); Kan^R, Tet^R	Present work
pacHK02	pacHK01 derivative, intergenic region between *npsP8* und *npsP4* based on annotation of the pacidamycin BGC by Zhang *et al.*[17] replaced by bidirectional promoter cassette P03-P04 (PC2); Kan^R, Tet^R	Present work
pacHK03	pacRS01 derivative, intergenic region between *pac3* and *pac4* based on annotation of the pacidamycin BGC by Rackham *et al.*[121] replaced by bidirectional promoter cassette P15-P16 (PC1); Kan^R, Tet^R	Present work
pacHK04	pacHK03 derivative, intergenic region between *npsP8* und *npsP4* based on annotation of the pacidamycin BGC by Rackham *et al.*[121] replaced by bidirectional promoter cassette P03-P04 (PC2); Kan^R, Tet^R	Present work
pacHK05	pacRS01 derivative, intergenic region between *npsP8* und *npsP4* replaced by bidirectional promoter cassette P03-P04 (PC2); Kan^R, Tet^R	Present work
pacHK06	pacRS01 derivative, intergenic region between *npsP8* und *npsP4* replaced by bidirectional promoter cassette P15-P16 (PC1); Kan^R, Tet^R	Present work

Plasmid/Cosmid	Description	Reference
pacHK07	pacRS01 derivative, intergenic region between *npsP8* und *npsP4* replaced by I-SceI- *aac(3)IV* cassette; Kan^R, Tet^R	Present work
pacHK08	pacHK03 derivative, intergenic region between *npsP8* und *npsP4* replaced by bidirectional promoter cassette P15-P16 (PC1); Kan^R, Tet^R	Present work
pacHK09	pacRS03 derivative, intergenic region between *pac3* and *pac4* based on annotation of the pacidamycin BGC by Rackham *et al.*[121] replaced by bidirectional *ermE** promoter cassette (PC3); Kan^R, Tet^R	Present work
pacHK10	pacRS03 derivative, intergenic region between *pac3* and *pac4* based on annotation of the pacidamycin BGC by Rackham *et al.*[121] replaced by bidirectional *ermE*-kasOp*SP44* promoter cassette (PC4); Kan^R, Tet^R	Present work
pacHK11	pacRS03 derivative, intergenic region between *pac3* and *pac4* based on annotation of the pacidamycin BGC by Rackham *et al.*[121] replaced by bidirectional promoter cassette P15-P16 (PC1); Kan^R, Tet^R	Present work
pacHK12	pacHK03 derivative, intergenic region between *npsP8* und *npsP4* replaced by bidirectional *ermE** promoter cassette; Kan^R, Tet^R	Present work
pacHK13	pacHK11 derivative, operon consisting of *npsP4*, *pac13* and *npsP3* inverted with a simultaneous knock-in of promoter *ermE** in front of *npsP4*; Kan^R, Tet^R	Present work
pacHK14	pacHK13 derivative, unidirectional promoter cassette P15 knocked in between *npsP3* and *npsP8*; Kan^R, Tet^R	Present work
pacNH01	Derivative of integrative cosmid SuperCos1 containing the pacidamycin biosynthetic gene cluster, *bla* gene replaced by cassette from pIJ787 (*oriT, tet, attP, int* of phage ϕC31); Kan^R, Tet^R	Rackham *et al.* (2010)[121]
pacRS01	pacNH01 derivative, *pac14*, *pac15* and *pac2* replaced by *npsP4*, *npsP8* and *npsN* of the napsamycin BGC, respectively; Kan^R, Tet^R	Richard Sonnengruen
pacRS03	pacRS01 derivative, *pac21* knocked out and *pac12* replaced by *npsP3* of the napsamycin BGC; Kan^R, Tet^R	Richard Sonnengruen
pAG03	Promoter cassette 1 cloned into pBluescript II SK (-); $Carb^R$	Franziska Wiker, Dissertation
pAG05	Promoter cassette 2 cloned into pBluescript II SK (-); $Carb^R$	Franziska Wiker, Dissertation
pBluescript II SK (-)	Cloning vector; $Carb^R$	Stratagene Inc., La Jolla, CA, USA

Plasmid/Cosmid	Description	Reference
pGGAselect	High-copy-number ColE1/pMB1/pBR322/pUC origin of replication; Cml^R	NEB, Ipswich, MA, USA
pHK01	pGGAselect derivative containing bidirectional *ermE** promoter cassette (PC3) cloned into BsaI restriction sites; Cml^R	Present work
pHK02	pGGAselect derivative containing bidirectional *ermE*-kasOp*SP44* promoter cassette (PC4) cloned into BsaI restriction sites; Cml^R	Present work
pHK03	pBluescript II SK (-) derivative, inversion cassette consisting of SwaI_site/300 bp *pac11*/*ermE** promoter/*npsP4*/*pac13*/*npsP3*/300 bp *npsP8/*SwaI_site cloned into EcoRV-digested vector with Gibson assembly; $Carb^R$	Present work
pIJ773	pBluescript SK(+)-derivative, *P1*-FRT-*oriT*-*aac(3)IV*-FRT-*P2*, $Apra^R$	Gust *et al.* (2003)[122]
pIJ774	pBluescript SK(+)-derivative, *P1*-loxP-*oriT*-*aac(3)IV*-loxP-*P2*, $Apra^R$	Gust *et al.* (2003)[122]
pIJ787	SuperCos1-derivative, *bla* gene replaced by a cassette containing *oriT, tet, attP* and *int* of phage *φ*C31; Tet^R, Kan^R	Eustáquio *et al*. (2005)[123]
pIJ790	Recombineering plasmid: λ/RED (*gam*, *bet*, *exo*), *araC*, *rep101^{ts}*; Cml^R; Temperature sensitive origin of replication	Gust *et al.* (2003)[122]
pMVM3100	Integrative plasmid, derivative of pRT801, *attP*/*int* BT1, synthetic cassette [TermFd + promoter P57+ N12 UTR + NdeI-SpeI cloning sites + TermFd] cloned into SpeI-EcoRV sites; $Apra^R$	Martha V. Mendes, University of Porto
pRS02	pMVM3100 derivative, *ermE*p_pac21h_phhA* cloned into SpeI/HindIII restriction sites; $Apra^R$	Richard Sonnengruen
pRS04	pRS02 derivative, *ermE*p_npsM* cloned into EcoRV restriction site; $Apra^R$	Richard Sonnengruen
pRS07	pRS04 derivative, *ermE*p_npsK* cloned into PvuII restriction site; $Apra^R$	Richard Sonnengruen
pUB307	Conjugative plasmid, helper element to mobilize vectors in triparental conjugations; Kan^R	Flett *et al.* (1997)[124]
pUZ8002	Conjugative plasmid used in biparental conjugations; Kan^R	Paget *et al*. (1999)[125]
SuperCos1	Cosmid vector; $Carb^R$, Kan^R	Stratagene Inc., La Jolla, CA, USA

2.1.10 Buffers and Solutions

2.1.10.1 Solutions for DNA Isolation (plasmids and cosmids)

Unless stated otherwise, autoclaving was carried out for 20 min at 121 °C at a pressure of 2 bar.

Solution I

Glucose	50 mM
EDTA (pH = 8)	10 mM
Tris-HCl (pH = 8)	25 mM
ddH_2O	

The solution was autoclaved and stored at 4 °C. RNase A (1 µL/mL) was added before use.

Solution II

NaOH	0.2 M
SDS	1 %
ddH_2O	

The solution was not autoclaved but prepared directly before use and stored at room temperature.

Solution III

Potassium acetate	3 M
ddH_2O	

The pH was adjusted to 5.2 with glacial acetic acid. Then the solution was autoclaved, stored at 4 °C and put on ice before use.

Sodium Acetate Solution

Sodium acetate	3 M
ddH_2O	

The pH was adjusted to 5.2 with acetic acid. The solution was autoclaved and stored at room temperature.

Lithium Chloride Solution

Lithium chloride	4 M
ddH_2O	

The solution was autoclaved and stored at room temperature.

2.1.10.2 Buffers and Solutions for Agarose Gel Electrophoresis

50x TAE-Buffer

Tris base	2 M
Na_2-EDTA	0.05 M
Glacial acetic acid	1 M

The pH was adjusted to 8. The solution was autoclaved and stored at room temperature. Before use, the buffer was diluted to its working concentration (1x).

6x Loading Buffer

Bromophenol blue	30 mg
Xylene cyanol	30 mg
Glycerol 98 %	60 mL
50x TAE – buffer	500 µL
ddH_2O	ad 100 mL

The buffer was stored at 4 °C.

GeneRuler 1 kb

DNA ladder	100 µL
6x loading buffer	100 µL
ddH_2O	400 µL

The solution was stored at 4 °C.

PeqGREEN (DNA dye)

A 1:50 dilution of the 20.000x stock solution was prepared with ddH_2O. The solution was stored at 4 °C, protected from light. PeqGREEN was added to prepared agarose solutions to a concentration of 1 µL/1 mL.

2.1.10.3 Solutions for Blue/White Selection of *E. coli*

IPTG Stock Solution

IPTG	0.5 M
ddH_2O	

The solution was sterilized by filtration (0.2 µm pore size) and stored at - 20 °C.

X-Gal Stock Solution

X-Gal	0.24 M
DMSO	

The solution was stored under light protection at - 20 °C.

2.1.10.4 Further Solutions

Magnesium Chloride Solution

Magnesium chloride hexahydrate	1 M
ddH_2O	

The solution was autoclaved and stored at room temperature.

L-Arabinose

L-Arabinose	1 M
ddH_2O	

The solution was sterilized by filtration (0.2 µm pore size) and stored at 4 °C.

2.1.11 Culture Media

All media were prepared by published procedures and autoclaved directly after preparation (unless stated otherwise: 121 °C, 2 bar, 20 min). If necessary for selection purposes, the appropriate antibiotics were added to solid media after their cooling to around 50 °C and to liquid cultures prior to inoculation.

2.1.11.1 Media for Cultivation of *Escherichia coli*

LB Medium (Luria Bertani; Sambrook and Russell)[126]

Tryptone	10.0 g
Yeast extract	5.0 g
NaCl	10.0 g
NaOH	ad pH = 7
ddH_2O	ad 1 L

LB Agar

Identical to LB Medium with an additional 2 g of agar per 100 mL medium.

SOB (SOC) Medium (Super Optimal Broth; Sambrook and Russell)[126]

Tryptone	20 g
Yeast extract	5 g
NaCl	0.5 g
KCl	0.186 g
NaOH	ad pH = 7
ddH_2O	ad 1 L

Prior to inoculation, 20 mM $MgCl_2$ were added.

For the preparation of SOC medium, 20 mM glucose was added.

2.1.11.2 Media for Cultivation of *Streptomyces*

MS (Mannitol Soya Flour) Agar (Kieser *et al.*)[127]

Mannitol	20.0 g
Soya flour	20.0 g
Agar	20.0 g
Tap water	1 L

Mannitol was dissolved in 1 L tap water and 100 mL aliquots were poured into 300 mL flasks. Subsequently, 2 g soy flour and 2 g agar were added per flask. The mixture was autoclaved twice (115 °C, 2 bar, 15 min) with gentle interim shaking.

2xYT Medium (Yeast Extract Tryptone; Kieser *et al.*)[127]

Tryptone	16 g
Yeast extract	10 g
NaCl	5 g
ddH_2O	ad 1 L

TSB (Tryptone Soya Broth) Medium (Kieser *et al.*)[127]

Tryptone soya broth	30.0 g
ddH_2O	1 L

P - Medium (Production-Medium) (Fronko *et al.*)[128]

The medium was prepared fresh in order to avoid starch precipitation at room temperature.

Soytone	20.0 g
Soluble starch	20.0 g
D-Maltose	20.0 g
1xTrace element sol.	5 mL
ddH_2O	ad 1 L

Adjusted to pH 6.7, sterilized by autoclaving.

Trace element solution (sterilized by filtration, kept at 4°C):

$ZnCl_2$	40 mg
$FeCl_3 \cdot 6\ H_2O$	200 mg
$CuCl_2 \cdot 2\ H_2O$	10 mg
$MnCl_2 \cdot 4\ H_2O$	10 mg
$Na_2B_4O_7 \cdot 10\ H_2O$	10 mg
$(NH_4)_6Mo_7O_{24} \cdot 4\ H_2O$	10 mg
ddH_2O	ad 1 L

The soluble starch was dissolved in approximately half the water volume under heating and constant stirring. After the solution was cooled to room temperature, the remaining components were added. Subsequently, the pH was adjusted to 6.7 and the medium was autoclaved.

2.1.12 Bacterial Strains

2.1.12.1 *Escherichia coli* strains

Table 12: *E. coli* strains

Organism	Strain	Description	Reference	Application
E. coli	BT340	*E. coli* DH5α/pCP20	Cherepanov & Wakernagel, 1995[129]	Site-specific recombination by Flp recombinase
E. coli	BW25113	Δ*(araD-araB)567*, Δ*(rhaD-rhaB)568*, Δ*lacZ4787(::rrnB-3)*, *hsdR514, rph-1*	Datsenko and Wanner, 2000[130]	λ-RED recombination

Organism	Strain	Description	Reference	Application
E. coli	DH10β	*F'mcrAΔ-(mrr hsdRMS-mcrBC), φ80dlacZΔM15, ΔlacX74, deoR, recA1, araD139,* Δ *(ara, leu)7697, galUgalKλ⁻rpsL, end, A1, nupG*	Stratagene Inc., La Jolla, CA, USA	Cloning strain for large constructs
E. coli	DH5α	*huA2, lacΔU169, phoA, glnV44,* Φ *80', lacZΔM15, gyrA96, recA1, relA1, endA1, thi-1, hsdR17*	Stratagene Inc., La Jolla, CA, USA	Cloning strain
E. coli	ET12567	*dam-13::Tn9, dcm-6, hsdM, hsdR, recF14 zjj201::Tn10 galK2, gal T22, ara14, lacY1, xyl5, leuB6, thi1, tonA31, rpsL136, hisG4, tsx78, mtli, glnV44*; Cml^R	MacNeil *et al.*, 1992[131]	Intergenic conjugation
E. coli	XL1 - Blue	*recA1, endA1, gyrA96 (nal^r), thi-1, hsdR17($r_k^-m_k^+$), supE44, relA1, lac [F´, proAB$^+$, lacI^{q}ZΔM15, Tn10, (Tet^r)]*	Stratagene Inc., La Jolla, CA, USA	Cloning strain

2.1.12.2 *Streptomyces* strains

Table 13: *Streptomyces* strains

Organism	Strain	Description	Reference
Streptomyces albus	J1074	WT, Heterologous host (HH)	Chater and Wilde (1976)[132]
Streptomyces sp.	DSM5940	WT, Napsamycin producer strain	Kaysser *et al*. (2011)[14]
Streptomyces albus	Del14	Derivative of *S. albus* J1074 with deletion of 15 biosynthetic gene clusters	Myronovskyi *et al.* (2018)[133]
Streptomyces albus	B2P1	Derivative of Del14 with one additional *attB* site	Myronovskyi *et al.* (2018)[133]
Streptomyces griseus	CS065	WT, Heterologous host (HH)	Malmierca *et al.* (2018)[134]
Streptomyces albus	J1074/pacRS01	HH strain with modified pacidamycin gene cluster pacRS01	Richard Sonnengruen
Streptomyces albus	J1074/pRS02/pacRS01	HH strain with modified pacidamycin gene cluster pacRS01 and integrative plasmid pRS02	Richard Sonnengruen
Streptomyces albus	J1074/pRS04/pacRS01	HH strain with modified pacidamycin gene cluster pacRS01 and integrative plasmid pRS04	Richard Sonnengruen

Organism	Strain	Description	Reference
Streptomyces albus	J1074/pacHK01	HH strain with modified pacidamycin gene cluster pacHK01	Present work
Streptomyces albus	J1074/pRS02/pacHK01	HH strain with modified pacidamycin gene cluster pacHK01 and integrative plasmid pRS02	Present work
Streptomyces albus	J1074/pRS04/pacHK01	HH strain with modified pacidamycin gene cluster pacHK01 and integrative plasmid pRS04	Present work
Streptomyces albus	J1074/pacHK02	HH strain with modified pacidamycin gene cluster pacHK02	Present work
Streptomyces albus	J1074/pRS02/pacHK02	HH strain with modified pacidamycin gene cluster pacHK02 and integrative plasmid pRS02	Present work
Streptomyces albus	J1074/pRS04/pacHK02	HH strain with modified pacidamycin gene cluster pacHK02 and integrative plasmid pRS04	Present work
Streptomyces albus	J1074/pacHK03	HH strain with modified pacidamycin gene cluster pacHK03	Present work
Streptomyces albus	J1074/pRS02/pacHK03	HH strain with modified pacidamycin gene cluster pacHK03 and integrative plasmid pRS02	Present work
Streptomyces albus	J1074/pRS04/pacHK03	HH strain with modified pacidamycin gene cluster pacHK03 and integrative plasmid pRS04	Present work
Streptomyces albus	J1074/pacHK04	HH strain with modified pacidamycin gene cluster pacHK04	Present work
Streptomyces albus	J1074/pRS02/pacHK04	HH strain with modified pacidamycin gene cluster pacHK04 and integrative plasmid pRS02	Present work
Streptomyces albus	J1074/pRS04/pacHK04	HH strain with modified pacidamycin gene cluster pacHK04 and integrative plasmid pRS04	Present work
Streptomyces albus	J1074/pacHK05	HH strain with modified pacidamycin gene cluster pacHK05	Present work

Organism	Strain	Description	Reference
Streptomyces albus	J1074/pRS02/pacHK05	HH strain with modified pacidamycin gene cluster pacHK05 and integrative plasmid pRS02	Present work
Streptomyces albus	J1074/pRS04/pacHK05	HH strain with modified pacidamycin gene cluster pacHK05 and integrative plasmid pRS04	Present work
Streptomyces albus	J1074/pRS02/pacHK08	HH strain with modified pacidamycin gene cluster pacHK08 and integrative plasmid pRS02	Present work
Streptomyces albus	J1074/pRS04/pacHK08	HH strain with modified pacidamycin gene cluster pacHK08 and integrative plasmid pRS04	Present work
Streptomyces albus	Del14/pacRS01	HH strain with modified pacidamycin gene cluster pacRS01	Richard Sonnengruen
Streptomyces albus	Del14/pacHK03	HH strain with modified pacidamycin gene cluster pacHK03	Present work
Streptomyces albus	Del14/pacHK08	HH strain with modified pacidamycin gene cluster pacHK08	Present work
Streptomyces albus	B2P1/pacRS01	HH strain with modified pacidamycin gene cluster pacRS01	Richard Sonnengruen
Streptomyces albus	B2P1/pacHK03	HH strain with modified pacidamycin gene cluster pacHK03	Present work
Streptomyces albus	B2P1/pacHK08	HH strain with modified pacidamycin gene cluster pacHK08	Present work
Streptomyces albus	J1074/pacHK06	HH strain with modified pacidamycin gene cluster pacHK06	Present work
Streptomyces albus	J1074/pRS02/pacRS03	HH strain with modified pacidamycin gene cluster pacRS03 and integrative plasmid pRS02	Richard Sonnengruen
Streptomyces albus	J1074/pRS04/pacRS03	HH strain with modified pacidamycin gene cluster pacRS03 and integrative plasmid pRS04	Richard Sonnengruen
Streptomyces albus	J1074/pRS02/pacHK11	HH strain with modified pacidamycin gene cluster pacHK11 and integrative plasmid pRS02	Present work

Organism	Strain	Description	Reference
Streptomyces albus	J1074/pRS04/pacHK11	HH strain with modified pacidamycin gene cluster pacHK11 and integrative plasmid pRS04	Present work
Streptomyces albus	Del14/pRS02/pacHK03	HH strain with modified pacidamycin gene cluster pacHK03 and integrative plasmid pRS02	Present work
Streptomyces albus	Del14/pRS04/pacHK03	HH strain with modified pacidamycin gene cluster pacHK03 and integrative plasmid pRS04	Present work
Streptomyces albus	B2P1/pRS02/pacHK03	HH strain with modified pacidamycin gene cluster pacHK03 and integrative plasmid pRS02	Present work
Streptomyces albus	B2P1/pRS04/pacHK03	HH strain with modified pacidamycin gene cluster pacHK03 and integrative plasmid pRS04	Present work
Streptomyces albus	J1074/pRS02/pacHK12	HH strain with modified pacidamycin gene cluster pacHK12 and integrative plasmid pRS02	Present work
Streptomyces albus	J1074/pRS04/pacHK12	HH strain with modified pacidamycin gene cluster pacHK12 and integrative plasmid pRS04	Present work
Streptomyces albus	J1074/pRS02/pacHK09	HH strain with modified pacidamycin gene cluster pacHK09 and integrative plasmid pRS02	Present work
Streptomyces albus	J1074/pRS04/pacHK09	HH strain with modified pacidamycin gene cluster pacHK09 and integrative plasmid pRS04	Present work
Streptomyces albus	J1074/pRS02/pacHK10	HH strain with modified pacidamycin gene cluster pacHK10 and integrative plasmid pRS02	Present work
Streptomyces albus	J1074/pRS04/pacHK10	HH strain with modified pacidamycin gene cluster pacHK10 and integrative plasmid pRS04	Present work
Streptomyces griseus	CS065/pacHK03	HH strain with modified pacidamycin gene cluster pacHK03	Present work

Organism	Strain	Description	Reference
Streptomyces albus	B2P1/pRS04/pacHK11	HH strain with modified pacidamycin gene cluster pacHK11 and integrative plasmid pRS04	Present work
Streptomyces albus	Del14/pRS04/pacHK11	HH strain with modified pacidamycin gene cluster pacHK11 and integrative plasmid pRS04	Present work
Streptomyces griseus	CS065/pRS04/pacHK11	HH strain with modified pacidamycin gene cluster pacHK11 and integrative plasmid pRS04	Present work
Streptomyces albus	J1074/npsXT01	HH strain with napsamycin gene cluster npsXT01	Nils Hauck
Streptomyces albus	J1074/npsPK01	HH strain with modified napsamycin gene cluster npsPK01	Present work - Philipp Konrad
Streptomyces albus	J1074/pRS02/npsPK01	HH strain with modified napsamycin gene cluster npsPK01 and integrative plasmid pRS02	Present work - Philipp Konrad
Streptomyces albus	J1074/pRS04/npsPK01	HH strain with modified napsamycin gene cluster npsPK01 and integrative plasmid pRS04	Present work - Philipp Konrad
Streptomyces albus	J1074/npsPK02	HH strain with modified napsamycin gene cluster npsPK02	Present work - Philipp Konrad
Streptomyces albus	J1074/pRS02/npsPK02	HH strain with modified napsamycin gene cluster npsPK02 and integrative plasmid pRS02	Present work - Philipp Konrad
Streptomyces albus	J1074/pRS04/npsPK02	HH strain with modified napsamycin gene cluster npsPK02 and integrative plasmid pRS04	Present work - Philipp Konrad
Streptomyces albus	J1074/npsPK03	HH strain with modified napsamycin gene cluster npsPK03	Present work - Philipp Konrad
Streptomyces albus	J1074/pRS02/npsPK03	HH strain with modified napsamycin gene cluster npsPK03 and integrative plasmid pRS02	Present work - Philipp Konrad
Streptomyces albus	J1074/pRS04/npsPK03	HH strain with modified napsamycin gene cluster npsPK03 and integrative plasmid pRS04	Present work - Philipp Konrad

Organism	Strain	Description	Reference
Streptomyces albus	J1074/npsHK01	HH strain with modified napsamycin gene cluster npsHK01	Present work
Streptomyces albus	J1074/npsHK02	HH strain with modified napsamycin gene cluster npsHK02	Present work
Streptomyces albus	Del14/npsHK02	HH strain with modified napsamycin gene cluster npsHK02	Present work
Streptomyces albus	Del14/pRS04/pacRS03	HH strain with modified pacidamycin gene cluster pacRS03 and integrative plasmid pRS04	Richard Sonnengruen
Streptomyces albus	Del14/pRS07/pacRS03	HH strain with modified pacidamycin gene cluster pacRS03 and integrative plasmid pRS07	Richard Sonnengruen
Streptomyces albus	Del14/pRS07/pacHK11	HH strain with modified pacidamycin gene cluster pacHK11 and integrative plasmid pRS07	Present work
Streptomyces griseus	CS065/pRS07/pacHK11	HH strain with modified pacidamycin gene cluster pacHK11 and integrative plasmid pRS07	Present work
Streptomyces albus	J1074/npsHK03	HH strain with modified napsamycin gene cluster npsHK03	Present work
Streptomyces albus	Del14/npsHK03	HH strain with modified napsamycin gene cluster npsHK03	Present work
Streptomyces albus	J1074/pRS04/pacHK13	HH strain with modified pacidamycin gene cluster pacHK13 and integrative plasmid pRS04	Present work
Streptomyces albus	Del14/pRS04/pacHK13	HH strain with modified pacidamycin gene cluster pacHK13 and integrative plasmid pRS04	Present work
Streptomyces albus	J1074/pRS04/pacHK14	HH strain with modified pacidamycin gene cluster pacHK14 and integrative plasmid pRS04	Present work
Streptomyces albus	Del14/pRS04/pacHK14	HH strain with modified pacidamycin gene cluster pacHK14 and integrative plasmid pRS04	Present work

Organism	Strain	Description	Reference
Streptomyces albus	J1074/npsHK04	HH strain with modified napsamycin gene cluster npsHK04	Present work
Streptomyces albus	Del14/npsHK04	HH strain with modified napsamycin gene cluster npsHK04	Present work

The plasmids pRS02, pRS04 and pRS07 were integrated into the ϕBT1 *attB* site, while all cosmids were integrated into the ϕC31 *attB* site(s) of the heterologous hosts.

2.1.13 Software

Table 14: Software used in this study

Name	Specification	Manufacturer
Artemis	16.0.0	Wellcome Sanger Institute, Hinxton, UK
ChemDraw Professional	Version 22.2.0	PerkinElmer, Waltham, MA, USA
Clone Manager	Clone Manager Professional Suite Version 8	Sci Ed Software, Westminster, CO, USA
DataAnalysis	6300 Series Ion Trap LC/MS Software Version 6.1	Agilent Technologies, Santa Clara, CA, USA
Integrated Genome Browser	9.1.10	Affymetrix, Santa Clara, CA, USA
ImageJ	1.46r, Java 1.8.0.112 (32-bit)	National Institutes of Health, Bethesda, Maryland, USA
SeqMan Pro	Lasergene 7, Version: 7.1.0 (44.1)	DNA STAR, Madison, WI, USA

2.2 Methods

2.2.1 Methods of molecular biology

2.2.1.1 Isolation of cosmid/plasmid DNA of *E. coli*

Plasmids and cosmids were isolated from *E. coli* strains by alkaline lysis. The stated amounts apply for a minipreparation, while the amounts given in brackets were used for a maxipreparation. Firstly, the cells contained in 1.5 mL (50 mL) of an overnight liquid culture were harvested by centrifugation at 13300 rpm for 3 minutes at room temperature. The supernatant was discarded, and the cell pellet resuspended in 100 µL (5 mL) Solution I, supplemented with RNase. Then, 200 µL (10 mL) of Solution II was added and the contents were mixed thoroughly by inverting the vessel several times. Subsequently, 150 µL (7.5 mL) ice-cold Solution III was added and mixed again by gently inverting the vessel. The suspension was centrifuged at 13300 rpm (4000 rpm) for 5 minutes (10 min) at 4 °C in order to separate the white precipitate, containing proteins, cell wall components and chromosomal DNA, from the supernatant, containing the plasmids. The supernatant was transferred to fresh Eppendorf tubes, where it was either purified by phenol/chloroform extraction (2.2.1.2) or precipitated (2.2.1.3).

2.2.1.2 Purification/Extraction of DNA with phenol/chloroform/isoamyl alcohol

The DNA solution to be purified was transferred into a 2 mL Eppendorf tube with safety lock and an equal volume of phenol/chloroform/isoamyl alcohol (25:24:1, *v/v*) was added. The tubes were vortexed thoroughly for 30 seconds and afterwards centrifuged at 13300 rpm for 15 minutes at 4 °C. Thus, phase separation was accomplished. While the organic phase is enriched with proteins, the aqueous upper layer, containing the plasmids or cosmids, was transferred into a fresh vessel without disturbing the interphase. Subsequently, the DNA was precipitated (2.2.1.3).

2.2.1.3 Precipitation of DNA

The precipitation of DNA with alcohol was used to both concentrate and purify the DNA by removing salts and other substances with low molecular weight, which remain in the supernatant. For this purpose, one-tenth volume of sodium acetate and one volume of isopropanol were added to one volume of DNA solution. The contents were mixed thoroughly by inverting the tube and afterwards incubated on ice for 10 minutes. The mixture was centrifuged at 13300 rpm for 30 minutes at 4 °C and the supernatant discarded. The resulting pellet was washed with 500 µL ethanol (70 % *v/v*) by centrifugation at 13300 rpm for 10 minutes at 4 °C. The supernatant was removed carefully and

completely with a pipette and the pellet dried at room temperature. Lastly, the DNA pellet was dissolved in 30 - 50 µL ddH_2O, depending on its size. The DNA solution was stored at - 20 °C.
Whenever a high-efficiency DNA precipitation was deemed necessary, an optimized version of the aforementioned method was implemented. This consisted of the substitution of the sodium acetate solution with a lithium chloride solution, the use of 2.5 volumes of 100 % ethanol instead of isopropanol and an incubation of 20 minutes at - 80 °C instead of 10 minutes on ice prior to centrifugation.

2.2.1.4 DNA restriction

Enzymatic digestion was conducted by restriction endonucleases, which recognize and cleave specific restriction sites in DNA, in order to excise specific DNA fragments from vectors, prepare vectors and inserts for ligation or perform an analytical digest to investigate whether the resulting fragments are correct. Typically, the reaction mixture for an analytical digestion was set to have a total volume of 20 µL, containing 0.5 - 1 µL restriction enzyme, 2 µL of the corresponding 10x reaction buffer, 2 - 10 µL DNA and ddH_2O. DNA and restriction enzyme concentrations were adjusted each time, knowing that 1 U of enzyme digests 1 µg of DNA per hour. For preparative digestions, multiple 20 µL - digestions were pooled after incubation, or the total volume increased to 50 µL and the components' concentrations increased accordingly. For each enzyme, ideal restriction conditions as specified by the manufacturer were implemented, while analytical restrictions were typically incubated for one hour at 37 °C and 300 rpm and preparative ones for two hours at 37 °C and 300 rpm. If deemed necessary, the reaction mixture was subsequently heat inactivated for 10 - 20 minutes at the temperature specified by the enzyme manufacturer.

2.2.1.5 DNA ligation

DNA ligation was conducted by T4 DNA ligase, which catalyzes the formation of a phosphodiester bond between 5'-phosphate and 3'-hydroxyl termini in DNA molecules. The total volume of reaction mixtures was chosen to be 10 µL, consisting of 1 µL T4 DNA ligase, 1 µL T4 DNA ligase buffer, the DNA fragments to be ligated and ddH_2O and was incubated at 4 °C overnight. The ligation of an insert and a vector was set to feature the respective DNA fragments at a 3:1 ratio. When deemed necessary, dephosphorylation of vectors was performed in order to prevent re-circularization during ligation. In this case, the digested vector was mixed with 2 µL CutSmart buffer, 1 µL rSAP (Shrimp Alkaline Phosphatase) and ddH_2O to a total reaction volume of 20 µL and incubated for 1 h at 37 °C and

300 rpm. The reaction mixture was purified with a spin column-based purification kit (2.2.1.8) and then ligated overnight, as stated above.

2.2.1.6 Agarose gel electrophoresis

2.2.1.6.1 Analytical gel electrophoresis

Analytical gel electrophoresis was performed for the separation of DNA fragments in order to determine their size and examine whether the correct fragments were present in a mixture. Agarose gels were prepared by dissolving 1 % (*w/v*) agarose in 1x TAE buffer under constant heating until a clear solution was obtained. After the solution was cooled down to room temperature, 1 µL/mL peqGREEN could be added. Then the solution was poured into the tray of a gel chamber, a comb was added, small bubbles were removed with a pipette tip and the gel was left to cool down and polymerize completely. Subsequently, the comb was removed, and the gel was placed into the chamber, which contained 1x TAE - buffer. The DNA samples were mixed with loading dye to a ratio of 6:1 and then loaded into the gel wells. Typically, the entire 20 µL of a DNA restriction was loaded into one pocket, while only 10 µL of a PCR reaction was used. As a reference for the determination of size and concentration of the DNA fragments, 6 µL (corresponding to 500 ng DNA) of the GeneRuler 1 kb DNA Ladder was loaded into the two outer pockets next to the DNA samples. Afterwards, the gel was run at a constant voltage of 100 - 120 V for 1 - 2 hours. The DNA banding pattern was visualized with a gel documentation system under UV_{213nm} - light.

2.2.1.6.2 Preparative gel electrophoresis

Preparative gel electrophoresis was performed in order to isolate specific DNA fragments after their separation from other ones. The gel was prepared identically to an analytical gel, but for this purpose, combs forming bigger pockets were used, their separate wells were joined by adhesive tape and, thus, larger sample volumes loaded into them. Furthermore, exposure to UV - light was kept to a minimum (70 % of the usual intensity), while the desired bands were excised from the gel with a scalpel. Subsequently, the gel fragments were purified with a spin column-based purification kit (2.2.1.8) and thus the DNA fragments were isolated.

2.2.1.7 Polymerase chain reaction (PCR)

DNA amplification was performed by PCR in appropriate reaction tubes, which were filled with 50 µL aliquots of PCR reactions. Reaction mixtures were assembled on ice in accordance with the pipetting schemes described below, placed into a thermocycler and the respective program was run, depending on the polymerase. The annealing temperature was determined through a Gradient-PCR, where annealing temperatures of 50 - 70 °C were tested for specific primer pairs. Elongation time was set under consideration of the expected product length, knowing that Taq polymerase, on average, synthesizes 1 kb of DNA per minute. Afterwards, successful amplification of the DNA fragments was examined by analytical gel electrophoresis (2.2.1.6) and comparison of the fragment size with a positive control, while false positives were excluded by a negative control.

A) Amplification of DNA by Taq/Pfu - polymerase

For standard DNA amplification, a Taq:Pfu (9:1) polymerase mixture was used in a reaction comprised of the components stated in Table 15. In this case, the PCR program of Table 16 was implemented.

Table 15**:** Composition of Taq/Pfu PCR reactions

Component	**Volume (µL)**
DNA Template	1
FW - Primer (10 µM)	1
RV - Primer (10 µM)	1
10x Taq-polymerase-buffer	5
Taq:Pfu polymerase (9:1)	1
dNTPs (2.5mM each)	4
DMSO	5
ddH_2O	32
Total	**50**

Table 16**:** Temperature program for Taq/Pfu PCR reactions

Phase	**Temperature (°C)**	**Duration (sec)**	**Cycles**
Denaturing	94	300	1
Denaturing	94	45	
Annealing	X = 50 - 70	45	25
Elongation	72	Y = 30 - 120	
Terminal elongation	72	600	1
Storage	4	∞	

B) Amplification of DNA by Q5 - polymerase

DNA amplifications, which were impeded due to high GC content or the possibility of forming secondary structures, were performed by the Q5 High-Fidelity DNA polymerase in accordance with the pipetting scheme of Table 17 and the program depicted in Table 18.

Table 17**:** Composition of Q5 PCR reactions

Component	**Volume (µL)**
DNA Template	2
FW - Primer (10 µM)	1
RV - Primer (10 µM)	1
5x Q5 Reaction Buffer	10
5x Q5 High GC Enhancer	10
Q5 High-Fidelity DNA Polymerase	0.5
dNTPs (2.5 mM each)	4
ddH_2O	21.5
Total	**50**

Table 18**:** Temperature program for Q5 PCR reactions

Phase	**Temperature (°C)**	**Duration (sec)**	**Cycles**
Denaturing	98	30	1
Denaturing	98	10	
Annealing	X = 50 - 70	30	30
Elongation	72	Y = 30 - 120	
Terminal elongation	72	120	1
Storage	4	∞	

C) Colony PCR of *E. coli*

Colony PCR was utilized as a method of high - throughput screening of *E. coli* mutant strains for colonies harboring plasmids or cosmids with specific modifications, for example subsequent to a cloning experiment. This was accomplished by picking single colonies with sterile toothpicks and resuspending them as PCR templates in standard PCR reactions, as described above. Thereafter, colony residues on the toothpick were plated onto LB agar containing the appropriate antibiotics to preserve the mutant

strains. In order to ensure cell lysis, the initial denaturation phase of the PCR program had to be prolonged to 10 min, while the remaining program was conducted unaltered (2.2.1.7 A).

D) PCR - mediated verification of *Streptomyces* exconjugants

In order to examine whether conjugations were successful and the desired cosmids were transferred into a heterologous host and integrated into their genome, PCR-mediated verification of the mutant strains was conducted. For this purpose, 10 µL of each spore suspension was inoculated into 4 mL LB medium without antibiotics and incubated for 2 - 3 days at 30 °C and 220 rpm. After the incubation, a potential *E. coli* contamination could be ruled out, when the supernatant was clear and only *Streptomyces* mycelia growth was observed. The suspension was vortexed thoroughly in order to distribute the mycelia evenly throughout the medium and afterwards 1.5 mL of the suspension was transferred into an Eppendorf tube and centrifuged at 13.000 rpm for 3 min at room temperature. Subsequently, the supernatant was discarded, and the pellet resuspended as evenly as possible in 50 µL DMSO. Then, the mixture was incubated for 10 min at 95 °C and 300 rpm, vortexed and centrifuged briefly. The resulting supernatant was utilized as PCR template in a typical Taq-polymerase PCR reaction (2.2.1.7 A).

2.2.1.8 Spin column - based DNA purification

Spin column - based DNA purification was implemented after a DNA restriction, ligation or PCR to purify the DNA fragments, plasmids or PCR products, after a preparative gel electrophoresis to extract the DNA fragments from the agarose gel or to purify DNA prior to sequencing. For this purpose, a gel extraction or DNA purification kit, containing spin columns and the required buffers was used. The DNA solution was mixed with 5 volumes of binding buffer PB and a maximal amount of 750 µL was added on the column. The column was then centrifuged at 13000 rpm for 1 min at room temperature. This process was repeated until the entire DNA sample was bound to the column. In the case of a gel extraction, the mixture of agarose slice and buffer was incubated at 50 °C for 10 min prior to the loading of the column. The flow-through was discarded and 750 µL wash buffer PE was added to the column, which was then centrifuged twice for 1 min under the same conditions. After each step, the flow-through was discarded. Subsequently, the column was placed in an Eppendorf tube and the sample was eluted with 10 - 50 µL ddH_2O, depending on the desired DNA concentration. After the addition of ddH_2O, the vessel was incubated for 3 min at 50 °C to improve the DNA yield, if deemed necessary, and then centrifuged for 1 min. The elution process was then repeated into a second Eppendorf tube. The DNA samples were stored at - 20 °C.

2.2.1.9 DNA sequencing

DNA sequencing was performed to verify modified DNA sequences in plasmids or cosmids. For this purpose, a mixture of 5 µL DNA sample, consisting of plasmid/cosmid DNA or purified PCR product, 2 µL primer (5 pmol/µL) and 10 µL ddH_2O was sent to the company "Eurofins Genomics GmbH" (Ebersberg, Germany), where the sample was sequenced using the chain-terminating Sanger method. DNA concentration was adjusted to fulfill the set requirements of 60 - 250 ng/µL for plasmid DNA, 250 - 500 ng/µL for cosmid DNA or 20 - 40 ng/µL for purified PCR products. The obtained sequences were analyzed with the SeqMan software by Lasergene.

2.2.1.10 λRed/ET- mediated homologous recombination

Promoter knock-ins and gene knockouts were conducted through λRed/ET- mediated homologous recombination, which is a method described by Gust *et al.* (2003)[122]. This strategy allows for the replacement of specific DNA sequences on plasmids and cosmids through the recombination with linear DNA fragments in the targeted strain, which is facilitated by the λ-Red proteins encoded on pIJ790. The linear DNA fragments in question contain selection markers and are generated by PCR, where 39 nucleotide long overhangs are added to the disruption cassette through each long PCR primer. These constitute homology arms to the sequences flanking the DNA region intended to be replaced.

The PCR for extension and amplification of resistance or bidirectional promoter cassettes was conducted as described in 2.2.1.7.A, regarding the pipetting scheme, while the temperature program of Table 19 was implemented.

Table 19**:** Temperature program for PCR-targeting

Phase	**Temperature (°C)**	**Duration (sec)**	**Cycles**
Denaturing	94	300	1
Denaturing	94	45	
Annealing	50	45	10
Elongation	72	90	
Denaturing	94	45	
Annealing	55	45	15
Elongation	72	90	
Terminal elongation	72	300	1
Storage	4	∞	

The length of PCR products was verified by analytical agarose gel electrophoresis (2.2.1.6.1) and successful reactions were then purified as described in 2.2.1.8.

Single colonies of *E. coli* BW25113/pIJ790/cosmid was inoculated into 5 mL LB medium containing Cml/Kan and incubated at 30 °C, 200 rpm overnight. The next day, 200 µL overnight culture was inoculated into 10 mL SOB medium containing 10 µL Cml, 10 µL Kan and 100 µL L-arabinose (1 M) and incubated at 30 °C, 200 rpm until the cultures reached an OD_{600} of 0.4 - 0.6. Maintaining the temperature at 30 °C was crucial due to the temperature-sensitive origin of replication of plasmid pIJ790, while L-arabinose was added to induce the *red* genes. Subsequently the cells were harvested by centrifugation at 4000 rpm for 5 minutes at 4 °C. While the supernatant was discarded, the cell pellets were resuspended in 10 mL ice - cold glycerol 10 % and harvested once again by centrifugation under the same conditions. The washing process was repeated with 5 mL ice - cold glycerol 10 %, the supernatant discarded, and the cell pellet resuspended in the residual glycerol (ca. 100 µL). A 50 µL cell aliquot was electroporated with 2 - 4 µL (ca. 100 ng) of PCR product, as described in 2.2.2.2. Immediately after electroporation, 500 µL SOC medium was added to the cells and mixed thoroughly, before transferring the suspension into a fresh Eppendorf tube and incubating at 37 °C and 300 rpm for 1 hour. For selection, the cell suspension was plated on LB agar containing the appropriate antibiotics (typically Kan/Apra) and incubated at 37 °C overnight. The following day, single colonies were investigated regarding the recombination, by minipreparation and restriction digest (after overnight incubation, 2.2.1.1 and 4) or colony-PCR (2.2.1.7.C).

2.2.1.11 Golden Gate Assembly

Golden Gate Assembly, as described by Engler *et al.* (2008)[135], was used to construct promoter cassettes 3 and 4. This constitutes a cloning technique that utilizes type IIS restriction enzymes, which cleave DNA at a defined distance to their non-palindromic, asymmetric recognition sites and, thus, form unique 4-base-pair overhangs. This allows for seamless and efficient cloning, since enzyme recognition sites are eliminated, and the fragments can be assembled only in the desired sequence and direction. Simultaneously, T4 DNA ligase and a Golden Gate destination vector are included in the reaction kit. The former joins the overhangs subsequent to their annealing with neighboring fragments, while the latter harbors a multiple cloning site, which is cleaved in order to receive the assembling DNA fragment. Since enzyme recognition sites are removed during the process, continuous restriction-ligation cycles are conducted.

DNA fragments to be assembled comprised a total volume of 15 µL (2:1 molar ratio of insert: vector), and were mixed with 1 µL pGGA Destination Plasmid, 2 µL T4 DNA Ligase Buffer and 2 µL NEB Golden

Gate Enzyme Mix. The mixture was incubated in a thermocycler overnight, according to the program depicted in Table 20.

Table 20: Thermocycling program GGA

Temperature (°C)	Duration (min)	Cycles
37	5	30
16	5	
6	5	1
4	∞	

The reaction mixtures were directly introduced into chemically competent *E. coli* by heat shock transformation (2.2.2.3), which were then screened for positive colonies, in accordance with aforementioned methods.

2.2.1.12 Gibson Assembly

Gibson Assembly constitutes a standard cloning method, by which DNA fragments are combined through 20 - 30 bp of overlapping ends by three enzymes, which are present in the reaction. Firstly, a 5' exonuclease digests 5' end sequences, while revealing the complementary sequence for the annealing of overlapping segments. Gaps caused by the exonuclease, which neighbor annealing regions, are filled by a DNA polymerase, while a DNA ligase seals the remaining nicks between adjacent fragments. All the aforementioned processes are carried out in a single-tube isothermal reaction.
The linearized vector (typically pBluescript II SK (-)) and the inserts to be assembled composed a total of 10 µL of the reaction, mixed in equal concentration, which was supplemented with 10 µL of Gibson Assembly Master Mix or NEBuilder® HiFi DNA Assembly Master Mix. The reaction was incubated at 50 °C for 60 min, transformed by heat shock (2.2.2.3) and plated on LB agar, containing carbenicillin (in the case of pBluescript), IPTG and X - Gal for Blue-White-Screening of the resulting colonies.

2.2.1.13 Blue-White-Screening

For the simplified identification of positive colonies in cloning experiments, vectors harboring the gene *lacZ* for β-galactosidase (e.g., pBluescript II SK (-)) within their MCS were utilized. Successful cloning of a gene into the MCS constitutes a disruption of the *lacZ* gene, and, thus, β-galactosidase inactivation. This enzyme physiologically cleaves lactose into glucose and galactose and its analog X - Gal into a blue dye (5,5'-dibromo-4,4'-dichloro-indigo). Therefore, negative clones with an intact β-galactosidase

appear blue, while successful cloning and subsequent disruption of β-galactosidase activity leads to uncolored colonies, which can be analyzed further. The inductor IPTG is added to the agar since *lacZ* is controlled by an IPTG-inducible promoter.
After the respective cloning experiments, the plasmids to be analyzed were transformed into *E. coli* XL1-Blue (2.2.2.2) and plated on LB agar containing the appropriate antibiotic, 4 mM IPTG and 80 µg/mL X - Gal and incubated overnight at 37 °C.

2.2.1.14 FLP-mediated excision of resistance genes

The enzyme FLP recombinase allows for the site-specific recombination and deletion of DNA sequences, which was used in the present work for the removal of resistance cassettes. FLP recombinase recognizes FRT sites (FLP recombinase target), which also flank the apramycin resistance cassette on plasmid pIJ773, promotes recombination and, therefore, deletion of sequences in between. For the bidirectional promoter cassette PC1, which was based on pIJ773, and knockouts conducted with this cassette, FLP-mediated recombination was performed to remove resistance markers.
For this purpose, the cosmid to be recombined, which contained the FRT sites, was transformed into *E. coli* BT340, which harbors the genes for FLP recombination. The cells were incubated for 2 days at 30 °C on LB agar containing the appropriate antibiotics. Resulting colonies were carefully streaked for single colonies on LB agar without antibiotics and incubated overnight at 42 °C, to induce expression of the FLP recombinase. The obtained colonies were plated first onto LB agar containing Apra/Kan and then plates containing only Kan, to test for apramycin sensitivity. Colonies growing only on kanamycin plates were further investigated by restriction digests (2.2.1.4), PCR (2.2.1.7) and sequencing (2.2.1.9).

2.2.1.15 Cre-mediated excision of resistance genes

Similar to the previously described FLP recombinase, the enzyme Cre recombinase also catalyzes site-specific recombination events. Since these enzymes recognize distinct sites, Cre was utilized to perform recombination on constructs with loxP sites, which already harbored a FRT scar. Cre-loxP sites flank the apramycin resistance cassette on plasmid pIJ774, which was used for knockouts and as the template for bidirectional promoter cassettes PC2, PC3 and PC4. Therefore, the Cre-loxP system was utilized to remove resistance markers in related experiments.
For this purpose, the cosmid to be recombined was incubated at 37 °C for 30 min, in accordance with the pipetting scheme of Table 21. Subsequently, the reaction was heat inactivated at 70 °C for 10 min,

precipitated with LiCl (2.2.1.3), and transformed into *E. coli* DH10β. After incubation overnight at 37 °C, the colonies were tested regarding their apramycin sensitivity, as described in 2.2.1.14.

Table 21: Pipetting scheme Cre recombinase

Component	**Volume (µL)**
Cre recombinase	1
10x Cre recombinase reaction buffer	1
DNA	2 - 8
ddH_2O	0 - 6

2.2.2 Methods of horizontal gene transfer in bacteria

2.2.2.1 Preparation of electrocompetent cells

For the preparation of fresh electrocompetent *E. coli* cells, 100 mL LB medium containing the appropriate antibiotics was inoculated with 500 µL of an overnight culture of *E. coli* and incubated at 37 °C, 200 rpm until the cultures reached an OD_{600} of 0.4 to 0.6. Then, the culture was split into two pre-cooled 50 mL tubes and the cells were harvested by centrifugation at 4000 rpm for 5 min at 4 °C. While the supernatant was discarded, the cell pellets were resuspended in 25 mL ice - cold glycerol 10 % and harvested once again by centrifugation under the same conditions. The washing process was repeated and afterwards the supernatant discarded once again. The cell pellet was resuspended in the residual glycerol and aliquots of 50 µL stored at - 80 °C.

2.2.2.2 Transformation of *E. coli*

Electroporation involves the exposure of electrocompetent cells and plasmids, cosmids or DNA - fragments to a brief pulse of a high - voltage electric field, which causes cell pores to open and, thus, permits the DNA to enter the cells. One aliquot of electrocompetent cells was thawed on ice, mixed with 2 - 4 µL of the DNA sample to be transformed, and transferred into a clean, dry 2 mm electroporation cuvette that had previously been stored on ice. Electroporation was conducted in an electroporator set to EC2 with a pulse of 12.5 kV/cm and a desired time constant of 4 - 5 ms. Immediately after electroporation, 500 µL LB medium was added to the cells and mixed thoroughly before transferring the suspension into a fresh Eppendorf tube and incubating at 37 °C (or 30 °C for temperature-sensitive constructs) and 300 rpm for at least 1 hour. The cell suspension was plated on LB agar containing the appropriate antibiotics for selection and incubated at 37 °C (or 30 °C) overnight.

2.2.2.3 Heat shock transformation

Chemically competent *E. coli* NEB 10β cells (50 µL aliquots) with a partially developed cell wall were obtained from NEB and thawed on ice. Subsequently, 2 - 10 µL of the DNA sample to be transformed was added and distributed carefully in the cell suspension, which was then incubated on ice for 30 min. Afterwards, heat shock was conducted for 30 sec at 42 °C and followed by another incubation period of 5 min on ice. Warm 10β Stable Outgrowth Medium (500 µL) was added to the cells, which were then incubated at 37 °C, 300 rpm for at least 1 h. The cell suspension was plated on warm LB agar containing the appropriate antibiotics for selection and incubated at 37 °C overnight.

2.2.2.4 Intergenic conjugation of *E. coli* with *Streptomyces*

Triparental conjugation

Conjugation constitutes one of the three methods of horizontal gene transfer in bacteria and was utilized in this study in order to transfer cosmids and plasmids into *Streptomyces.* For cosmids conferring the same resistance as the helper plasmids (pUB307/pUZ8003, Kan^R), triparental conjugations were conducted. For this purpose, the cosmids in question were first transformed into the methylation deficient strain *E. coli* ET12567 by electroporation, according to published procedures. Furthermore, another *E. coli* ET12567 strain, which contained the self-transmissible helper plasmid pUB307, played a crucial role, since it contains the necessary *tra* genes for the activation of the *oriT* of the cosmids to be transferred.

Firstly, 20 µL glycerol stock *E. coli* ET12567/pUB307 and single colonies of *E. coli* ET12567/cosmid that had been obtained through electroporation (2.2.2.2) were inoculated each into 5 mL of LB medium containing the appropriate antibiotics (Cml/Kan) and incubated at 37 °C, 200 rpm overnight. The main cultures were prepared by inoculating 200 µL overnight culture into 10 mL LB medium containing the appropriate antibiotics (Cml/Kan) and incubating at 37 °C and 200 rpm until the cultures reached an OD_{600} of 0.4 to 0.6. Simultaneously, *Streptomyces* spores were prepared by inoculating 500 µL 2xYT medium with 20 µL spore stock, conducting a heat shock in order to activate germination at 50 °C for 10 min at 300 rpm and then incubating for 2 - 4 hours at 28 °C at 300 rpm.

Meanwhile, pre-cultures of *E. coli* ET12567/cosmid strains were verified by minipreparation, phenol/chloroform extraction, DNA precipitation and a subsequent enzymatic restriction analysis. Only a clone exhibiting the desired banding pattern and, thus, harboring the cosmid to be conjugated, was eventually conjugated.

Once the cells had reached the required OD_{600}, they were harvested by centrifugation at 4000 rpm for 5 min at 4 °C. While the supernatant was discarded, the cell pellets were resuspended in 10 mL

LB medium and harvested once again by centrifugation under the same conditions. The washing process was repeated with 10 mL LB medium and afterwards the supernatant discarded once again. The cell pellet was resuspended in 1 mL LB medium, and, subsequently, mixed with the heat-shocked spores. To each 500 µL *Streptomyces* aliquot, 250 µL *E. coli* ET12567/pUB307 and 250 µL *E. coli* ET12567/cosmid were added. The vessel containing the cells was inverted carefully a few times and centrifuged briefly (ca. 10 sec) at 7000 rpm. Afterwards, 800 µL of the supernatant was removed and the residue resuspended. The obtained cell suspension was carefully plated in a dilution series of 10^0, 10^{-1} and 10^{-3} on MS agar, containing 1 mL $MgCl_2$ (1 M). The necessary dilution was carried out with sterile ddH_2O. After 16 - 20 h of incubation at 30 °C, the plates were flooded completely with 1 mL of an antibiotic solution containing 25 µL Kan (50 mg/mL) and 25 µL Ndx (25 mg/mL) per plate. Then, incubation was continued for 4 - 8 days until exconjugants appeared. Four exconjugants were transferred as a serial dilution onto separate MS - $MgCl_2$ plates, containing the appropriate antibiotics (Kan/Ndx) and further incubated at 30 °C for 4 - 8 days. This process was repeated with the four separate exconjugants, picked from the first-generation plates and spread onto the second-generation of dilution plates. Lastly, all four exconjugants were plated confluent onto separate MS - $MgCl_2$ plates (Kan/Ndx), from where they were eventually harvested (2.2.3.3) and verified by colony PCR (2.2.1.7.D). When the plasmids pRS02 and pRS04 had previously been integrated into the respective strains, verification was conducted with the additional primers pRS02_TF1 and pRS02_TR1.

Biparental conjugation

For cosmids conferring a different resistance than the helper plasmids (Kan^R), biparental conjugations were conducted (e.g., for pRS02/04, $Apra^R$). In this case, the non-transmissible helper plasmid pUZ8002, which also harbors the *tra*-genes, was used to transfer genetic material. The plasmid to be conjugated was, therefore, transformed into electrocompetent *E. coli* ET12567/pUZ8002 and the remaining procedure conducted unaltered, except for the addition of apramycin to selection media and MS plates. Furthermore, instead of 250 µL of each *E. coli* strain, 500 µL of *E. coli* ET12567/pUZ8002/cosmid was added to the heat-shocked spores at conjugation.

2.2.3 Microbiological Methods

2.2.3.1 Growth conditions and maintenance of *E. coli* strains

Liquid cultures of *E. coli* were grown overnight in LB medium at 37 °C with the appropriate antibiotics for selection and aerated by shaking at 200 - 300 rpm depending on the culture size. Typically, 4 mL LB medium containing appropriate antibiotics was inoculated with a single colony stemming from an

LB plate, 10 - 20 µL of a glycerol stock or 10 - 100 µL of an overnight culture and cultivated at 300 rpm. In order to prepare electrocompetent cells or for a maxi - preparation, 100 mL of LB medium was inoculated.

Single *E. coli* colonies were grown overnight on LB agar plates at 37 °C with the appropriate antibiotics and stored at 4 °C. One exception consists of the strain *E. coli* BW25113/pIJ790, which was incubated at 30 °C prior to the homologous recombination, for which it was utilized.

For long-term storage, glycerol stocks of *E. coli* were prepared. For this purpose, 1 mL of a liquid culture was mixed with 500 µL 80 % glycerol (*v/v*), vortexed briefly and then stored at - 80 °C.

2.2.3.2 Growth conditions and maintenance of *Streptomyces*

For strain maintenance and medium-term storage, single colonies of *Streptomyces* strains were grown at 30 °C on MS agar containing the appropriate antibiotics and 10 mM $MgCl_2$ for enhanced sporulation. Plates were stored at 4 °C. Single colonies were plated confluent on MS agar containing 10 mM $MgCl_2$ and the appropriate antibiotics, in order to be harvested to form spore suspension and be stored long-term.

2.2.3.3 Preparation of *Streptomyces* spore suspension stocks

Spore suspensions were harvested from MS agar plates, containing the appropriate antibiotics and 10 mM $MgCl_2$, on which one single colony had been streaked out confluent and incubated for 5 -7 days at 30 °C until extensive sporulation. The plate was flooded with 5 mL sterile ddH_2O and the spores suspended with a sterile cotton stick. The suspension was then filtered through a sterile cotton-filled syringe into a 50 mL falcon tube in order to remove mycelium and agar residues. Immediately after filtration, the syringe was disposed of, and the falcon tube closed and stored on ice until centrifugation at 4000 rpm for 10 min at 4 °C. The supernatant was discarded, and the spore pellet resuspended in 200 - 800 µL 20 % glycerol, depending on pellet size, and then transferred into an Eppendorf tube. The suspensions were stored at - 80 °C.

Furthermore, a potential contamination of the spore suspensions had to be ruled out and, thus, 5 mL LB medium was inoculated with 10 µL of each suspension and without antibiotics and incubated for 2 - 3 days at 30 °C and 220 rpm. If after that period no *E. coli* growth was visible and only the *Streptomyces* mycelium was apparent, the spore suspension was deemed free of contamination. Additionally, spore suspensions harboring recombinant DNA had to be verified by PCR (2.2.1.7.D).

2.2.3.4 Cultivation of *Streptomyces* strains

Streptomyces strains were cultivated in 24-square deep-well plates. For this purpose, precultures were inoculated in pre-weighed 50 mL tubes. More specifically, 10 mL TSB medium was inoculated with 10 µL of the respective spore suspension and the appropriate antibiotics: 10 µL nalidixic acid to prevent *E. coli* contamination, 10 µL kanamycin for the generated cosmids, and 10 µL apramycin for the pRS02/pRS04 plasmids, if present. The precultures were incubated at 30 °C, 220 rpm. After 2 - 3 days, the precultures were centrifuged at 4000 rpm for 10 minutes at 4 °C. The supernatant was discarded, and the tubes weighed in order to determine the mass of the pellets. The pellet with the smallest mass was dissolved in 500 µL TSB medium and the obtained concentration was calculated in mg/mL. By adding different volumes of TSB medium to the other pellets, concentrations were adjusted to be equal. Each well of the sterile deep-well plates was filled with 3 mL P-medium without antibiotics. The medium was inoculated with 50 µL of the respective preculture and the bioreactors incubated at 30 °C and 240 rpm for 7 days, unless stated otherwise. For precursor feeding, stock solutions of the respective amino acids were prepared, sterilized by filtration, and added to the wells prior to cultivation.

For upscaled cultivation, 50 mL of TSB medium in baffled 300 mL flasks with a metal coil was inoculated with 20 µL spore suspension and the abovementioned antibiotics. After cultivation at 30 °C and 200 rpm for 2 - 3 days, 70 mL P-medium contained in baffled 300 mL flasks with a metal coil was inoculated with 1 mL preculture and cultivated at 30 °C for 7 days at 200 rpm.

2.2.4 Analytical Methods

Cultivations of *Streptomyces* strains were analyzed by the determination of cell dry weight and LC-MS analysis of UPA production.

2.2.4.1 Determination of cell dry weight

Cell dry weight was determined by transferring a 1 mL sample of each cultivated strain into a pre-weighed 1.5 mL Eppendorf tube (dried at 80 °C to remove adsorbed water) and harvesting the cells by centrifugation (13200 rpm, 10 min). The supernatant was discarded, the pellet washed with 1 mL ddH_2O, and the tube centrifuged under the same conditions. The supernatant was discarded once again, and the pellet left to dry at 80 °C for 24 - 48 h. At that point, the pellets were weighed, and cell dry weight determined by subtracting the weight of the tubes.

2.2.4.2 LC-MS analysis of UPA production

Samples were prepared by acidifying 700 µL of main culture with HCl (1 M) to pH = 3 - 4 and, subsequently, extracting twice with equal volumes of n-butanol. The samples were centrifuged, after adding n-butanol and shaking vigorously, for better phase separation (13300 rpm, 10 min). The supernatant was collected each time and afterwards dried in a centrifugal vacuum concentrator (Speedvac). The extract was dissolved in 100 µL MeOH/ddH_2O (1:1), centrifuged again and the supernatant analyzed by LC-MS.

LC-MS measurements were kindly conducted by Andreas Kulik (University of Tuebingen) with a LC/MSD Ultra Trap System XCT 6330 (Agilent Technologies). Separation was accomplished on a Nucleosil-100 C18 column (100 × 2 mm, 3 µm) at a flow rate of 0.4 ml/min, while the injection volume was kept at 5 µl. Elution was achieved with a linear gradient from 0 to 100 % of solvent B, which was implemented for 20 min (solvent A: 0.1 % formic acid in water; solvent B: 0.06 % formic acid in acetonitrile; Table 22). MS analysis was performed with electrospray ionization in Ultra Scan mode with a capillary voltage of 3.5 kV and a heated capillary temperature of 350 °C. Peaks corresponding to UPAs were identified through comparison with the peaks of the native producer strain.

Table 22: LC-MS solvent program

Time (min)	**Solvent B (%)**
0	0
20	100
23	100
28	0

3. Results

3.1 Pacidamycin biosynthetic gene cluster

3.1.1 Increased production by promoter replacements

3.1.1.1 Introduction of bidirectional promoter cassettes *P15_aac(3)IV_P16* and *P03_aac(3)IV_P04* into modified pacidamycin biosynthetic gene clusters

The first strategy designed to improve production rates of uridyl peptide antibiotics (UPAs) focused on the replacement of native promoters of the pacidamycin biosynthetic gene cluster with strong, constitutively active promoters, which would ensure full transcription of all genes situated on the respective operon. In a first analysis of the modified pacidamycin gene cluster on cosmid pacRS01, it became apparent that two sites harboring bidirectional promoters are located within the cluster: the first one between *pac3* and *pac4* and the second one between *npsP4* and *npsP8* (Fig. 7). These could be responsible for the transcription of the entire cluster except for *pac1*. In previous studies conducted by Dr. Nils Hauck in our working group, the transcriptional regulator Pac1 was found to decrease mass spectrometry (MS) signal intensities and therefore production levels of UPAs[18], indicating Pac1 to be acting as a transcriptional repressor of pacidamycin biosynthesis. In these experiments an additional copy of *pac1* was cloned under the control of an *ermE** promoter in the replicative plasmid pUWL-*aac(3)IV-oriT* and introduced into *S. sp.* DSM5940 (napsamycin wild type producer), *S. albus* J1074/npsXT01 (heterologous expression of napsamycin/mureidomycin BGC) and *S. albus* J1074/pacNH01 (heterologous expression of pacidamycin BGC prior to further gene swaps). For all three combinations, a reduction in signal intensity was observed upon introduction of the plasmid. Thus, *pac1* and the respective promoter were excluded from the promoter replacements and only the two bidirectional sites taken into consideration.

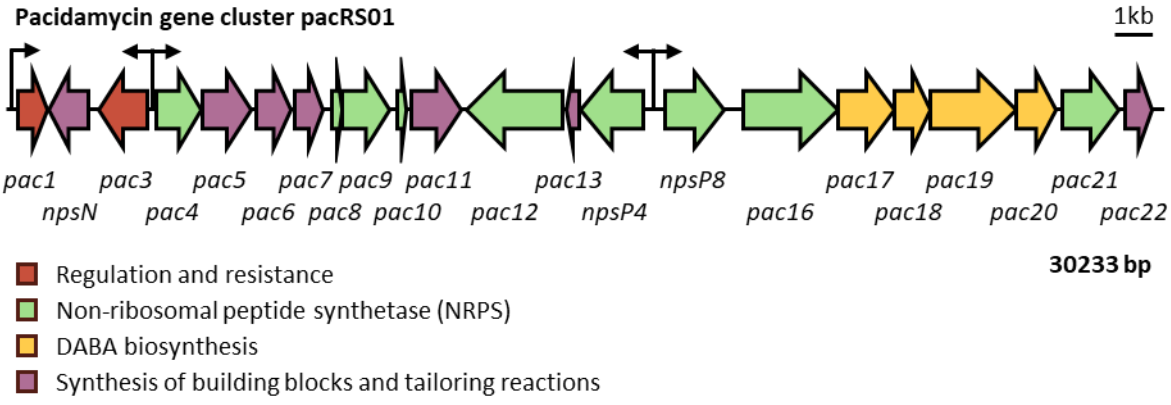


Fig. 7: Genetic organization of the modified pacidamycin BGC on cosmid pacRS01, sites harboring uni - or bidirectional promoters are displayed by thin arrows. Coloring of genes correlates to the noted function, respectively.

Soon another issue manifested itself, since two different annotations of the pacidamycin biosynthetic gene cluster have been published. The first was discovered by Rackham *et al.* (2010)[121] and the second only a few months later by Zhang *et al.* (2010)[17]. The annotations are identical, except for *pac3* and the intergenic region between *pac3* and *pac4*. According to Rackham *et al.* (2010), *pac3* amounts to 1311 bp while the intergenic region (IGR) between the genes consists of 236 bp. Contrastingly, Zhang *et al.* (2010) describe *pac3* to be consisting of 1152 bp and the intergenic region to be spanning 395 bp (Fig. 8). Both annotations utilize start codons, which are common in Streptomycetes, and for both the observed GC-plot increase, as investigated with the software Artemis, could be considered reasonable. Unfortunately, the intergenic region between *pac3* and *pac4* is one of the two bidirectional promoter sites of the gene cluster, where a promoter swap was to be conducted. Thus, it was decided that the knock-in for this site should be conducted twice, once for each possible annotation. The eventual production data should indicate which annotation turns out to be correct.

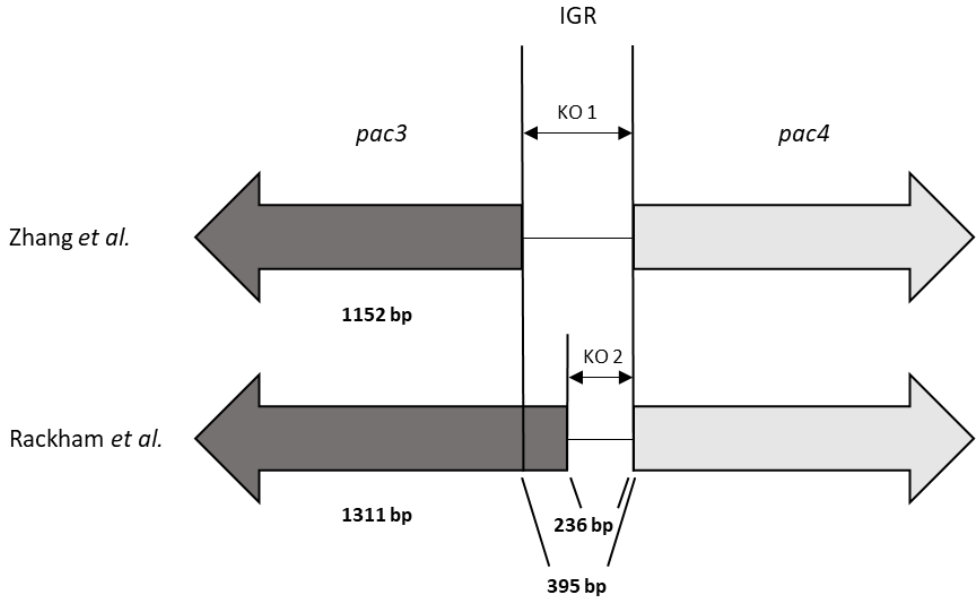


Fig. 8: Schematic representation of the annotations of the pacidamycin biosynthetic gene cluster by Zhang *et al*. (2010) and by Rackham *et al.* (2010). The regions knocked out in the promoter replacements KO 1 and KO 2, based on the two annotations respectively, were labeled alongside the length of the intergenic regions (IGR) and *pac3.*

Subsequently, suitable promoters for the knock-ins had to be chosen. For this purpose, a study published by Montiel *et al.* (2015)[136] was consulted, which tested synthetic constitutively-active promoter cassettes in order to determine the ones optimal for the activation of silent biosynthetic gene clusters and for production increase of natural products in Streptomycetes. Based on these findings, bidirectional promoter cassettes harboring the most promising candidates were constructed in previous experiments in our working group by Dr. Franziska Wiker[137]. The respective sequences P03, P04, P15 and P16 are displayed in Table 23, where the - 35 and - 10 regions were underlined.

Table 23: Organization and sequences (5' → 3') of promoter cassettes

Name	Promoter sequence (45 bp)	Insulation (15 bp)	RBS (12 - 16 bp)
P03	GAGTGCGAGATTGACGTAATGAGGGTG TGTGCCTAGGTTCTGTA	GGGAGCCTAATGTGC	AAGGAGTCGCGG
P04	TTATTTAGAGTTGACTGTGTTCTCGTCTT CCCATAGCGTGGAAA	CTGGGGAGTAGCGGA	TAGGAGGAGCTGG
P15	AATTGCCCACTTGACGTTGAGAGTGAAG CAATATAGGTTAACCT	GCCACGTGTTCGTTA	TGAGAGGTGGTCCTCA
P16	GGTGATCAGTTTGACGCCCCTGACATCG GGTGGTAGCGTCGCTG	GTGGTCCGTCAAGCC	ATAGAGGTCCGCT

The first bidirectional promoter cassette (PC1) was fused to an apramycin resistance cassette from plasmid pIJ773 and harbors the promoter sequences P15 and P16 on either side of the cassette, respectively. Plasmid pIJ773 is widely used for gene deletions through Red/ET-mediated homologous recombination (Gust *et al.* 2003)[122] and contains an apramycin resistance marker flanked by FRT sites, which allow for the subsequent deletion of the resistance marker via a site-specific recombination through the FLP recombinase. The second cassette (PC2) contains P03, P04, and an apramycin resistance marker based on the resistance cassette of plasmid pIJ774, on which the apramycin marker is flanked by loxP sites, which can be excised by a Cre-recombinase (Fig. 9).

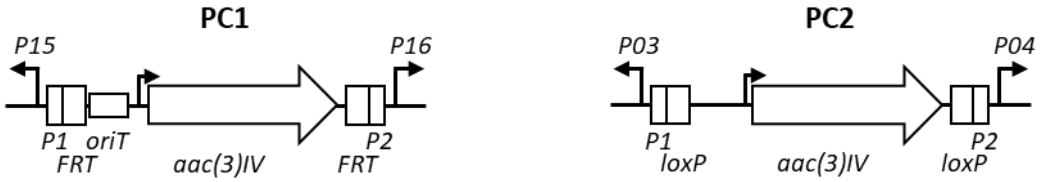


Fig. 9: Schematic representation of promoter cassettes 1 and 2, constructed by Franziska Wiker[137]. PC1 contains promoters P15 and P16, priming sites *P1* and *P2*, *FRT* sites, an *oriT* and an apramycin resistance marker, while PC2 harbors promoters P03 and P04, priming sites *P1* and *P2*, *loxP* sites and an apramycin resistance marker.

In order to replace the native intergenic regions of the BGC with the synthetic bidirectional promoter cassettes, both cassettes were amplified by PCR with elongated primers containing 33 bp-overhangs complementary to the respective genes adjacent to the intergenic region to be replaced. For the knock-in of PC1 between *pac3* and *pac4*, the primers BidPrCas1_FW and BidPrCas1_RV were utilized for a knock-in based on the annotation by Zhang *et al.* (2010)[17] and BidPrCas1_FW_vol2 and BidPrCas1_RV for a knock-in based on the annotation by Rackham *et al.* (2010)[121]. In both cases, the orientation of PC1 was chosen to set *pac3* under the control of P15 and *pac4* under the control of P16. In order to knock-in PC2 into the second bidirectional site of the cluster, which is located between *npsP4* and *npsP8*, the primers BidPrCas2_FW and BidPrCas2_RV were used for the amplification of PC2.

Moreover, P03 was inserted upstream of *npsP4* and P04 upstream of *npsP8*. PC1 was amplified out of the template plasmid pAG03 and PC2 of pAG05, which had both been obtained from Dr. Franziska Wiker[137]. After the isolation of the PCR products out of a preparative agarose gel and a subsequent spin column - based DNA purification, the amplified cassettes were utilized via Red/ET-mediated homologous recombination to replace the respective intergenic regions, as previously described. In the case of PC1, targeting was conducted on *E. coli* BW25113/pIJ790/pacRS01 (once for each annotation), while PC2 was targeted on *E. coli* BW25113/pIJ790/pacRS01 and *E. coli* BW25113/pIJ790/pacRS01_PC1 (once for each annotation). After a retransformation of the resulting cosmid DNA in order to isolate the positive candidates, in which recombination had taken place, the resulting clones were verified by enzymatic digest, PCR and sequencing. Afterwards, the resistance marker was removed by FRT-mediated or Cre-mediated recombination. The successful loss of apramycin resistance was tested and the clones were verified by enzymatic digest, PCR and sequencing. Thus, the following cosmids were constructed: pacHK01 (based on the annotation by Zhang *et al.,* pacRS01 harboring PC1), pacHK02 (based on the annotation by Zhang *et al.,* pacRS01 harboring PC1 and PC2), pacHK03 (based on the annotation by Rackham *et al.,* pacRS01 harboring PC1), pacHK04 (based on the annotation by Rackham *et al.,* pacRS01 harboring PC1 and PC2) and pacHK05 (pacRS01 harboring PC2) (Fig. 10). Construct verification by PCR was conducted with the primers pac3_test_FW, neu_pac3_test_FW and pac4_test_RV in the case of a PC1 knock-in, where each forward primer was utilized for one of the differing annotations. For the verification of PC2 knock-ins, npsP8_test_FW and npsP4_test_RV were utilized.

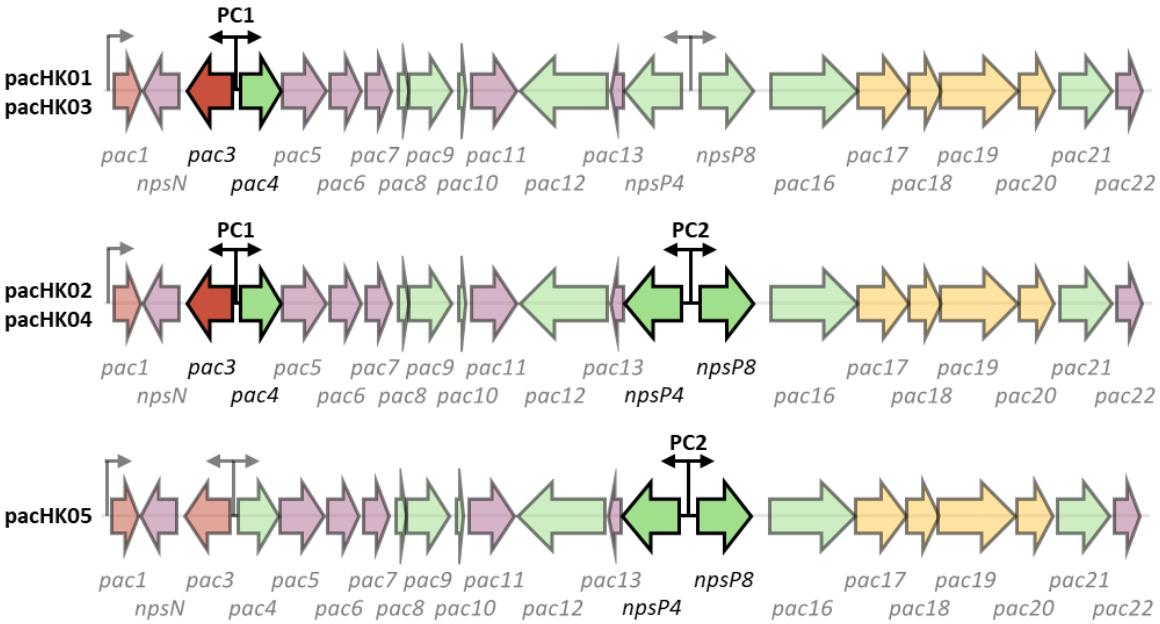


Fig. 10: Schematic representation of the conducted promoter replacements on pacRS01 and resulting BGCs pacHK01 - pacHK05.

All five cosmids were introduced by triparental conjugation, each into the following *Streptomyces* strains: *S. albus* J1074 wild type (WT), *S. albus* J1074/pRS02 (containing the phenylalanine hydroxylase *phhA* and the NRPS A-domain *pac21h*) and *S. albus* J1074/pRS04 (containing *phhA*, *pac21h* and the cluster-specific positive regulator *npsM* of the napsamycin BGC). Biological triplicates and technical duplicates of each of the 15 resulting mutant strains were cultivated in 3 mL deep well plates and extracted after 2 days of preculture and 7 days of main culture (see 2.2.3.4).

Firstly, production rates regarding the two different annotations were examined. For this purpose, the mutant strains *S. albus* J1074/pRS02/pacRS01 and *S. albus* J1074/pRS02/pacHK01 were compared, in order to examine the results of knock-ins based on the annotation by Zhang *et al.* (2010)[17]. Since production rates were overall quite low, compound detection in UV (λ = 260 nm) was not determinatively feasible, although a slight reduction in intensity was observed for all mutant strains based on this annotation, as demonstrated by met-pacidamycin S in Fig. 11. More specifically, the UV-chromatogram of *S. albus* J1074/pRS02/pacHK01 displayed closer similarity to the wild type than to the strains harboring the BGC, regarding the retention times of UPAs t_R = 8.0 - 9.4 min.

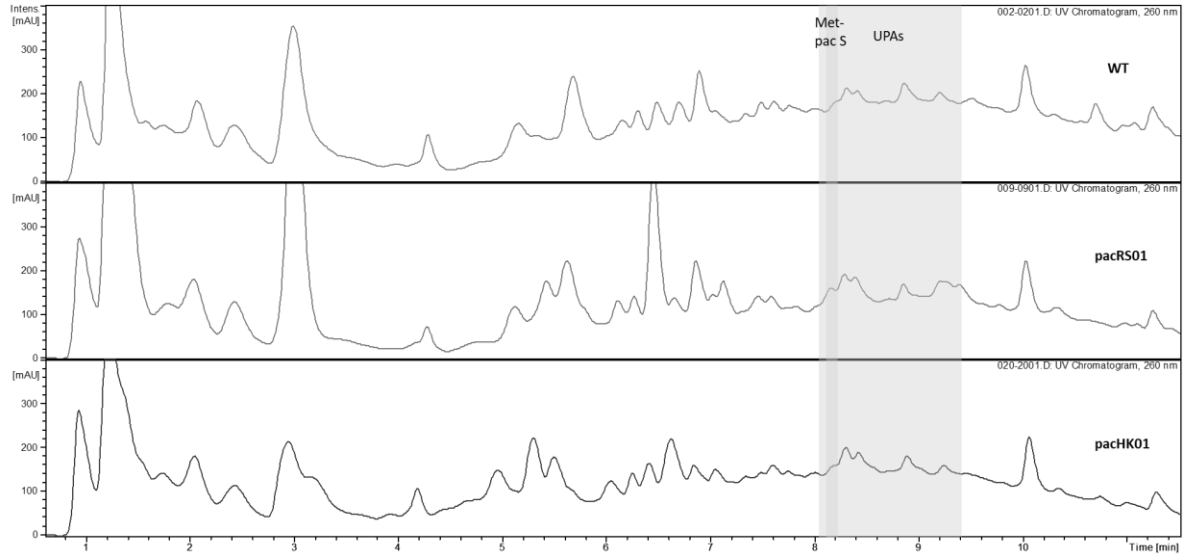


Fig. 11: LC-MS analysis of knock-ins of PC1 on pacRS01 based on annotation by Zhang *et al.* (2010): UV-Chromatograms 260 nm, top to bottom: 1) *S. albus* J1074 WT, 2) *S. albus* J1074/pRS02/pacRS01 and 3) *S. albus* J1074/pRS02/pacHK01; The light gray area correlates to the retention times of UPAs and the dark gray column displays the exemplary compound met-pacidamycin S.

This reduction became more apparent through comparison of extracted ion chromatogram (EICs) of the main compounds for the respective strains. Prior to the integration of the plasmids pRS02 and pRS04 into the alternative attachment site, the major compounds produced by *S. albus* J1074/pacRS01 were met-pacidamycin S and met-pacidamycin D. Once the plasmids were integrated, the BGC synthesizes met-pacidamycin S, met-pacidamycin D, met-pacidamycin 4, met-pacidamycin 5 and mureidomycin A. All aforementioned compounds were detectable in the extracts of *S. albus* J1074/pRS02/pacRS01, which was not the case for extracts of *S. albus* J1074/pRS02/pacHK01,

where the knock-in had been conducted based on the annotation by Zhang *et al.* (2010)[17]. Extracted ion chromatograms of mureidomycin A are displayed in Fig. 12, in which the gray area corresponds to the retention time determined by Nils Hauck in his PhD thesis[18], which was also verified by the respective MS^2 fragmentation pattern. A further verification derives from the comparison with the respective peaks of *S. sp.* DSM5940 and *S. albus* J1074/npsXT01, the former being the native napsamycin/mureidomycin producer and the latter the heterologous producer strain of the napsamycin/mureidomycin biosynthetic gene cluster. The slight peak shift observed in these chromatograms might derive from LC-MS factors over the course of running all 110 analyses consecutively, while mureidomycin A corresponds to the right shoulder of the split peaks. In the EIC of mureidomycin A, derived from the analysis of the extract of *S. albus* J1074/pRS02/pacHK01, no peak could be detected, and thus, mureidomycin A production could not be observed.

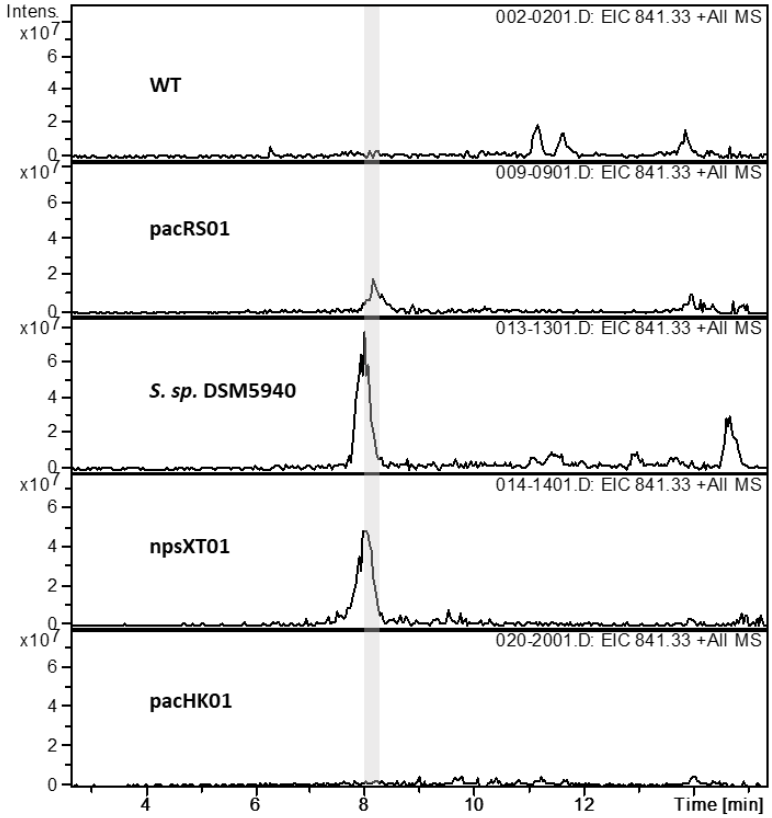


Fig. 12: LC-MS analysis of knock-ins of PC1 on pacRS01 based on annotation by Zhang *et al.* (2010): Extracted ion chromatograms of mureidomycin A (*m/z* 841.3 $[M+H]^+$) are displayed for (top to bottom): 1) *S. albus* J1074 WT, 2) *S. albus* J1074/pRS02/pacRS01, 3) *S. sp.* DSM5940 (native napsamycin/mureidomycin producer), 4) *S. albus* J1074/npsXT01 (heterologous expression of the native napsamycin BGC) and 5) *S. albus* J1074/pRS02/pacHK01 (PC1 knock-in on the native pacidamycin BGC); The gray area correlates to the retention time of mureidomycin A.

A similar picture was presented by the EICs of met-pacidamycin 4, which are depicted in Fig. 13. The respective peak could be readily observed in extracts of *S. albus* J1074/pRS02/pacRS01, while the knock-in decreased compound production below detection limit in *S. albus* J1074/pRS02/pacHK01, as was the case for all other UPAs (data not shown). As described for mureidomycin A, the retention time

and MS^2 fragmentation pattern for met-pacidamycin 4 correspond to the ones determined by Dr. Nils Hauck[18], who utilized an identical LC-MS program.

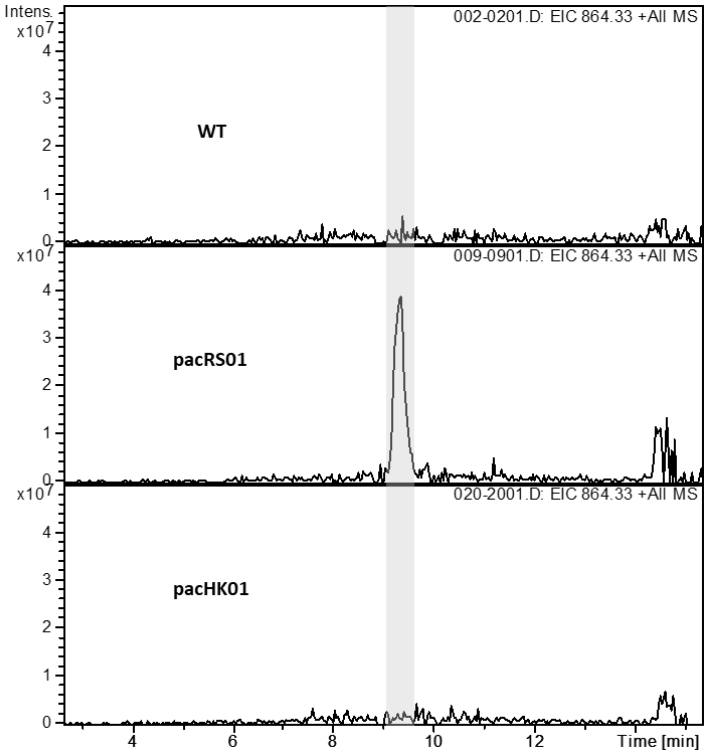


Fig. 13: LC-MS analysis of knock-ins of PC1 on pacRS01 based on annotation by Zhang *et al.* (2010): Extracted ion chromatograms of met-pacidamycin 4 (*m/z* 864.3 $[M+H]^+$) are displayed for (top to bottom): 1) *S. albus* J1074 WT, 2) *S. albus* J1074/pRS02/pacRS01 and 3) *S. albus* J1074/pRS02/pacHK01; The gray area correlates to the retention time of met-pacidamycin 4.

Identical results were observed for the mutant strains *S. albus* J1074/pacHK01, *S. albus* J1074/pRS04/pacHK01, *S. albus* J1074/pacHK02, *S. albus* J1074/pRS02/pacHK02 and *S. albus* J1074/pRS04/pacHK02, where no UPA compounds were detectable (data not shown). In contrast, UPA production was increased by promoter replacements based on the annotation by Rackham *et al.* (2010)[121], which will be described subsequently in more detail. These results strongly indicate the latter annotation to be correct and thus this annotation was used for the design of further experiments.

Production levels of major compounds were investigated in mutants harboring PC1 containing promoters *P15* and *P16* at the first bidirectional promotor site based on the correct annotation. For the mutant strain *S. albus* J1074/pacHK03, which did not carry the additional plasmids pRS02 or pRS04 at the alternative attachment site, production levels of met-pacidamycin S and met-pacidamycin D were significantly increased in comparison with *S. albus* J1074/pacRS01 (data not shown). More interestingly, a significant production increase could also be observed for strains harboring these plasmids within their genome, and thus, synthesize the desired compound mureidomycin A. The UV

chromatogram of the mutant strain *S. albus* J1074/pRS02/pacHK03 depicts increased signal intensities for UPAs, when compared with the native *S. albus* J1074/pRS02/pacRS01 (Fig. 14).

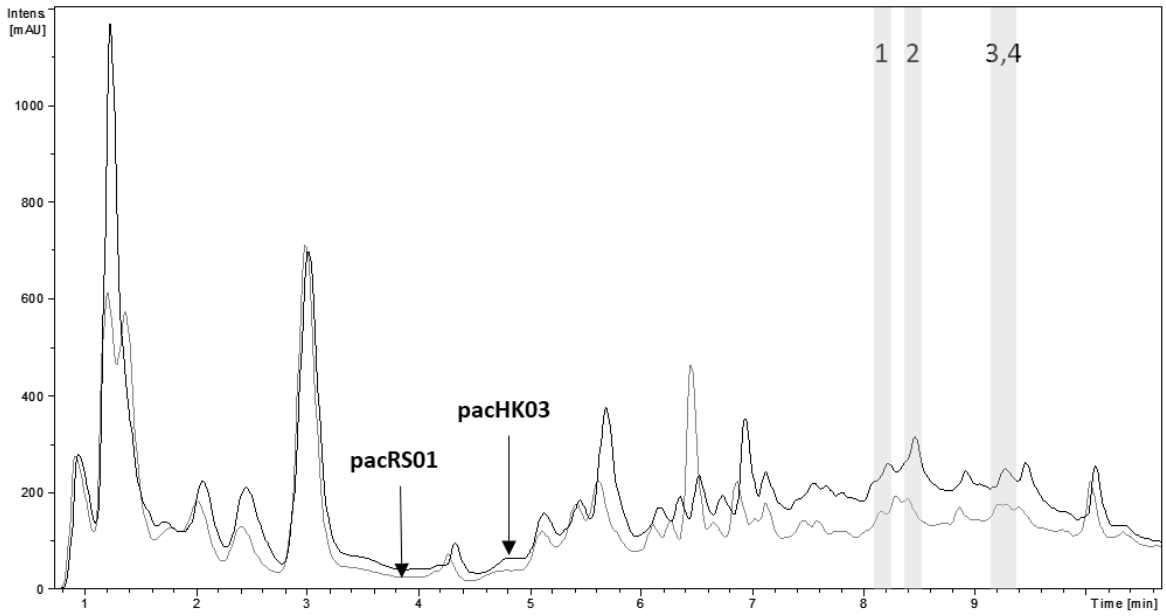


Fig. 14: LC-MS analysis of knock-ins of PC1 on pacRS01 based on annotation by Rackham *et al.* (2010): UV-Chromatograms 260 nm, light gray: *S. albus* J1074/pRS02/pacRS01 and black: *S. albus* J1074/pRS02/pacHK03; exemplary UPAs and the respective increase in signal intensities have been labeled: 1) Met-pacidamycin S, 2) Met-pacidamycin D, 3) Met-pacidamycin 5 and 4) Met-pacidamycin 4.

The investigation of the extracted ion chromatograms further revealed an increased peak area of mureidomycin A (*m/z* 841.3 $[M+H]^+$) subsequent to the promoter replacement, when comparing the aforementioned strains (Fig. 15A). This data was summarized in the graph displayed in Fig. 15B. Therein, mureidomycin A levels were compared in biological triplicates and technical duplicates for the mutant strains harboring the modified pacidamycin BGCs and in technical duplicates only for the native producer strain *S. sp.* DSM 5940 and the heterologous host strain *S. albus* J1074/npsXT01 (harboring the napsamycin/mureidomycin BGC). While the promoter knock-in increased production rates in *S. albus* J1074/pRS02/pacHK03 approximately to the same level of *S. albus* J1074/npsXT01, the subsequent addition of *npsM* on pRS04 did not further increase mureidomycin A levels. The gene *npsM* constitutes the cluster-specific positive regulator of the napsamycin/mureidomycin BGC, which had been found to elevate UPA production in the work of Dr. Nils Hauck, however, this observation could not be replicated in this experiment. Regarding the remaining UPAs, production rates were either slightly improved or not affected (Appendix Fig. S1), while mureidomycin C production could not be detected in any mutant (Richard Sonnengruen, personal communication).

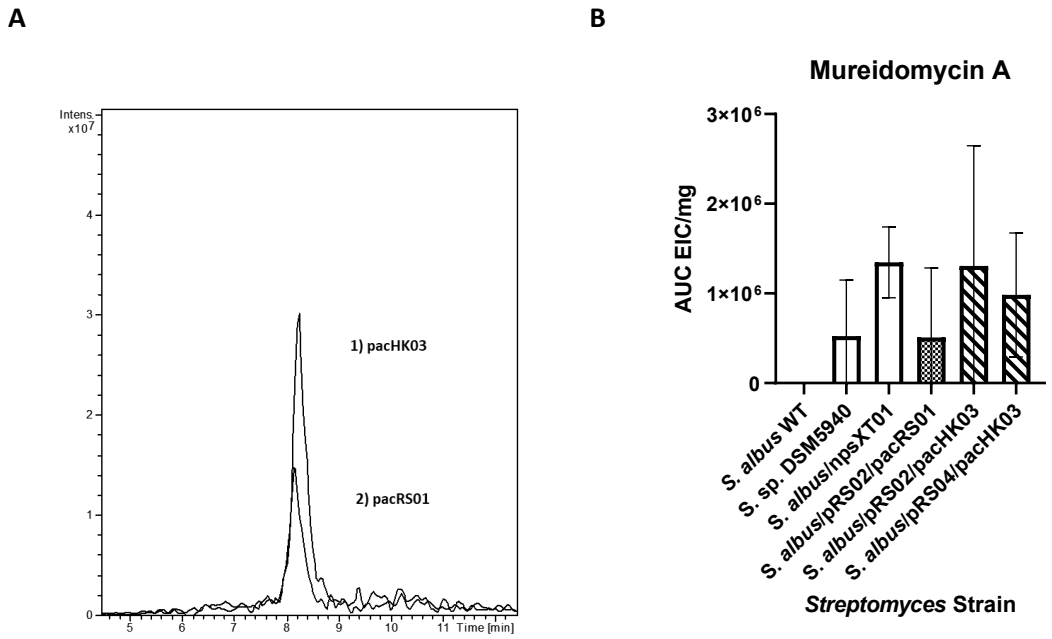
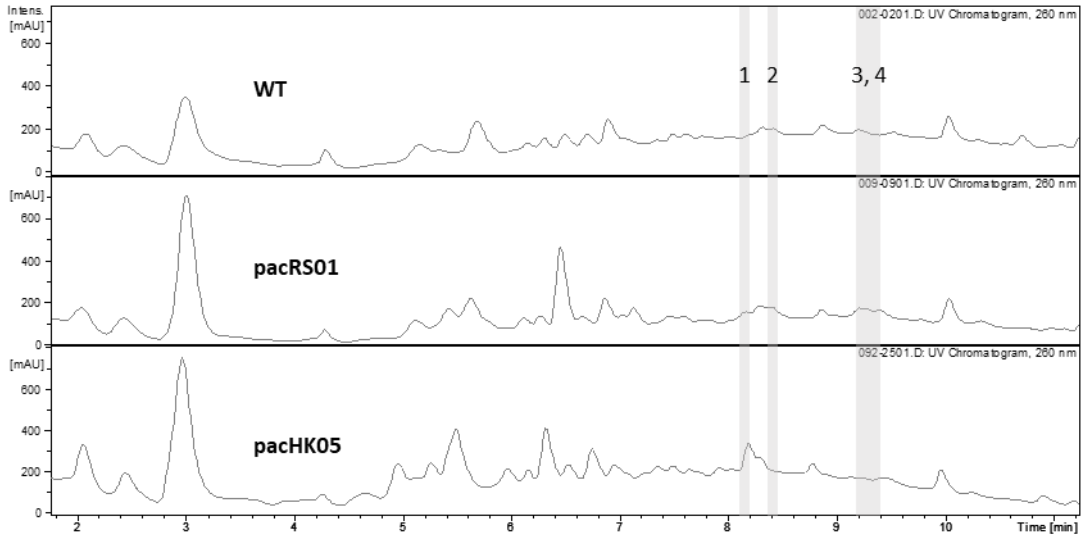


Fig. 15: LC-MS analysis of knock-in of PC1 in between *pac3* and *pac4* on pacRS01 based on annotation by Rackham *et al.* (2010): A) Extracted ion chromatograms of mureidomycin A (*m/z* 841.3 $[M+H]^+$; smoothed 2.24, 1, Gauss), are displayed for: 1) *S. albus* J1074/pRS02/pacHK03 and 2) *S. albus* J1074/pRS02/pacRS01; B) AUCs (Area under curve) of mureidomycin A EICs are plotted against mutant strains harboring the promoter swap, reference strains and the wild type strain in biological and technical replicates, normalized by cell dry weight.

Subsequently, the knock-in of promoter cassette PC2 containing promoters P03 and P04 between *npsP4* and *npsP8* on the modified pacidamycin gene cluster pacRS01 was investigated. For this purpose, production levels of the major compounds were compared in *S. albus* J1074/pRS02/pacRS01 and *S. albus* J1074/pRS02/pacHK05. However, compound production was abolished in mutants harboring PC2, as displayed in the respective UV- and base-peak chromatograms (Fig. 16A and B), as well as shown for the EICs of mureidomycin A and met-pacidamycin 4 of the same strains (Fig. 17A and B). Identically, the complete cessation of UPA production was noted in *S. albus* J1074/pacHK05 and *S. albus* J1074/pRS04/pacHK05 (data not shown).

A



B

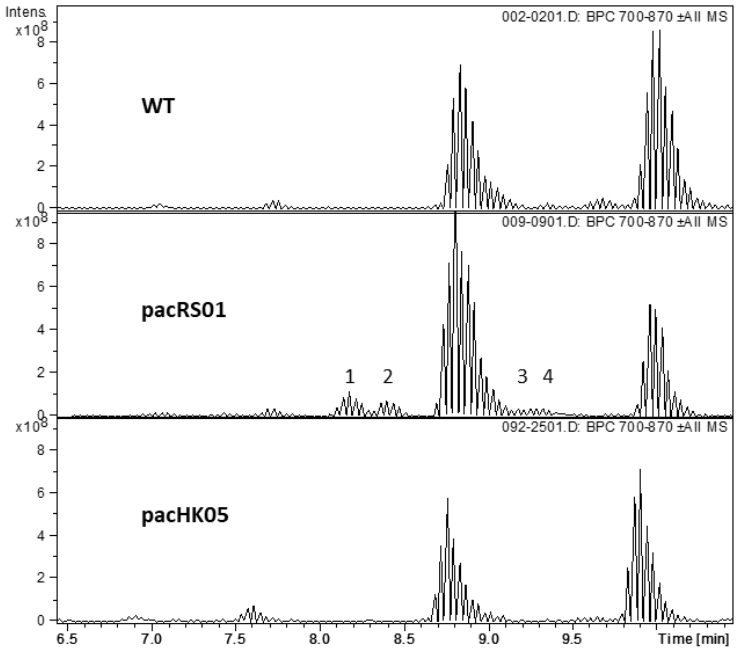


Fig. 16: LC-MS analysis of knock-in of PC2 in between *npsP4* and *npsP8* on pacRS01: A) UV-Chromatograms 260 nm and B) Base Peak Chromatogram (+ MS 700-870 *m/z*), each top to bottom: a) *S. albus* J1074 WT, b) *S. albus* J1074/pRS02/pacRS01 and c) *S. albus* J1074/pRS02/pacHK05; UPAs were labeled: 1) Met-pacidamycin S, 2) Met-pacidamycin D, 3) Met-pacidamycin 5 and 4) Met-pacidamycin 4.

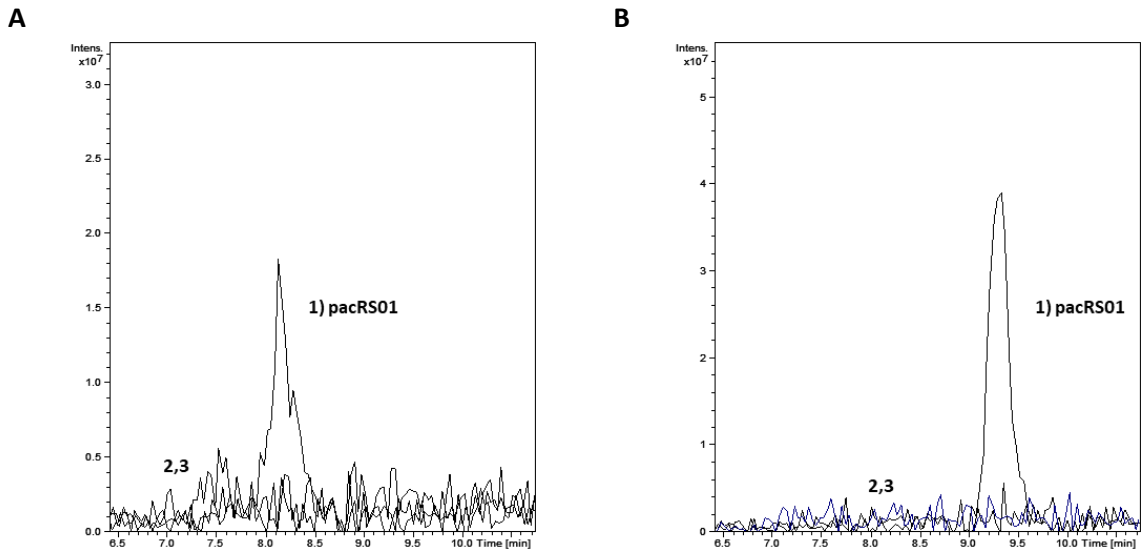


Fig. 17: LC-MS analysis of knock-ins of PC2 on pacRS01 between *npsP4* and *npsP8*: Extracted ion chromatograms of A) mureidomycin A (*m/z* 841.3 $[M+H]^+$) and B) met-pacidamycin 4 (*m/z* 864.3 $[M+H]^+$) are displayed for: 1) *S. albus* J1074/pRS02/pacRS01, 2) *S. albus* J1074/pRS02/pacHK05 and 3) *S. albus* J1074 WT. Since UPA production was not detectable in *S. albus* J1074/pRS02/pacHK05, the respective EICs were not separable from WT noise.

Similar results were obtained for the respective knock-in on the modified pacidamycin cluster, which already harbored PC1 between *pac3* and *pac4*, since no UPA compound production was detectable in *S. albus* J1074/pacHK04, *S. albus* J1074/pRS02/pacHK04 or *S. albus* J1074/pRS04/pacHK04 (data not shown). Due to the observed production abolishment whenever PC2 was inserted into a BGC, this cassette was hypothesized to be inactive under the experimental conditions.

Knock-ins of PC1 between *npsP4* and *npsP8*

Since promoter cassette 2 (PC2) did not lead to the desired effects when inserted into the second bidirectional site between *npsP4* and *npsP8*, it was decided to knock in the first, efficient promoter cassette into that side, in order to position most of the BGC under the control of strong, synthetic promoters, as intended by the original strategy. Theoretically, this could ensure optimized transcription and, thus, mureidomycin A production levels. For this purpose, two additional modified pacidamycin biosynthetic gene clusters were constructed, one containing PC1 with promoters P15 and P16 only at the second bidirectional promotor site (between *npsP4* and *npsP8*) and one containing the same cassette at both bidirectional sites of the gene cluster (*pac3*/*pac4* and *npsP4*/*npsP8*) (Fig. 18). The latter was meant to further enhance production rates, while the former was planned to reveal the impact of strong, synthetic promoters on the second site. In both cases, promoter P15 was inserted upstream of *npsP4* and promoter P16 upstream of *npsP8*.

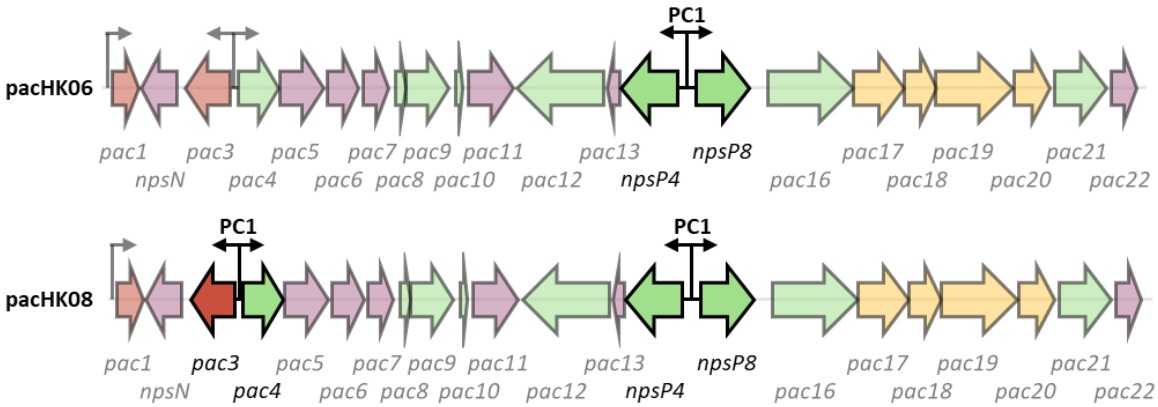


Fig. 18: Schematic representation of further knock-ins on pacRS01 and resulting BGCs pacHK06 and pacHK08.

For the knock-in of PC1 between *npsP4* and *npsP8* into pacRS01 resulting in pacHK06, the same procedure as previously described for the construction of pacHK03 was followed with the sole exception that novel primers were designed for cassette amplification out of pAG03. These primers (HB_FW and HB_RV) introduced long overhangs complementary to the genes adjacent to the second bidirectional promoter site. Thus, the modified pacidamycin BGC harboring PC1 between *npsP4* and *npsP8* encoded on pacHK06 was obtained and verified by PCR, sequencing and restriction digest. This construct was transformed into *E. coli* ET12567 and then conjugated with *S. albus* J1074, which was chosen due to the reduced variety of compounds produced in the absence of the plasmids pRS02 and pRS04, which facilitated drawing conclusions regarding the overall effect on production rates. Subsequent to cultivation and extraction procedures according to previously described methods, LC-MS measurements of extracts of *S. albus* J1074/pacRS01 and *S. albus* J1074/pacHK06 were compared regarding compound yield of met-pacidamycin D and S. Both compounds have been discussed in the work of Nils Hauck[18], where they were identified and verified by MS^2 measurements. Evidently, the respective extracted ion chromatograms display a very significant reduction in production rates for both major compounds (Fig. 19).

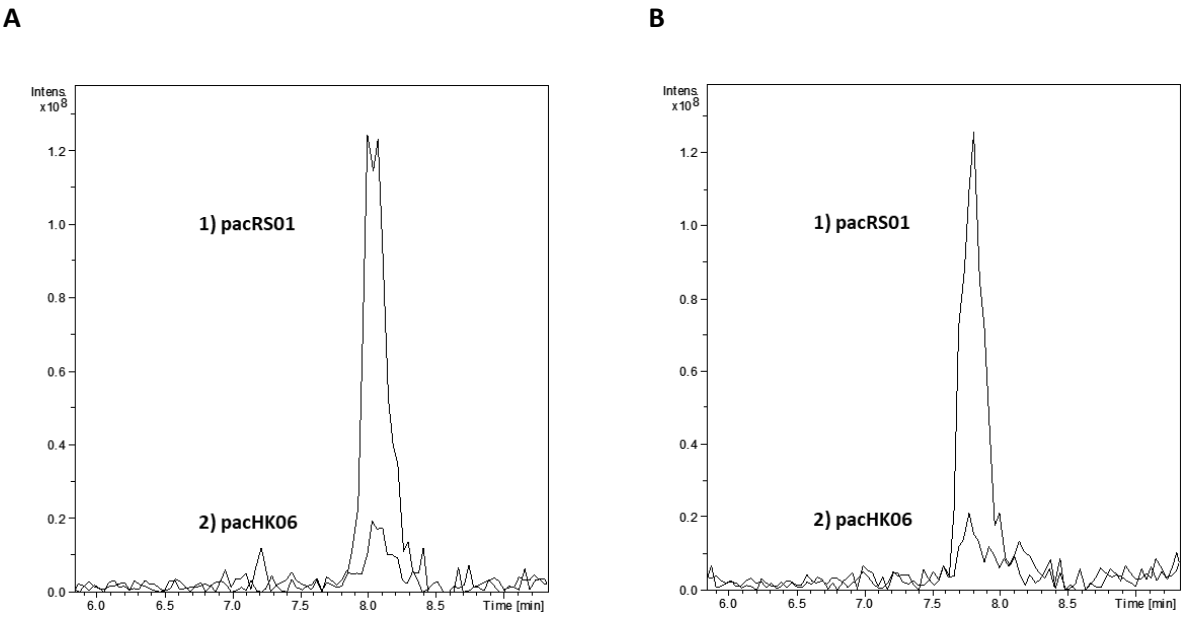


Fig. 19: LC-MS analysis of knock-ins of PC1 into pacRS01 between *npsP4* and *npsP8*: Extracted ion chromatograms of A) Met-pacidamycin D (*m/z* 772.3 $[M+H]^+$) and B) Met-pacidamycin S (*m/z* 733.3 $[M+H]^+$) are displayed for: 1) *S. albus* J1074/pacRS01 and 2) *S. albus* J1074/pacHK06.

In order to design a cosmid harboring the modified pacidamycin BGC, in which both intergenic regions have been replaced by the synthetic promoter cassette PC1, the following strategy utilizing a resistance cassette with a rare restriction site was devised (Fig. 20). A simple insertion of PC1 was not feasible herein, due to the FRT scar present in the cosmid after the first knock-in. Firstly, the apramycin resistance cassette encoded on pRS03 was amplified with primers PromB_ISce_FW and PromB_ISce_RV. The obtained PCR product was purified and then utilized in a Red/ET-dependent recombination on pacHK03 in accordance with the aforementioned procedure. Once the resulting cosmid was isolated after a retransformation and verification by PCR, restriction digest and sequencing, an I-SceI digest was performed[138]. This enzyme recognizes and cleaves a restriction site, which rarely occurs due to its length of 18 bp. Therefore, this digest allows for the linearization of the pacidamycin biosynthetic gene cluster, which harbors the corresponding cassette. After heat inactivation, the mixture was precipitated with 100 % EtOH and LiCl for increased efficiency. Simultaneously, a fragment containing PC1 was amplified out of pacHK06. The primers PC1B_Amp_FW and PC1B_Amp_RV were designed to bind at a distance of 459 bp and 483 bp on either side of PC1. This resulted in a PCR product consisting of PC1 at its core flanked by a 459 bp overhang to *npsP4* and a 483 bp overhang to *npsP8*. Moreover, the linearized cosmid and this fragment could be utilized in a co-transformation into Red/ET proficient strains, where recircularization occurred due to the homologous recombination of the corresponding overhangs utilized as a selection mechanism. Thus, the desired pacidamycin BGC was obtained, which harbors PC1 at both bidirectional promoter sites.

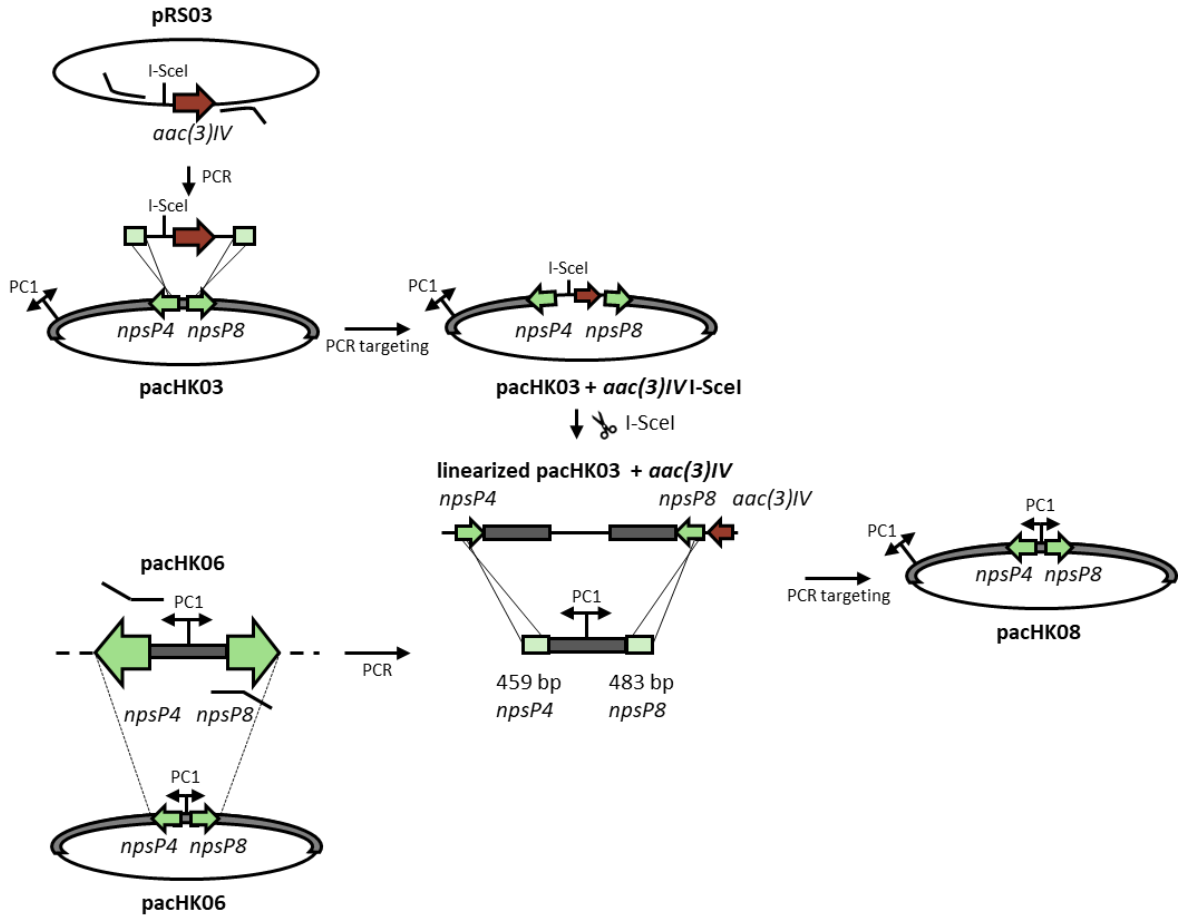


Fig. 20: Schematic representation of the strategy designed to construct pacHK08.

The resulting cosmid pacHK08 was verified by restriction digest, PCR (Primers: pacHK08_test_FW and pacHK08_test_RV) and sequencing, transformed into *E. coli* ET12567 and conjugated with *S. albus* J1074/pRS02, in order to examine whether a beneficial effect on mureidomycin A yield in comparison with *S. albus* J1074/pRS02/pacHK03 could be observed. The isolated and verified mutant strains were cultivated, as previously mentioned. LC-MS analysis of the extracts revealed a very significant decline in UPA production of *S. albus* J1074/pRS02 containing pacHK08 compared to the strain containing pacHK03 (Fig. 21). While production rates of mureidomycin A, met-pacidamycin 4 and met-pacidamycin 5 were decreased below the detection limit, met-pacidamycin S and met-pacidamycin D were significantly decreased, as displayed in the respective EICs.

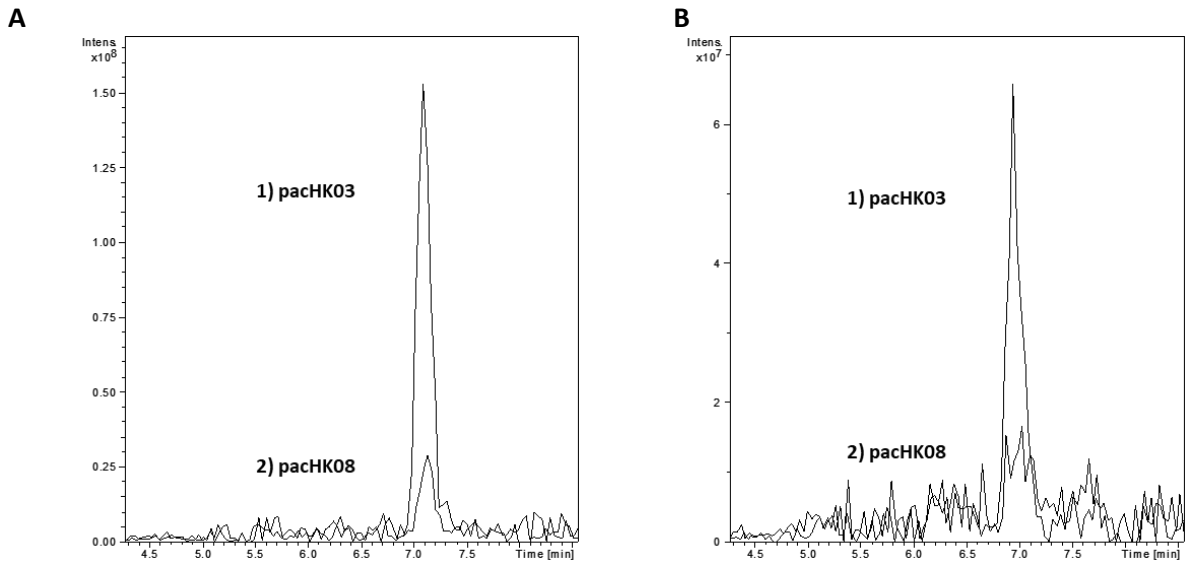


Fig. 21: LC-MS analysis of knock-ins of PC1 into pacHK03 between *npsP4* and *npsP8*: Extracted ion chromatograms of A) Met-pacidamycin D (*m/z* 772.3 $[M+H]^+$) and B) Met-pacidamycin S (*m/z* 733.3 $[M+H]^+$) are displayed for: 1) *S. albus* J1074/pRS02/pacHK03 and 2) *S. albus* J1074/pRS02/pacHK08.

Feeding studies

Since the latter promoter exchanges did not improve UPA yield, a novel approach was conceived. Dr. Nils Hauck conducted several feeding experiments of amino acids in his thesis, owing to the UPA structure scaffold, which for the varying compounds mainly diverges in the different amino acids incorporated in the pseudo tetra- or pentapeptide moiety. Out of all successfully fed amino acids in his work, solely the feeding of *m*-tyrosine for the incorporation at position 5 of the amino acid scaffold is beneficial for the biosynthesis of mureidomycins A and C. Therefore, feeding studies with *m*-tyrosine were conducted to steer compound production toward mureidomycin A and C. Additionally, glycine was fed, in order to potentially cause the production of UPAs containing glycine in the scaffold, which had not been detected hitherto. For this purpose, *m*-tyrosine (5 mM) and glycine (5 mM) were added to 70 mL main cultures of *S. albus* J1074/pRS02/pacHK03, prior to cultivation. After compound extraction, LC-MS analysis revealed the glycine feeding to be ineffective, since mureidomycin C production was not detected. UV chromatograms depict a slight intensity decrease for compounds like met-pacidamycin D and 4 (Fig. 22A), which do not contain *m*-tyrosine at position 5 of the UPA scaffold, while production rates for the other compounds were too low to observe effects in UV-chromatograms. Similarly, EICs of Met-pacidamycin 4, 5, S and D (all harboring phe or trp at position 5) display a very significant production decrease upon feeding, while mureidomycin A peak intensity was strongly increased. This was expected and correlates with the data of Dr. Nils Hauck, since *m*-tyrosine is incorporated at position 5 of the amino acid scaffold of mureidomycin A (Fig. 22B for

mureidomycin A and Fig. 22C for met-pacidamycin 4; Appendix Fig. S2 and Fig. S3 for met-pacidamycins 5, S and D).

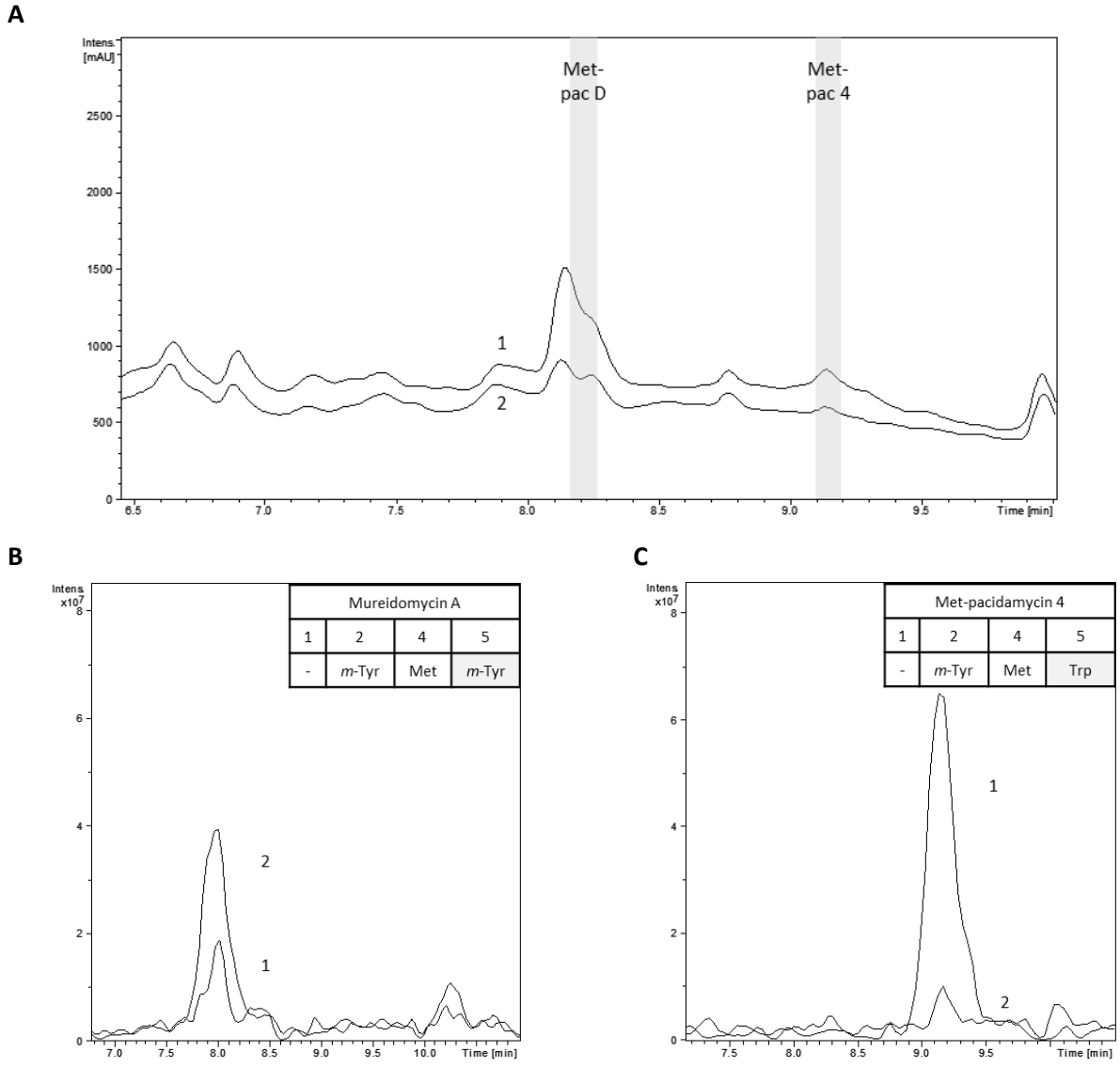


Fig. 22: LC-MS analysis of feeding studies of *S. albus* J1074/pRS02/pacHK03: 1) No feeding, 2) Feeding of *m*-tyrosine (5 mM) and glycine (5 mM). A) UV-Chromatograms 260 nm, B) Extracted ion chromatograms of mureidomycin A (*m/z* 841.3 $[M+H]^+$) and C) Extracted Ion Chromatograms of met-pacidamycin 4 (*m/z* 864.3 $[M+H]^+$) are displayed, the respective amino acid composition has been noted; EICs have been processed by Gaussian smoothing (2.24,1).

Promoter exchange on further modified pacidamycin BGC

Meanwhile, further modifications of the pacidamycin gene cluster were carried out by Richard Sonnengruen. The NRPS adenylation domain *pac21* was knocked out due to its preference for the incorporation of an N-terminal alanine instead of *m*-tyrosine, which can be found in both mureidomycins C and A. This necessitates the complementation with either pRS02 or pRS04, since both plasmids carry the orthologous adenylation domain *pac21h*, which displays a preference for

m-tyrosine. Furthermore, the adenylation domain *pac12* was swapped for its napsamycin ortholog *npsP3*, in order to restrict the variety of possible amino acids recognized by *pac12* and incorporated at the UPA C-terminus from L-phe, L-trp and *m*-tyrosine to only *m*-tyrosine, and to, thus, eliminate the need for feeding *m*-tyrosine. Since the A-domain *npsP3* displays a preference for *m*-tyrosine, all mureidomycins and napsamycins harbor this amino acid at position 5 of the scaffold. The resulting mutant strain containing the mutated pacidamycin gene cluster pacRS03 therefore mainly produced mureidomycin A and met-pacidamycin 5. Hence, promoter cassette no. 1 was knocked into the first bidirectional promoter site of the novel pacidamycin cluster pacRS03 to increase mureidomycin A yield, prompted by the promising results observed for PC1, which have been described above.

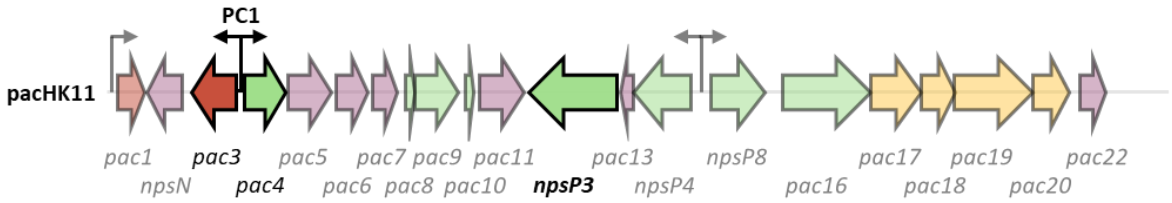


Fig. 23: Schematic representation of the novel modified pacidamycin BGC on pacRS03 containing PC1.

Accordingly, promoter P15 was inserted upstream of *pac3* and P16 upstream of *pac4* (Fig. 23). This was accomplished by the same procedure mentioned above to knock in PC1 in between *npsP4* and npsP8 on cosmid pacHK03, resulting in pacHK08 (see 3.1.1.1). After conjugation with *S. albus* J1074/pRS02 and *S. albus* J1074/pRS04, isolated and verified mutant strains were cultivated and analyzed by LC-MS, as stated above.

The graph of Fig. 24 depicts production rates of mureidomycin A for different mutant strains. When comparing *S. albus* J1074/pRS02/pacRS03 harboring only native promoters, with *S. albus* J1074/pRS02/pacHK11, a slight production increase could be noticed. However, in combination with the plasmid pRS04, which additionally contains the positive regulator *npsM*, this increase becomes most significant. While the addition of *npsM* to *S. albus* J1074/pRS02/pacRS03 had no effect on mureidomycin A production, the combination of *npsM* and promoter replacement seemed to be highly beneficial for mureidomycin A production (Fig. 24). This effect is displayed in detail in the respective EICs of mureidomycin A, while met-pacidamycin 5 was increased to a lesser extent (Fig. 25). Therefore, the most promising candidate hitherto for mureidomycin A production was *S. albus* J1074/pRS04/pacHK11.

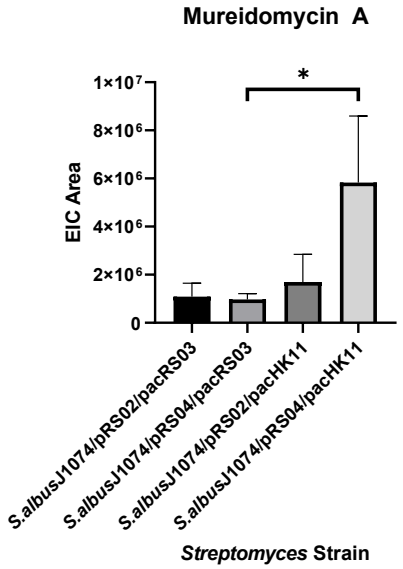


Fig. 24: LC-MS analysis of knock-in of PC1 in between *pac3* and *pac4* on pacRS03; AUCs of mureidomycin A EICs have been normalized by cell dry weight and plotted against mutant strains with and without promoter swap in biological and technical replicates. Statistical analysis: unpaired t-test, two-tailed P value, P value style: GraphPad, one asterisk signifies $P \leq 0.05$.

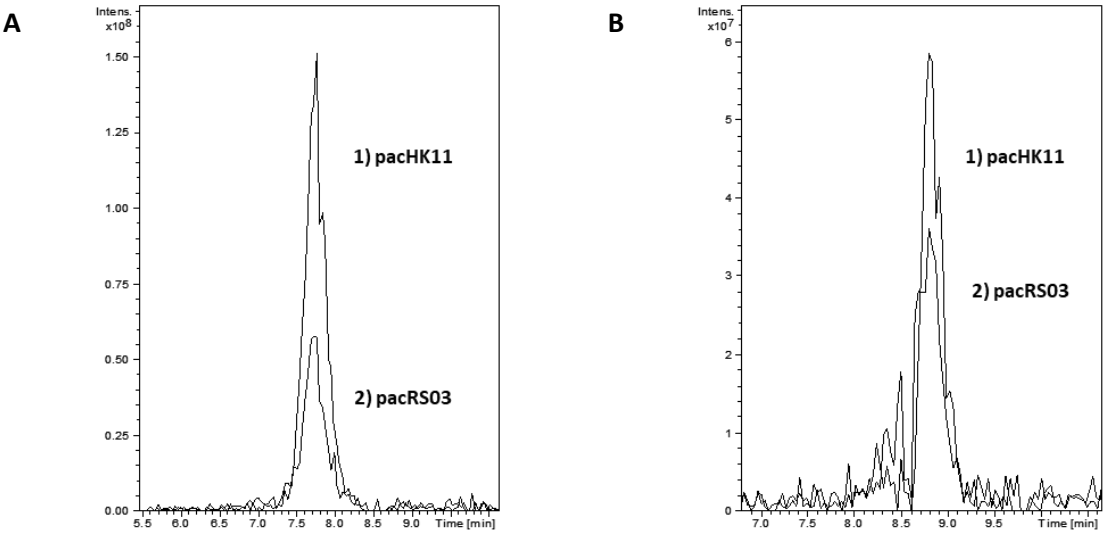


Fig. 25: LC-MS analysis of knock-in of PC1 in between *pac3* and *pac4* on pacRS03: Extracted ion chromatograms of A) mureidomycin A (*m/z* 841.3 $[M+H]^+$) and B) met-pacidamycin 5 (*m/z* 825.3 $[M+H]^+$) are displayed for: 1) *S. albus* J1074/pRS04/pacHK11 and 2) *S. albus* J1074/pRS04/pacRS03.

3.1.1.2 Introduction of bidirectional promoter cassettes *ermE*p_aac(3)IV_ermE*p* (PC3) and *ermE*p_aac(3)IV_kasOp*-SP44* (PC4) into modified pacidamycin biosynthetic gene clusters

In order to further increase UPA production, two novel bidirectional promoter cassettes were constructed by golden gate assembly (Fig. 26). The first one consists of a bidirectional *ermE**p cassette (PC3), where one *ermE** spacer RBS sequence correlates to the one described by Montiel *et al.* (2015)[136] and the other corresponds to the *ermE*p* of cloning vector pUWL201. The second bidirectional promoter cassette consists of the same *ermE*p* spacer RBS cassette[136] and an optimized derivative of *kasO*p[139,140] (PC4). These promoters were selected due to their common use as strong, constitutively active promoters, which were, therefore, well established to be used in Streptomycetes.[141]

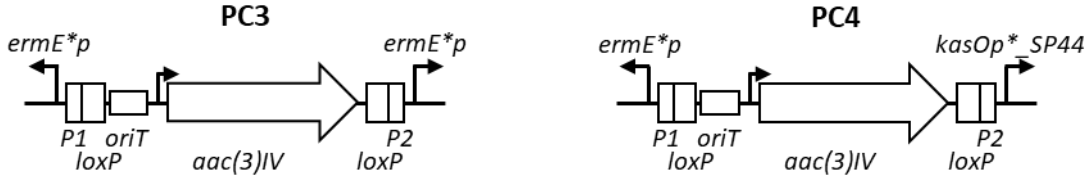


Fig. 26: Schematic representation of promoter cassettes 3 and 4. PC3 consists of two *ermE*p*, priming sites *P1* and *P2*, two *loxP* sites, an *oriT* and an apramycin resistance gene. PC4 harbors *ermE*p* and *kasOp*_SP44*, priming sites *P1* and *P2*, two *loxP* sites, an *oriT* and an apramycin resistance gene.

Both cassettes were based on the apramycin resistance cassette of plasmid pIJ774, which was excised through a HindIII/EcoRI digest, purified, and then amplified by PCR with primers GGA_774_FW and GGA_774_RV, which introduced overhangs harboring recognition sites for the type IIS restriction enzyme BsaI and the desired homologous 4 bp-overhangs for assembly. Thus, the purified PCR product was mixed with gBlocks containing the promoter sequences and used for Golden Gate Assembly. For the construction of pHK01 harboring PC3, the gBlocks ermE_Mon and ermE_pUWL were mixed with the amplified insert from pIJ744 and vector DNA, and for pHK02 harboring PC4, the gBlocks ermE_Mon and kasOP*_SP44 were mixed accordingly (Fig. 27). The resulting plasmids were verified by restriction digest, PCR (GGA_test_FW and GGA_test_RV) and sequencing.

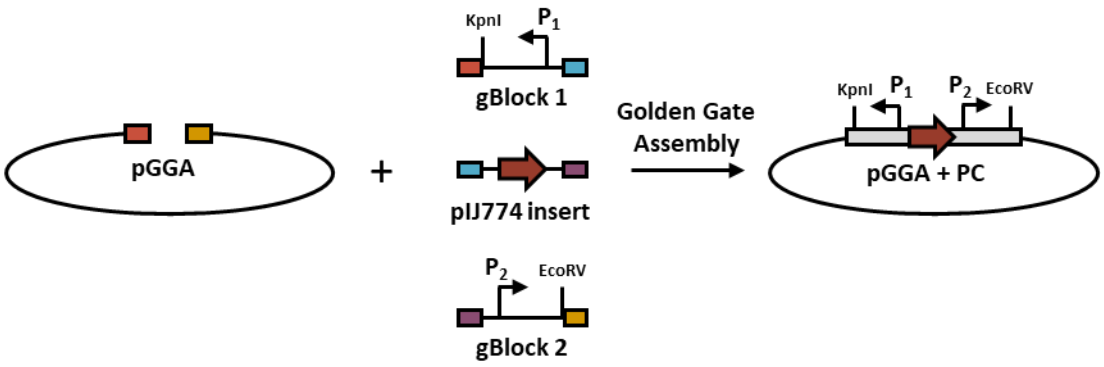


Fig. 27: Schematic representation of the strategy designed to construct bidirectional promoter cassettes PC3 and PC4 by Golden Gate Assembly.

In order to insert these promoters into both bidirectional intergenic regions of the pacidamycin gene cluster by homologous recombination, the cassettes were excised out of pHK01 and pHK02 with KpnI/EcoRV. The respective enzyme recognition sites had been introduced to the borders of the cassette through the promoter gBlocks. After purification, PCR products were amplified with the following primers, which introduced long overhangs for recombination at the desired sites of the BGC: a) PC3-4_npsP8P4_FW and PC3_npsP8P4_RV for PC3 in between *npsP4* and *npsP8*, b) PC3-4_pac4_FW and PC3_pac3_RV for PC3 in between *pac3* and *pac4* and c) PC3-4_pac4_FW and PC4_pac3_RV for PC4 in between *pac3* and *pac4* (Fig. 28). The former fragment was targeted on pacHK03, whilst the latter two were knocked into pacRS03. On pacHK12 and pacHK09, *ermE*p* (pUWL-apra_oriT) was inserted upstream of *npsP4* and *pac3*, respectively, and *ermE*p* (Montiel *et al.*)[136] upstream of *npsP8* and *pac4*. Regarding the PC4 knock-in, *kasOp*_SP44* was inserted upstream of *pac3* and *ermE*p* (Montiel *et al.*)[136] upstream of *pac4*.

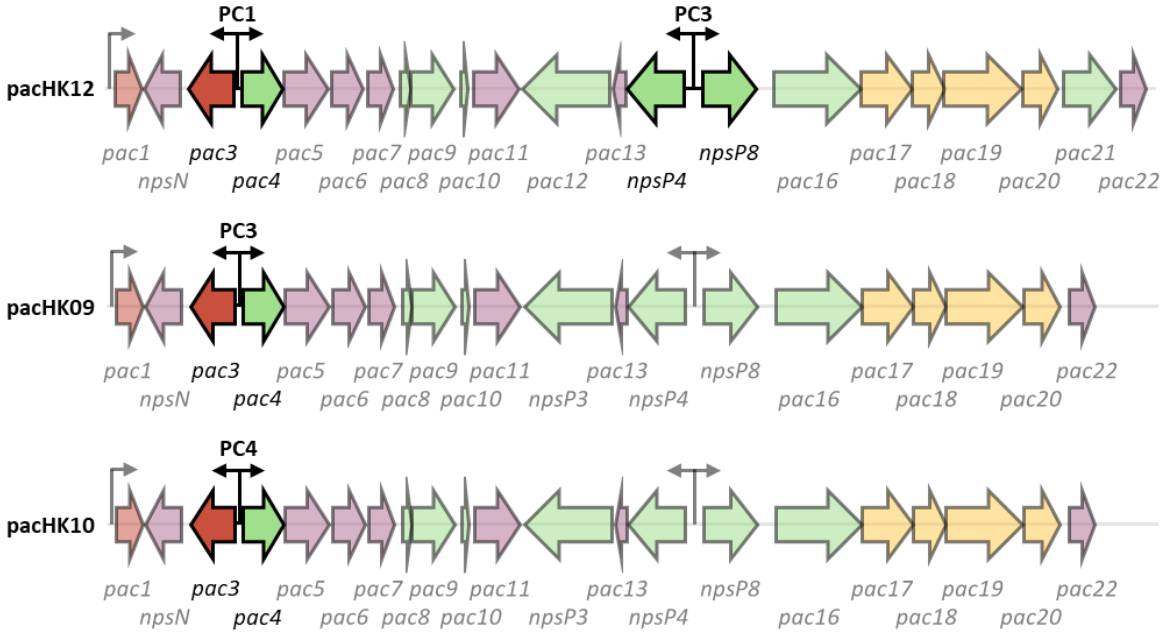


Fig. 28: Schematic representation of the promoter replacements conducted with PC3 and PC4 and the resulting BGCs encoded on pacHK12, pacHK09 and pacHK10.

Otherwise, the process was conducted as previously described for PC2, where the apramycin resistance marker was removed by Cre-mediated excision. The resulting cosmids pacHK09, pacHK10 and pacHK12 were verified by restriction analysis, PCR and sequencing. After conjugation with *S. albus* J1074/pRS02 and *S. albus* J1074/pRS04, the obtained and verified mutant strains were cultivated and analyzed by LC-MS.

Firstly, the mutant strains *S. albus* J1074/pRS02/pacHK03 and *S. albus* J1074/pRS02/pacHK12 were compared to investigate the effect of the knock-in of PC3 in between *npsP4* and npsP8 on pacHK03. As displayed in Fig. 29, no UPA production was detectable subsequent to the promoter exchange. While the first three chromatograms correspond to *S. albus* J1074/pRS02/pacHK03, where clear peaks are visible in the EICs of met-pacidamycin 4 (*m/z* 864.3 $[M+H]^+$) and met-pacidamycin D (*m/z* 772.3 $[M+H]^+$) and smaller ones in the UV-chromatogram, the latter three correlate to *S. albus* J1074/pRS02/pacHK12. Herein, no EIC peaks are visible, while the UV-chromatogram displays a slight decrease in signal intensity at the respective retention times. Similar results were obtained for the remaining major compounds mureidomycin A, met-pacidamycin 5 and met-pacidamycin S (EICs depicted in Appendix Fig. S4). Since three separate promoter replacements between *npsP4* and *npsP8* were unsuccessful, this site seemed to be unsuitable for the insertion of a strong, bidirectional promoter cassette.

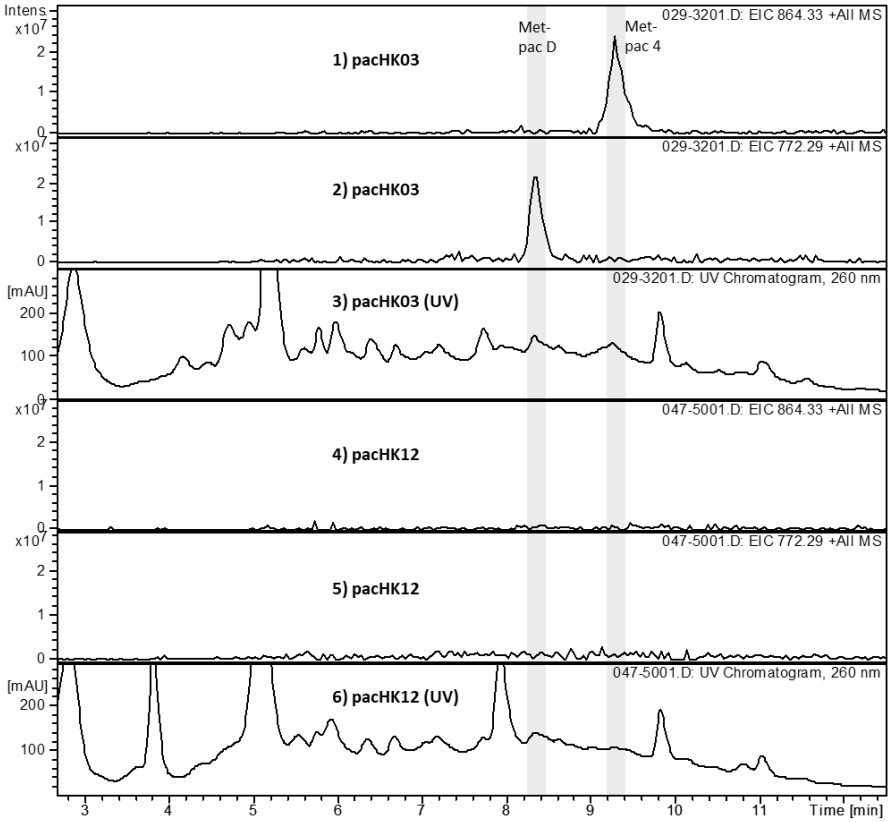


Fig. 29: LC-MS analysis of knock-in of PC3 between *npsP4* and *npsP8* on pacHK03 (top to bottom): 1) EIC of met-pacidamycin 4 (*m/z* 864.3 $[M+H]^+$) in *S. albus* J1074/pRS02/pacHK03, 2) EIC of met-pacidamycin D (*m/z* 772.3 $[M+H]^+$) in *S. albus* J1074/pRS02/pacHK03, 3) UV-Chromatogram 260 nm of *S. albus* J1074/pRS02/pacHK03, 4) EIC of met-pacidamycin 4 (*m/z* 864.3 $[M+H]^+$) in *S. albus* J1074/pRS02/pacHK12, 5) EIC of met-pacidamycin D (*m/z* 772.3 $[M+H]^+$) in *S. albus* J1074/pRS02/pacHK12 and 6) UV-Chromatogram 260 nm of *S. albus* J1074/pRS02/pacHK12.

When comparing *S. albus*/pRS02/pacRS03 and *S. albus*/pRS02/pacHK10 in order to determine the influence of the PC4 knock-in between *pac3* and *pac4*, a very significant production decrease could be noted for both major compounds mureidomycin A and met-pacidamycin 5 (Fig. 30). This cassette was, therefore, considered unsuitable for a promoter replacement at this site.

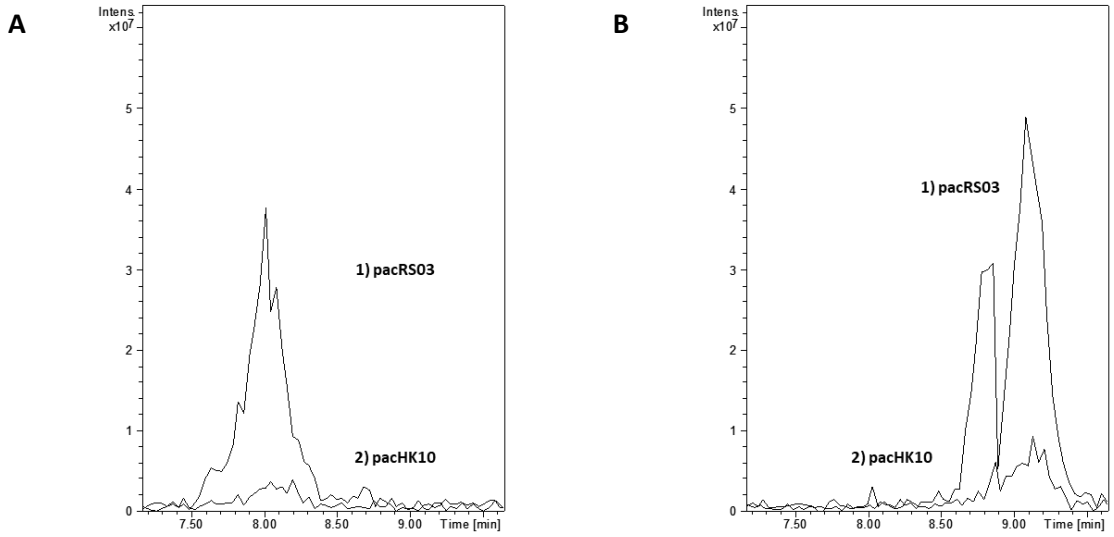


Fig. 30: LC-MS analysis of knock-in of PC4 in between *pac3* and *pac4* on pacRS03: Extracted ion chromatograms of A) mureidomycin A (*m/z* 841.3 $[M+H]^+$) and B) met-pacidamycin 5 (*m/z* 825.3 $[M+H]^+$) are displayed for: 1) *S. albus* J1074/pRS02/pacRS03 and 2) *S. albus* J1074/pRS02/pacHK10.

Furthermore, no significant influence on mureidomycin A production was detected after the knock-in of PC3 between *pac3* and *pac4* (Fig. 31). While compound production could only be detected in one exconjugant of *S. albus*/pRS02/pacHK09, a slight production increase was noted for mureidomycin A in comparison with *S. albus*/pRS02/pacRS03. Regarding met-pacidamycin 5, no significant influence on production rates was observed. For the respective mutants harboring pRS04, met-pacidamycin 5 production was again not affected by the promoter swap, while mureidomycin A levels were slightly decreased.

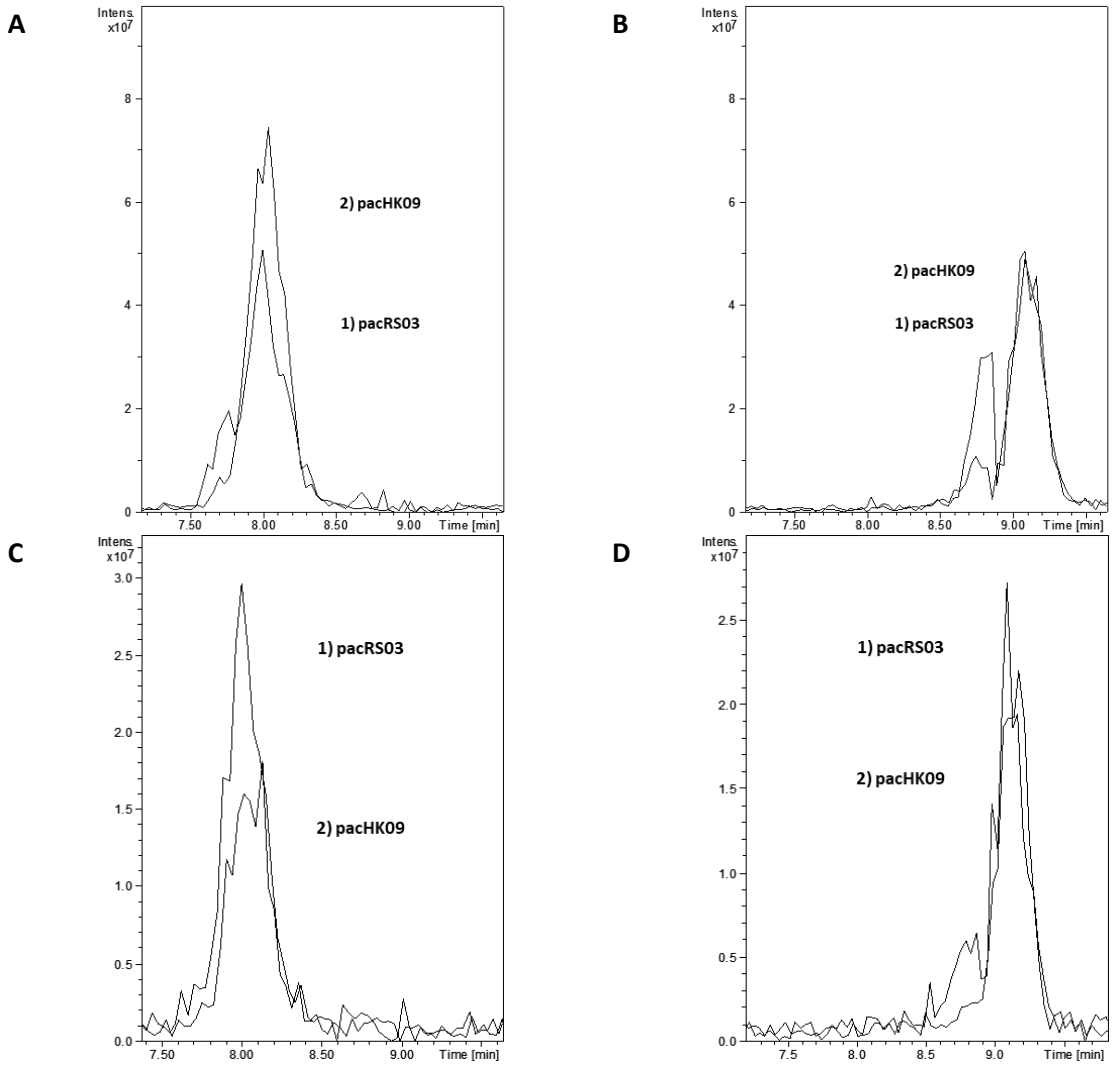


Fig. 31: LC-MS analysis of knock-in of PC3 in between *pac3* and *pac4* on pacRS03: Extracted ion chromatograms of mureidomycin A (*m/z* 841.3 $[M+H]^+$, A and C) and met-pacidamycin 5 (*m/z* 825.3 $[M+H]^+$, B and D) are displayed for:
Top: 1) *S. albus* J1074/pRS02/pacRS03 and 2) *S. albus* J1074/pRS02/pacHK09
Bottom: 1) *S. albus* J1074/pRS04/pacRS03 and 2) *S. albus* J1074/pRS04/pacHK09.

The previous findings were summarized in the graph of Fig. 32, where AUCs of mureidomycin A EICs were normalized by cell dry weight and then plotted against the respective producer strains. The significant reduction in UPA levels caused by PC4 is evident. Contrastingly, while the PC3 insertion led to a slight production improvement, when combined with the positive regulator *npsM*, the minimally positive effect was negated. Overall, the promoter replacement with PC3 did not affect UPA production yield significantly in comparison with the native promoters.

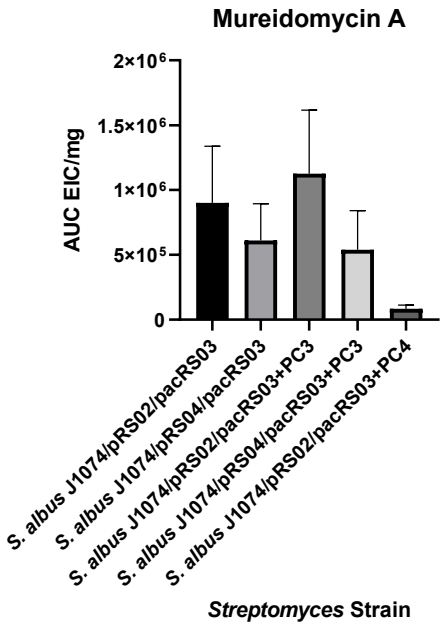


Fig. 32: LC-MS analysis of further promoter swaps on pacRS03; AUCs of mureidomycin A EICs are plotted against mutant strains harboring PC3 and PC4 (between *pac3* and *pac4*) and reference strains in biological and technical replicates (normalized by cell dry weight).

3.1.2 Investigation of operon structure by RNA-sequencing

Since the promoter replacement between *pac3* and *pac4* with PC1 had led to increased mureidomycin A production levels, the respective mutants were analyzed by mRNA sequencing (RNA-seq), in order to investigate, whether this elevation was directly correlated to transcription levels of biosynthetic genes. This data could also elucidate operon structure, visualize silencing effects potentially caused by read-through due to leaky terminators and determine additional sites for promoter replacements or other modifications.

The cultivation and sample preparation for this experiment were carried out in collaboration with Richard Sonnengruen (Pharmaceutical Biology, University of Tuebingen), by whom mutant strains *S. albus* J1074/pacRS01 (exconjugants II and III) and *S. albus* J1074/pRS02/pacRS01 (exconjugant I) were supplied, which harbor the modified pacidamycin BGC. Furthermore, mutants carrying the native pacidamycin BGC prior to any modifications (*S. albus* J1074/pacNH01, exconjugants I, II and III) were obtained from previous work by Dr. Nils Hauck[18]. These strains were prepared in 50 mL TSB precultures, alongside *S. albus* J1074/pRS02/pacHK03 (exconjugants I and III) and *S. albus* J1074/pRS04/pacHK03 (exconjugants I and II), which contained the modified gene cluster with the first promoter swap. Prior to inoculation of the main culture, all preculture pellets were normalized by bacterial wet weight. Subsequent to cultivation for 2 or 4 days, pellets were harvested by centrifugation, immediately frozen with liquid nitrogen and sent on dry ice to Vertis Biotechnologie AG (Freising, Germany) for further processing. There, RNA isolation and sequencing were conducted

according to the succeeding procedure, as described in the respective SOP (standard operating procedure) developed by Vertis Biotechnologie AG. Firstly, total RNA of all samples was isolated, by treatment with a bead mill for cell disruption and homogenization and by subsequently treating samples with the mirVana RNA isolation kit (with DNase treatment). Verification was conducted by capillary electrophoresis, and the respective concentrations and specific amounts of isolated total RNA preparations were displayed in Table 24.

Table 24: RNA-Seq samples and respective amount of total isolated RNA

No.	Sample description	Concentration (ng/µL)	Total amount (µg)
1	Sa_pacNH01_I_S11	553.7	33.2
2	Sa_pacNH01_II_S12	218.1	13.1
3	Sa_pacNH01_III_S13	174.5	10.5
4	Sa_pacRS01_II_S15	501.0	30.1
5	Sa_pacRS01_III_S16	596.2	35.8
6	Sa_pacRS01_pRS02_I_S17	435.8	26.1
7	Sa_pacHK03_pRS02_I_2d_S26	756.3	45.4
8	Sa_pacHK03_pRS02_I_4d_S29	1,117.9	67.1
9	Sa_pacHK03_pRS02_III_4d_S31	468.1	28.1
10	Sa_pacHK03_pRS04_I_2d_S32	1,002.1	60.1
11	Sa_pacHK03_pRS04_I_4d_S35	1,114.5	66.9
12	Sa_pacHK03_pRS04_II_4d_S36	901.3	54.1

After ribosomal RNA depletion, the samples were fragmented by ultrasound and linked with a 3' end oligonucleotide adapter. Hence, cDNA synthesis was conducted, utilizing the adapter as a primer. This procedure was repeated with a 3' adapter of the newly synthetized strand, after interim purification. In the ensuing PCR, the resulting cDNA was amplified by PCR to about 10 -20 ng/µL and then purified and examined by capillary electrophoresis once more. The resulting cDNA samples were pooled in approximately equimolar amounts, size fractionated in the range of 200 - 600 bp and sequenced on an Illumina NextSeq 500 system.

The obtained data was kindly processed and aligned by Theresa Harbig of the working group of Prof. Dr. Kay Nieselt (University of Tuebingen), by whom also the percentages of reads which aligned with *S. albus* J1074 and *E. coli* DNA and the percentage of the samples mapped with rRNA after depletion were supplied (Table 25). While for all samples a slight contamination with *E. coli* was observed, the majority of reads (82.2 - 93.2 %) were aligned with *S. albus* J1074 cDNA. However, following criteria should be taken into consideration knowing that, typically, alignment to the sequenced sample exceeds 95 %. Moreover, a sample is generally considered to be of high quality, when less than 5 % of reads are aligned with rRNA[142]. Therefore, exemplary samples were chosen to be displayed based on high *S. albus* J1074 DNA and low rRNA alignment, while the remaining ones were depicted in Appendix Fig. S15 - Fig. S21.

Table 25: Percentage of reads in RNA-Seq samples aligned to *S. albus* J1074 DNA, *E. coli* DNA and *S. albus* J1074 rRNA

No.	**Sample description**	***S. albus* J1074 (% aligned)**	***E. coli* (% aligned)**	**rRNA *S. albus* J1074 (%)**
1	Sa_pacNH01_I_S11	86.10	3.50	5.33
2	Sa_pacNH01_II_S12	82.20	4.60	2.33
3	Sa_pacNH01_III_S13	91.90	1.90	27.71
4	Sa_pacRS01_II_S15	85.00	4.60	12.06
5	Sa_pacRS01_III_S16	93.20	1.10	62.86
6	Sa_pacRS01_pRS02_I_S17	87.10	3.70	13.26
7	Sa_pacHK03_pRS02_I_2d_S26	86.50	3.80	1.82
8	Sa_pacHK03_pRS02_I_4d_S29	85.20	4.60	4.60
9	Sa_pacHK03_pRS02_III_4d_S31	88.50	3.00	1.60
10	Sa_pacHK03_pRS04_I_2d_S32	83.90	4.00	2.18
11	Sa_pacHK03_pRS04_I_4d_S35	90.20	2.20	0.70
12	Sa_pacHK03_pRS04_II_4d_S36	86.30	2.40	0.69

Visualization of alignments was conducted in the present study with the software IGB (Integrated Genome Browser). Firstly, the alignment graphs of *S. albus* J1074/pacNH01 were observed (Fig. 33, Appendix Fig. S15 and Fig. S16). Therein, an increase in transcription levels was observed upstream of *pac3* (*pacC*)/*pac4* (*pacD*) and *pac14* (*pacN*)/*pac15* (*pacO*) in both directions, which was expected at these bidirectional promoter sites. Additionally, transcription rates were elevated starting at *pac16* (*pacP*) and *pac21* (*pacU*), which indicates the presence of unidirectional promoters upstream of the respective genes. Transcription rates are increased at the beginning of the operons and decline over the length of the respective gene sequence, which led to the hypothesis that the pacidamycin BGC is transcribed in the following operon structure:

- Operon 1: *pac1* (*pacA*)
- Operon 2: *pac3* and *pac2* (*pacC* and *pacB*)
- Operon 3: *pac4* - *pac11* (*pacD* - *pacK*)
- Operon 4: *pac14* - *pac12* (*pacN* - *pacL*)
- Operon 5: *pac15* (*pacO*)
- Operon 6: *pac16* - *pac20* (*pacP* - *pacT*)
- Operon7: *pac21* and *pac22* (*pacU* and *pacV*)

While *pac1* (*pacA*) was not transcribed properly, a promoter needs to be situated upstream of *pac1*, since this gene is located at the border of the cluster. In the three examined mutants, reads were mapped on the opposite strand of *pac1*, which might indicate further silencing of the few detected reads on the sense strand. Otherwise, no read-through was observed. While the remaining operons were transcribed, only few reads mapped at the last gene of operon 3 (*pac11*/*pacK*) and transcription of operon 6 dropped shortly after the expected promoter region. Highly similar pictures were observed for the other two exconjugants (Appendix Fig. S15 and Fig. S16), regarding operon structure, read quantities and tendencies in shapes of mapped reads. Overall, reads counts were low, averaging 200 - 500. Maximal read height, where promoters were situated, was 4500.

Modifications, which were conducted in order to transform pacNH01 into pacRS01, were the exchanges of *pac2* for *npsN*, *pac14* for *npsP4* and *pac15* for *npsP8* (orthologous genes of the napsamycin BGC). In the respective mutant strains *S. albus* J1074/pacRS01 (exconjugants II and III), transcription levels were visibly reduced in all operons to less than 250 mapped reads (Fig. 34 and Appendix Fig. S17). The swapped gene *npsN* was hardly transcribed, while in operons 4 and 5, which each harbor a swapped gene at its 5' end, mapped reads at the beginning of the operons dropped from 4500 to approximately 500, and, hence, transcription was low throughout the operons.

Furthermore, the integration of plasmid pRS02 slightly reduced transcription levels of the entire cluster (Fig. 35), when compared with *S. albus* J1074/pacRS01 lacking plasmid pRS02. Operons 1, 2, 5 and 6 were barely transcribed, while mapped reads for all remaining operons were below 200. Coverage

plots of the plasmid within the same sample were also low, with mostly less than 500 reads mapped to the sequence. The first gene, the NRPS A-domain *pac21h* was transcribed in a low rate, while the phenylalanine hydroxylase *phhA* was hardly transcribed, despite the native promoter being situated upstream of *phhA* (Fig. 36).

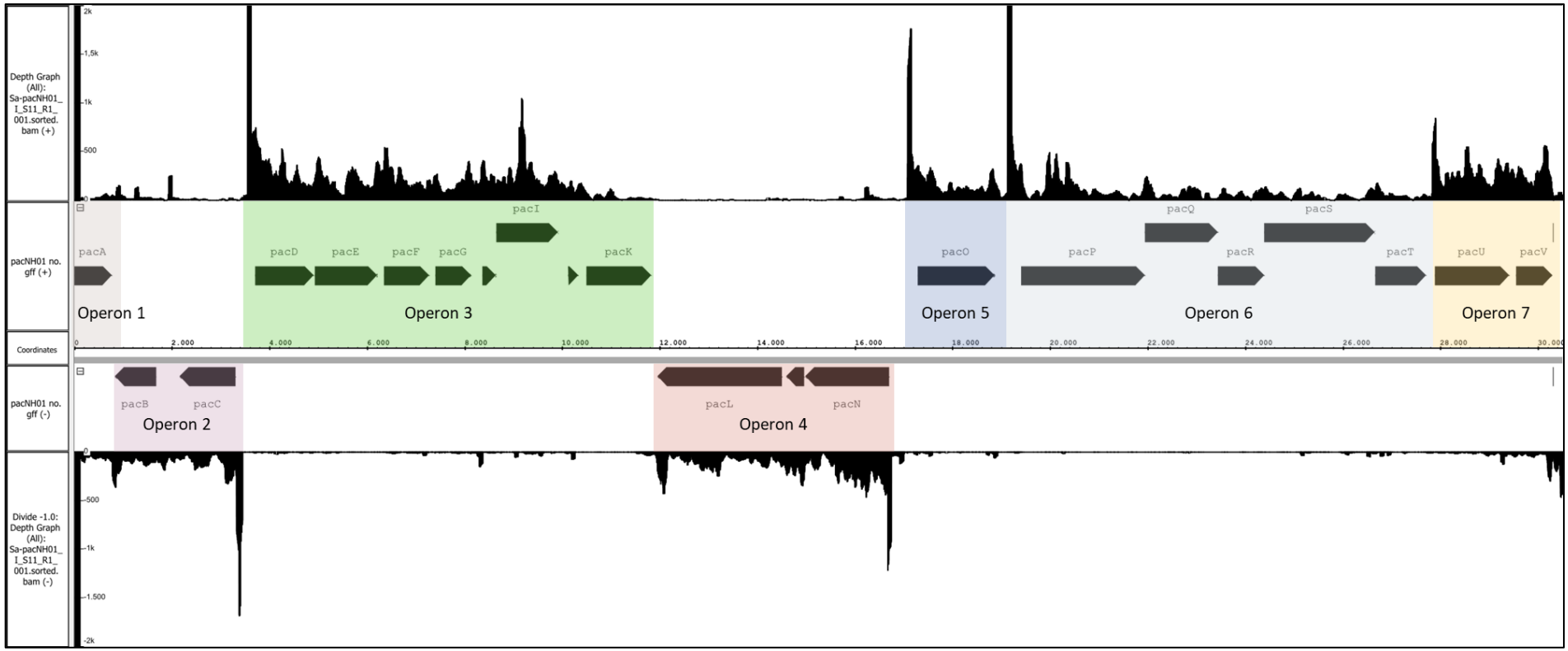


Fig. 33: RNA sequencing results regarding the pacidamycin BGC of strain *S. albus* J1074/pacNH01; exconjugant I (native pacidamycin biosynthetic gene cluster) after 4 days of cultivation. While the annotation of the BGC is depicted with arrows on the x-axis in the middle of the graph and separated into sense and antisense strands, the y-axis displays the coverage plots for the respective strands. The postulated operons 1 - 7 were labeled with different colors, depending on sites displaying a strong increase in transcription or due to the genetic organization (*pacA*). In this case, the annotation of Zhang *et al.* (2010)[17] was utilized, by which the genes were labeled *pacA* - *pacV* (see 1.2). Furthermore, the gene cluster was inverted in all following graphs.

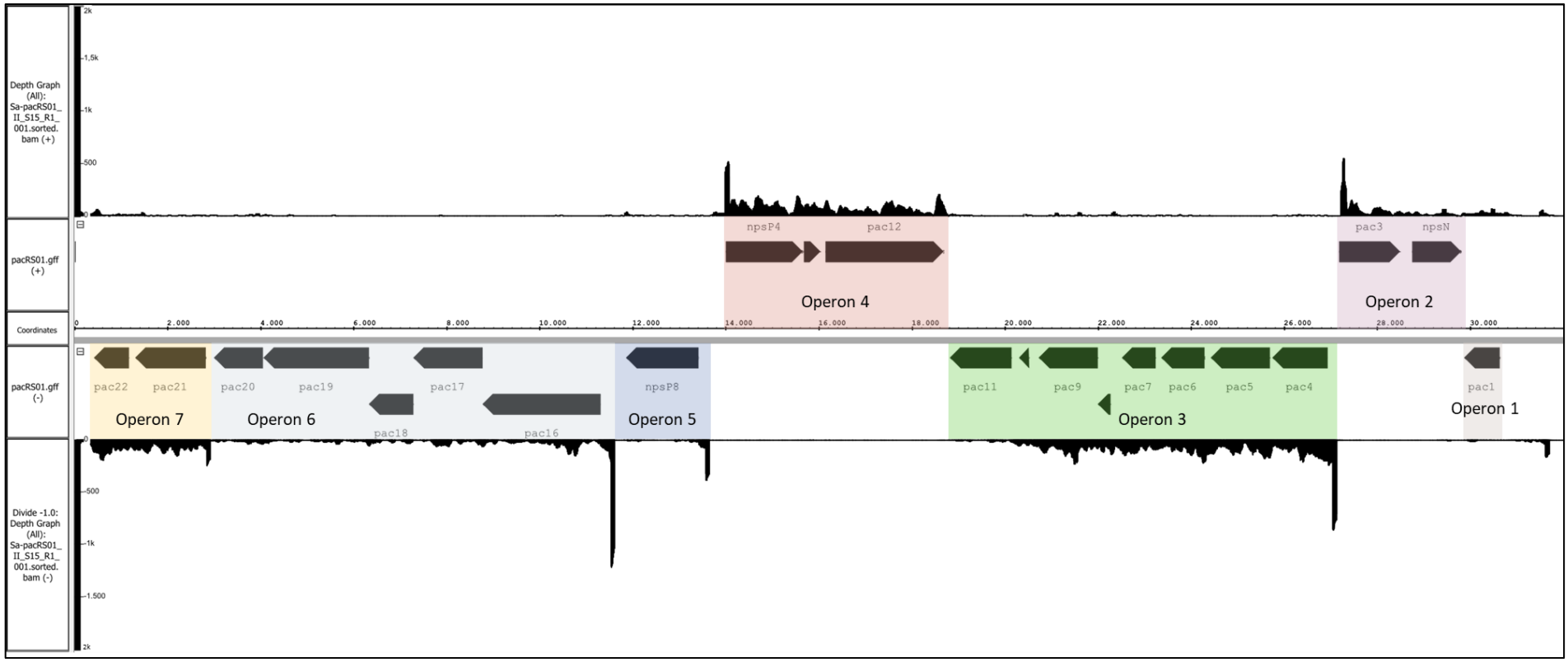


Fig. 34: RNA sequencing results regarding the pacidamycin BGC of strain *S. albus* J1074/pacRS01; exconjugant II (modified pacidamycin biosynthetic gene cluster) after 4 days of cultivation. While the annotation of the BGC is depicted with arrows on the x-axis in the middle of the graph and separated into sense and antisense strands, the y-axis displays the coverage plots for the respective strands. The postulated operons 1 - 7 were labeled with different colors in accordance with the other graphs, depending on sites displaying a strong increase in transcription or due to the genetic organization (*pac1*). In this and all following cases, the annotation of Rackham *et al.* (2010)[121] was utilized, by which the genes were labeled *pac1* - *pac22* (see 1.2).

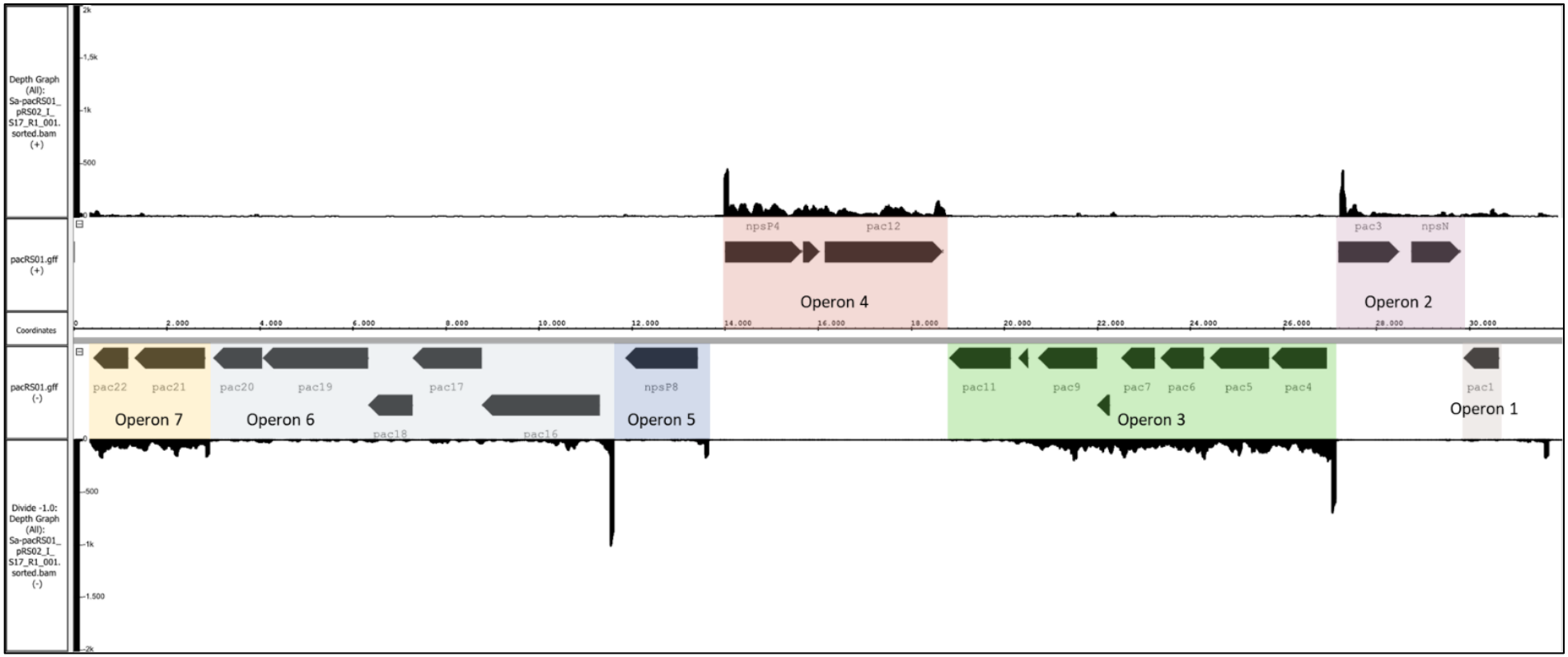


Fig. 35: RNA sequencing results regarding the pacidamycin BGC of strain *S. albus* J1074/pRS02/pacRS01; exconjugant I (modified pacidamycin biosynthetic gene cluster in combination with plasmid pRS02 harboring genes for *m*-tyrosine incorporation and biosynthesis) after 4 days of cultivation. While the annotation of the BGC is depicted with arrows on the x-axis in the middle of the graph and separated into sense and antisense strands, the y-axis displays the coverage plots for the respective strands. The postulated operons 1 - 7 were labeled with different colors in accordance with the other graphs, depending on sites displaying a strong increase in transcription or due to the genetic organization (*pac1*).

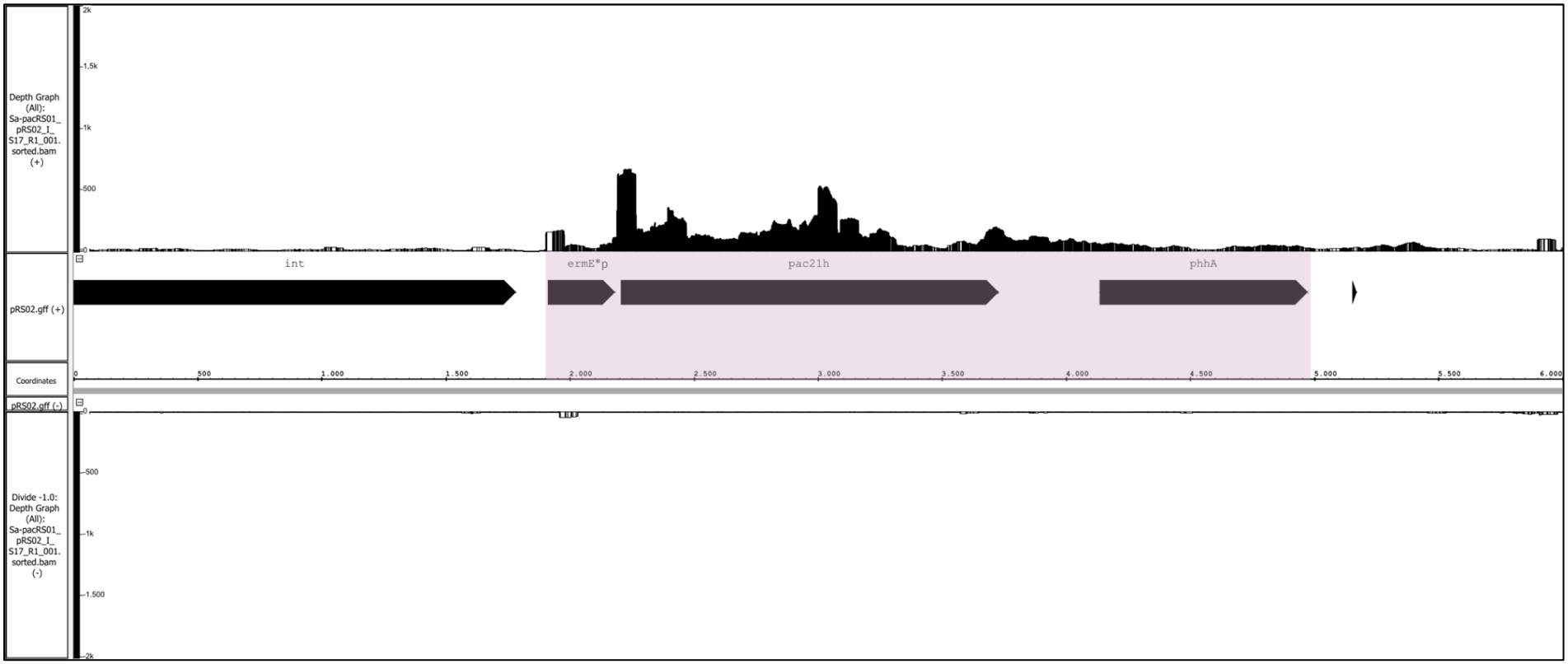


Fig. 36: RNA sequencing results regarding the plasmid pRS02 of strain *S. albus* J1074/pRS02/pacRS01; exconjugant I (modified pacidamycin biosynthetic gene cluster in combination with plasmid pRS02 harboring genes for *m*-tyrosine incorporation and biosynthesis) after 4 days of cultivation. While part of the annotation of the plasmid is depicted with arrows on the x-axis in the middle of the graph and separated into sense and antisense strands, the y-axis displays the coverage plots for the respective strands. The postulated operon was labeled with a colored box, depending on sites displaying a strong increase in transcription.

Contrastingly, in *S. albus* J1074/pRS02/pacHK03 the replacement of the intergenic region between *pac3* and *pac4* with promoter cassette 1 (PC1) drastically improved transcription levels, with the maximal read count at the promoter site upstream of *pac3* nearing 40,000 (Fig. 37, Fig. 39 and Appendix Fig. S18). Herein, operon structure remained as previously observed. While operons 2 and 3, which were situated under direct control of the synthetic promoters, were most strongly transcribed (read count up to 1000), for all remaining operons transcription was elevated, as well. However, transcription rates of operon 1 and operon 5 remained low, while generally, read count distribution was observed to be highly similar in all mutants. Furthermore, a strong increase in reads on the antisense strand of *pac1* was noted, which indicated silencing of the gene. Additionally, transcription appeared to be slightly higher in mutant strains after 2 days of cultivation, in contrast with the ones cultivated for 4 days, although solely one mutant had been measured at 2 days. Regarding the plasmid pRS02 within the respective samples, transcription levels were strongly elevated in contrast to *S. albus* J1074/pRS02/pacRS01 (Fig. 38, Fig. 40 and Appendix Fig. S19). Read counts were comparable between the three exconjugants (after 2 and 4 days of cultivation) and increased to up to 5500. Moreover, the phenylalanine hydroxylase *phhA* was fully transcribed within these constructs on the same operon.

Lastly, alignments for mutant strains harboring pacHK03 and plasmid pRS04 were examined. This plasmid had been constructed through the knock-in of the cluster-specific positive regulator of the napsamycin BGC *npsM* into pRS02 under the control of the strong, constitutive promoter *ermE*p*. After 2 days of cultivation, transcription levels were strongly increased in *S. albus* J1074/pRS04/pacHK03 (maximal read count of approximately 40,000) in comparison with the respective mutants at 4 days of cultivation and also in comparison to *S. albus* J1074/pRS02/pacHK03 after 2 days (Fig. 41, Fig. 43 and Appendix Fig. S20). Patterns of transcription and gaps in the read count within a gene remained very similar within the mutants. Furthermore, operons 3 and 7 were most strongly transcribed, followed by operons 2, 4 and then 6. Regarding the remaining two operons 1 and 5, transcription was visibly elevated, yet comparatively low. Since for operon 2 read counts were highly increased, the reads indicating silencing of pac1 were further increased as read-through. Concerning the alignments for the plasmids pRS04 of the respective samples, mapped reads increased from 2 to 4 days of cultivation and were comparable to pRS02 in *S. albus* J1074/pRS02/pacHK03, regarding *pac21h* and *phhA* (Fig. 42, Fig. 44 and Appendix Fig. S21). However, not only was *npsM* transcribed at a lower rate than *pac21h*, especially after 4 days of cultivation, a high count of reads was mapped to the respective antisense strand, which might be silencing *npsM* and, thus, downregulating the production increase caused by the regulator.

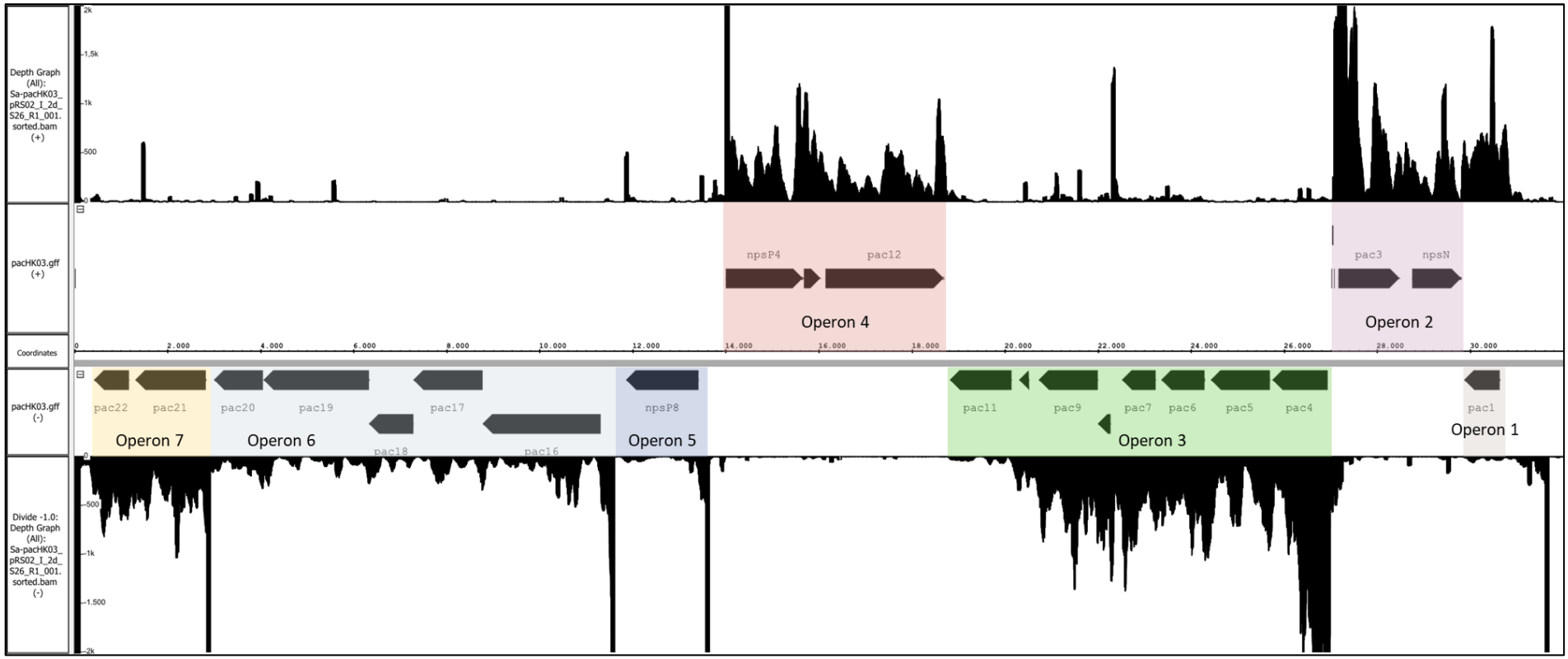


Fig. 37: RNA sequencing results regarding the pacidamycin BGC of strain *S. albus* J1074/pRS02/pacHK03; exconjugant I (modified pacidamycin biosynthetic gene cluster with bidirectional promoter cassette 1 between *pac3* and *pac4* in combination with plasmid pRS02 harboring genes for *m*-tyrosine incorporation and biosynthesis) after 2 days of cultivation. While the annotation of the BGC is depicted with arrows on the x-axis in the middle of the graph and separated into sense and antisense strands, the y-axis displays the coverage plots for the respective strands. The postulated operons 1 - 7 were labeled with different colors in accordance with the other graphs, depending on sites displaying a strong increase in transcription or due to the genetic organization (*pac1*).

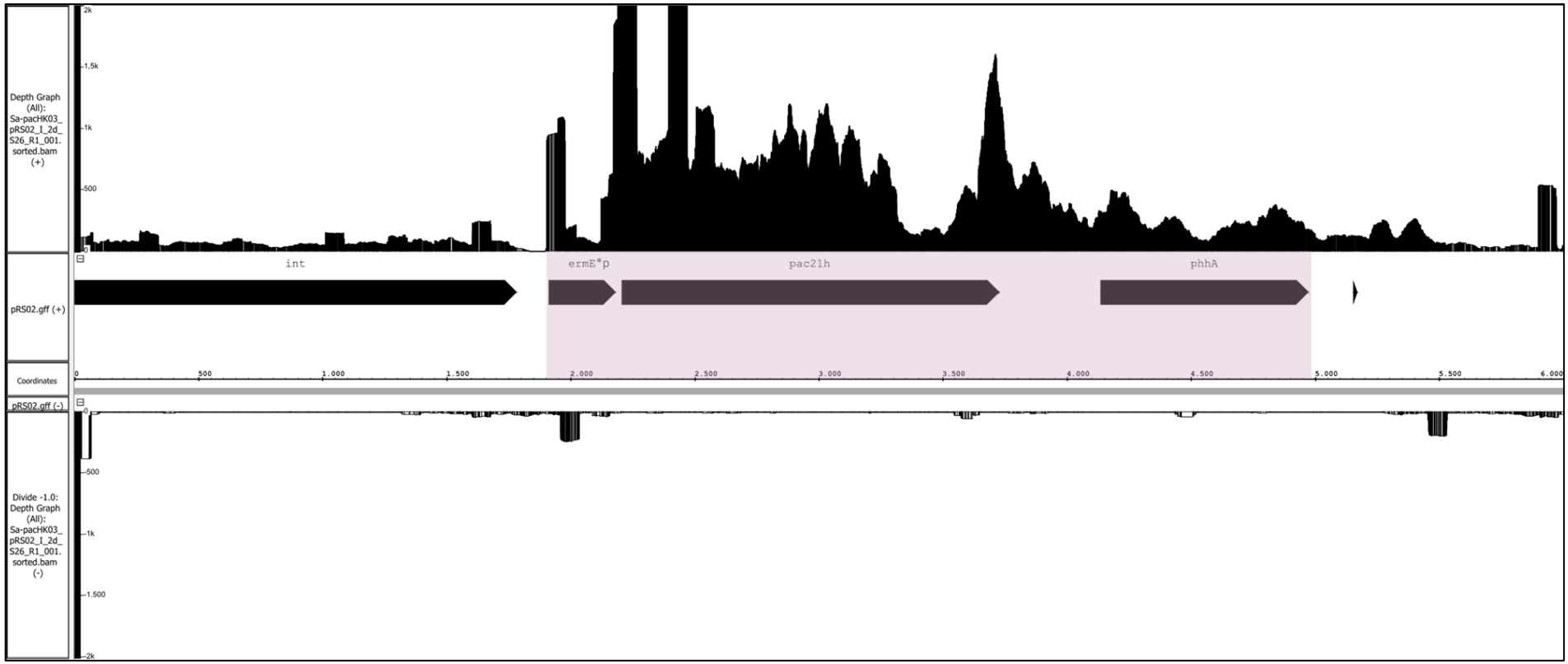


Fig. 38: RNA sequencing results regarding the plasmid pRS02 of strain *S. albus* J1074/pRS02/pacHK03; exconjugant I (modified pacidamycin biosynthetic gene cluster with bidirectional promoter cassette 1 between *pac3* and *pac4* in combination with plasmid pRS02 harboring genes for *m*-tyrosine incorporation and biosynthesis) after 2 days of cultivation. While part of the annotation of the plasmid is depicted with arrows on the x-axis in the middle of the graph and separated into sense and antisense strands, the y-axis displays the coverage plots for the respective strands. The postulated operon was labeled with a colored box.

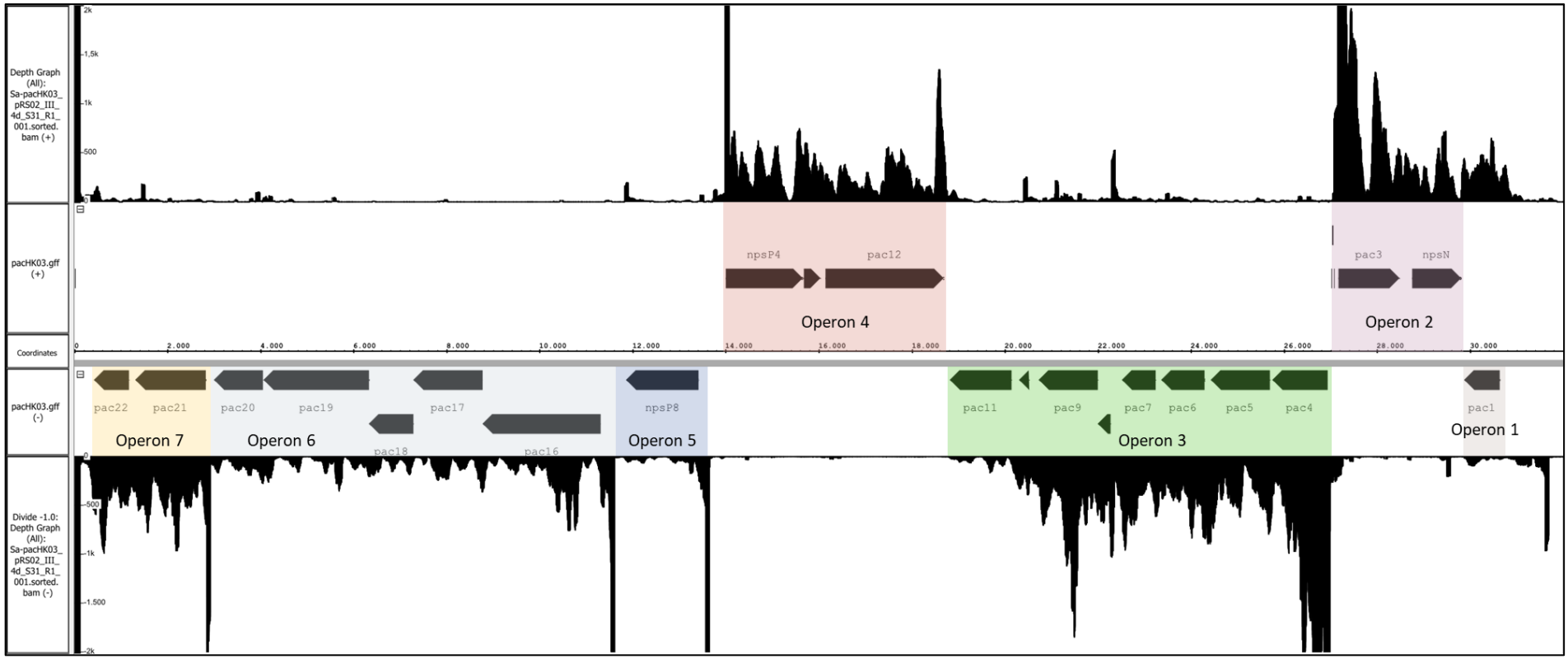


Fig. 39: RNA sequencing results regarding the pacidamycin BGC of strain *S. albus* J1074/pRS02/pacHK03; exconjugant III (modified pacidamycin biosynthetic gene cluster with bidirectional promoter cassette 1 between *pac3* and *pac4* in combination with plasmid pRS02 harboring genes for *m*-tyrosine incorporation and biosynthesis) after 4 days of cultivation. While the annotation of the BGC is depicted with arrows on the x-axis in the middle of the graph and separated into sense and antisense strands, the y-axis displays the coverage plots for the respective strands. The postulated operons 1 - 7 were labeled with different colors in accordance with the other graphs, depending on sites displaying a strong increase in transcription or due to the genetic organization (*pac1*).

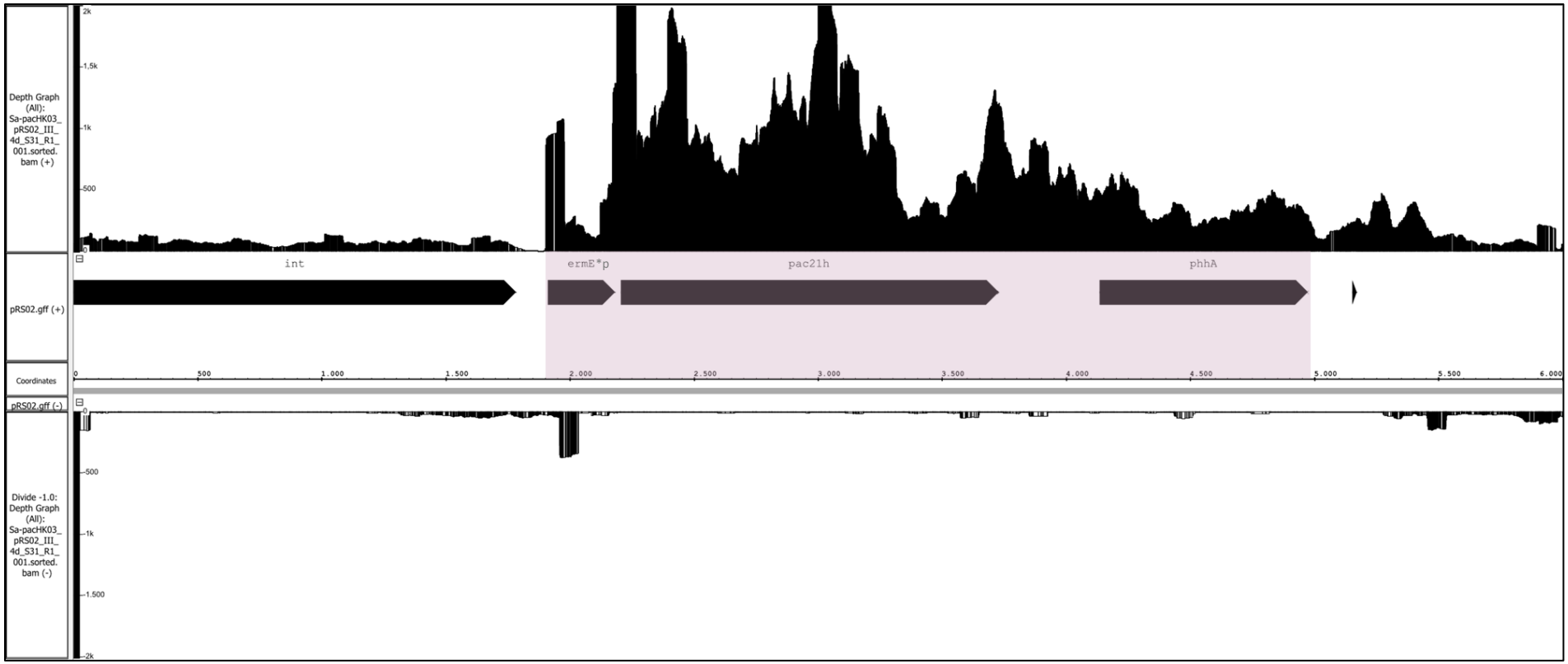


Fig. 40: RNA sequencing results regarding the plasmid pRS02 of strain *S. albus* J1074/pRS02/pacHK03; exconjugant III (modified pacidamycin biosynthetic gene cluster with bidirectional promoter cassette 1 between *pac3* and *pac4* in combination with plasmid pRS02 harboring genes for *m*-tyrosine incorporation and biosynthesis) after 4 days of cultivation. While part of the annotation of the plasmid is depicted with arrows on the x-axis in the middle of the graph and separated into sense and antisense strands, the y-axis displays the coverage plots for the respective strands. The postulated operon was labeled with a colored box.

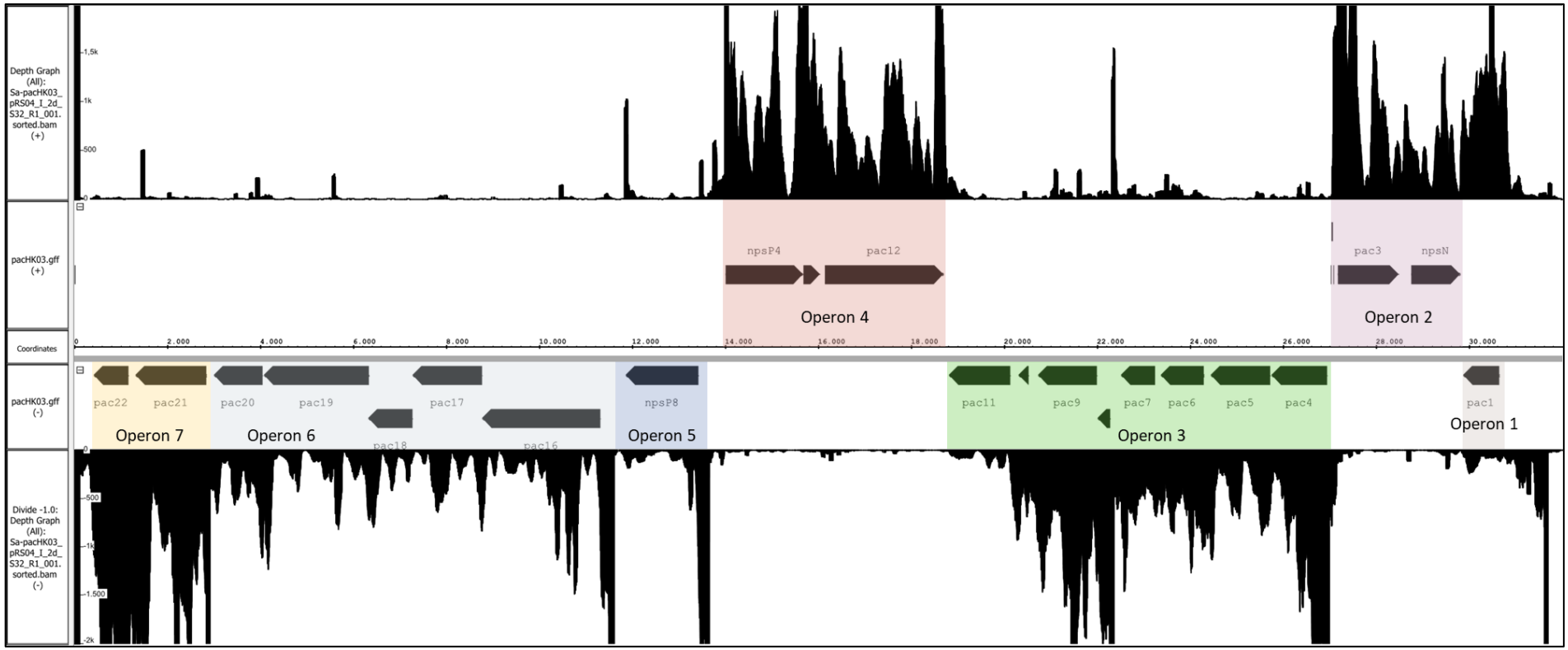


Fig. 41: RNA sequencing results regarding the pacidamycin BGC of strain *S. albus* J1074/pRS04/pacHK03; exconjugant I (modified pacidamycin biosynthetic gene cluster with bidirectional promoter cassette 1 between *pac3* and *pac4* in combination with plasmid pRS04 harboring genes for *m*-tyrosine incorporation and biosynthesis and the cluster-specific positive regulator of the napsamycin BGC *npsM*) after 2 days of cultivation. While the annotation of the BGC is depicted with arrows on the x-axis in the middle of the graph and separated into sense and antisense strands, the y-axis displays the coverage plots for the respective strands. The postulated operons 1 - 7 were labeled with different colors in accordance with the other graphs, depending on sites displaying a strong increase in transcription or due to the genetic organization (*pac1*).

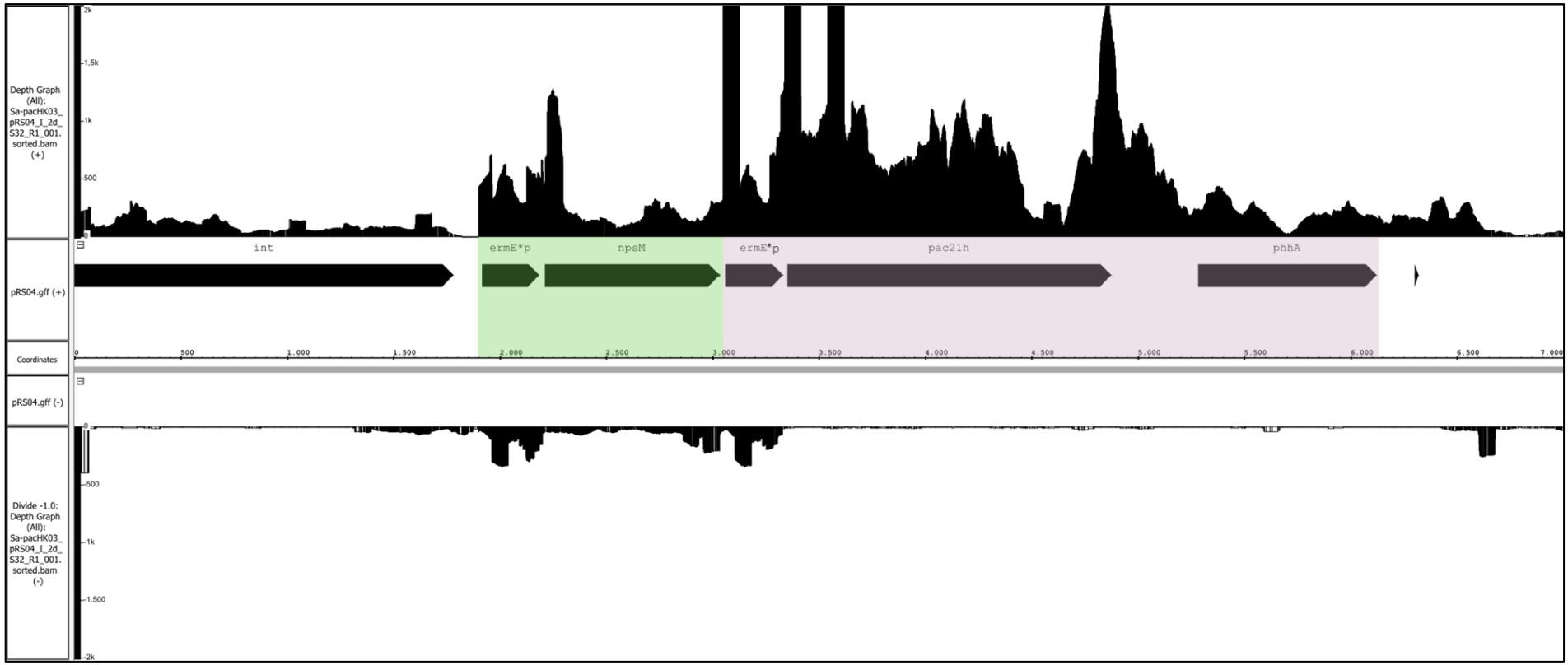


Fig. 42: RNA sequencing results regarding the plasmid pRS04 of strain *S. albus* J1074/pRS04/pacHK03; exconjugant I (modified pacidamycin biosynthetic gene cluster with bidirectional promoter cassette 1 between *pac3* and *pac4* in combination with plasmid pRS04 harboring genes for *m*-tyrosine incorporation and biosynthesis and the cluster-specific positive regulator of the napsamycin BGC *npsM*) after 2 days of cultivation. While part of the annotation of the plasmid is depicted with arrows on the x-axis in the middle of the graph and separated into sense and antisense strands, the y-axis displays the coverage plots for the respective strands. The postulated operons were labeled with colored boxes.

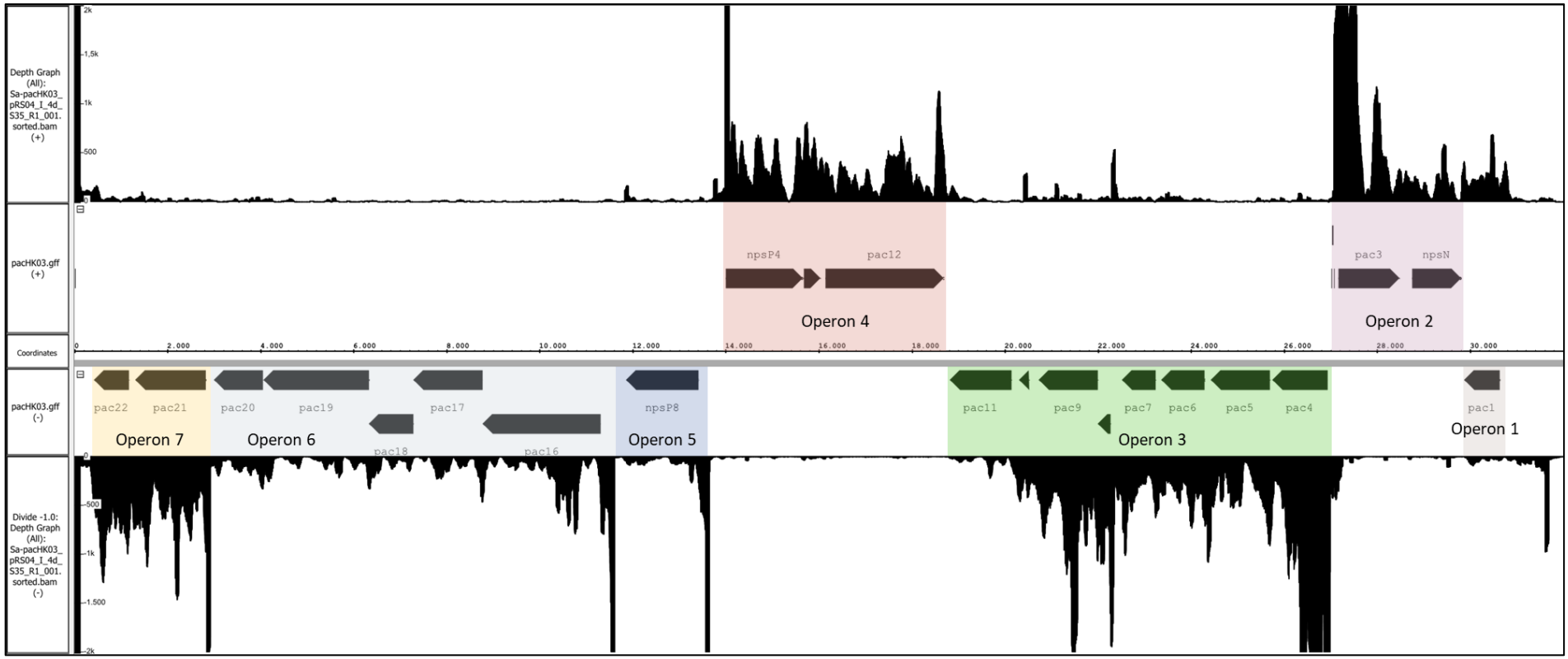


Fig. 43: RNA sequencing results regarding the pacidamycin BGC of strain *S. albus* J1074/pRS04/pacHK03; exconjugant I (modified pacidamycin biosynthetic gene cluster with bidirectional promoter cassette 1 between *pac3* and *pac4* in combination with plasmid pRS04 harboring genes for *m*-tyrosine incorporation and biosynthesis and the cluster-specific positive regulator of the napsamycin BGC *npsM*) after 4 days of cultivation. While the annotation of the BGC is depicted with arrows on the x-axis in the middle of the graph and separated into sense and antisense strands, the y-axis displays the coverage plots for the respective strands. The postulated operons 1 - 7 were labeled with different colors in accordance with the other graphs, depending on sites displaying a strong increase in transcription or due to the genetic organization (*pac1*).

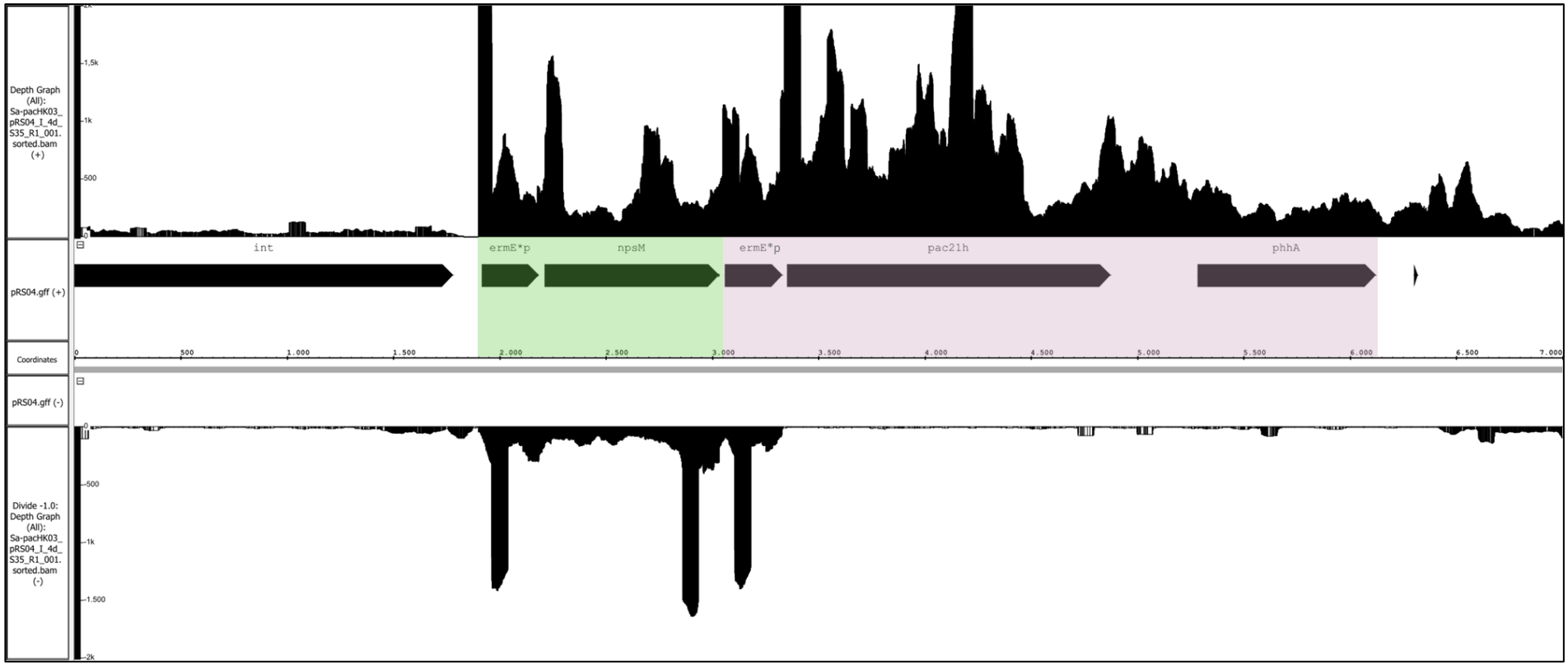


Fig. 44: RNA sequencing results regarding the plasmid pRS04 of strain *S. albus* J1074/pRS04/pacHK03; exconjugant I (modified pacidamycin biosynthetic gene cluster with bidirectional promoter cassette 1 between *pac3* and *pac4* in combination with plasmid pRS04 harboring genes for *m*-tyrosine incorporation and biosynthesis and the cluster-specific positive regulator of the napsamycin BGC *npsM*) after 4 days of cultivation. While part of the annotation of the plasmid is depicted with arrows on the x-axis in the middle of the graph and separated into sense and antisense strands, the y-axis displays the coverage plots for the respective strands. The postulated operons were labeled with colored boxes.

3.1.3 Increased production by optimized heterologous hosts

Moreover, the optimized heterologous hosts *S. albus* Del14 and *S. albus* B2P1 were kindly provided by Prof. Dr. Andriy Luzhetskyy (Saarland University)[133], in order to further improve production yields. More specifically, 15 non-essential biosynthetic gene clusters of secondary metabolites were deleted in *S. albus* J1074, resulting in *S. albus* Del14, in order to reduce the metabolic background, facilitate compound isolation and improve production rates. Its derivative *S. albus* B2P1 was generated through the integration of an additional *phi*C31 *attB* site into its chromosome, to allow for the insertion of multiple copies of biosynthetic gene clusters, which would, theoretically, lead to further production improvements. Furthermore, the fungus-growing attini ant-derived host *S. griseus* CS065 was obtained from an in-lab collection of Actinomycetes strains of Prof. Dr. Carmen Méndez (Universidad de Oviedo)[134,143], and was proven to harbor the potential to increase the biosynthesis of natural products.[144]

The cosmid containing the modified pacidamycin biosynthetic gene cluster harboring the first bidirectional promoter cassette between *pac3* and *pac4* (pacHK11) was transformed into *E. coli* ET12567 and conjugated with the aforementioned hosts, which had already integrated pRS04 into their genome in a previous conjugation. Thus, obtained exconjugants were verified, cultivated and analyzed by LC-MS, as previously described.

LC-MS measurements revealed a significant production increase for all tested hosts. Extracted ion chromatograms of mureidomycin A display significantly enhanced signal intensities for *S. albus* Del14 and *S. albus* B2P1, while mureidomycin A was increased to a lesser, yet still significant, extent in *S. griseus* CS065. While most exconjugants depicted similar production rates (Fig. 45A), two overproducer mutant strains were measured (Fig. 45B): one *S. albus* Del14/pRS04/pacHK11 and one *S. albus* J1074/pRS04/pacHK11. In these strains, mureidomycin A production was approximately doubled, when compared with the remaining exconjugants, respectively. Correspondingly, met-pacidamycin 5 yield was significantly and similarly improved in *S. albus* Del14 and *S. albus* B2P1, while still being increased to a lesser extent in *S. griseus* CS065 (Fig. 45C).

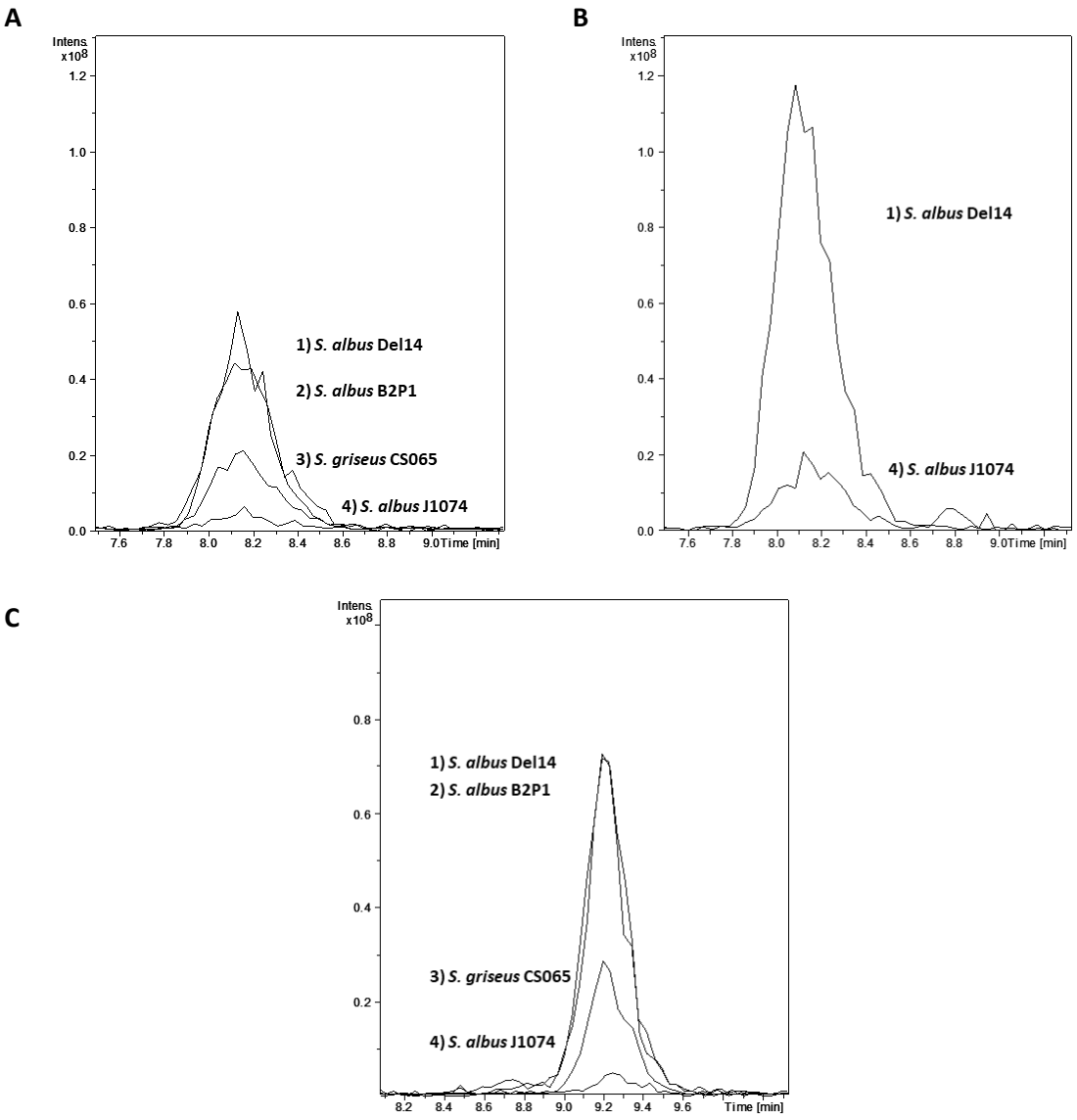


Fig. 45: LC-MS analysis of extracts of optimized heterologous hosts harboring the modified pacidamycin BGC pacHK11: Extracted ion chromatograms of A) mureidomycin A (*m/z* 841.3 $[M+H]^+$) and C) met-pacidamycin 5 (*m/z* 825.3 $[M+H]^+$) are displayed for: 1) *S. albus* Del14/pRS04/pacHK11, 2) *S. albus* B2P1/pRS04/pacHK11, 3) *S. griseus* CS065/pRS04/ pacHK11 and 4) *S. albus* J1074/pRS04/pacHK11
B) Extracted ion chromatograms of two selected mureidomycin A (*m/z* 841.3 $[M+H]^+$) overproducer mutant strains.

These results were summed up in the statistical analysis of Fig. 46, in order to reach a conclusion regarding the optimal heterologous host. UPA production was significantly increased in *S. albus* Del14, which, despite exhibiting a high variance between exconjugants, constituted the most beneficial mureidomycin A producer strain. *S. albus* B2P1 mutant strains elevated compound yield almost equally, but no overproducer mutants were observed, and variance remained high. Out of all examined hosts, production levels observed for *S. griseus* CS065 were most consistent between biological replicates, resulting in low variance between mutants, but, regardless, not improved on the same scale. Therefore, experiments were henceforth also conducted with *S. albus* Del14, which displayed the double benefit of the highest detected production increase and the simplified metabolic background,

thus facilitating compound isolation. Contrastingly, *S. griseus* CS065 is suited for quantification of compound production, due to the consistency in production levels.

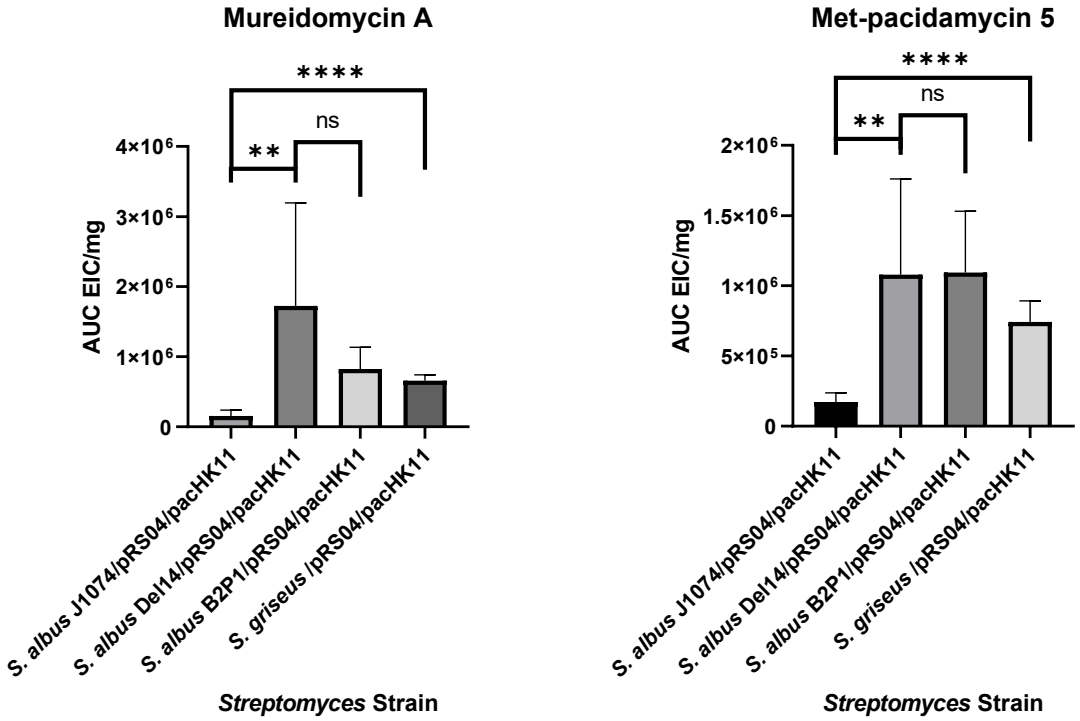


Fig. 46: LC-MS measurements of extracts of different heterologous hosts carrying the pacidamycin gene cluster harboring the first promoter swap; AUCs of UPA EICs are plotted against mutant strains in biological and technical replicates (normalized by cell dry weight). Statistical analysis: unpaired t-test, two-tailed P value, P value style: GraphPad, two asterisks signify P ≤ 0.01, four asterisks signify P ≤ 0.0001.

3.1.4 Genetic reorganization of the pacidamycin BGC by operon inversion

Since UPA biosynthesis was not increased further by the latter promoter swaps and due to the cessation of compound production when a bidirectional promoter was knocked in between *npsP4* and *npsP8*, a novel approach to improve UPA production rates was devised. This consisted of an inversion of operon 4 (*npsP3_pac13_npsP4*) with a simultaneous insertion of two strong, constitutive, unidirectional promoters in front of *npsP4* and *npsP8* (Fig. 47). Thus, all genes starting from *pac4* until *pac22* (operon 3 - operon 7) would be transcribed into the same direction as one continuous operon. Transcription would be enhanced by the three strong, consecutive, unidirectional promoters, which were all positioned into the same direction (P_{pac4}, P_{npsP4} and P_{npsP8}). Therefore, strong transcription levels of operons 3 and 4 might continue over operons 5 and 6, for which transcription had not been increased as strongly. Moreover, the intergenic region between *npsP4* and *npsP8*, which had not been amenable to genetic manipulation and production improvements hitherto, would be eliminated.

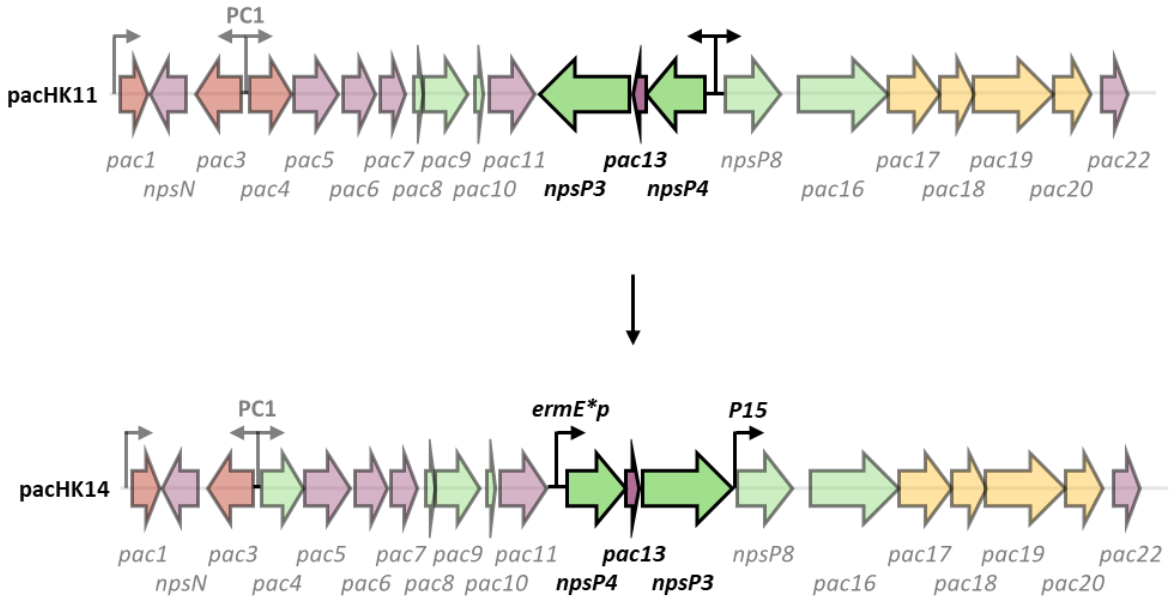


Fig. 47: Genetic organization of pacHK11 and pacHK14, areas modified in the inversion strategy were highlighted.

Firstly, an inversion cassette was designed, which consisted of the three genes to be inverted under the control of a unidirectional *ermE*p* promoter (Fig. 48A). This operon was flanked on either side by a 300 bp overhang of the respective newly adjacent genes, which were flanked, in turn, by SwaI recognition sites. Hence, *npsP4* was flanked by 300 bp of *pac11* and *npsP3* by 300 bp of *npsP8* sequences. For the construction of this cassette, a 5-fragment Gibson assembly was conducted, where one fragment consisted of EcoRV-digested pBluescript. The operon harboring *npsP4_pac13_npsP3* was amplified by PCR out of pacHK11 in two overlapping fragments, utilizing primers npsP4Frag_FW/npsP4Frag_RV and npsP3_Frag_FW/ npsP3_Frag_RV. Furthermore, the first 281 bp of *npsP8* was amplified out of pacHK11 with primers 300P8_FW and 300P8_RV, which introduced 20 bp Gibson overhangs, complementary to *npsP3* at the start of *npsP8* and 20 bp to pBluescript and a SwaI restriction site on the other side. The last fragment, containing 25 bp overhang to pBluescript, a SwaI recognition site, the 300 last base pairs of *pac11*, an *ermE*p* promoter sequence, and 21 bp homology to the start of *npsP4*, was ordered as gBlock Inv_R3pac11ermE. Gibson assembly was conducted as previously described and the isolated plasmid, carrying the entire insert, verified by restriction digest, PCR and sequencing of the entire insert with primers 47 - 60. Simultaneously, the *npsP4_pac13_npsP3* operon was knocked out of pacHK11 with the previously utilized I-SceI cassette encoded on pRS03, which had been amplified with primers ISceI_Del_3gen_FW and ISceI_Del_3gen_RV. As aforementioned in the construction of pacHK08 (3.1.1.1), the cosmid was linearized with an I-SceI digest and then co-transformed and circularized through Red/ET-mediated homologous recombination. The resulting cosmid pacHK13 was again verified by enzymatic digest, PCR and sequencing of the entire inverted insert (Fig. 48B).

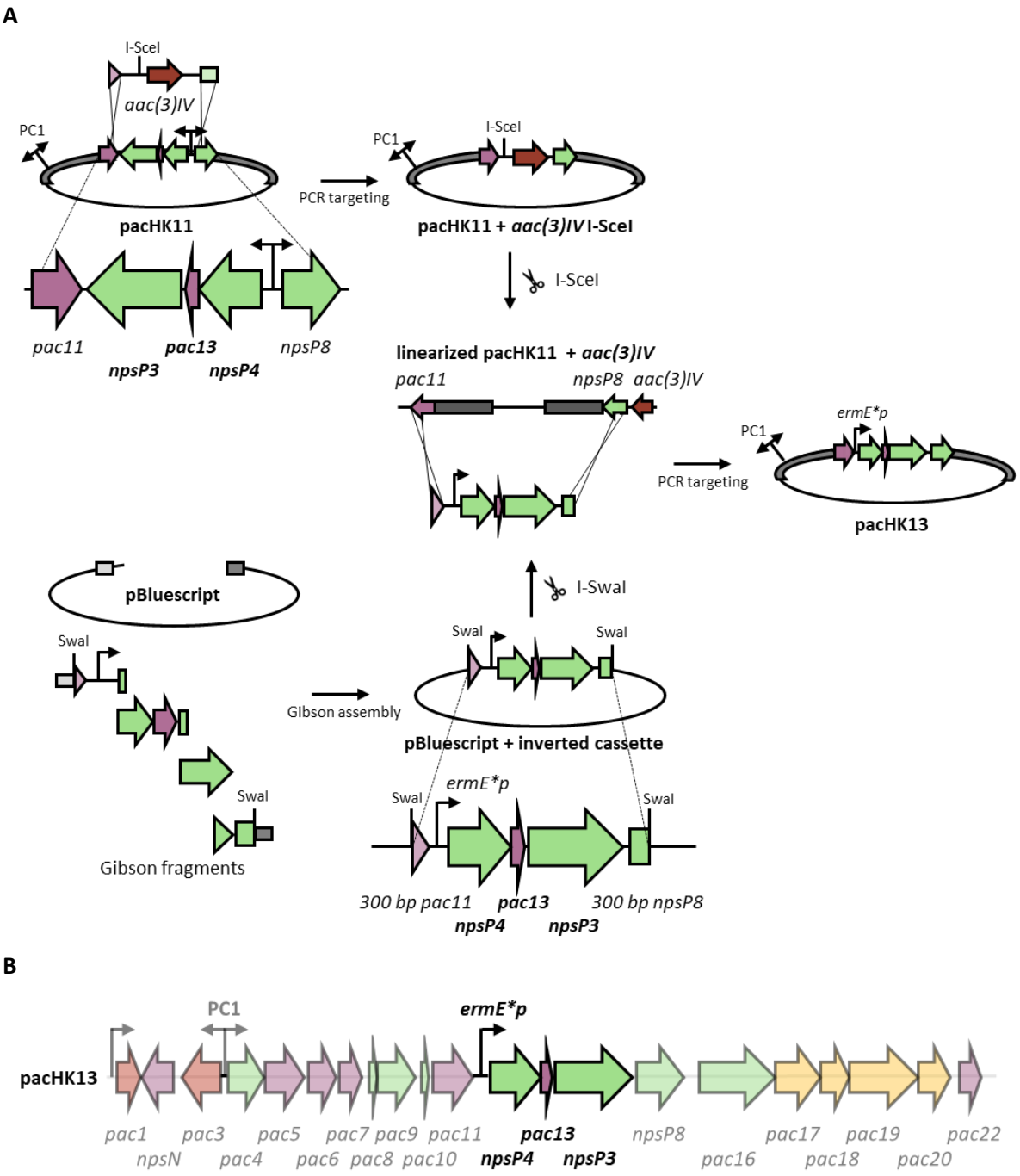


Fig. 48: A) Schematic representation of the strategy designed to construct pacHK13
B) Genetic organization of pacHK13, modified regions in comparison to pacHK11 are highlighted.

Since the synchronous insertion of the second unidirectional promoter *P15* complicated the designed Gibson assembly, its ensuing insertion into pacHK13 was implemented. For this purpose, the *aac(3)IV_I-SceI* cassette was amplified with primers ISceI_npsP8_3_P15_FW and ISceI_npsP8_3_P15_RV and knocked in between *npsP3* and *npsP8*. After linearization of the cosmid by I-SceI digestion, it was circularized, as aforementioned, by Red/ET-mediated homologous recombination with a gBlock containing *P15* with the respective spacer and RBS, flanked by 200 bp of

npsP3 and *npsP8* on either side (Fig. 49). The resulting cosmid pacHK14 was verified by enzymatic digest, PCR (primers Test_Inv_P15_FW and Test_Inv_P15_RV) and sequencing.

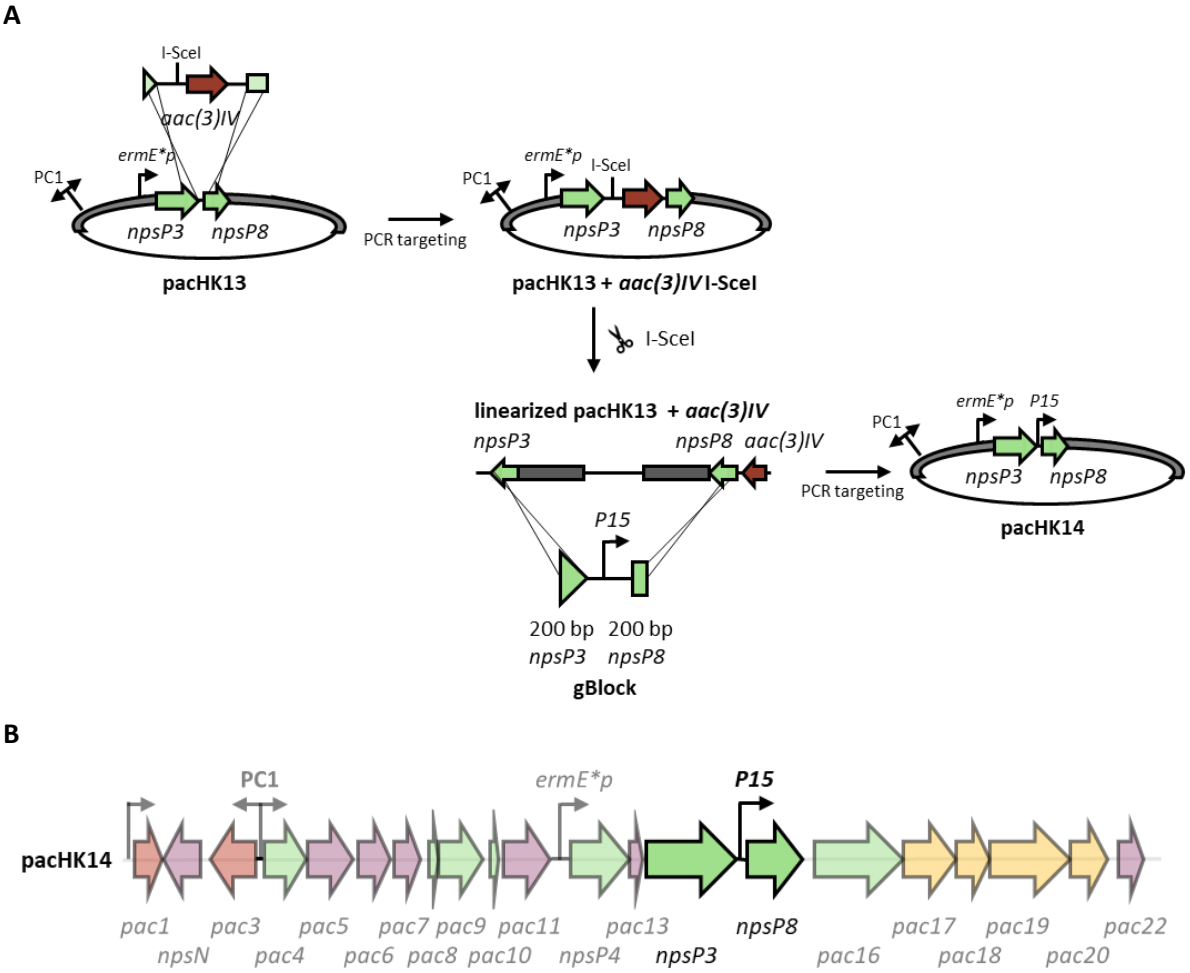


Fig. 49: A) Schematic representation of the strategy designed to construct pacHK14
B) Genetic organization of pacHK14, modified regions in comparison to pacHK13 were highlighted.

After conjugation with *S. albus* J1074/pRS04 and *S. albus* Del14/pRS04, mutant strain isolation and verification, the respective strains were cultivated, extracted and measured by LC-MS, as mentioned before. Extracted ion chromatograms for the two main compounds mureidomycin A and met-pacidamycin 5 revealed a very significant drop in production rates. For *S. albus* J1074, where less UPA production was detected in general, the inversion almost decreased met-pacidamycin 5 levels below the detection limit (Fig. 50B), while mureidomycin A was decreased below detection (Fig. 50A). The more efficient heterologous host *S. albus* Del14 displayed increased compound levels for both, the cluster prior to the inversion and the inverted derivative, when compared with *S. albus* J1074. Nevertheless, UPA production was still severely decreased, especially for met-pacidamycin 5 (Fig. 50D). Regarding mureidomycin A, while biosynthesis was still low, compound production was detectable (Fig. 50C).

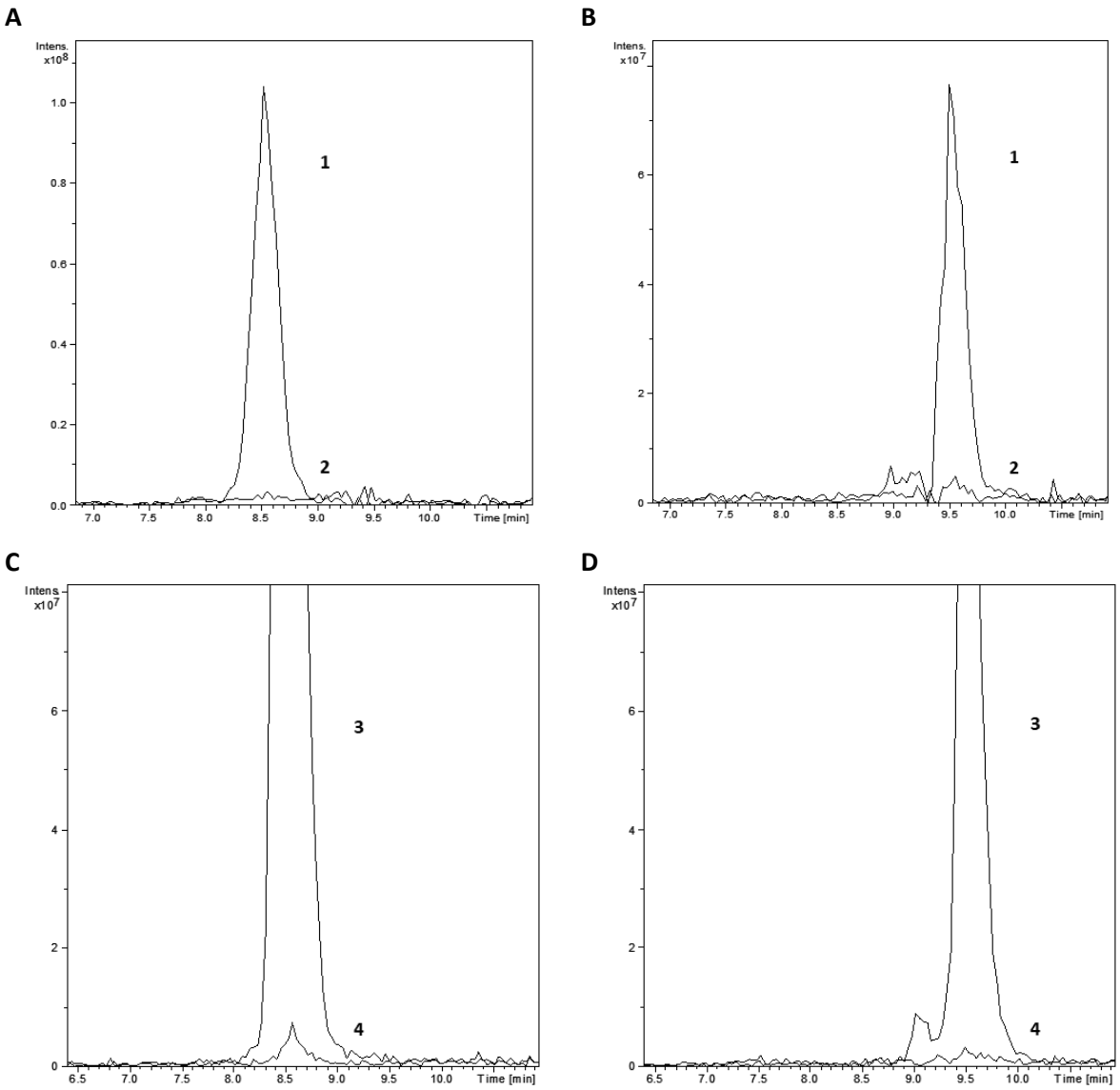


Fig. 50: LC-MS analysis of mutant strain extracts, which harbor the inverted pacidamycin BGC pacHK11 or pacHK14: Extracted ion chromatograms of A+C) mureidomycin A (*m/z* 841.3 $[M+H]^+$) and B+D) met-pacidamycin 5 (*m/z* 825.3 $[M+H]^+$) are displayed for:
1) *S. albus* J1074/pRS04/pacHK11, 2) *S. albus* J1074/pRS04/pacHK14, 3) *S. albus* Del14/pRS04/pacHK11 and 4) *S. albus* Del14/pRS04/pacHK14; full chromatograms displayed in Appendix Fig. S5.

3.1.5 Comparison of constructed UPA producer strains

The constructed bacterial strains harboring the modified pacidamycin biosynthetic gene clusters, which exhibited the most beneficial impact on UPA production yield, were summed up in the following table (Table 26). Therein, the strains were listed alongside the respective major compounds, the fold-change in UPA production and the reference strain, by which the fold-change had been calculated. Fold-change refers to mureidomycin A levels (exception: met-pacidamycin S was calculated for *S. albus* J1074/pacHK03) and, more specifically, the increase in the EIC peak area, which was normalized by cell dry weight. Where possible, three biological and two technical replicates were considered, and the respective average of the reference strain compared with the average of the mutant to be investigated. For *S. albus* J1074/pacRS01 and *S. albus* J1074/pRS04/ pacRS01 one biological replicate was measured as technical duplicates.

Table 26**:** Mutant strains constructed in this study displaying a positive effect on compound production

Strain	**Major compounds**	**Fold-change**	**Reference strain by which fold-change was calculated**
S. albus J1074/pacHK03	Met-pacidamycin D Met-pacidamycin S	25.52	*S. albus* J1074/pacRS01
S. albus J1074/pRS02/pacHK03	Met-pacidamycin D Met-pacidamycin S Met-pacidamycin 4 Met-pacidamycin 5 Mureidomycin A	2.57	*S. albus* J1074/pRS02/ pacRS01
S. albus J1074/pRS04/ pacHK03	Met-pacidamycin D Met-pacidamycin S Met-pacidamycin 4 Met-pacidamycin 5 Mureidomycin A	8.44	*S. albus* J1074/pRS04/ pacRS01
S. albus J1074/pRS02/pacHK11	Met-pacidamycin 5 Mureidomycin A	1.55	*S. albus* J1074/pRS02/ pacRS03
S. albus J1074/pRS04/pacHK11	Met-pacidamycin 5 Mureidomycin A	4.10	*S. albus* J1074/pRS04/ pacRS03
S. griseus CS065/pRS04/ pacHK11	Met-pacidamycin 5 Mureidomycin A	4.42	*S. albus* J1074/pRS04/ pacHK11
S. albus B2P1/pRS04/pacHK11	Met-pacidamycin 5 Mureidomycin A	5.55	*S. albus* J1074/pRS04/ pacHK11
S. albus Del14/pRS04/pacHK11	Met-pacidamycin 5 Mureidomycin A	11.58	*S. albus* J1074/pRS04/ pacHK11

3.2 Napsamycin biosynthetic gene cluster

3.2.1. Increased production by promoter replacements and an NRPS knockout

The napsamycin biosynthetic gene cluster encodes for the biosynthesis of a variety of different napsamycins and mureidomycins, but, as described by Dr. Nils Hauck in his PhD thesis[18], low production yields impede compound isolation of the desired UPAs. Therefore, in this work it was attempted to increase compound yield of the napsamycin BGC in parallel to the work done on the pacidamycin gene cluster, and more specifically, to increase mureidomycin A yield. The first series of modifications of the napsamycin biosynthetic gene cluster was undertaken by Philipp Konrad during his Master Thesis, where the bidirectional promoter cassette 1 was knocked into two separate sites of the cluster, one with a simultaneous knockout of an NRPS A-domain. Finally, both promoter replacements were combined. More specifically, the first promoter cassette (PC1), which had resulted in a significant UPA production increase when inserted into the pacidamycin gene cluster, was knocked into two bidirectional promoter sites of the napsamycin gene cluster (Fig. 51). In contrast to the pacidamycin BGC, the napsamycin BGC harbors four sites where bidirectional promoters have to be located and one site where a unidirectional promoter must be situated, in order for all genes to be expressed. Therefore, the first two sites for the promoter replacements were chosen based on which seemed most promising for production improvements.

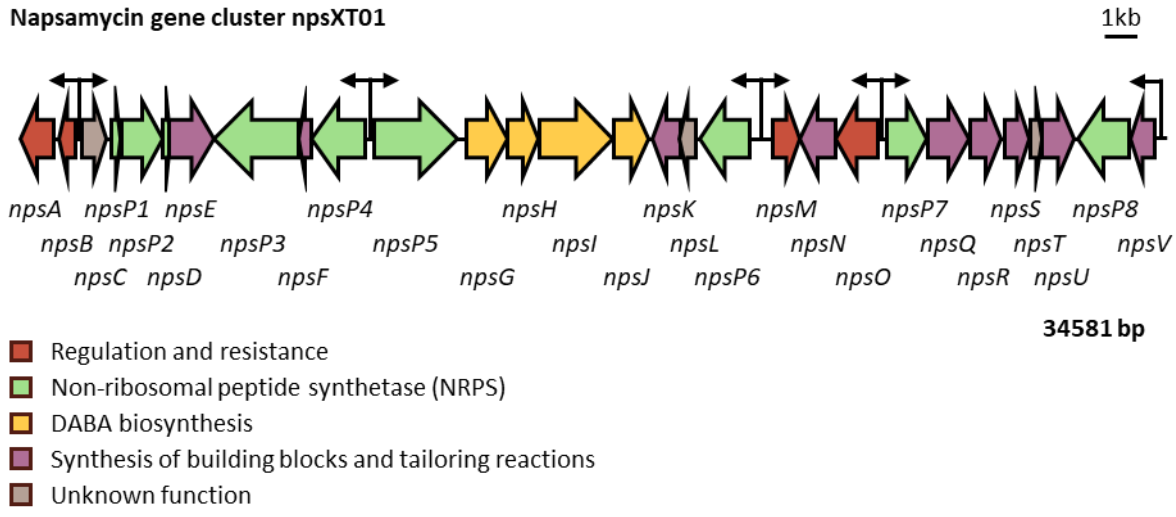


Fig. 51: Genetic organization of the napsamycin biosynthetic gene cluster. Coloring of genes correlates to the noted function, respectively.

At first, PC1 was knocked-in between *npsL* and *npsM* with a simultaneous knockout of *npsP6*, an NRPS adenylation domain which has been postulated to be responsible for the activation of 6-OH-tetrahydro-isoquinoline carboxylate (Htia) and *m*-tyrosine.[14] This knockout could downregulate napsamycin and mureidomycin E and F production, which contain a bicyclic derivative of Htia in their

scaffold (see Table 1), because complementation was intended with an A-domain specific for *m*-tyrosine. Since the orthologous gene to *npsP6* of the pacidamycin BGC is *pac21* with a preference for the activation of alanine, the adenylation domain function was complemented with *pac21h*, situated on pRS02 and pRS04. The enzyme encoded by the latter gene displays a preference for the activation of *m*-tyrosine and, thus, could increase mureidomycin A-D production. Further production improvement was expected from the combination with PC1 (npsPK01), since one promoter was knocked-in directly upstream of *npsM*, the cluster-specific positive regulator of the napsamycin BGC. Secondly, PC1 was knocked-in between *npsO* and *npsP7* on the native napsamycin gene cluster (npsPK02), since this region is orthologous to *pac3* and *pac4* of the pacidamycin gene cluster (see Table 2), where a promoter replacement by PC1 had been proven successful. Lastly, both promoter swaps and the knockout were combined in the third resulting cosmid npsPK03. In all cases, P15 was introduced upstream of *npsO* and *npsM*, and P16 upstream of *npsP7* and *npsL* (Fig. 52).

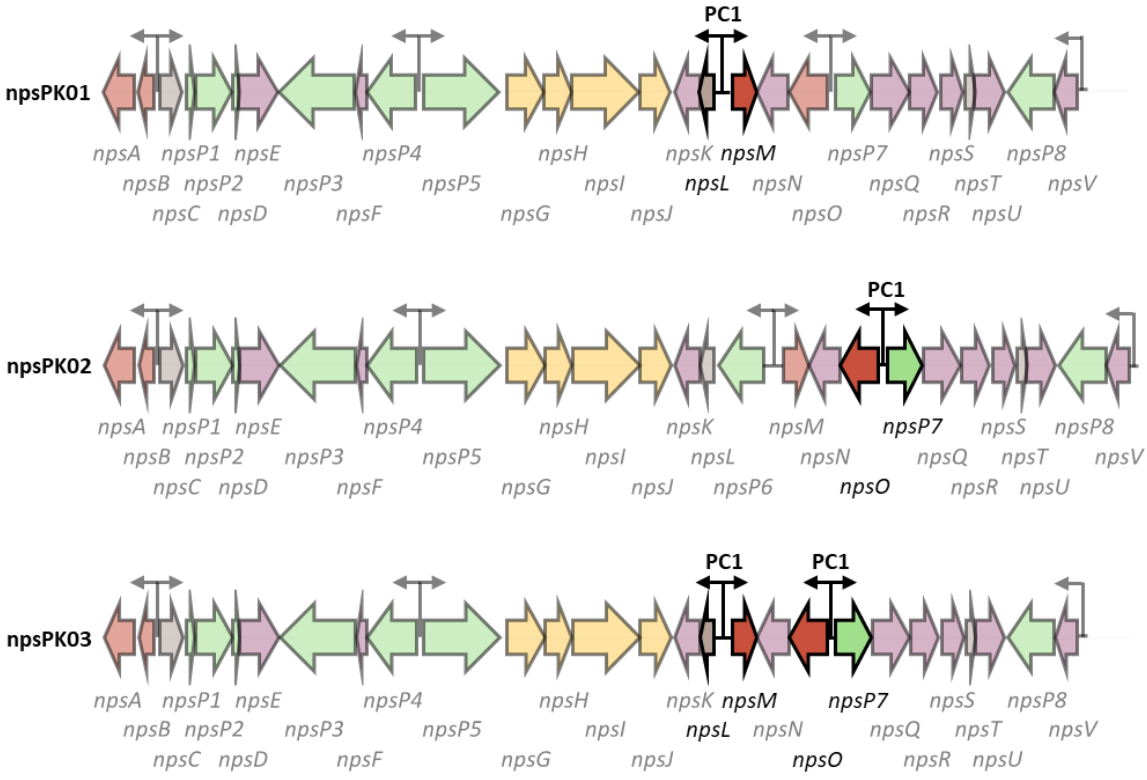


Fig. 52: Genetic organization of the napsamycin biosynthetic gene cluster, modifications conducted by Philipp Konrad are highlighted on the constructed cosmids npsPK01, npsPK02 and npsPK03.

In order to conduct the first promoter replacement/A-domain knockout, the same workflow as for the construction of pacHK03 was followed (see 3.1.1.1). The excised and purified PC1 fragment, isolated from pAG03, was amplified with the long primers KOnpsP6_FW and KOnpsP6_RV, which introduced overhangs complementary to *npsL* and *npsM*. After homologous recombination with npsXT01,

harboring the entire napsamycin BGC, and FLP-mediated resistance marker excision, the resulting cosmid npsPK01 was verified by enzymatic digestion, sequencing and PCR (primers: Test_KOnpsP6_FW and Test_KOnpsP6_RV). For the construction of npsPK02, the same procedure was implemented with different cassette-specific primers (npsP7_PC1_FW and npsP7_PC1_RV), which harbored sequences homologous to *npsO* and *npsP7* and different test primers (Test_npsPK02_FW and Test_npsPK02_RV). The combination of modifications required a different approach, due to the FRT sites present subsequent to every promoter replacement. Therefore, the strategy presented in the assembly of pacHK08 was followed (see 3.1.1.1), where the fragment harboring PC1 at its core, flanked by overhangs to *npsO* and *npsP7*, was amplified out of npsPK02 with primers Amp_npsXT01_PS2_FW and Amp_npsXT01_PS2_RV. Simultaneously, the intergenic region between *npsO* and *npsP7* was knocked out in npsPK01 and replaced by an apra_I-SceI cassette, which had been amplified with primers ISceI_O_P7_FW and ISceI_O_P7_RV. Hence, the linearized cosmid and amplified fragment were recombined, as aforementioned. The obtained construct was verified by enzymatic digestion, PCR (primers Test_PC1_P7_O_FW and Test_PC1_P7_O_RV) and sequencing. All assembled cosmids were transformed into *E. coli* ET12567 and conjugated with *S. albus* J1074, *S. albus* J1074/pRS02 and *S. albus* J1074/pRS04, and mutant strains isolated, verified and cultivated alongside the heterologous napsamycin producer strain *S. albus* J1074/npsXT01, as previously elucidated. The respective LC-MS analysis can be found below.

Upon heterologous expression of the napsamycin gene cluster encoded on npsXT01 in *S. coelicolor* M1154, the compounds mureidomycins A and B and napsamycin C were detected and verified by ESI-MS and MS^2 spectra, as described by Kaysser *et al.* (2011)[14]. Therein, napsamycin A was detected and verified after inactivation of *npsU*, which encodes for an oxidoreductase. Other napsamycins (B and D) could only be detected in trace amounts. These compounds were further verified by Dr. Nils Hauck in his dissertation[18], in which the same gene cluster was heterologously expressed in *S. albus* J1074. Production of mureidomycin A, mureidomycin B, mureidomycin E/napsamycin A and napsamycin C was confirmed by LC-MS analysis and MS^2 fragmentation at corresponding retention times. Thus, the heterologous expression of the napsamycin gene cluster in *S. albus* J1074/npsXT01 was repeated in this study as a reference for the further modifications. In this analysis, new peaks were detected in the UV-chromatogram at 260 nm of *S. albus* J1074/npsXT01, in comparison with the wild type, in the range t_R = 7.2 - 9.8 min (Fig. 53A), which correspond to retention times of mureidomycins and napsamycins, as described by Dr. Nils Hauck. The respective base peak chromatogram revealed five new major peaks (Fig. 53B), which were assigned to masses of the +MS spectrum (Fig. 53C), depending on the most abundant mass of the peak. Detected masses A) *m/z* 843.3 $[M+H]^+$ (t_R = 7.6 min) and B) *m/z* 855.3 $[M+H]^+$ (t_R = 8.0 min) correspond to mureidomycin B and napsamycin C, respectively. Contrastingly, mureidomycin A

(*m/z* 841.3 $[M+H]^+$, t_R = 7.8 min) and mureidomycin E/napsamycin A were detected solely in traces. These five compounds will be investigated herein in detail, since mureidomycin A was determined to be the most promising UPA structure in MIC and IC_{50} studies[18]. The other masses observed in the heterologous expression of npsXT01 were congruent with the ones observed by Tang *et al.* (2013)[145]. More specifically, compounds with *m/z* values of 825.4, 827.4, 867.4 (D), 885.4 (C) and 899.4 were investigated in the respective work. It was postulated that a derivative of mureidomycin B containing leucine or *iso*-leucine at position four of the amino acid scaffold accounted for *m/z* 825.4 $[M+H]^+$, while the *m/z* value of 827.4 was suggested to correspond to mureidomycin B with phenylalanine at position 5 instead of *m*-tyrosine. Due to the lack of definitive evidence (for example by NMR analysis) to support these hypotheses, these masses were not investigated in the present study. Tang *et al.* (2013)[145] further examined compound D and the compound with an *m/z* value of 899.4 $[M+H]^+$ by ESI-MS^2, but structure elucidation was not possible. Although the slightly shifted *m/z* values of 867.3 $[M+H]^+$ (compound D) and 869.4 (compound E) could correspond to napsamycins B and D in theory, the respective retention times of t_R = 9.2 and t_R = 9.6 were measured 1.2 min and 1.6 min after napsamycin C, which differs from napsamycin D only in one methyl moiety. Therefore, the identity as napsamycins was considered highly doubtful and the respective masses not regarded in the present study. Lastly, the compound with an *m/z* value of 885.4 $[M+H]^+$ was investigated by Tang *et al.* (2013)[145] and concluded to correlate to the inactive *N*-acetylmureidomycin B, which was supported by HRMS, MS^2 fragmentation, genetic and biochemical data and suggested to be the product of the *N*-acetyltransferase NpsB.

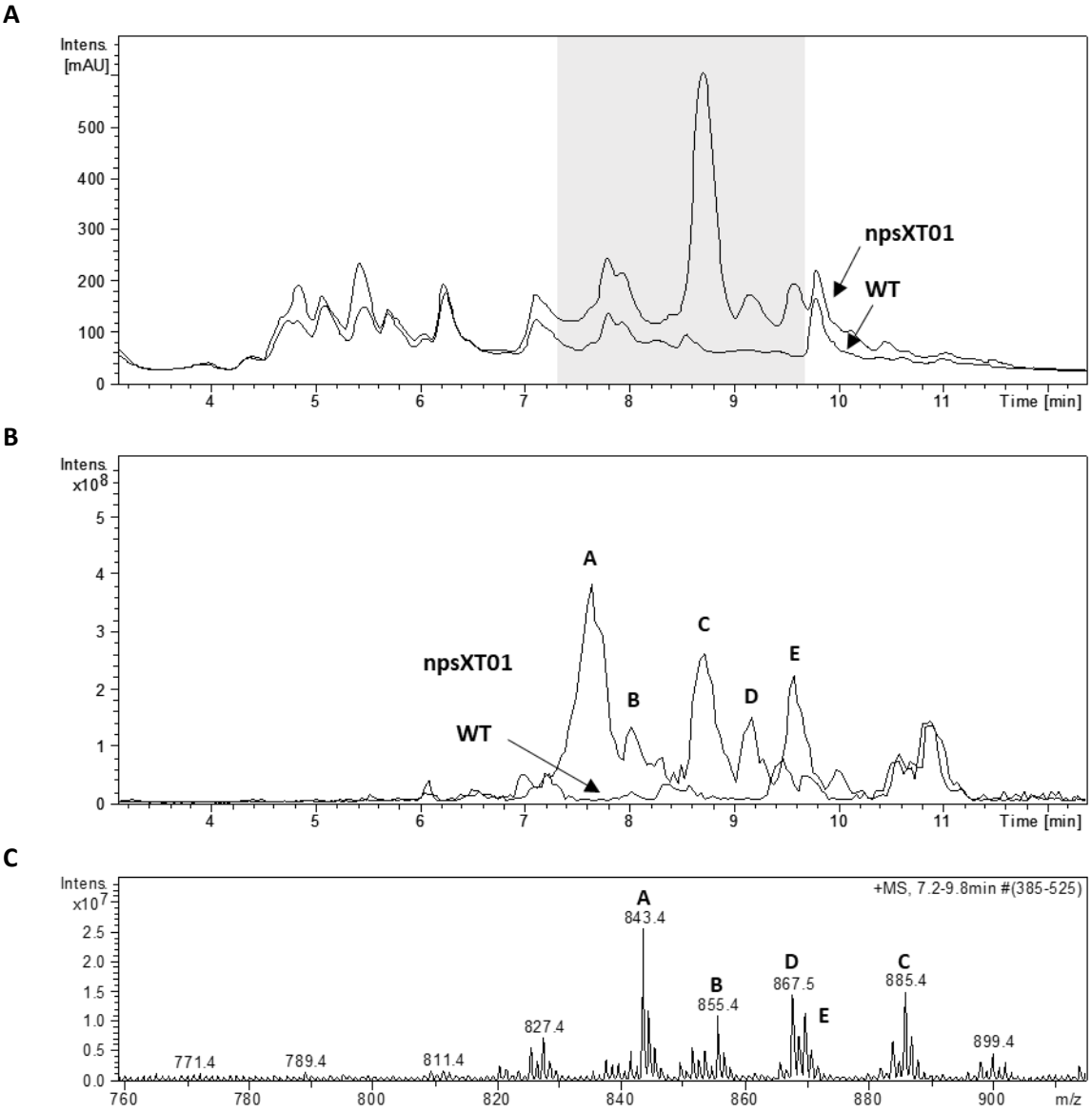


Fig. 53: LC-MS analysis of heterologous expression of the napsamycin BGC on cosmid npsXT01: a) UV-chromatogram 260 nm of *S. albus* J1074 WT and *S. albus* J1074/npsXT01, b) Base Peak Chromatogram +MS 700-900 *m/z* of *S. albus* J1074 WT and *S. albus* J1074/npsXT01, and c) + MS spectrum of *S. albus* J1074/npsXT01 at t_R = 7.2 - 9.8 min. The major detected compounds were labeled.

When cultivating mutants harboring the promoter replacement between *npsL* and *npsM*, UPA production was not detected in the strains *S. albus* J1074/npsPK01 and *S. albus* J1074/pRS02/npsPK01 (Appendix Fig. S6). Solely when the *npsP6* knockout was complemented with the plasmid pRS04, harboring *npsM*, UPA production was restored. Nevertheless, EIC signal intensity in *S. albus* J1074/pRS04/npsPK01 was unaffected regarding mureidomycin B and decreased for mureidomycin A, mureidomycin E/napsamycin A and napsamycin C (Fig. 54 and Appendix Fig. S7).

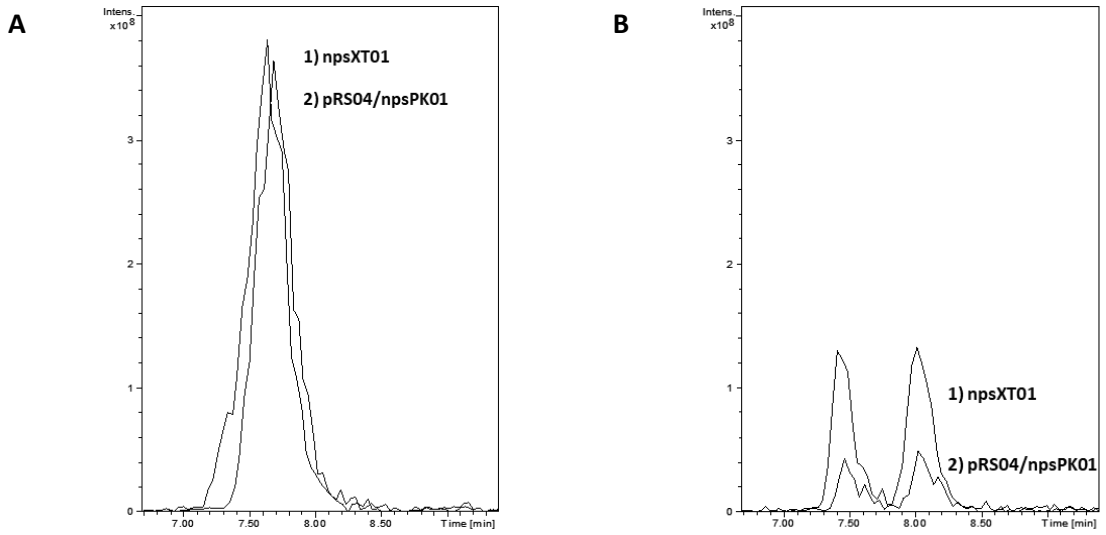


Fig. 54: LC-MS analysis of mutant strain extracts, which harbor the napsamycin gene cluster carrying promoter cassette 1 between *npsL* and *npsM*. Extracted ion chromatograms of A) mureidomycin B (*m/z* 843.3 $[M+H]^+$) and B) napsamycin C (*m/z* 855.3 $[M+H]^+$) are displayed for: 1) *S. albus* J1074/npsXT01 and 2) *S. albus* J1074/pRS04/npsPK01.

Different tendencies were observed in extracts of mutant strains, which harbored PC1 between *npsO* and *npsP7*. Regarding mureidomycin A, all mutant strains (*S. albus* J1074/npsPK02, *S. albus* J1074/pRS02/npsPK02 and *S. albus* J1074/pRS04/npsPK02) significantly increased mureidomycin A production and decreased mureidomycin B, each to a comparable extent (Fig. 55). Mureidomycin E/napsamycin A yield was decreased in *S. albus* J1074/npsPK02 and *S. albus* J1074/pRS02/npsPK02 and lowered to a lesser extent in *S. albus* J1074/pRS04/npsPK02. Corresponding observations were made for napsamycin C levels, which were decreased very significantly in the former two strains (Appendix Fig. S8).

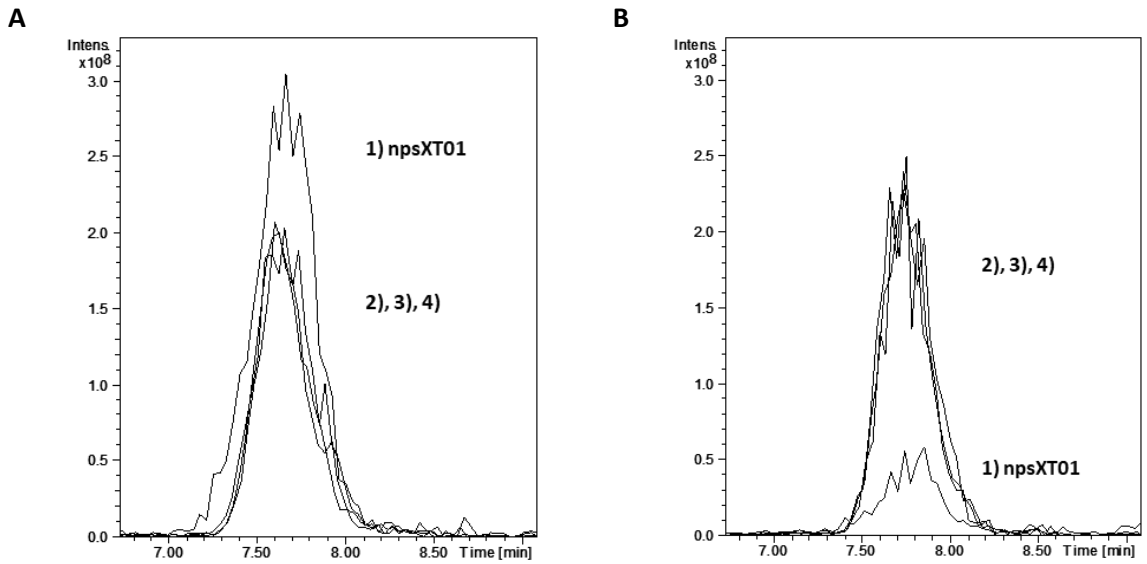


Fig. 55: LC-MS analysis of mutant strain extracts, which harbor the napsamycin gene cluster carrying promoter cassette 1 between *npsO* and *npsP7*. Extracted ion chromatograms of A) mureidomycin B (*m/z* 843.3 $[M+H]^+$) and B) mureidomycin A (*m/z* 841.3 $[M+H]^+$) are displayed for: 1) *S. albus* J1074/npsXT01, 2) *S. albus* J1074/npsPK02 3) *S. albus* J1074/pRS02/npsPK02 and 4) *S. albus* J1074/pRS04/npsPK02.

Similar results to the knock-in of PC1 between *npsL* and *npsM* were observed for the combination of modifications in npsPK03, with no UPA production being detected in *S. albus* J1074/npsPK03 and *S. albus* J1074/pRS02/npsPK03 (Appendix Fig. S9). Again, compound production was restored, when the knockout was complemented with pRS04. Mureidomycin A levels were slightly increased in *S. albus* J1074/pRS04/npsPK03, in contrast to *S. albus* J1074/pRS04/npsPK01, while for mureidomycin B, mureidomycin E/napsamycin A and napsamycin C a significant drop in compound yield was observed. Mureidomycin E/napsamycin A were detected in trace amounts (Fig. 56 and Appendix Fig. S10).

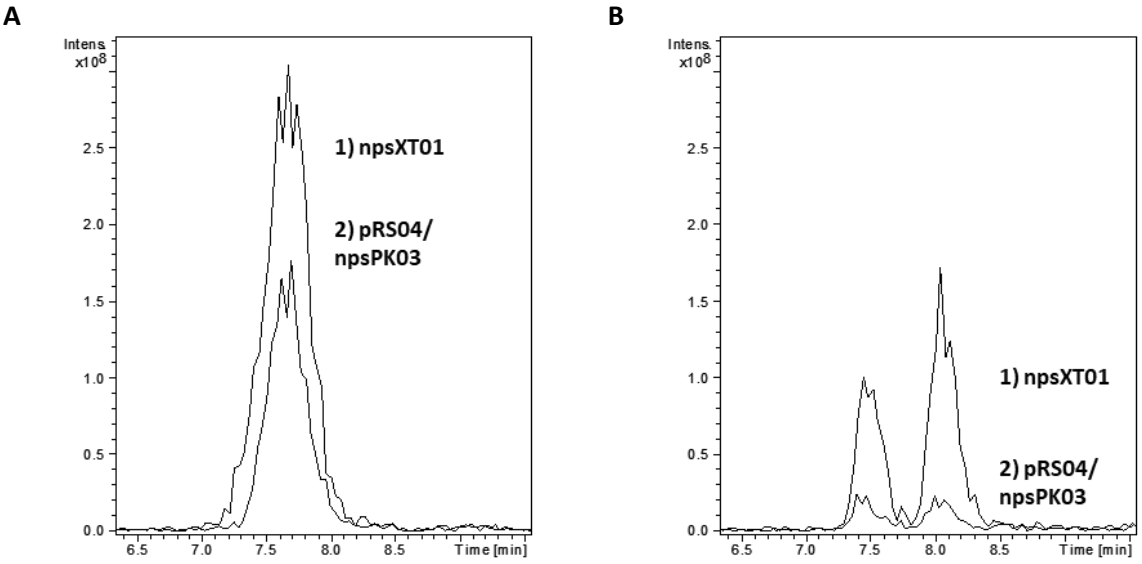


Fig. 56: LC-MS analysis of mutant strain extracts, which harbor the napsamycin gene cluster carrying promoter cassette 1 between *npsL* and *npsM* and between *npsO* and *npsP7*; *npsP6* was knocked out. Extracted ion chromatograms of A) mureidomycin B (*m/z* 843.3 $[M+H]^+$) and B) napsamycin C (*m/z* 855.3 $[M+H]^+$) are displayed for: 1) *S. albus* J1074/npsXT01 and 2) *S. albus* J1074/pRS04/npsPK03.

This data was further analyzed in biological triplicates (duplicates of *S. albus* J1074/npsXT01 and *S. albus* J1074/pRS04/npsPK01) and the area of mureidomycin A EIC peaks in all mutants normalized by cell dry weight and portrayed in the graph of Fig. 57. While UPA compounds were not detected in the wild type, mureidomycin A was produced in low amounts in *S. albus* J1074/npsXT01, which was utilized as the reference strain. Regarding the *npsP6* knockout-mutants, the abolishment of mureidomycin A production was noted without complementation of A-domain function, as expected, but also after complementation with pRS02. Solely in the case of complementing with pRS04, compound biosynthesis was restored to a level not significantly different from the unaltered producer. Contrastingly, mureidomycin A levels were significantly elevated by the promoter replacement between *npsO* and *npsP7*. More specifically, in the mutant strains *S. albus* J1074/npsPK02 and *S. albus* J1074/pRS02/npsPK02, mureidomycin A signal intensity was increased 4.58-fold and 4.51-fold, respectively. Furthermore, by combining the same gene cluster with mutant strains harboring pRS04, mureidomycin A production was increased 5.28-fold. Therefore, the second promoter insertion

constitutes the most promising candidate for further modifications, also considering the reduction in napsamycin signal intensity. However, no significant influence on UPA production was detected subsequent to the insertion of pRS02 and pRS04.

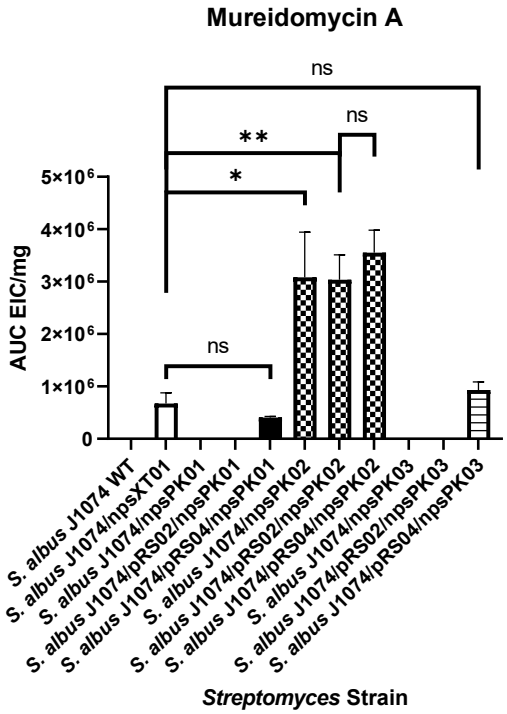


Fig. 57: LC-MS measurements of extracts of mutant strains carrying the napsamycin gene cluster harboring npsPK01, npsPK02 or npsPK03; AUCs of mureidomycin A (*m/z* 841.3 $[M+H]^+$) EICs are plotted against mutant strains in biological replicates normalized by cell dry weight. Statistical analysis: unpaired t-test, two-tailed P value, P value style: GraphPad, one asterisk signifies P ≤ 0.05, two asterisks signify P ≤ 0.01.

Furthermore, masses with *m/z* values of 885.4 $[M+H]^+$ and 883.4 $[M+H]^+$ were detected. While the former was identified by Tang *et al.* (2013)[145] to correspond to *N*-acetylmureidomycin B, the latter was postulated to be the respective dihydro-derivative, which would be *N*-acetylmureidomycin A. This hypothesis has not been proven, since attempted MS^2 analyses were unsuccessful. Nevertheless, both masses will be investigated herein, since compound yield of mureidomycin A and B might be affected by conversion to acetylated derivatives. In the abovementioned mutants, where UPA production was not detected, the masses in question were not present, while in *S. albus* J1074/pRS04/npsPK01 the *m/z* value 883.4 $[M+H]^+$ was detected only in traces (while mureidomycin A levels were also low) and 885.4 $[M+H]^+$ was slightly reduced. In *S. albus* J1074/pRS04/npsPK03 the former was increased slightly, while the latter was not affected (Appendix Fig. S11A, B and C). However, in all mutant strains harboring npsPK02, similar observations were made, which consisted of a strong increase in the signal intensity in the compound with *m/z* 883.4 $[M+H]^+$, while 885.4 $[M+H]^+$ was slightly decreased, which correlates with the respective tendencies observed for mureidomycins A and B (Appendix Fig. S11D and E).

3.2.2. Increased production and compound specificity by knockouts

The napsamycin/mureidomycin gene cluster, encoded on the SuperCos1-based cosmid npsXT01, produces a variety of compounds in small amounts. In order to restrict the compound spectrum and thereby putatively increase the yield of mureidomycin A by increasing precursor availability, the strategy of knocking out *npsU* and *npsE* was devised. The FMN-dependent oxidase *npsU* had previously been inactivated in *S. coelicolor* M1154 by Kaysser *et al.* (2011)[14], who noted the subsequent production abolishment of UPAs carrying a dihydrouracil moiety (mureidomycin B and napsamycin C). They postulated the role of *npsU* to be the reduction of deoxyuridine to dihydrodeoxyuridine. Another gene of interest, the FAD-dependent oxidoreductase *npsE*, was hypothesized to catalyze the synthesis of the bicyclic Htia (6-hydroxytetrahydroisoquinoline carboxylic acid) from *m*-tyrosine and a one- or two-carbon adduct, which is present in all napsamycins and mureidomycin E. As shown in Table 27, combining these knockouts could, in theory, steer the biosynthesis effectively toward the production of mureidomycins C and A.

Table 27: UPAs produced by the napsamycin/mureidomycin gene cluster with an overview over the amino acid sequence in their scaffold. Postulated effect of knockouts on different compounds are indicated.

Name	**R_1**	**AA2**	**AA4**	**AA5**	**Other**	**Targeted by KO**
Mureidomycin A	H	*m*-Tyr	Met	*m*-Tyr		
Mureidomycin B	H	*m*-Tyr	Met	*m*-Tyr	Dihydrouracil	Δ*npsU*
Mureidomycin C	Gly	*m*-Tyr	Met	*m*-Tyr		
Mureidomycin D	Gly	*m*-Tyr	Met	*m*-Tyr	Dihydrouracil	Δ*npsU*
Mureidomycin E	H	Bicyclic a	Met	*m*-Tyr		Δ*npsE*
Napsamycin A	H	Bicyclic b	Met	*m*-Tyr		Δ*npsE*
Napsamycin C	H	Bicyclic b	Met	*m*-Tyr	Dihydrouracil	Δ*npsU*

Firstly, both single knockouts were planned to be conducted with different cassettes, in order to facilitate a potential subsequent combination of both. In the process of knocking out *npsE*, the resistance cassette of plasmid pIJ774 was used. This cassette had been situated at the core of promoter cassette 2, and, therefore, the method by which this knockout was executed, was based on the procedure for the construction of pacHK05 (see 3.1.1.1). The cassette was obtained from pIJ774, amplified by primers KO_npsE_FW and KO_npsE_RV, purified, and used in the Red/ET-mediated homologous recombination of npsXT01. After Cre-mediated resistance marker excision, the resulting cosmid npsHK01 was verified by enzymatic digestion, PCR (npsE_test_FW and npsE_test_RV) and sequencing. For the knockout of *npsU*, the apramycin resistance cassette of plasmid pIJ773, which was

described as part of the composition of PC1, was utilized. Hence, the respective procedure described herein closely resembles the one presented in the construction of pacHK03 (see 3.1.1.1). After excision from plasmid pIJ773 by HindIII/EcoRI and purification, the cassette was amplified with primers npsU_KO_FW and npsU_KO_RV. This fragment was utilized for Red/ET-mediated homologous recombination of npsXT01, as previously described, and the resulting clones were verified, subsequent to a retransformation. After removal of the resistance cassette by FLP-mediated recombination, the resulting cosmid npsHK02 was verified by enzymatic digestion, PCR (primers: npsU_KO_test_FW and npsU_KO_test_RV) and sequencing. The cosmids harboring both novel modified napsamycin gene clusters were transformed into *E. coli* ET12567 and then conjugated with *S. albus* J1074 and the isolated mutants verified, as previously described. Biological triplicates and technical duplicates of the strains in question and of *S. albus* J1074/npsXT01 and *S. albus* J1074/npsPK02 as references were cultivated and the resulting extracts analyzed by LC-MS.

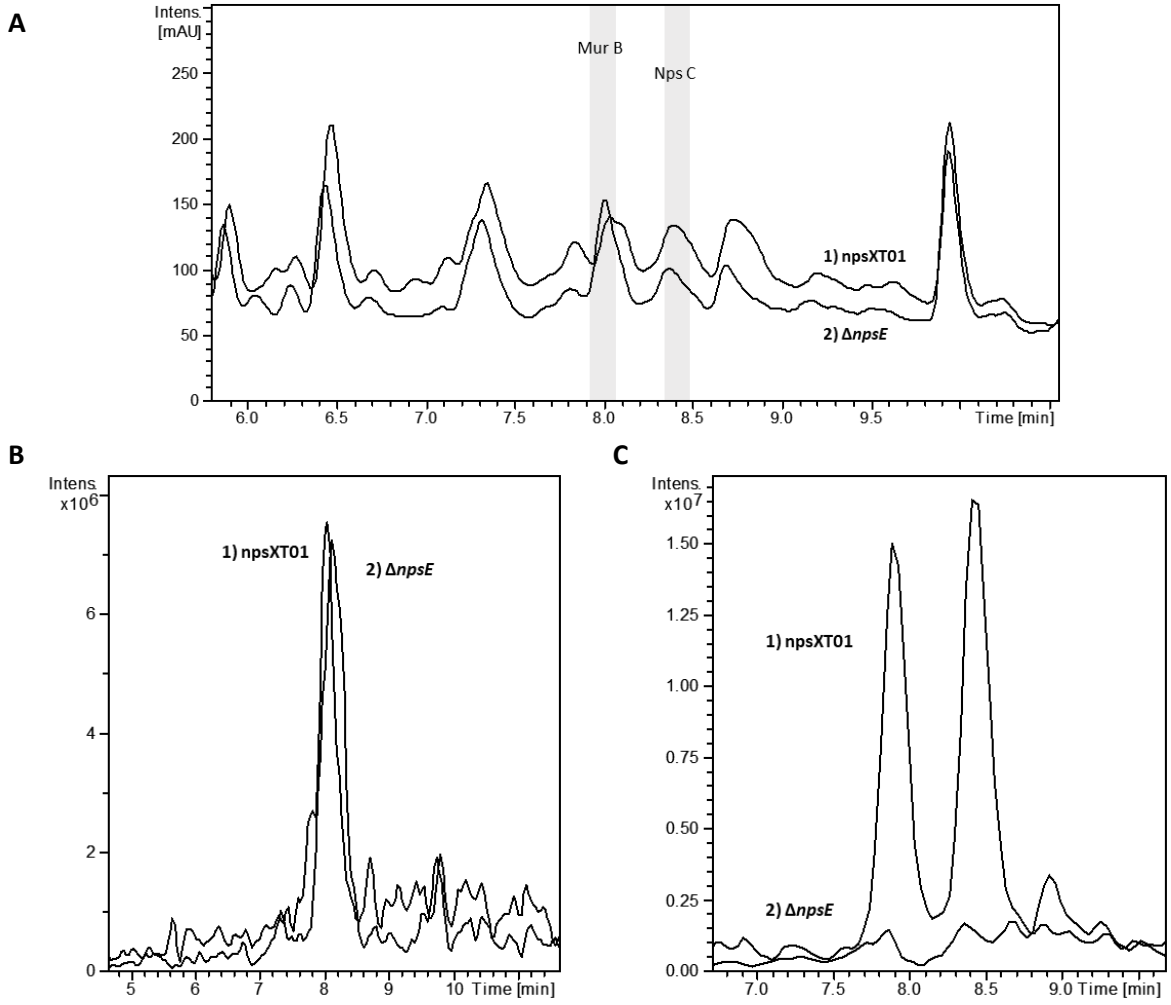


Fig. 58: LC-MS analysis of Δ*npsE* mutant strain extracts, in comparison with the original napsamycin gene cluster. A) UV-chromatogram at 260 nm of 1) *S. albus* J1074/npsXT01 and 2) *S. albus* J1074/npsHK01 (Δ*npsE*), peaks corresponding to mureidomycin B and napsamycin C were labeled, B) EICs of mureidomycin B (*m/z* 843.3 $[M+H]^+$) in 1) *S. albus* J1074/npsXT01 and 2) *S. albus* J1074/npsHK01 (Δ*npsE*) and C) EICs of napsamycin C (*m/z* 855.3 $[M+H]^+$) in 1) *S. albus* J1074/npsXT01 and 2) *S. albus* J1074/npsHK01 (Δ*npsE*). The EICs were smoothed by Gaussian processing (2.28, 1, GA).

As displayed above in the UV-chromatogram and the respective extracted ion chromatograms, signal intensity was significantly decreased for compounds, which contain a bicyclic moiety within their scaffold, such as napsamycin C and mureidomycin E/napsamycin A (Fig. 58, data not shown for mureidomycin E/napsamycin A). Contrastingly, compounds containing *m*-tyrosine at position two of the amino acid scaffold instead of a bicyclic moiety were not affected by the modification, as seen in the EICs of mureidomycin B (Fig. 58) and mureidomycin A, which was produced in traces, as was the compound with an *m/z* value of 883.4 $[M+H]^+$ (data not shown). Furthermore, in *npsE* knockout mutant strains (containing npsHK01) signal intensity of the compound with an *m/z* value of 885.4 $[M+H]^+$ was decreased in comparison with the respective peak in *S. albus* J1074/npsXT01, but still higher than mureidomycin B peaks in either of these strains, which did not differ significantly (Fig. 59). Therefore, this knockout was deemed successful in limiting the compound spectrum produced by the napsamycin BGC. These observations were verified by the statistical analysis of all cultivated mutants, which were summarized in Fig. 60.

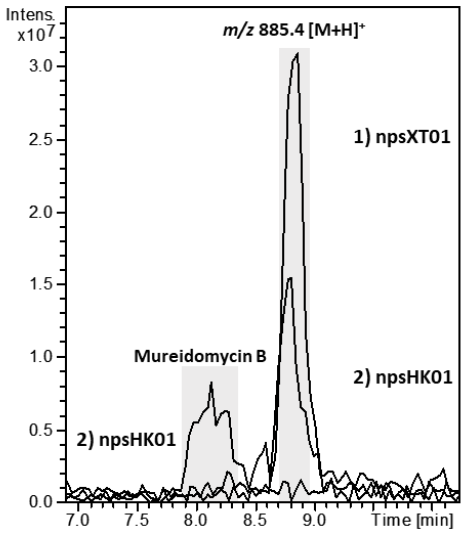


Fig. 59: LC-MS analysis of Δ*npsE* mutant strain extracts, in comparison with the original napsamycin gene cluster. EICs of mureidomycin B (*m/z* 843.3 $[M+H]^+$) and the compound with *m/z* 885.4 $[M+H]^+$ in 1) *S. albus* J1074/npsXT01 and 2) *S. albus* J1074/npsHK01.

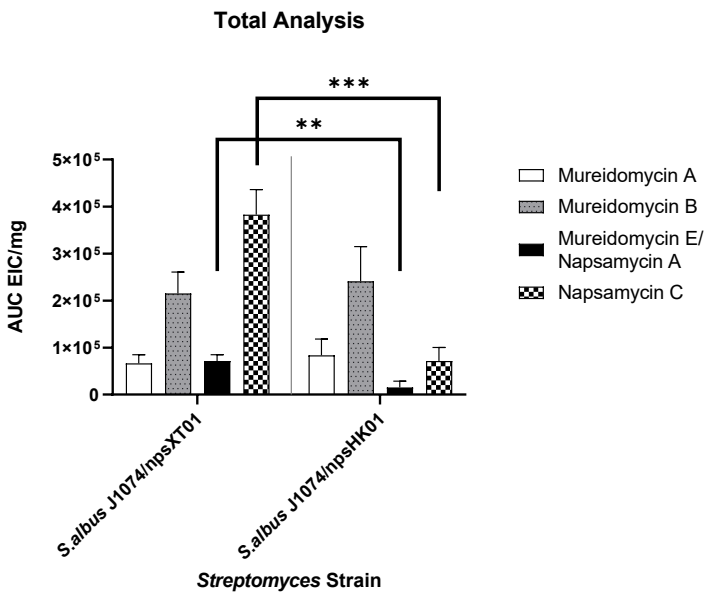


Fig. 60: LC-MS measurements of extracts of Δ*npsE* knockout strains; AUCs of EICs of produced UPAs were normalized by cell dry weight in biological triplicates and technical duplicates and plotted against the respective producer strains *S. albus* J1074/npsXT01 and *S. albus* J1074/npsHK01. Statistical analysis: unpaired t-test, two-tailed P value, P value style: GraphPad, two asterisks signify P ≤ 0.01, three asterisks signify P ≤ 0.001.

Regarding the knockout of *npsU*, compounds containing a dihydrouracil moiety could not be detected in the respective extracts, while a very significant production increase was measured for compounds not containing the former moiety. More specifically, mureidomycin A signal intensity was increased 90.22-fold, on average, in comparison with the native napsamycin/mureidomycin gene cluster of *S. albus* J1074/npsXT01, where mureidomycin A production was barely detected. Additionally, one overproducer mutant of mureidomycin A was isolated. A distinct increase in signal intensity in the UV-chromatogram peak corresponding to mureidomycin A was observed (Fig. 61A and B). Mureidomycin E/napsamycin A production was also increased (Fig. 61C).

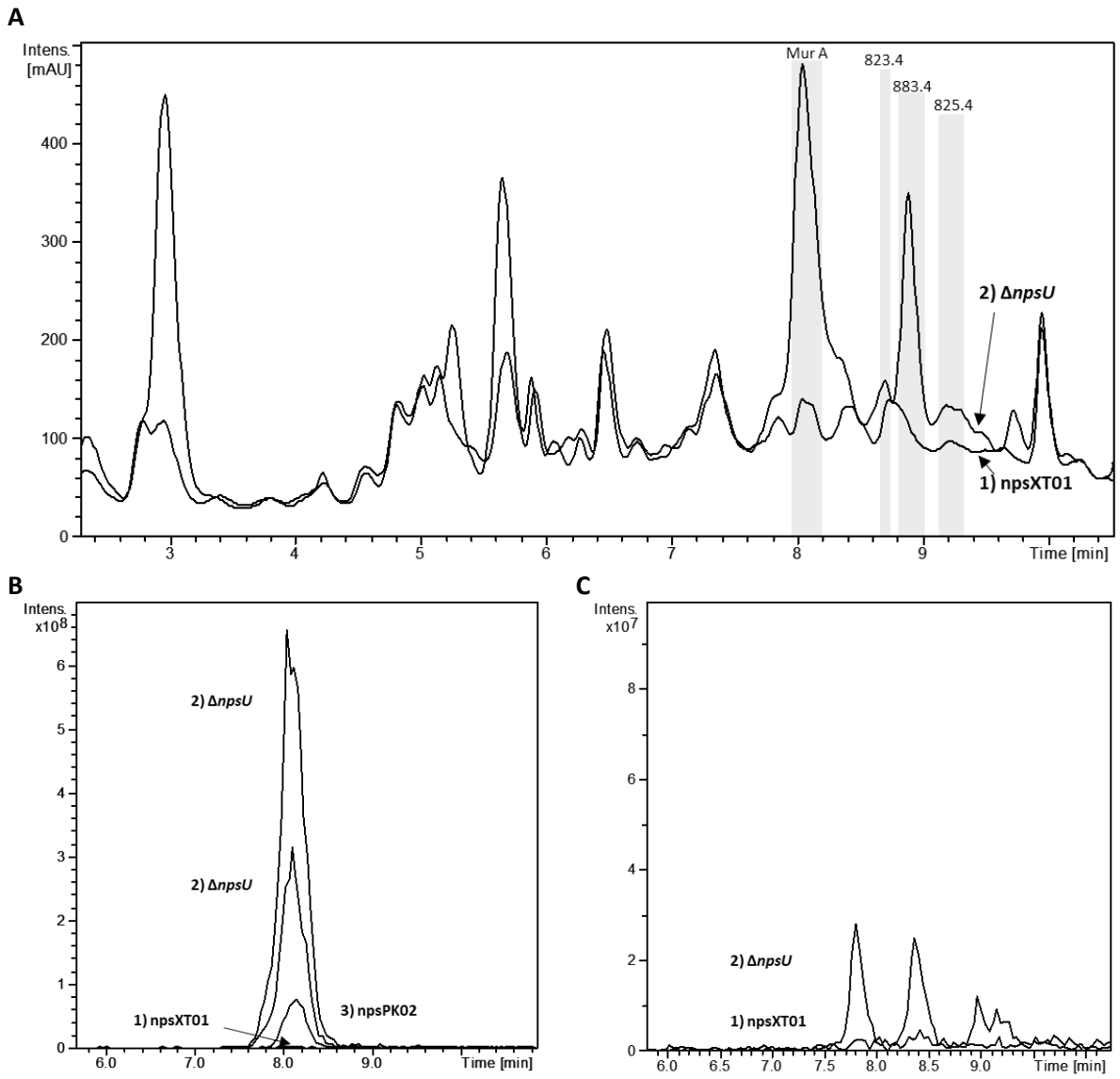


Fig. 61: LC-MS analysis of Δ*npsU* mutant strain extracts, in comparison with the original napsamycin gene cluster. A) UV-chromatogram at 260 nm of 1) *S. albus* J1074/npsXT01 and 2) *S. albus* J1074/npsHK02, the peak corresponding to mureidomycin A was marked, B) Extracted Ion Chromatogram of mureidomycin A (*m/z* 841.3 $[M+H]^+$) in 1) *S. albus* J1074/npsXT01, 2) *S. albus* J1074/npsHK02 and 3) *S. albus* J1074/npsPK02. The highest peak corresponds to the mureidomycin A overproducer mutant. C) Extracted Ion Chromatogram of mureidomycin E/napsamycin A (*m/z* 853.3 $[M+H]^+$) in 1) *S. albus* J1074/npsXT01 and 2) *S. albus* J1074/npsHK02.

Furthermore, the mureidomycin B derivative containing a leucine or *iso*-leucine at position 4 of the amino acid scaffold (*m/z* 825.4 $[M+H]^+$) was described by Tang *et al.* (2013)[145] to appear in *npsU* knockout mutants with a minus 2 Da shift, which correlates to the mass present in the UV-chromatogram 260 nm with an *m/z* value of 823.4 $[M+H]^+$ (leucine or *iso*-leucine derivative of mureidomycin A). Additionally, Tang *et al.* (2013)[145] observed and verified by MS^2 analysis a mureidomycin B derivative containing a phenylalanine at position 5 of the amino acid scaffold (m/z value of 827.4 $[M+H]^+$, variable sequence H - *m*-Tyr - Met - Phe - dihydrouracil), which in *npsU* knockout mutants becomes the compound herein called met-pacidamycin 5 (m/z value of 825.4 $[M+H]^+$, variable

sequence H - *m*-Tyr - Met - Phe - uracil), due to the cessation of the reduction of the uridyl moiety (2 Da shift). Moreover, the compound elutes at the same retention time and is, therefore, highly likely to be met-pacidamycin 5. Production levels of the postulated met-pacidamycin 5 are displayed in Fig. 64. Contrastingly, in *npsE* knockout mutants neither peak was detected.

Moreover, the postulated *N*-acetylmureidomycin A with an *m/z* value of 883.4 $[M+H]^+$ was detected in the *npsU* knockout mutants, where signal intensity was elevated in comparison with the respective peak in *S. albus* J1074/npsXT01, but lower than mureidomycin A levels in the same exconjugants (Fig. 62A). While a peak with an *m/z* value 885.4 $[M+H]^+$ was detected, the retention time was shifted and, as displayed in the respective +MS spectrum, the peak derives from an isotope of the compound with an *m/z* value of 883.4 $[M+H]^+$ (Fig. 62B).

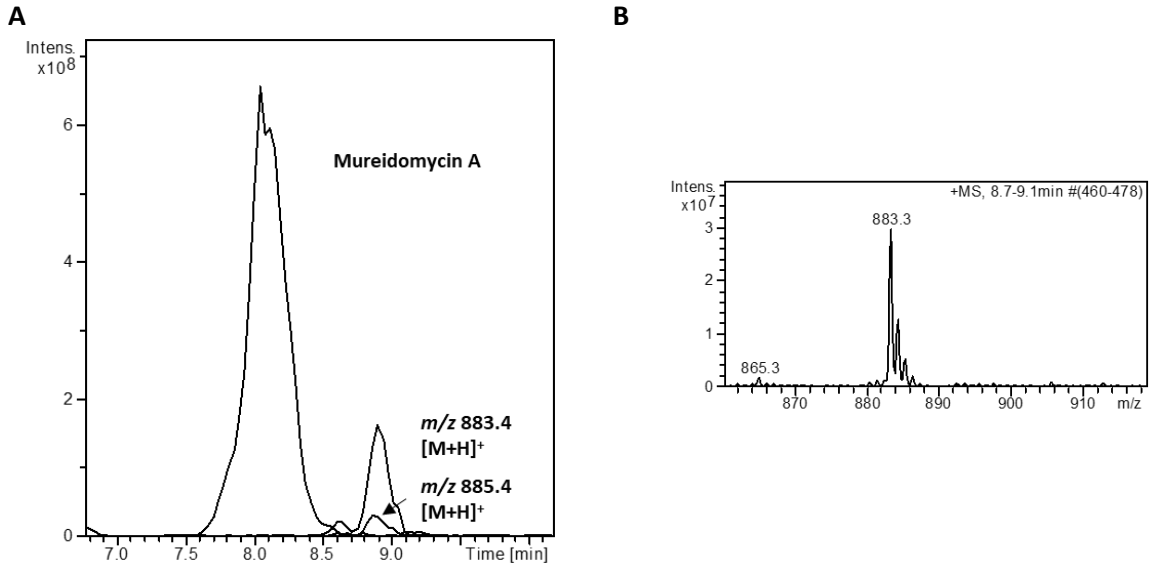


Fig. 62: LC-MS analysis of Δ*npsU* mutant strain extracts. A) Extracted ion chromatograms of mureidomycin A (*m/z* 841.3 $[M+H]^+$) and compounds with *m/z* values of 883.4 $[M+H]^+$ and 885.4 $[M+H]^+$, B) +MS spectrum at t_R = 8.7 - 9.1 min, corresponding to the compound with an *m/z* value of 883.4 $[M+H]^+$.

Simultaneously, mureidomycin B and napsamycin C production was not detected. While a peak of *m/z* 843.3 $[M+H]^+$ appears at the same retention time (t_R = 8.1 min) as mureidomycin B, the +MS spectrum indicates this mass to only consist of an isotope of mureidomycin A (Fig. 63A and C). This was further verified in a previous MS^2 analysis by Kaysser *et al.* (2011)[14], who concluded the respective peak to not correspond to mureidomycin B. Similarly, peaks detected in the EIC of napsamycin C (*m/z* 855.3 $[M+H]^+$) at t_R = 7.6 - 8.7 min correlate to an isotope of mureidomycin E/napsamycin A (Fig. 63B and D).

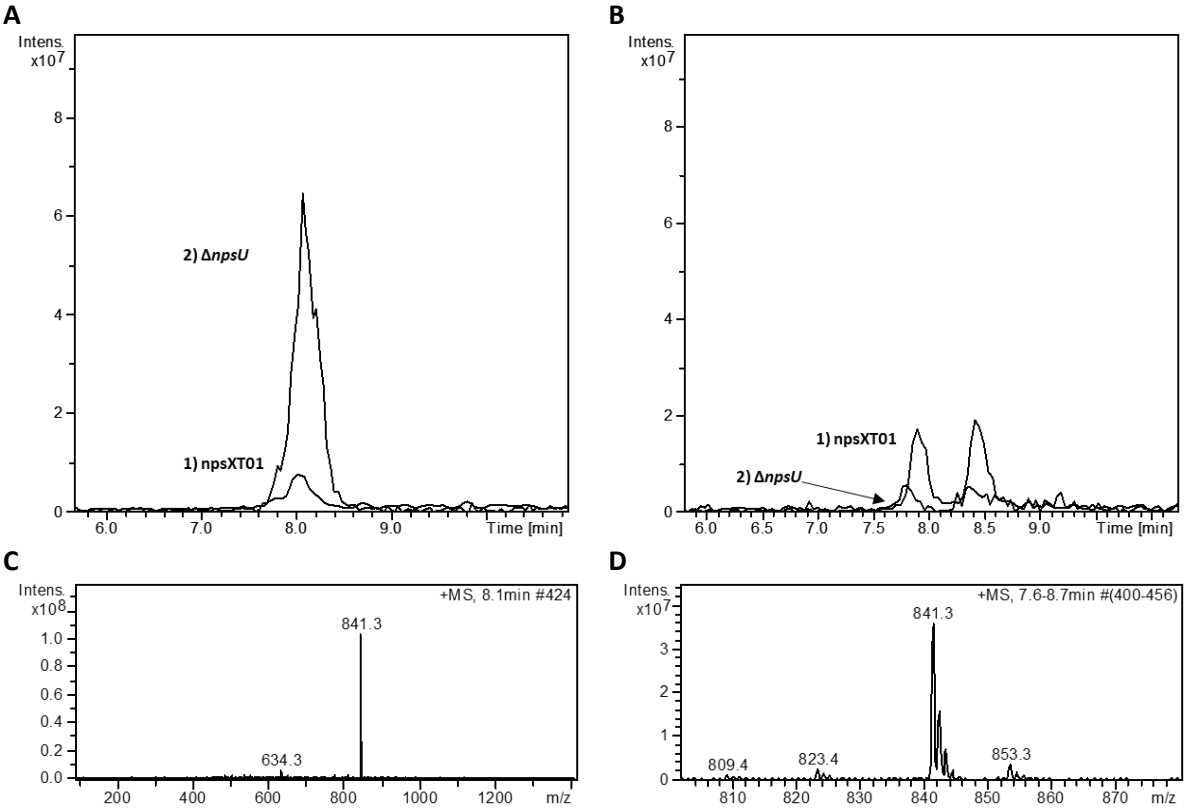


Fig. 63: LC-MS analysis of Δ*npsU* mutant strain extracts in comparison with the original napsamycin gene cluster. A) Extracted ion chromatograms of mureidomycin B (*m/z* 843.3 $[M+H]^+$) in 1) *S. albus* J1074/npsXT01 and 2) *S. albus* J1074/npsHK02, B) Extracted Ion Chromatograms of napsamycin C (*m/z* 855.3 $[M+H]^+$) in 1) *S. albus* J1074/npsXT01 and 2) *S. albus* J1074/npsHK02, C) +MS spectrum at t_R = 8.1 min, corresponding to mureidomycin A and D) +MS spectrum at t_R = 7.6 - 8.7 min.

This data was summarized in the graph of Fig. 64, where UPAs produced by the strains *S. albus* J1074/npsXT01, *S. albus* J1074/npsHK02 and *S. albus* J1074/npsPK02 are depicted and can, thus, be compared. The production rates of mureidomycin A in the Δ*npsU* strains are surpassing the other compounds in all three strains by far.

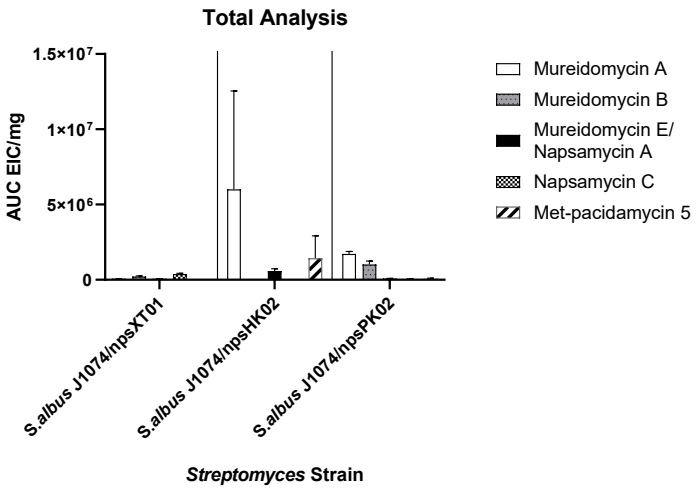


Fig. 64: LC-MS measurements of extracts of Δ*npsU* knockout strains; AUCs of EICs of produced UPAs were normalized by cell dry weight in biological triplicates and technical duplicates and plotted against the respective producer strains *S. albus* J1074/npsXT01, *S. albus* J1074/npsHK02 and *S. albus* J1074/npsPK02.

Subsequently, *E. coli* ET12567/npsHK02 was conjugated with *S. albus* Del14, which had been proven beneficial in the work concerning the pacidamycin biosynthetic gene cluster, regarding an increased production of UPAs and a reduced metabolic background. Indeed, signal intensity of mureidomycin A EICs (*m/z* 841.3 $[M+H]^+$) was increased in *S. albus* Del14/npsHK02 when compared with *S. albus* J1074/npsHK02 (Fig. 65). Mureidomycin E/napsamycin A production levels were significantly reduced in three exconjugants and not affected in the fourth (Appendix Fig. S12). Additionally, the postulated *N*-acetyl-mureidomycin A (*m/z* 883.4 $[M+H]^+$) was detected in similar peak intensities in all exconjugants of *S. albus* Del14/npsHK02, while mureidomycin A production displayed high fluctuations. Congruent observations were made for the respective peaks in *S. albus* J1074/npsHK02, contrasting to data of a previous cultivation. Furthermore, *N*-acetylmureidomycin B (*m/z* 885.4 $[M+H]^+$) was not detected (Appendix Fig. S13). Moreover, the abovementioned compounds with *m/z* values of 823.4 $[M+H]^+$ and 825.4 $[M+H]^+$ were also detected, in various intensities in both compared strains.

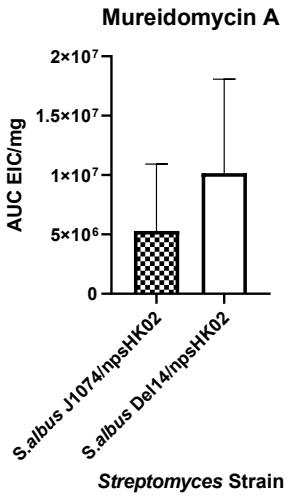


Fig. 65: LC-MS measurements of extracts of Δ*npsU* knock-out strains, comparison of the heterologous hosts *S. albus* J1074 and *S. albus* Del14; AUCs of EICs of mureidomycin A (*m/z* 841.3 $[M+H]^+$) were normalized by cell dry weight in biological triplicates and technical duplicates and plotted against the respective producer strains *S. albus* J1074/npsHK02 and *S. albus* Del14/npsHK02.

Mureidomycin A yield was significantly increased in the *npsU* knockout strain, but mureidomycin E/napsamycin A peaks were still detected at retention times directly prior and subsequent to mureidomycin A. Furthermore, the *npsE* knockout significantly decreased mureidomycin E/napsamycin A levels without affecting mureidomycin A yield. Therefore, a combination of both knockouts in one cosmid was attempted, in order to further restrict the compounds produced by the napsamycin gene cluster and facilitate compound isolation. This was accomplished by repeating the *npsE* knockout precisely as previously described, with only the targeting being conducted on npsHK02 instead of npsXT01. The resulting cosmid npsHK04 harboring the

napsamycin BGC with both knockouts was verified, as aforementioned, transformed into *E. coli* ET12567 and conjugated with *S. albus* Del14. After cultivation, the extracts of the resulting mutants were analyzed by LC-MS measurements.

Unfortunately, peak intensity of all major compounds was decreased in the double knockout mutants. Mureidomycin A was decreased 3.92-fold, while mureidomycin E/napsamycin A levels were lowered on average 5.04-fold (Fig. 66). Signal intensity of the compound with an *m/z* value of 883.4 $[M+H]^+$ was also decreased and lower than the respective one of mureidomycin A, while a peak with an *m/z* value of 885.4 $[M+H]^+$ was detected once more in low amounts (Appendix Fig. S14). Although the undesired compounds were more strongly decreased, the steep and almost equal loss in mureidomycin A yield is not preferable, and, thus, more modifications were carried out on the *npsU* single-knockout mutant strain. Moreover, mureidomycin A signal intensity displayed only slight fluctuations between exconjugants.

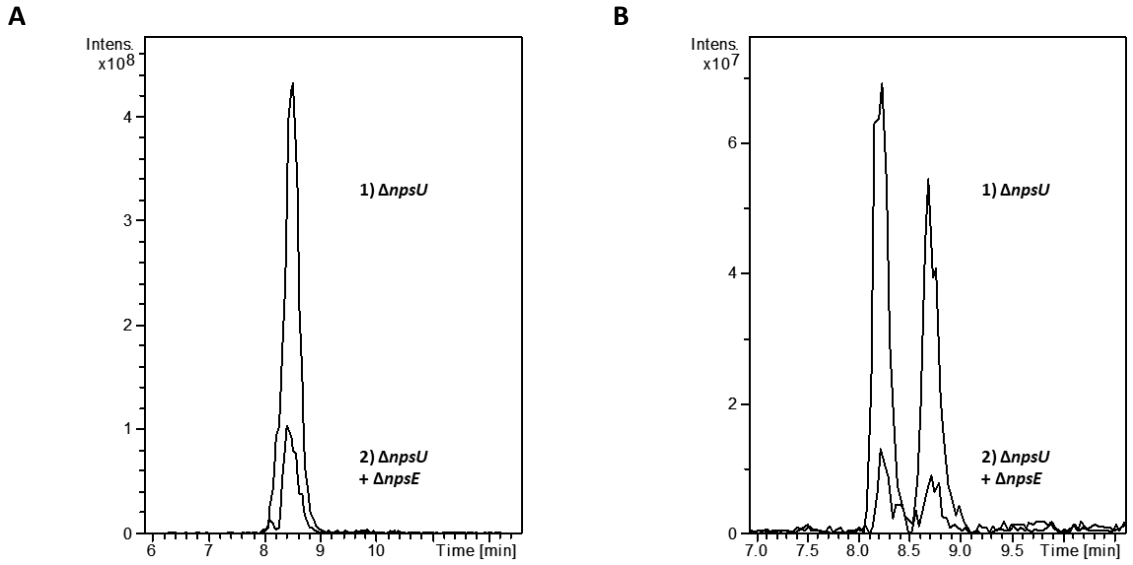


Fig. 66: LC-MS analysis of extracts of Δ*npsU* and Δ*npsE* double knockout mutant strain, compared with Δ*npsU* mutants. A) Extracted ion chromatograms of mureidomycin A (*m/z* 841.3 $[M+H]^+$) in 1) *S. albus* Del14/npsHK02 and 2) *S. albus* Del14/npsHK04 and B) Extracted Ion Chromatograms of mureidomycin E/napsamycin A (*m/z* 853.3 $[M+H]^+$) in 1) *S. albus* Del14/npsHK02 and 2) *S. albus* Del14/npsHK04.

3.2.3. Combination of promoter replacements and knockout

Subsequently, the two modifications, which had been beneficial for mureidomycin A production, were combined on one gene cluster. More specifically, promoter cassette 1 (PC1) was knocked-in between *npsO* and *npsP7* on the napsamycin gene cluster, in which *npsU* had already been knocked out. For this purpose, the aforementioned strategy of the construction of pacHK08 (see 3.1.1.1) was implemented. The apra_I-SceI cassette of pRS03 was amplified with primers ISceI_O_P7_FW and ISceI_O_P7_RV and

knocked into the intergenic region between *npsO* and *npsP7*. The resulting cosmid was linearized and then recombined with a fragment harboring PC1 flanked by overhangs of *npsO* and *npsP7*, which had been amplified with primers Amp_npsXT01_PS2_FW and Amp_npsXT01_PS2_RV out of npsPK02. The obtained cosmid npsHK03, harboring both modifications, was verified by enzymatic digestion, PCR (Test_PC1_P7_O_FW and Test_PC1_P7_O_RV) and sequencing. The mutant strains, into which npsHK03 had been conjugated, were verified and cultivated, and the respective extracts analyzed by LC-MS.

Regarding compound yield of mureidomycin E/napsamycin A, no significant influence was detected upon inserting the bidirectional promoter cassette. Similarly, mureidomycin A production was on average hardly affected. However, no exconjugant was detected to overproduce mureidomycin A as it was the case in *S. albus* Del14/npsHK02 (Fig. 67). Therefore, the promoter replacement did not lead to further production improvements and *S. albus* Del14/npsHK02 remained the favored mureidomycin A producer. Regarding the postulated *N*-acetylmureidomycin A (*m/z* 883.4 $[M+H]^+$), signal intensity was detected with low fluctuation. Due to the high fluctuations in mureidomycin A production, the peak corresponding to the postulated *N*-acetylmureidomycin A was detected to variate between a lower signal intensity than mureidomycin A and even a higher one. Simultaneously, the postulated met-pacidamycin 5 peak (m/z 825.4 $[M+H]^+$) was almost decreased below detection limit.

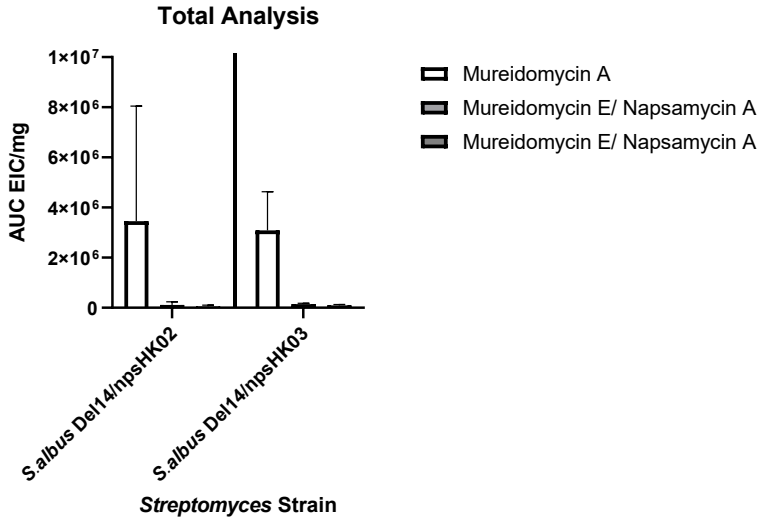


Fig. 67: LC-MS measurements of extracts of *S. albus* J1074/npsHK02 (Δ*npsU*) and *S. albus* Del14/npsHK03 (Δ*npsU*, PC1); AUCs of EICs of mureidomycin A (*m/z* 841.3 $[M+H]^+$) and mureidomycin E/napsamycin A (*m/z* 853.3 $[M+H]^+$) were normalized by cell dry weight in biological triplicates and plotted against the respective producer strains.

3.2.4. Comparison of constructed UPA producer strains

As previously conducted for the pacidamycin BGC (see 3.1.5), the bacterial strains carrying the napsamycin/mureidomycin biosynthetic gene cluster, which were favorable regarding mureidomycin A production, were summarized in the following table (Table 28). Besides the respective major compounds, the fold-change in UPA production was recorded in regards to the listed reference strain. Fold-change was calculated by the average increase in EIC peak area of mureidomycin A, which had been normalized by cell dry weight. Three biological replicates were considered for each genotype and the respective average of the reference strain compared with the average of the mutant to be investigated. For *S. albus* J1074/npsXT01 two biological replicates were measured in comparison with mutants harboring npsPK02. Contrastingly, for comparison of *S. albus* J1074/npsXT01 and *S. albus* J1074/npsHK02, biological triplicates in technical duplicates were measured. The asterisk indicates the aforementioned compound postulated to be met-pacidamycin 5.

Table 28**:** Mutant strains, harboring the napsamycin BGC, constructed in this study displaying a positive effect on compound production

Strain	**Produced compounds**	**Fold-change**	**Reference strain by which fold-change was calculated**
S. albus J1074/npsPK02	Mureidomycin B Mureidomycin A Mureidomycin E/ Napsamycin A Napsamycin C	4.58	*S. albus* J1074/npsXT01
S. albus J1074/pRS02/npsPK02	Mureidomycin B Mureidomycin A Mureidomycin E/ Napsamycin A Napsamycin C	4.51	*S. albus* J1074/npsXT01
S. albus J1074/pRS04/npsPK02	Mureidomycin B Mureidomycin A Mureidomycin E/ Napsamycin A Napsamycin C	5.28	*S. albus* J1074/npsXT01
S. albus J1074/npsHK02	Mureidomycin A Mureidomycin E/ Napsamycin A Met-pacidamycin 5 *	90.22	*S. albus* J1074/npsXT01
S. albus J1074/npsHK02	Mureidomycin A Mureidomycin E/ Napsamycin A Met-pacidamycin 5 *	3.49	*S. albus* J1074/npsPK02
S. albus Del14/npsHK02	Mureidomycin A Mureidomycin E/ Napsamycin A Met-pacidamycin 5 *	1.92	*S. albus* J1074/npsHK02

3.3 Optimized mutant strain for mureidomycin A production

Lastly, the most promising candidate strains, constructed in this study, were cultivated under the same conditions, in order to compare final mureidomycin A production yields and identify the optimal producer strain. For the pacidamycin gene cluster, the most promising candidate was *S. albus* Del14/pRS04/pacHK11, which harbored PC1 between *pac3* and *pac4*, and, regarding the napsamycin/mureidomycin BGC, highest production yield was observed in *S. albus* Del14/npsHK02 (Δ*npsU*). The major compounds, as detected at typical retention times for UPAs, are depicted in the UV-chromatograms and base peak chromatograms of Fig. 68. For *S. albus* Del14/npsHK02 (Fig. 68A + B), the major compound was mureidomycin A (*m/z* 841.3 $[M+H]^+$), followed by the mureidomycin A derivative with a leucine or *iso*-leucine at position four of the amino acid scaffold (*m/z* 823.4 $[M+H]^+$), *N*-acetylmureidomycin A (*m/z* 883.4 $[M+H]^+$), met-pacidamycin 5 (*m/z* 825.4 $[M+H]^+$) and an unidentified compound with an *m/z* value of 867.3 $[M+H]^+$. Contrastingly, while UPA production rates of the modified pacidamycin BGC are lower, only two major compounds were detected: mureidomycin A (*m/z* 841.3 $[M+H]^+$) and met-pacidamycin 5 (*m/z* 825.4 $[M+H]^+$) (Fig. 68A + C).

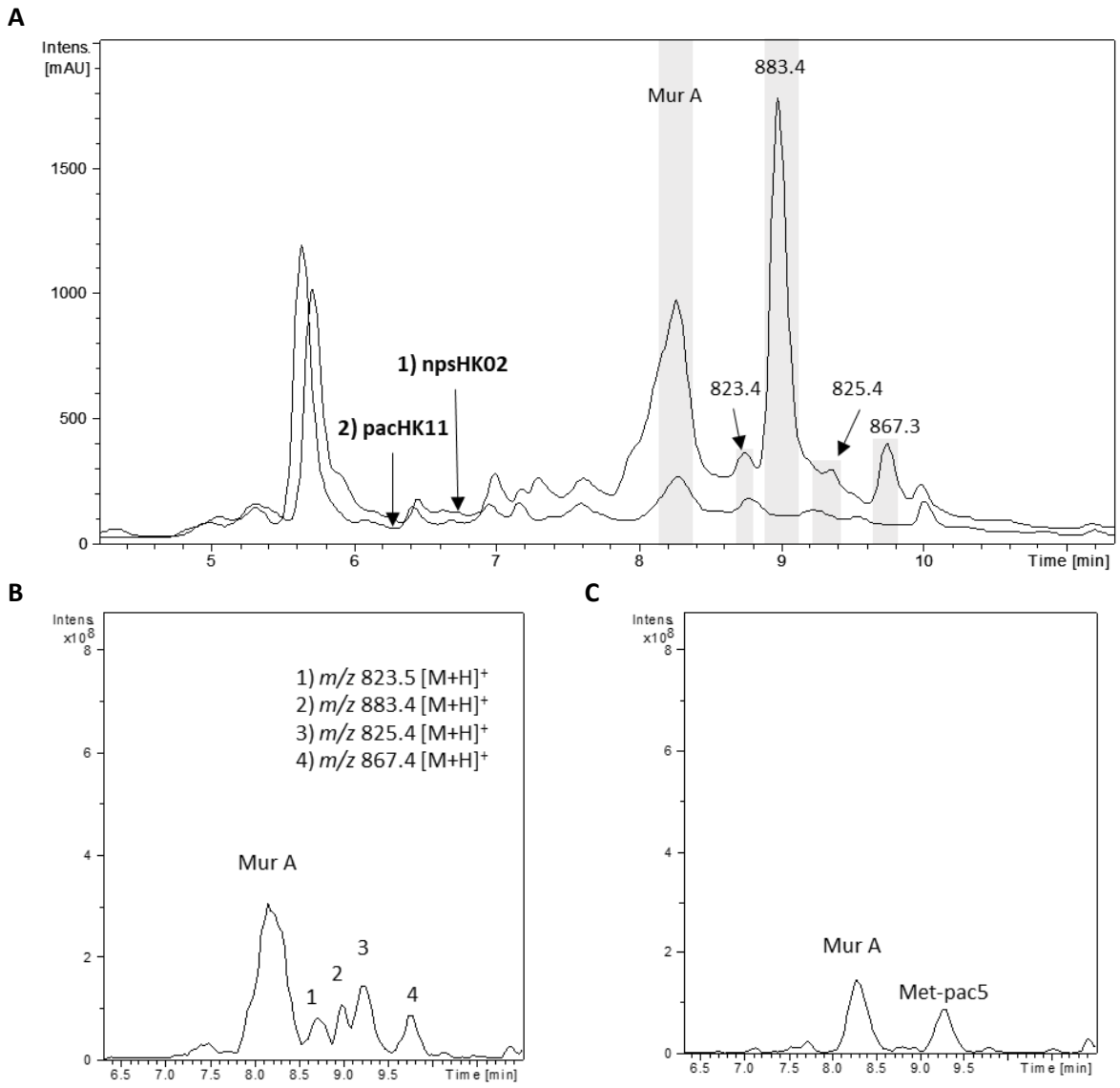


Fig. 68: LC-MS analysis of final mutant strains *S. albus* Del14/npsHK02 and *S. albus* Del14/pRS04/pacHK11.
A) UV-chromatograms at 260 nm of 1) *S. albus* Del14/npsHK02 and 2) *S. albus* Del14/pRS04/pacHK11, major peaks within the range of UPA retention times were marked and labeled with the most abundant mass, B) Base Peak Chromatogram 700 - 900 +ALL MS of *S. albus* Del14/npsHK02, major peaks were labeled with the most abundant mass and C) Base Peak Chromatogram 700 - 900 +ALL MS of *S. albus* Del14/pRS04/pacHK11, major peaks were labeled with the most abundant mass.

More specifically, when comparing mureidomycin A EIC signal intensities for the optimized gene clusters, on average a 3.01-fold increase from *S. albus* Del14/pRS04/pacHK11 to *S. albus* Del14/npsHK02 was measured. Therefore, the bacterial strain displaying the highest mureidomycin A production was concluded to be *S. albus* Del14/npsHK02 (Fig. 69).

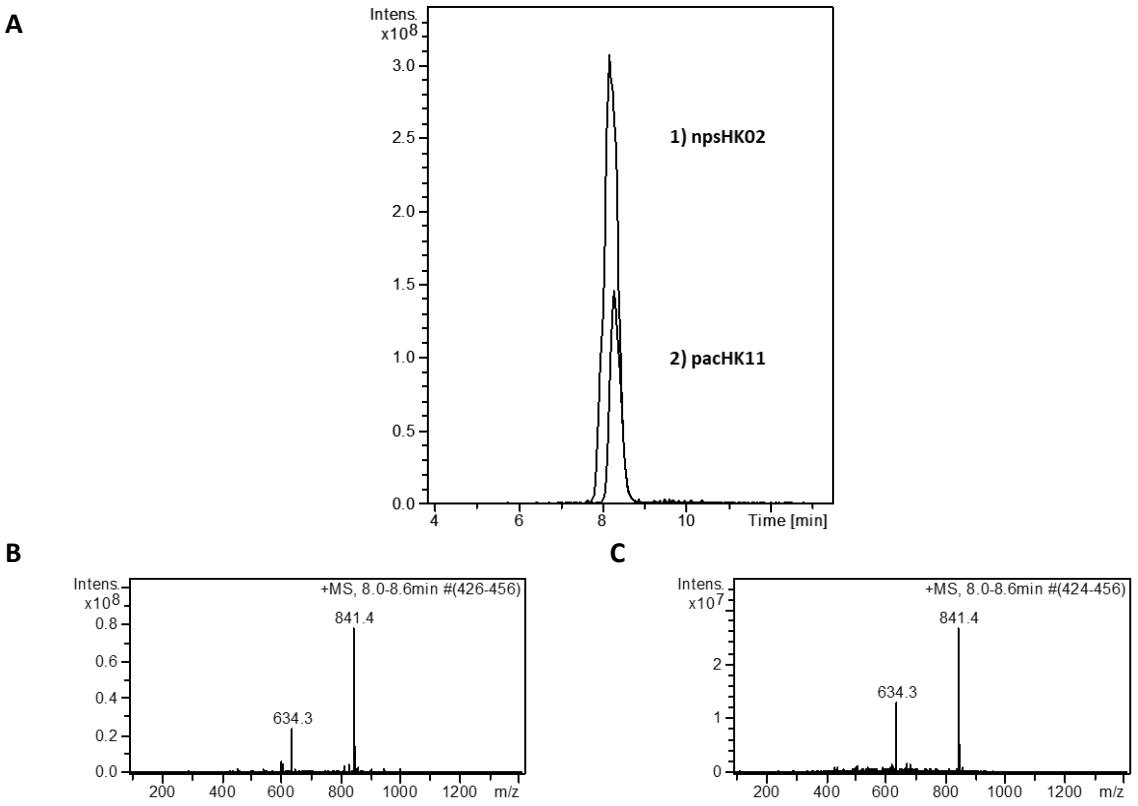


Fig. 69: LC-MS analysis of final mutant strains *S. albus* Del14/npsHK02 and *S. albus* Del14/pRS04/pacHK11. A) Extracted Ion Chromatograms of mureidomycin A *m/z* 841.3 $[M+H]^+$ in 1) *S. albus* Del14/npsHK02 and 2) *S. albus* Del14/pRS04/pacHK11, B) +MS spectrum of *S. albus* Del14/npsHK02 at t_R = 8.0 - 8.6 min, and C) +MS spectrum of *S. albus* Del14/pRS04/pacHK11 at t_R = 8.0 - 8.6 min.

4. Discussion

4.1 Increased production by expression of the pacidamycin gene cluster

The overarching goal of this study involved increasing mureidomycin production yield, which was attempted with different strategies. Generally, a plethora of different methods has been implemented in the genus *Streptomyces* to activate silent biosynthetic gene clusters and improve yield of compounds with low production rates. This stems from the estimation that out of all antimicrobial and otherwise interesting compounds encoded in this genus only a fraction has been discovered hitherto, partly due to secondary metabolite gene clusters being seldomly expressed under standard laboratory conditions[146–150].

Chemical and physical mutagenesis

The traditional approach to increase secondary metabolite production consists of random chemical and physical mutagenesis, especially for industrial strain enhancement. This was, for example, demonstrated by Mo *et al.* (2013)[151], who utilized the chemical mutagen *N*-methyl-*N*'-nitro-*N*-nitrosoguanidine in combination with exposure to UV radiation as a physical mutagen, in order to improve FK506 production in *Streptomyces* sp. RM7011. The combined effect on compound yield was an 11.63-fold increase in comparison with the wild type strain. This method could be used in the future to further improve mureidomycin production of the constructed mutant strains, to facilitate upscaling of production for industrial fermentations.

Media optimization

Furthermore, media screening constitutes a commonly applied strategy for improved secondary metabolite production in bacteria. In the case of the anthracycline-type antitumor compound doxorubicin, the two aforementioned methods were combined by Wang *et al.* (2018)[152], who induced mutations in the producer strain *Streptomyces peucetius* SIPI-11 by repeated UV and ARTP (atmospheric and room temperature plasma) treatment. Thus, doxorubicin production was increased from 119 mg/L to 570 mg/L (4.79-fold). The subsequent optimization of the culture medium further increased the yield to 850 mg/L (1.49-fold). A different study conducted by Zettler *et al.* (2014)[153] elevated yield of aminocoumarins cacibiocin A and B from 10.7 mg/L to 60 mg/L through media screening in cultivations in the heterologous host *Streptomyces coelicolor* M1152, which amounts to a 5.61-fold increase. Media optimization concerning UPAs was carried out by Dr. Nils Hauck in his PhD thesis[18], where six media described in literature for UPA production were compared. Therein, it was

concluded that cultivation in P-medium led to the highest UPA production rates for *Streptomyces* sp. DSM5940 (wild type producer of napsamycins/mureidomycins), *S. albus* J1074/npsXT01 (heterologous host harboring the napsamycin BGC) and *S. albus* J1074/pacNH01 (heterologous host harboring the pacidamycin BGC). Thus, this medium was utilized for cultivations in the present study.

One Strain Many Compounds (OSMAC)

Moreover, a simple yet effective strategy to activate silent biosynthetic gene clusters, which also incorporates media composition optimization, is the OSMAC approach (One Strain Many Compounds). This strategy is based on the hypothesis that bacterial strains harbor the potential to express different secondary metabolites under different conditions, like medium composition, cultivation conditions (pH, aeration and culture temperature), co-cultivation with other strains and adding biosynthetic precursors or enzyme inhibitors. Armin *et al.* (2021)[154] applied a combined chemical and biological OSMAC approach to cultures of *Streptomyces ciscaucasicus* GS2, which consisted of the testing of six different cultivation media and co-cultivation with the endophytic *Streptomyces pulveraceus* ES16 and the pathogen *Cylindrocarpon olidum,* separately. Thus, the iron-chelated siderophores ferrioxamines and the unchelated desferrioxamines were elucidated. Additionally, the antiviral geninthiocins E and F were isolated and elucidated from *Streptomyces* sp. CPCC 200267 by Fang *et al.* (2023)[155] through an OSMAC approach. Such a methodology might be used in the future to derivatize and potentially discover novel UPAs.

Metabolomics, proteomics, genomics and transcriptomics

More recent advances include ‘‘-omics’’-based methods to enhance production of secondary metabolites, which include metabolomics, proteomics, genomics and transcriptomics. Engineering of metabolic networks, for instance, led to enhanced oxytetracycline (OTC) titers in *Streptomyces rimosus* M4018. This was accomplished through the deletion of genes *zwf1* and *zwf2*, which encode for isoenzymes of G6PDH (glucose-6-phosphate dehydrogenase) in *Streptomyces*. Thus, supply of the OTC precursor malonyl-CoA was improved and OTC yield increased by up to 28.6 %[156]. Moreover, engineered proteomics increased doxorubicin (DXR) production in *Streptomyces peucetius* ATCC 27952. Pantothenate kinase (*panK*) from *E. coli* had been integrated into this strain to elevate coenzyme A pool and improve production yield. However, aglycon accumulation and a decrease in DXR production were observed. This effect was explored by the examination of proteome changes in the modified strain. Thus, the down-regulated DXR exporter DrrAB was overexpressed to secrete the toxic compound, which improved DXR production 9.4-fold in comparison with the *panK*-integrated strain[157]. Another highly utilized strategy, which has been developed to enhance secondary metabolite

production, is ribosome engineering. This involves, for instance, introducing mutations in ribosomal proteins against drugs targeting ribosomes, which improves antibiotic production[158], or work on *rpoB* (encoding for the RNA polymerase β-subunit) mutant strains, displaying increased transcription levels[159]. Furthermore, genomic approaches include the introduction of additional copies of entire biosynthetic gene clusters into native producer strains, as was demonstrated by Liao *et al.* (2010)[160]. In the respective study, the nikkomycin BGC was inserted into *Streptomyces ansochromogenes* 7100 and, thus, a 4-fold increase in nikkomycin X and 1.8-fold increase in nikkomycin Z production was observed. A differing genomic approach consists of genome shuffling, which is initiated by random mutagenesis followed by protoplast fusion of the resulting mutant strains and concluded by screening for strains displaying highest yields. This was applied by Zhang et al. (2002)[161], who improved tylosin yield in *Streptomyces fradiae* up to 9-fold.

Engineered transcriptomics involve, inter alia, investigations regarding the complex regulatory network governing secondary metabolite expression in *Streptomyces*[162]. One strategy to improve transcription levels or activate silent biosynthetic gene clusters consists of the overexpression of global or cluster-specific positive regulators, to which a plethora of corresponding examples can be found in literature. A semi-targeted approach was conceived by Mingyar *et al.* (2021)[163], who simultaneously integrated multiple positive regulators (cluster-situated and *Streptomyces* antibiotic regulatory proteins - SARPs) into the genomes of several *Streptomyces* sp. (TÜ10, 17 and 102) and thereby triggered the production of secondary metabolites of previously silent BGCs. Furthermore, silent biosynthetic gene clusters can also be activated or silenced by global regulators, as observed by Xu et al. (2017)[164]. In the respective study, the deletion of global regulator AdpA simultaneously activated a cryptic oviedomycin BGC and hindered nikkomycin production, displaying the complex regulatory mechanisms governing production of secondary metabolites. Moreover, deletion of repressors of compound biosynthesis has also been proven beneficial for secondary metabolite production. For instance, the deletion of putative GntR-like transcriptional regulator *ptmR1* in *Streptomyces platensis* MA7327 and *Streptomyces platensis* MA7339 led to overproduction of antibiotics platensimycin and platencin, respectively. The observed production yield for platensimycin increased from 56 mg/L to 323 mg/L[165]. Contrastingly, Xu *et al.* (2019)[166] identified and overexpressed the cluster-specific positive regulator for toyocamycin biosynthesis ToyA (large ATP-binding regulator of the LuxR family, LAL-family) in *Streptomyces diastatochromogenes* 1628, which increased production up to 2-fold. Closely-related work was done by Jiang *et al.* (2017)[167], who described the TetR family regulator GdmRIII to act as a positive regulator on geldanamycin biosynthesis and as a negative regulator of elaiophylin biosynthesis. Therefore, its deletion led to the detection of elaiophylin production. Thus, the effect of regulator manipulation on UPA yield was investigated by Dr. Nils Hauck in his PhD thesis[18]. Therein, the putative ArsR-type regulator NpsA of the napsamycin

biosynthetic gene cluster was investigated, which had been postulated to act as a repressor, due to its classification as a member of the ArsR-family of transcriptional repressors[168]. Interestingly, UPA production was abolished in *npsA*-knockout mutants as well as mutants where *npsA* had been overexpressed. This suggests a delicate balance of *npsA* levels is necessary for UPA production. While no homolog of *npsA* can be found in most UPA gene clusters, a different type of regulator has been described for this compound family. Li *et al.* (2013)[84] characterized the first regulator of UPA biosynthesis SsaA as a critical, cluster-specific activator of sansanmycin biosynthesis, belonging to a new family of transcriptional regulators. This class harbors an N-terminal fork head-associated domain and a C-terminal LuxR-type helix-turn-helix motif. Furthermore, SsaA was found to bind to several putative promoter regions of the respective cluster and to exert a feedback mechanism, sensing sansanmycin A and H accumulation. More specifically, sansanmycins A and H inhibited SsaA in a concentration-dependent manner via direct interaction with the regulator. SsaA was utilized by Jiang *et al*. (2015)[15] for the activation of a cryptic mureidomycin gene cluster in *S. roseosporus* NRRL 15998, while overexpression of the *ssaA* homolog *SSGG_02995*, situated within the cluster, did not stimulate mureidomycin production. The respective orthologous genes of the napsamycin and pacidamycin gene clusters are *npsM* and *pac1*. Their influence on UPA production was investigated by Dr. Nils Hauck in his PhD thesis[18], who cloned *ssaA*, *npsM* and *pac1* into replicative plasmids, which were then conjugated with *S. albus* J1074/pacNH01 (heterologous expression of pacidamycin BGC), *S. albus* J1074/npsXT01 (heterologous expression of napsamycin BGC) and *S*. sp. DSM 5940 (napsamycin wild type producer), while *S. coeruleorubidus* NRRL 18370 (pacidamycin wild type producer) was not amenable to conjugation efforts. The insertion of *pac1* and *ssaA* reduced UPA production in all three strains, which is congruent with results of the RNA-sequencing conducted in the present study, where *pac1* was found to be silenced in the pacidamycin BGC and might therefore have negative effects on UPA production. Furthermore, compound yield was nearly doubled when *npsM* was inserted. A subsequent integration of *npsM* into *S. albus* J1074/pacNH01 via the integrative vector pSET152 led to a 1.5-fold increase in pacidamycin D yield. Thus, the work on NpsM was continued by Richard Sonnengruen of our working group, who cloned the respective gene into the integrative plasmid pRS02, harboring genes for the integration of *m*-tyrosine at position 2 of the UPA scaffold, resulting in pRS04 (unpublished data). The effect of the integration of these two plasmids into different mutant strains was further compared in the present study. No significant influence on UPA production was observed upon integrating *npsM* encoded on pRS04 into *S. albus* J1074/pacHK03 (pacidamycin BGC pacRS01 harboring PC1) in comparison with *S. albus* J1074/pRS02/pacHK03, while the EIC signal intensity of mureidomycin A was even slightly decreased (see 3.1.1.1). A first possible explanation for these unexpected observations stems from the RNA-sequencing analysis conducted of the respective mutants (see 3.1.2), where *npsM* seemed to be silenced on plasmid pRS04. However,

differing observations were made regarding the further modified pacidamycin gene cluster pacRS03. In this case, neither the combination of pacRS03 with the positive regulator, nor the promoter replacement on pacRS03 resulting in pacHK11 improved production rates significantly, while the latter led to slightly increased compound production. Contrastingly, for the combination of synthetic promoter cassette PC1 with regulator NpsM a synergistic effect was observed, leading to significantly increased mureidomycin A production. This might partly be explained by the study of Li *et al.* (2013)[84], who found the NpsM-homolog SsaA to be inhibited by sansanmycins A and H in a regulatory feedback mechanism. Sansanmycin A is structurally identical to met-pacidamycin 4, which is only produced by pacHK03, but not pacRS03 or pacHK11. A potentially similar feedback mechanism regarding NpsM might therefore inhibit regulator function on pacHK03 (potentially explaining the lack of benefits on UPA production in this combination), but not in the novel clusters pacRS03 and pacHK11. Therefore, increased UPA production was expected as a result of the influence of NpsM on pacRS03 and pacHK11, but only observed for pacHK11. However, in data of cultivations conducted by Richard Sonnengruen of our working group, this positive effect in the combination of pacRS03 with regulator NpsM was detected, supporting the previous hypothesis. Furthermore, compound production of pacRS03 and pacHK11 might be more amenable to improvements, since only two main compounds are being produced in comparison with pacHK03, where five main UPAs can be detected. This prompted the decision to favor the integration of pRS04 in contrast to pRS02 in subsequent experiments.

Reconstruction of biosynthetic pathways

The reconstruction of biosynthetic pathways has been utilized to uncouple the expression of secondary metabolites of the complex regulatory network of the host strains[169]. For example, Basitta *et al.* (2017)[170] assembled four operons of the novobiocin biosynthetic gene cluster in the Artificial Gene Operon assembly System (AGOS) via Red/ET-mediated homologous recombination. Thus, heterologous expression in *S. coelicolor* M1146 was facilitated and novobiocin production was detected alongside novobiocin precursors. However, production rates of novobiocin were strongly decreased from 36 mg/L in the wild type cluster (*S. coelicolor* M1146/novBG01) to approximately 40 µg/L in the AGOS expression system. Therefore, Basitta *et al.* (2017)[170] investigated the influence of terminators in the AGOS constructs and detected a slight production increase upon terminator insertion (~10 µg/L novclobiocic acid 106 to ~65 µg/L). It was, thus, postulated that the inclusion of terminator sequences in artificial operons benefits mRNA stability and reduces degradation processes, causing increased translation and availability of biosynthetic enzymes leading to product synthesis. Another example of a plug-and-play system for BGC reconstruction was demonstrated by Shao *et al.* (2015)[169], who reorganized and thus reactivated the silent BGC of spectinabilin in *S. lividans*. This was accomplished by assembling all biosynthetic genes, except for the gene encoding for the

cluster-specific repressor *norD*, in a scaffold, where each gene was situated under the control of a separate promoter and simultaneously all native terminators were preserved. Moreover, all genes were placed downstream of strong, constitutive promoters, except for *norG*, which encodes for the first enzyme of the biosynthetic pathway and was coupled with an inducible promoter. This approach was chosen in order to alleviate the competition between primary and secondary metabolism, since NorG catalyzes the conversion of the shikimate pathway-derived chorismate to *p*-aminobenzoic acid. Furthermore, *norE* was inverted in this design, since it was the sole gene encoded on the opposite strand from all remaining genes of the cluster. Hence, spectinabilin production was activated in *S. lividans*, amounting to 105 +/- 21 µg/L. In a more recent study conducted by Tian *et al*. (2023)[171], a cryptic biosynthetic pathway encoding for kitaniitetronins was identified in *Kitasatospora niigatensis* DSM 44781. For this purpose, the postulated core biosynthetic genes were assembled in a synthetic operon under the control of the strong constitutive promoter *kasO*p*, where *kntB* was inverted, *ktnG* was inserted at a different position to its native location and several genes with unknown functions were deleted. The heterologous expression of this synthetic cluster in *S. coelicolor* M1154 led to the isolation and structure elucidation of kitaniitetronin A. These studies constitute a proof-of-concept for the gene inversion conducted in the present work (see 3.1.4), since Shao *et al.* (2013)[169] and Tian *et al*. (2023)[171] inverted single genes and situated them under the control of strong promoters in the resulting BGCs. The dramatic drop in compound production detected in this work is congruent with the decreased novobiocin production observed by Basitta *et al.* (2017)[170]. Therefore, the insertion of terminators downstream of *pac11* and *npsP3* might cause a slight elevation in UPA production, based on the hypothesis of Basitta *et al.* (2017)[170] on mRNA stability. This corresponds to the experimental design of Shao *et al.* (2013)[169], who preserved the native terminators. However, production levels in the novobiocin study were not restored to the yield of the native producer. Therefore, the effect of including terminators in pacHK14 might also be minute.

Promoter engineering and RNA-sequencing analysis

In *Streptomyces*, one of the most effective and well-established methods to activate silent biosynthetic gene clusters and improve production of lowly-expressed clusters consists of promoter engineering, which encompasses the replacement of native promoters with constitutive or inducible ones, leading to the desired transcription levels. For this purpose, a plethora of promoters active in *Streptomyces* have been described[141,172]. For example, Bauman *et al.* (2019)[173] activated a cryptic phenazine-type BGC from the marine *Streptomyces* sp. CNB-091 by inserting a bidirectional *sp44_p21* promoter cassette upstream of key structural elements, which led to the discovery of potent antibiotic streptophenazines and a phylogenetically distinct group of adenylation domains. Moreover, Du *et al*. (2013)[174] improved yield of the peptidyl nucleoside antibiotic gougerotin in *S. coelicolor* M1146 up to

10-fold through the promoter replacements with P_{hrdB} (constitutive promoter of *hrdB*, encoding for the principal sigma-like transcription factor of *Streptomyces*) upstream of key structural genes. A more recent development was reported by Zhang *et al.* (2017)[175], who adapted the CRISPR-Cas9 system to replace native promoters in silent biosynthetic gene clusters and, thus, activated BGCs in five *Streptomyces* species. Promoter engineering was also conducted in the present work. Firstly, bidirectional promoter cassettes PC1 and PC2, which had been constructed by Dr. Franziska Wiker in her PhD thesis[137], were knocked into different sites of the pacidamycin BGC. Therein, the promoter sequences P15_P16 and P03_P04 were included, which had been described by Montiel *et al.* (2015)[136]. In the respective study, bidirectional promoter cassettes, harboring these sequences and *Streptomyces* ribosomal binding sites, were constructed and validated by refactoring the well-characterized rebeccamycin BGC, which led to the production of comparable compound levels to the cluster harboring native promoters, activating the silent tetarimycin BGC and refactoring the silent eDNA-derived lazarimide BGC, all in *S. albus*. In the present study, promoter cassette PC1 led to increased UPA production, when knocked-in between *pac3* and *pac4*. This production increase might stem partly from the overexpression of *pac3*, which encodes for a putative major facilitator transporter, responsible for UPA efflux. This was postulated to cause a shift in the UPA production equilibrium, since the products of the biosynthetic pathway were removed from the cells more efficiently, which might prompt improved production rates through feedback mechanisms. The overexpression of *pac3* also constitutes an upregulated resistance mechanism, which might improve bacterial capacity to synthesize increased amounts of UPAs. This corresponds to data by Dr. Franziska Wiker, who detected novel peaks in the UV-chromatogram subsequent to promoter replacements with PC1 in a silent BGC of *Actinokineospora enzanensis* DSM 44649[137].

Furthermore, the improved compound yield was correlated with enhanced transcription rates of all operons, as observed in the respective RNA-sequencing results (see 3.1.2). This suggests a crosstalk between operons, likely through regulatory mechanisms, which enhance transcription rates of all operons, when operons 2 and 3 are more strongly transcribed due to the insertion of PC1. The RNA-sequencing further suggests transcription of genes encoding for the DABA-moiety (2,3-Diaminobutyric acid) to be a limiting factor for UPA biosynthesis, since operon 6 was one of the least transcribed. This issue might be addressed in the future by the insertion of a unidirectional promoter upstream of *pac16* or *pac17*, or by feeding *L*-threonine to cultures. This strategy stems from a study of Lam *et al.* (2008)[85], who proposed *L*-threonine as a precursor for DABA biosynthesis, which is converted in an unusual β-replacement reaction. Moreover, although transcription levels of *npsP8* were detected to be lower than in other operons, the respective A-domain is fully functional and successfully incorporates methionine at position four of the UPA scaffold. A further strategy to improve transcription levels in the future might consist of codon optimization, by identifying rare codons, where transcription rates

displayed a significant drop in the RNA-sequencing. Hence, these could be replaced by codons which are abundant and commonly utilized in *Streptomyces*. The RNA-sequencing of plasmid pRS02 revealed low transcription levels of the phenylalanine hydroxylase *phhA*, which is situated under the control of its native promoter, as isolated from *S. coeruleorubidus*[120]. Thus, the *m*-tyrosine pool available for incorporation into the UPA scaffold might be increased by a promoter replacement with a strong unidirectional promoter upstream of *phhA*.

Unfortunately, when PC1 was knocked-in between *npsP4* and *npsP8*, UPA production was significantly reduced in all resulting mutants, raising the hypothesis that RNA silencing could be an explanation due to excessive gene cluster activation and read-through over *pac11* caused by a potential leaky terminator situated between *pac11* and *pac12*. This was determined to be highly unlikely through the RNA-sequencing data (see 3.1.2), which depicted a full stop of transcription between *pac11* and *pac12*, without read-through. This hypothesis could, however, not be dismissed completely, since no RNA-sequencing data of strains containing the strong promoter cassette PC1 at both bidirectional regions were available. Another explanation might be the need for balanced transcription rates between the operons. As shown by Ji *et al.* (2022)[176], the highest improvement in production yield of daptomycin in *S. roseosporus* was detected upon refactoring the BGC with one strong, one weak and two medium strength promoters, which led to a titer improvement of 1780 % from the wild type. Thus, utilizing only strong promoters might not always conclude in the highest benefit for production yield.

Furthermore, complete abolishment of compound production was observed for all constructs containing bidirectional promoter cassette PC2 (P03_P04). These observations are in accordance with the results described in the work of Dr. Franziska Wiker[137]. In the respective PhD thesis, PC1 had been knocked into a silent gene cluster from *Actinokineospora enzanensis* DSM 44649, resulting in new peaks in the UV-chromatogram. However, upon the knock-in of PC2 into the cluster already harboring PC1, the novel peaks disappeared. It was, thus, hypothesized in the present work that PC2 might be transcriptionally inactive under these conditions.

Since mureidomycin C production was generally not detected, it was hypothesized that the incorporation of glycine at position one of the UPA scaffold was unsuccessful, although the tRNA-dependent aminoacyl transferase *pac2* had been swapped on pacRS01 with its ortholog *npsN,* which displays a preference for glycine. Moreover, the RNA-sequencing revealed *npsN* to be fully transcribed. The orthologous gene *pacB* is a tRNA-dependent aminoacyl transferase, which incorporates an amino acid residue at the N-terminus of the UPA scaffold, resulting in the formation of a pentapeptide. During the characterization of *pacB*, Zhang *et al.* (2011)[87] observed an abundance of pentapeptide production in early stages of cultivation, whilst tetrapeptides were predominantly detected later on. This led the group to hypothesize that proteolysis, efflux and metabolite limitations during the stationary phase could account for the lack of pentapeptidyl forms in later stages of cultivations. Since mureidomycin C

also comprises a pentapeptide with an N-terminal glycine moiety, it might be hypothesized that detection is only possible during the first days of cultivation. This will be analyzed further in the PhD thesis of Richard Sonnengruen of our working group.

Subsequently, two novel bidirectional promoter cassettes PC3 and PC4 were constructed. The former consisted of a bidirectional *ermE*p* and the latter of an *ermE*p* and the *kasOp* derivative *kasOp*_SP44*. These promoters were chosen based on their wide utilization as strong, constitutive promoters, well characterized in *Streptomyces*. The promoter region of the erythromycin resistance gene (*ermE*), consisting of ermEp1 and ermEp2, was isolated from *Saccharopolyspora erythraea*[177]. Bibb *et al.* (1994)[178] further modified *ermE* through the deletion of three nucleotides in the -35 region of ermEp1, resulting in the upregulated *ermE** promoter[178], which initially displayed an approximately 5-fold increase in transcripts. One example of successful activation of silent BGCs by promoter replacements with *ermE** was described by Olano *et al.* (2014)[179], who activated the gene cluster of the blue pigment indigoidine and a hybrid PKS-NRPS BGC in *S. albus* J1074. The latter gene cluster was found to encode for the novel compounds 6-*epi*-alteramides A and B, belonging to the family of polycyclic tetramate macrolactams. Additionally, the native promoter *kasOp* of *S. coelicolor* is situated upstream of *kasO* which encodes for a SARP transcriptional activator. This promoter was engineered by Wang *et al.* (2013)[140], who uncoupled the promoter from its native regulatory elements and implemented random mutagenesis to increase transcriptional activity, which resulted in *kasOp** with 2- to 5-fold stronger transcription than observed for *ermE*p*. An attempt at further optimization of *kasOp** was conducted by Bai *et al.* (2015)[139], who randomly mutated nucleotides in the spacer region between the -10 and -35 sequences and nucleotides downstream from the -10 sequence. This resulted in the promoter sequence *kasOp*_SP44*, utilized in the present study, for which a 187.5 % increase in activity compared to *kasOp** was noted. In a study by Zheng *et al.* (2019)[180] the engineered *kasOp** was used to enhance neomycin yield in *S. fradiae* CGMCC 4.576, by situating the longest operon of the BGC under the control of the semisynthetic promoter. This led to a yield improvement of 36 %. In the present study however, production levels of mutant strains harboring the bidirectional *ermE*p* cassette were not significantly differing from mutants with the native promoters, while the bidirectional *ermE*p_ kasOp*_SP44* cassette decreased compound yield significantly. Since both aforementioned promoters are considered strong, constitutive promoters and *kasOp*_SP44* might be 4- to 10-fold more active than *ermE*p*, these results might indicate that a more balanced fine-tuning of gene expression is necessary. This has, for instance, been demonstrated by Ji *et al.* (2022)[176], who fine-tuned daptomycin transcription with promoters displaying different activities and, thus, maximized compound yield.

4.2 Increased production by expression of the napsamycin gene cluster

The project regarding the napsamycin BGC was commenced, since this cluster produced the desired compounds mureidomycins in its native form, but in low amounts, while the pacidamycin gene cluster had to be modified first to produce mureidomycins. Since with every step of genetic engineering UPA yield dropped, the need arose to subsequently improve pacidamycin production, and thus efforts were directed toward enhancing compound production for both BGCs.

Firstly, a promotor replacement on the napsamycin BGC was conducted with PC1 between *npsL* and *npsM*, with a simultaneous knockout of the NRPS A-domain *npsP6*. Kaysser *et al*. (2011)[14] postulated the discrete A-domain NpsP6 to specifically activate hydroxylated aromatic amino acids. Thus, *m*-tyrosine or 6-hydroxy-tetrahydroisoquinoline carboxylic acid (Htia) are incorporated at position two of the UPA scaffold and the respective knockout could be complemented with the orthologous A-domain *pac21h*, specific for the recognition of *m*-tyrosine. While the knockout of *npsP6* led to the expected cessation of compound production in all mutant strains, production could, interestingly, not be complemented with pRS02 (harboring *pac21h* and *phhA*), but only pRS04, which additionally harbors the cluster-specific positive regulator *npsM* of the napsamycin gene cluster. This indicates that *npsM* could have been damaged during the promoter replacement, since *npsM* is the first gene downstream of PC1. However, since sequencing of the respective intergenic region and the start of *npsM* revealed the sequence to be correct, further investigations need to be conducted. As expected, production of compounds containing a bicyclic moiety derived from Htia at position two of the UPA scaffold, like mureidomycin E/napsamycin A and napsamycin C, was decreased, while mureidomycin B yield was unaffected. Mureidomycin A production was slightly decreased, but not to a statistically significant extend.

Subsequently, similarly to the promoter swaps conducted on the pacidamycin biosynthetic gene cluster, the bidirectional promoter cassette PC1 was knocked-in between *npsO* and *npsP7* of the napsamycin gene cluster and a significant production increase was observed. This was expected, since the region affected by the promoter replacement in the napsamycin gene cluster *npsN* - *npsS* is orthologous to the region consisting of *npsN* - *pac7* of the pacidamycin gene cluster, where the first promoter swap had been beneficial to UPA production. Therefore, *npsO*, which encodes for a putative major facilitator transporter of the napsamycin gene cluster, is upregulated. This transporter exports UPAs out of the cells and, thus, possibly improves intracellular production rates through an equilibrium shift. Moreover, this overexpression further constitutes the enhancement of a self-resistance mechanism potentially leading to reduced toxicity of UPAs for the host strain, as was investigated by Malla *et al.* (2010)[181] for the doxorubicin/daunorubicin biosynthesis. In the respective study, the resistance genes *drrABC* from *S. peucetius* ATCC 27952 were overexpressed in a high-copy vector

under the control of a strong *ermE** promoter. An ATP-dependent efflux pump is formed by DrrA and DrrB, which exports the two anthracycline-type antitumor compounds doxorubicin and daunorubicin out of the cell. The overexpression of this efflux pump increased doxorubicin yield 2.2-fold, which resembles the mechanism and magnitude of overproduction caused by the exporter NpsO in the napsamycin BGC. In general, most antibiotic-producing *Streptomyces* harbor at least one mechanism of self-resistance to increase tolerance to the produced toxic compounds. Frequently, resistance genes are situated within the BGC of the respective secondary metabolite and encode for efflux pumps, enzymes causing antibiotic modifications or degradation, proteins causing antibiotic sequestration, or enzymes leading to modifications/bypass/protection of the susceptible molecular target[181–183]. While solely the exporter Pac3 could be hypothesized to serve as a resistance mechanism regarding the pacidamycin BGC, only one other potential self-resistance mechanism besides NpsO has been investigated for the napsamycin BGC, which involves the *N*-acetyltransferase NpsB. Acetyltransfer constitutes a common method for antibiotic inactivation through the formation of covalent bonds with vulnerable amine groups (*N*-acetylation) or hydroxyl groups (O-acetylation) present in the secondary metabolite[184]. Prevalent examples consist of aminoglycoside acetyltransferases[185], chloramphenicol acetyltransferases[186] and streptogramin acetyltransferases[187]. Regarding the napsamycin BGC, the *N*-acetyltransferase NpsB was investigated by Tang *et al.* (2013)[145], who observed a compound with an *m/z* value of 885.4 $[M+H]^+$, corresponding to *N*-acetylmureidomycin B in an MS^2 analysis. In the respective study, in *npsB*-knockout mutant strains production of this compound was abolished, while a subsequent in vitro incubation of crude extracts with purified N-terminally His_8-tagged NpsB led to full conversion of mureidomycin B (*m/z* 843.4 $[M+H]^+$) to *N*-acetylmureidomycin B (*m/z* 885.4 $[M+H]^+$). Moreover, in the same assay conducted with purified sansanmycin A (*m/z* 864.4 $[M+H]^+$), conversion to *N*-acetylsansanmycin A was detected (*m/z* 906.4 $[M+H]^+$). These acetylated derivatives were investigated in agar diffusion assays against *E. coli* Δ*tolC*, which had been proven to be sensitive to UPAs, but bioactivity was abolished. The *N*-acetylation was postulated to constitute a self-protection mechanism, since *N*-acetylmureidomycin B was found to accumulate in the mycelium of *S. coelicolor* M1154/npsXT01, while mureidomycin B was predominately detected in the supernatant of cultures. Tang *et al.* (2013)[145] further constructed *npsO*-knockout mutants and observed the same intracellular accumulation of *N*-acetylmureidomycin B, while mureidomycin B was detected only in traces. This prompted the hypotheses that NpsO might hydrolyze the acetyl group, excreting the active compound, or that resistance might be mainly conferred by the export of UPAs, while the acetylation might constitute a secondary resistance mechanism. This postulated function of NpsO might be an additional explanation to the observed increase in mureidomycin A yield, subsequent to the overexpression of the exporter conducted in the present study. More specifically, yield of mureidomycin A and the postulated *N*-acetylmureidomycin A were increased significantly, while

mureidomycin B and the postulated *N*-acetylmureidomycin B were slightly decreased. This supports the idea of an equilibrium between the acetylated UPA and its counterpart over the postulated *N*-deacetylation function of NpsO. Moreover, based on the data by Tang *et al.* (2013)[145], the present study focused on investigating the influence of genetic modifications on non-acetylated UPAs, and not the likely inactive derivatives. Interestingly, in the aforementioned work by Jiang *et al.* (2015)[15], the cryptic mureidomycin BGC of *S. roseosporus* NRRL 15998 was described to produce an array of *N*-acetylated mureidomycins, subsequent to gene cluster activation with SsaA. More specifically, eight novel compounds were detected, which corresponded to the *m/z* values of 899.2, 885.3, 883.3, 869.3, 867.3, 865.3, 851.3 and 849.3 $[M+H]^+$. All eight compounds were investigated by ESI-MS and MS^2, while the compounds with *m/z* values of 899.2 and 883.3 $[M+H]^+$ were further investigated by NMR analysis. This led the authors to propose the structures displayed in Table 29. Additionally, the *npsB* ortholog *SSGG_02979*, situated within the cryptic gene cluster, was proposed to conduct the respective *N*-acetylation reactions.

Table 29: Compounds detected in study by Jiang *et al.* (2015)[15], mureidomycins A and B included as a reference. For UPA scaffold, see Fig. 1.

Name	**R**	**AA4**	**AA5**	**Uracil**	**MW (Da)**
Mureidomycin A	H	Met	*m*-Tyr		840
Mureidomycin B	H	Met	*m*-Tyr	Dihydro-	842
N-acetylmureidomycin A	Acetyl	Met	*m*-Tyr		882
N-acetylmureidomycin B	Acetyl	Met	*m*-Tyr	Dihydro-	884
N-acetylmureidomycin E	Acetyl	Met^{SO}	*m*-Tyr		898
N-acetylmureidomycin F	Acetyl	Met	Phe	Dihydro-	868
N-acetylmureidomycin G	Acetyl	Met	Phe		866
N-acetylmureidomycin H	Acetyl	Leu/Ile	*m*-Tyr		864
N-acetylmureidomycin I	Acetyl	Leu/Ile	Phe		848
N-acetylmureidomycin J	Acetyl	Leu/Ile	Phe	Dihydro-	850

While different cultivation and extraction procedures were followed in the present study, in the data of Jiang *et al.* (2015)[15] the postulated *N*-acetylmureidomycin A was verified. This raises the question, whether compounds produced by the cryptic mureidomycin BGC correspond to hitherto unexplained

compounds of the napsamycin BGC. In the final producer strain *S. albus* Del14/npsHK02 of the napsamycin BGC, the major compound mureidomycin A and compounds with *m/z* 823.5, 825.4, 883.3 and 867.4 $[M+H]^+$ were detected. The former three were postulated to be a mureidomycin A derivative with a leucine or *iso*-leucine at position four of the amino acid scaffold (*m/z* 823.4 $[M+H]^+$), *N*-acetylmureidomycin A (*m/z* 883.4 $[M+H]^+$) and met-pacidamycin 5 (*m/z* 825.4 $[M+H]^+$) (see 3.3). Based on the work by Jiang *et al.* (2015)[15], the hitherto unexplained compound with an *m/z* value of 867.3 $[M+H]^+$ might be *N*-acetylmureidomycin G, which is structurally identical to the *N*-acetylated derivative of met-pacidamycin 5.

Subsequent to first isolation attempts, Jiang *et al.* (2015)[15] investigated fractions containing different compounds in a bioassay against *Pseudomonas aeruginosa* PA14. Therein, *N*-acetylmureidomycins E and H displayed distinct inhibition zones, a fraction containing *N*-acetylmureidomycins F and G minor inhibition zones and the remaining compounds no activity. This supports the previously described hypothesis of *N*-acetylmureidomycins A and B not displaying bioactivity.

4.3 Increased production by engineered heterologous hosts

A commonly applied technique to improve production yield of bacterial secondary metabolites is the expression of biosynthetic gene clusters in optimized heterologous hosts, which have been engineered to be advantageous over the native producers. Desirable attributes of heterologous hosts are amenability to genetic manipulation, high compound yield, lack of endogenous metabolites with biological activity, a reduced amount of secondary metabolite BGCs and a well-characterized secondary metabolism[133,188]. The *Streptomyces* strains, which have been most commonly used for heterologous expression, are, inter alia, *S. coelicolor*, *S. avermitilis* and *S. albus*. Since these strains harbor antibiotic or other secondary metabolite BGCs and in order to enhance compound production, a plethora of attempts has been conducted to engineer heterologous hosts genetically, in accordance with the abovementioned criteria.

Firstly, the complete genome sequence of *S. coelicolor* A3(2) was reported by Bentley *et al.* (2002)[147] as the first of all *Streptomyces*. In the respective study, its prototrophic derivative *S. coelicolor* M145, which lacks the two plasmids SCP1 (encoding the antibiotic methylenomycin) and SCP2 in comparison with its parental strain A3(2), was sequenced. Thus, more than 20 BGCs encoding for secondary metabolites in the 8,667,507 bp-long, linear chromosome were predicted. To date, at least 29 BGCs have been predicted in *S. coelicolor* A3(2)[189]. Since this strain is genetically well characterized, it has been utilized as a model organism in the study of *Actinomycetes*. Furthermore, *S. coelicolor* A3(2) was genetically engineered by Floriano and Bibb (1996)[190] to construct *S. coelicolor* M512, in which the cluster-specific positive regulators of prodiginine and actinorhodin biosynthesis were deleted and compound production of the respective antibiotics abolished. In a subsequent study, Gomez-Escribano and Bibb (2011)[191] manipulated *S. coelicolor* M145, constructing a number of optimized derivative heterologous hosts. The first issue, addressed in the respective work, was the presence of four BGCs encoding for antibiotic compounds in *S. coelicolor* M145. More specifically, this strain produces actinorhodin (by type II polyketide synthase biosynthesis), prodiginines (by NRPS - PKS hybrid biosynthesis), CDA (calcium-dependent antibiotic, NRPS-derived) and CPK (by cryptic type I polyketide synthase biosynthesis)[192]. The respective BGCs were deleted in the resulting *S. coelicolor* M1146, in order to enhance precursor supply and simplify the metabolic background, thus facilitating compound isolation and bioactivity assays. Moreover, *rpoB* (encoding for the β-subunit of RNA polymerase) was mutated in *S. coelicolor* M1146, generating *S. coelicolor* M1152. Then, in the latter strain, *rpsL* (encoding for ribosomal protein S12) was mutated, leading to *S. coelicolor* M1154. These modifications strongly and unspecifically increased secondary metabolite production in the respective strains. Furthermore, Zhou *et al.* (2012)[193] constructed *S. coelicolor* M145 derivatives with minimized genomes, in which all ten PKS and NRPS gene clusters were sequentially deleted,

simultaneously with a 900-kb subtelomeric sequence (*S. coelicolor* FX-series and ZM-series). Following a similar approach, Thanapipatsiri *et al.* (2015)[194] genetically engineered *S. coelicolor* M1152 to obtain the heterologous host *S. coelicolor* M1317, optimized for the expression of type III PKS biosynthetic gene clusters. This novel host was constructed through the deletion of all three type III PKS genes in *S. coelicolor* M1152, in order to enhance precursor supply.

Moreover, Ikeda *et al.* (2003)[195] sequenced the complete genome of the pharmaceutically relevant strain *S. avermitilis*, and determined the linear chromosome to span 9,025,608 bp and to encode for at least 30 secondary metabolite BGCs. Additionally, the two linear plasmids SAP1 and SAP2 were detected. To date, at least 38 secondary metabolite BGCs have been predicted in *S. avermitilis* MA-4680[196], among which the anthelmintic compounds avermectins are encoded. Henceforth, this strain was utilized as a host for heterologous expression of secondary metabolites. Thus, efforts were conducted for further strain improvements. For this purpose, Komatsu *et al.* (2010)[197] minimized the genome of *S. avermitilis* by consecutively deleting nonessential genes. While *S. coelicolor* harbors ~ 1 Mb subtelomeric regions at each end of its linear chromosome, the respective regions of *S. avermitilis* are asymmetrical, consisting of 2 Mb and 0.5 Mb, respectively. These segments contain nonessential genes, involved in the secondary metabolism, and thus Komatsu *et al.* (2010)[197] consecutively deleted > 1.4 Mb from the left subtelomeric region, resulting in the derivative strains *S. avermitilis* SUKA2 - SUKA17. In the subsequent heterologous expression of streptomycin, a significant production increase was observed in comparison with the original producer *S. griseus* and the native *S. avermitilis*. This was further demonstrated in a later study by Komatsu *et al.* (2013)[198], in which 18 BGCs were expressed in the optimized host *S. avermitilis* SUKA17 and an isogenic derivative. Therein, a lack of interference by major endogenous metabolites was observed, which improved yield by increasing precursor availability. However, production rates were not improved for all investigated compounds.

Regarding Uridyl Peptide Antibiotics, the optimized heterologous hosts *S. coelicolor* M512, *S. coelicolor* M1146 and *S. coelicolor* M1154 were tested by Dr. Nils Hauck in his PhD thesis[18], alongside the hosts *S. lividans* TK24, *S. lividans* 1326, *S. venezuelae* ATCC 10712 and *S. albus* J1074, in agar diffusion assays against *E. coli* BW25113 Δ*tolC*. The hosts displaying the largest inhibitory zones in the bioassay, *S. albus* J1074, *S. coelicolor* M1146 and *S. coelicolor* M1154, were analyzed regarding the respective pacidamycin D production via LC-MS. While all strains increased compound production in comparison to the wild type producer *S. coeruleorubidus* NRRL 18370, the highest elevation was observed for *S. albus* J1074, which was, thus, concluded to be the optimal host for UPA production. Therefore, heterologous expression of the pacidamycin and napsamycin BGCs was conducted in *S. albus* J1074 in the work by Dr. Nils Hauck, as well as in the present work.

Generally, genetic manipulation of *S. coelicolor* has slowed, since a plethora of modifications has already been conducted, while *S. avermitilis* has been known to be less amenable to genetic manipulation. Contrastingly, optimized derivatives of *S. albus* G have been developed in recent years, which display rapid growth, high compound yield and amenability to genetic modifications[133]. Chater and Wilde (1976)[132] isolated the *S. albus* G mutant *S. albus* J1074, which, in contrast to the parental strain, harbors a defective SalI bacteriophage restriction system. Henceforth, this strain has been used for efficient heterologous expression of secondary metabolite BGCs, where one of the first successful applications was reported by Rodríguez *et al*. (1993)[199]. Further genetic optimizations of *S. albus* J1074 were conducted by Myronovskyi *et al.* (2018)[133], who deleted 15 nonessential secondary metabolite BGCs in the chromosome of *S. albus* J1074 and thus obtained strains *S. albus* Del1 - Del14. Therein, the aim was to simplify the metabolic background, enhance precursor supply and facilitate compound detection and isolation. The consecutively deleted BGCs and resulting mutant strains are displayed in Table 30.

Table 30: Consecutive secondary metabolite gene cluster deletions in optimized *S. albus* J1074 derivatives**,** adapted from Myronovskyi *et al.* (2018)[133]

Mutant strain	**Deleted biosynthetic gene cluster**	**Size of deletion**
S. albus Del1	Candicidin and antimycin	204.8 kb
S. albus Del2	Flaviolin	4.2 kb
S. albus Del3	Carotenoid isorenieratene	10.2 kb
S. albus Del4	NRPS/Blue pigment synthetase	8.3 kb
S. albus Del5	NRPS	9.4 kb
S. albus Del6	NRPS	67.4 kb
S. albus Del7	NRPS	33.7 kb
S. albus Del8	Lantibiotic	19.6 kb
S. albus Del9	Geosmin synthase	2.4 kb
S. albus Del10	NRPS	31.4 kb
S. albus Del11	Paulomycin	45.7 kb
S. albus Del12	Frontalamide	20.2 kb
S. albus Del13	Type I PKS-NRPS	18.8 kb
S. albus Del14	Type I PKS-NRPS	26.9 kb

Subsequently, additional *phi*C31 *attB* sites were integrated into the chromosome of *S. albus* Del14, resulting in strains *S. albus* B2P1 (containing two canonical *attB* sites and one pseudo-*attB* site), B3P1 (containing three canonical *attB* sites and one pseudo-*attB* site) and B4 (containing four canonical *attB* sites), thus allowing the integration of multiple copies of BGCs encoded on *phi*C31-based integrative vectors into the genome. One successful example regarding compound overexpression through multiple copies of a BGC was observed by Yanai *et al.* (2006)[200], who investigated the industrial kanamycin overproducer strain *S. kanamyceticus* 12-6. Therein, the largest amplifiable unit of DNA (AUD) reported in *Streptomyces* was discovered, which included the entire kanamycin BGC and in some mutants exceeded 36 copies. Since kanamycin yield correlated with the copy number of the BGC, the authors postulated DNA amplification to be caused by selection for increased kanamycin resistance. More specifically, kanamycin production in strain *S. kanamyceticus* 12-6 (three copies of BGC on average) was increased approximately 2-fold in comparison to an isolate containing solely one copy. In a more recent study, Li *et al.* (2021)[201] amplified the spinosad BGC in *S. coelicolor* M1146 to five copies via a Cas9-assisted targeting approach, leading to a drastic yield increase (224-fold).

In the aforementioned study by Myronovskyi *et al.* (2018)[133], production rates of eight secondary metabolite BGCs (polyketides, nucleoside, phosphoglycolipid and lantibiotic) were compared in the therein constructed hosts with compound yield in the parental strain *S. albus* J1074 and the hosts *S. coelicolor* M1152 and M1154. Solely for the lantibiotic cinnamycin, production yield was the highest in *S. coelicolor*, while in most cases production was significantly enhanced in the optimized *S. albus* hosts. More specifically, five compounds were detected in higher amounts in strains harboring additional attachment sites, in comparison with *S. albus* Del14. Interestingly, regarding production rates of the nucleoside antibiotic tunicamycin B2, the integration of additional attachment sites did not lead to further benefits.

In the present study, UPA yield was significantly increased in *S. albus* Del14, when compared with *S. albus* J1074, as was expected. A possible explanation might be the deletion of multiple NRPS biosynthetic gene clusters in the optimized host, which might increase precursor availability for UPA biosynthesis and thus increase production rates. However, the integration of one additional attachment site in *S. albus* B2P1 did not lead to a further production enhancement, which indicates that UPA biosynthesis is not hampered on a transcriptional level. If transcription were a limiting factor, increased compound production would be expected subsequent to the integration of an additional copy of the BGC. Rather, the bottleneck might be located on a translational level or in precursor availability. The last heterologous host examined in the present work was *S. griseus* CS065, which was chosen based on a study conducted by Botas *et al.* (2021)[144], who increased the production of the immunosuppressive compound brasilicardin A to a gram-scale level. This was accomplished by a combination of heterologous expression in *S. griseus* CS065, media optimization, overexpression of

the cluster-specific positive regulator of brasilicardin biosynthesis *bra12* and tuning of the terpenoid-pathway. Therein, brasilicardin production was investigated in more than 70 heterologous hosts, out of which *S. griseus* CS065 displayed the strongest increase in production yield. While production levels of UPAs were significantly increased in the present study through the heterologous expression in *S. griseus* CS065, the enhancement was inferior to the one detected in *S. albus* Del14 mutants. However, production rates between biological replicates were more consistent in *S. griseus* CS065, displaying low fluctuations. Thus, *S. griseus* CS065 might be an ideal candidate for the quantification of compound production, in order to investigate the exact influence of modifications on yield. Contrastingly, *S. albus* Del14 might be suited for compound isolation, since overproducer mutants appear with a high frequency, despite high fluctuations in compound yield. Furthermore, its reduced metabolic background constitutes a beneficial factor for simplified compound isolation.

4.4 Outlook

Regarding the pacidamycin biosynthetic gene cluster, transcription rates and UPA production rates were significantly increased subsequent to the successful promoter replacement with PC1. The replacement of additional native promoters of the cluster might be beneficial, if transcription rates are carefully monitored with RT-qPCR and adapted and fine-tuned, accordingly. Therein, the insertion of unidirectional or even inducible promoters might be considered. Steps should be taken to eliminate the potential bottleneck of the biosynthesis, consisting of the transcription rates of the DABA-genes. Potential strategies might be the insertion of a unidirectional promoter upstream of *pac16* or *pac17*, or feeding of *L*-threonine to cultures as the respective precursor. Additionally, the cosmid harboring the pacidamycin BGC with one inverted operon could be further optimized by inserting transcriptional terminators downstream of *pac11* and *npsP3.* Moreover, the functions of the UPA regulators NpsM, Pac1 and SsaA, especially regarding possible feedback mechanisms, need to be elucidated further. Additional methods for production improvement, which might be tested in the future, are chemical and physical mutagenesis to optimize the final production strain and metabolic engineering to optimize precursor supply. As far as the napsamycin biosynthetic gene cluster is concerned, a knockout of *npsB* could be attempted, in order to decrease the variety of acetylated compounds still produced by the *npsU*-knockout mutants. As far as mureidomycin A yield is concerned, genetic engineering in combination with heterologous expression in optimized host strains led to highly significant production enhancements. In conclusion, a robust platform for mureidomycin A production was constructed, which paves the way for compound isolation, testing of MIC and IC_{50} values and first preclinical studies.

5. Bibliography

1. Inukai, M. *et al.* Mureidomycins A-D, novel peptidylnucleoside antibiotics with spheroplast forming activity. I. Taxonomy, fermentation, isolation and physico-chemical properties. *J. Antibiot. (Tokyo)* **42**, 662–666 (1989).
2. Isono, F. *et al.* Mureidomycins A-D, novel peptidylnucleoside antibiotics with spheroplast forming activity. II. Structural elucidation. *J. Antibiot. (Tokyo)* **42**, 667–673 (1989).
3. Beyer, P. & Paulin, S. Priority pathogens and the antibiotic pipeline: an update. *Bull. World Health Organ.* **98**, 151 (2020).
4. Isono, F., Katayama, T., Inukai, M. & Haneishi, T. Mureidomycins A-D, novel peptidylnucleoside antibiotics with spheroplast forming activity. III. Biological properties. *J. Antibiot. (Tokyo)* **42**, 674–679 (1989).
5. Chen, R. H., Buko, A. M., Whittern, D. N. & Mcalpine, J. B. Pacidamycins, a novel series of antibiotics with anti-Pseudomonas aeruginosa activity. II. Isolation and structural elucidation. *J. Antibiot. (Tokyo)* **42**, 512–520 (1989).
6. Fernandes, P. B. *et al.* Pacidamycins, a novel series of antibiotics with anti-Pseudomonas aeruginosa activity. III. Microbiologic profile. *J. Antibiot. (Tokyo)* **42**, 521–526 (1989).
7. Karwowski, J. P. *et al.* Pacidamycins, a novel series of antibiotics with anti-Pseudomonas aeruginosa activity. I. Taxonomy of the producing organism and fermentation. *J. Antibiot. (Tokyo)* **42**, 506–511 (1989).
8. Chatterjee, S. *et al.* Napsamycins, new Pseudomonas active antibiotics of the mureidomycin family from Streptomyces sp. HIL Y-82,11372. *J. Antibiot. (Tokyo)* **47**, 595–598 (1994).
9. Xie, Y., Chen, R., Si, S., Sun, C. & Xu, H. A new nucleosidyl-peptide antibiotic, sansanmycin. *J. Antibiot. (Tokyo)* **60**, 158–161 (2007).
10. Bugg, T. D. H., Lloyd, A. J. & Roper, D. I. Phospho-MurNAc-pentapeptide translocase (MraY) as a target for antibacterial agents and antibacterial proteins. *Infect. Disord. Drug Targets* **6**, 85–106 (2006).

11. Isono, F. & Inukai, M. Mureidomycin A, a new inhibitor of bacterial peptidoglycan synthesis. *Antimicrob. Agents Chemother.* **35**, 234–236 (1991).

12. Fer, M. J. *et al.* Bacterial Transferase MraY, a Source of Inspiration towards New Antibiotics. *Curr. Med. Chem.* **25**, 6013–6029.

13. Rackham, E. J., Grüschow, S. & Goss, R. J. M. Revealing the first uridyl peptide antibiotic biosynthetic gene cluster and probing pacidamycin biosynthesis. *Bioeng. Bugs* **2**, 218–221 (2011).

14. Kaysser, L. *et al.* Identification of a napsamycin biosynthesis gene cluster by genome mining. *Chembiochem Eur. J. Chem. Biol.* **12**, 477–487 (2011).

15. Jiang, L. *et al.* Identification of novel mureidomycin analogues via rational activation of a cryptic gene cluster in Streptomyces roseosporus NRRL 15998. *Sci. Rep.* **5**, 14111 (2015).

16. Wang, L. *et al.* Draft Genome Sequence of Streptomyces sp. Strain SS, Which Produces a Series of Uridyl Peptide Antibiotic Sansanmycins. *J. Bacteriol.* **194**, 6988–6989 (2012).

17. Zhang, W., Ostash, B. & Walsh, C. T. Identification of the biosynthetic gene cluster for the pacidamycin group of peptidyl nucleoside antibiotics. *Proc. Natl. Acad. Sci.* **107**, 16828–16833 (2010).

18. Hauck, N. D. Investigation of Uridyl Peptide Antibiotics towards Mode of Action Studies and Generation of Novel Bioactive Pacidamycin Derivatives. (Eberhard Karls Universitaet Tuebingen, 2018).

19. Tacconelli, E. *et al.* Discovery, research, and development of new antibiotics: the WHO priority list of antibiotic-resistant bacteria and tuberculosis. *Lancet Infect. Dis.* **18**, 318–327 (2018).

20. Thi, M. T. T., Wibowo, D. & Rehm, B. H. A. Pseudomonas aeruginosa Biofilms. *Int. J. Mol. Sci.* **21**, 8671 (2020).

21. Garau, J. & Gomez, L. Pseudomonas aeruginosa pneumonia. *Curr. Opin. Infect. Dis.* **16**, 135 (2003).

22. Torres, A. *et al.* International ERS/ESICM/ESCMID/ALAT guidelines for the management of hospital-acquired pneumonia and ventilator-associated pneumonia: Guidelines for the

management of hospital-acquired pneumonia (HAP)/ventilator-associated pneumonia (VAP) of the European Respiratory Society (ERS), European Society of Intensive Care Medicine (ESICM), European Society of Clinical Microbiology and Infectious Diseases (ESCMID) and Asociación Latinoamericana del Tórax (ALAT). *Eur. Respir. J.* **50**, 1700582 (2017).

23. Therapeutic guidelines for Pseudomonas aeruginosa infections. *Int. J. Antimicrob. Agents* **16**, 103–106 (2000).

24. Torres, A. *et al.* Pneumonia. *Nat. Rev. Dis. Primer* **7**, 1–28 (2021).

25. Yoshimura, F. & Nikaido, H. Permeability of Pseudomonas aeruginosa outer membrane to hydrophilic solutes. *J. Bacteriol.* **152**, 636–642 (1982).

26. Pechère, J.-C. & Köhler, T. Patterns and modes of β-lactam resistance in Pseudomonas aeruginosa. *Clin. Microbiol. Infect.* **5**, S15–S18 (1999).

27. Strateva, T. & Yordanov, D. Pseudomonas aeruginosa - a phenomenon of bacterial resistance. *J. Med. Microbiol.* **58**, 1133–1148 (2009).

28. Thomson, J. M. & Lamont, I. L. Nucleoside Analogues as Antibacterial Agents. *Front. Microbiol.* **10**, 952 (2019).

29. Isono, K. Nucleoside antibiotics: structure, biological activity, and biosynthesis. *J. Antibiot. (Tokyo)* **41**, 1711–1739 (1988).

30. McErlean, M., Liu, X., Cui, Z., Gust, B. & Lanen, S. G. V. Identification and characterization of enzymes involved in the biosynthesis of pyrimidine nucleoside antibiotics. *Nat. Prod. Rep.* **38**, 1362–1407 (2021).

31. Gause, G. F. Recent Studies on Albomycin, a New Antibiotic. *Br. Med. J.* **2**, 1177–1179 (1955).

32. Pramanik, A. *et al.* Albomycin is an effective antibiotic, as exemplified with Yersinia enterocolitica and Streptococcus pneumoniae. *Int. J. Med. Microbiol. IJMM* **297**, 459–469 (2007).

33. Zeng, Y. *et al.* Biosynthesis of Albomycin δ2 Provides a Template for Assembling Siderophore and Aminoacyl-tRNA Synthetase Inhibitor Conjugates. *ACS Chem. Biol.* **7**, 1565–1575 (2012).

34. Turková, J., Mikeš, O. & Šorm, F. Determination of the structure of the peptide moiety of the antibiotic albomycin. *Experientia* **19**, 633–634 (1963).

35. Ushimaru, R., Chen, Z., Zhao, H., Fan, P. & Liu, H. The Enzymes Mediating Maturation of the Seryl-tRNA Synthetase Inhibitor SB-217452 during Biosynthesis of Albomycins. *Angew. Chem. Int. Ed Engl.* **59**, 3558–3562 (2020).

36. Hartmann, A., Fiedler, H. P. & Braun, V. Uptake and conversion of the antibiotic albomycin by Escherichia coli K-12. *Eur. J. Biochem.* **99**, 517–524 (1979).

37. Haskell, T. H. *et al.* The Isolation and Characterization of Three Crystalline Antibiotics from Streptomyces plicatus. *J. Am. Chem. Soc.* **80**, 743–747 (1958).

38. Konishi, M., Naruishi, M., Tsuno, T., Tsukiura, H. & Kawaguchi, H. Oxamicetin, a new antibiotic of bacterial origin. II. Structure of oxamicetin. *J. Antibiot. (Tokyo)* **26**, 757–764 (1973).

39. Bu, Y.-Y., Yamazaki, H., Ukai, K. & Namikoshi, M. Anti-Mycobacterial Nucleoside Antibiotics from a Marine-Derived Streptomyces sp. TPU1236A. *Mar. Drugs* **12**, 6102–6112 (2014).

40. Leviev, I. G. *et al.* A conserved secondary structural motif in 23S rRNA defines the site of interaction of amicetin, a universal inhibitor of peptide bond formation. *EMBO J.* **13**, 1682–1686 (1994).

41. DeBoer, C., Caron, E. L. & Hinman, J. W. AMICETIN, A NEW STREPTOMYCES ANTIBIOTIC. *J. Am. Chem. Soc.* **75**, 499–500 (1953).

42. Zhang, G. *et al.* Characterization of the Amicetin Biosynthesis Gene Cluster from Streptomyces vinaceusdrappus NRRL 2363 Implicates Two Alternative Strategies for Amide Bond Formation. *Appl. Environ. Microbiol.* **78**, 2393–2401 (2012).

43. Clark, J. M. & Gunther, J. K. GOUGEROTIN, A SPECIFIC INHIBITOR OF PROTEIN SYNTHESIS. *Biochim. Biophys. Acta* **76**, 636–638 (1963).

44. Takahashi, A., Ikeda, D., Naganawa, H., Okami, Y. & Umezawa, H. Bagougeramines A and B, new nucleoside antibiotics produced by a strain of Bacillus circulans. II. Physico-chemical properties and structure determination. *J. Antibiot. (Tokyo)* **39**, 1041–1046 (1986).

45. Niu, G. & Tan, H. Nucleoside antibiotics: biosynthesis, regulation, and biotechnology. *Trends Microbiol.* **23**, 110–119 (2015).

46. Contreras, A. & Carrasco, L. Selective inhibition of protein synthesis in virus-infected mammalian cells. *J. Virol.* **29**, 114–122 (1979).

47. Contreras, A., Vazquez, D. & Carrasco, L. Inhibition, by selected antibiotics, of protein synthesis in cells growing in tissue cultures. *J. Antibiot. (Tokyo)* **31**, 598–602 (1978).

48. Takahashi, A., Saito, N., Hotta, K., Okami, Y. & Umezawa, H. Bagougeramines A and B, new nucleoside antibiotics produced by a strain of Bacillus circulans. I. Taxonomy of the producing organism and isolation and biological properties of the antibiotics. *J. Antibiot. (Tokyo)* **39**, 1033–1040 (1986).

49. Niu, G., Li, L., Wei, J. & Tan, H. Cloning, Heterologous Expression, and Characterization of the Gene Cluster Required for Gougerotin Biosynthesis. *Chem. Biol.* **20**, 34–44 (2013).

50. Fox, J. J., Kuwasa, Y. & Watanabe, K. A. Nucleosides LVI. On the structure of the nucleotise antibiotic, gougerotin. *Tetrahedron Lett.* 6029–6032 (1968) doi:10.1016/s0040-4039(00)70784-2.

51. Dolak, L. The carbon-13 NMR spectrum of gougerotin. *J. Antibiot. (Tokyo)* **32**, 1346–1347 (1979).

52. Kirillov, S. V., Porse, B. T. & Garrett, R. A. Peptidyl transferase antibiotics perturb the relative positioning of the 3'-terminal adenosine of P/P'-site-bound tRNA and 23S rRNA in the ribosome. *RNA N. Y. N* **5**, 1003–1013 (1999).

53. Igarashi, M. *et al.* Caprazamycins, Novel Lipo-nucleoside Antibiotics, from Streptomyces sp. *J. Antibiot. (Tokyo)* **58**, 327–337 (2005).

54. Fujita, Y. *et al.* Muraminomicins, new lipo-nucleoside antibiotics from Streptosporangium sp. SANK 60501-structure elucidations of muraminomicins and supply of the core component for derivatization. *J. Antibiot. (Tokyo)* **72**, 943–955 (2019).

55. Fujita, Y. *et al.* A-90289 A and B, new inhibitors of bacterial translocase I, produced by Streptomyces sp. SANK 60405. *J. Antibiot. (Tokyo)* **64**, 495–501 (2011).

56. Kimura, K. *et al.* Selective inhibition of the bacterial peptidoglycan biosynthesis by the new types of liposidomycins. *J. Antibiot. (Tokyo)* **51**, 1099–1104 (1998).

57. Kaysser, L., Siebenberg, S., Kammerer, B. & Gust, B. Analysis of the Liposidomycin Gene Cluster Leads to the Identification of New Caprazamycin Derivatives. *ChemBioChem* **11**, 191–196 (2010).

58. Kaysser, L. *et al.* Identification and Manipulation of the Caprazamycin Gene Cluster Lead to New Simplified Liponucleoside Antibiotics and Give Insights into the Biosynthetic Pathway. *J. Biol. Chem.* **284**, 14987–14996 (2009).

59. Chi, X. *et al.* The muraminomicin biosynthetic gene cluster and enzymatic formation of the 2-deoxyaminoribosyl appendage. *MedChemComm* **4**, 239–243 (2012).

60. Funabashi, M. *et al.* The Biosynthesis of Liposidomycin-like A-90289 Antibiotics Featuring a New Type of Sulfotransferase. *ChemBioChem* **11**, 184–190 (2010).

61. Wiker, F., Hauck, N., Grond, S. & Gust, B. Caprazamycins: Biosynthesis and structure activity relationship studies. *Int. J. Med. Microbiol. IJMM* **309**, 319–324 (2019).

62. Igarashi, M. *et al.* Caprazamycin B, a novel anti-tuberculosis antibiotic, from Streptomyces sp. *J. Antibiot. (Tokyo)* **56**, 580–583 (2003).

63. Kagoshima, Y. *et al.* Muraminomicins, novel ester derivatives: in vitro and in vivo antistaphylococcal activity. *J. Antibiot. (Tokyo)* **72**, 956–969 (2019).

64. McDonald, L. A. *et al.* Structures of the Muraymycins, Novel Peptidoglycan Biosynthesis Inhibitors. *J. Am. Chem. Soc.* **124**, 10260–10261 (2002).

65. Niro, G., Weck, S. C. & Ducho, C. Merging Natural Products: Muraymycin-Sansanmycin Hybrid Structures as Novel Scaffolds for Potential Antibacterial Agents. *Chem. Weinh. Bergstr. Ger.* **26**, 16875–16887 (2020).

66. Yoshida, M. *et al.* A novel antifungal antibiotic, FR-900848. I. Production, isolation, physico-chemical and biological properties. *J. Antibiot. (Tokyo)* **43**, 748–754 (1990).

67. Yamaguchi, H. *et al.* Capuramycin, a new nucleoside antibiotic. Taxonomy, fermentation, isolation and characterization. *J. Antibiot. (Tokyo)* **39**, 1047–1053 (1986).

68. Biecker, A. L., Liu, X., Thorson, J. S., Yang, Z. & Van Lanen, S. G. Biosynthetic and Synthetic Strategies for Assembling Capuramycin-Type Antituberculosis Antibiotics. *Molecules* **24**, 433 (2019).

69. Fujita, Y., Murakami, R., Muramatsu, Y., Miyakoshi, S. & Takatsu, T. A-94964, Novel Inhibitor of Bacterial Translocase I, Produced by Streptomyces sp. SANK 60404. *J. Antibiot. (Tokyo)* **61**, 545–549 (2008).

70. Murakami, R. *et al.* A-94964, a Novel Inhibitor of Bacterial Translocase I, Produced by Streptomyces sp. SANK 60404: I. Taxonomy, Isolation and Biological Activity. *J. Antibiot. (Tokyo)* **61**, 537–544 (2008).

71. Dähn, U. *et al.* Stoffwechselprodukte von mikroorganismen. 154. Mitteilung. Nikkomycin, ein neuer hemmstoff der chitinsynthese bei pilzen. *Arch. Microbiol.* **107**, 143–160 (1976).

72. Suzuki, S. *et al.* A NEW ANTIBIOTIC, POLYOXIN A. *J. Antibiot. (Tokyo)* **18**, 131 (1965).

73. McCarthy, P. J., Troke, P. F. & Gull, K. Mechanism of action of nikkomycin and the peptide transport system of Candida albicans. *J. Gen. Microbiol.* **131**, 775–780 (1985).

74. Schlueter, U. Ultrastructural evidence for inhibition of chitin synthesis by nikkomycin. *Wilhelm Rouxs Arch. Dev. Biol.* **191**, 205–207 (1982).

75. Takatsuki, A., Arima, K. & Tamura, G. Tunicamycin, a new antibiotic. I. Isolation and characterization of tunicamycin. *J. Antibiot. (Tokyo)* **24**, 215–223 (1971).

76. Kuo, S. C. & Lampen, J. O. Tunicamycin--an inhibitor of yeast glycoprotein synthesis. *Biochem. Biophys. Res. Commun.* **58**, 287–295 (1974).

77. Bettinger, G. E. & Young, F. E. Tunicamycin, an inhibitor of Bacillus peptidoglycan synthesis: a new site of inhibition. *Biochem. Biophys. Res. Commun.* **67**, 16–21 (1975).

78. Brandish, P. E. *et al.* Modes of action of tunicamycin, liposidomycin B, and mureidomycin A: inhibition of phospho-N-acetylmuramyl-pentapeptide translocase from Escherichia coli. *Antimicrob. Agents Chemother.* **40**, 1640–1644 (1996).

79. Tkacz, J. S. & Lampen, J. O. Tunicamycin inhibition of polyisoprenyl N-acetylglucosaminyl pyrophosphate formation in calf-liver microsomes. *Biochem. Biophys. Res. Commun.* **65**, 248–257 (1975).

80. Inukai, M., Isono, F. & Takatsuki, A. Selective inhibition of the bacterial translocase reaction in peptidoglycan synthesis by mureidomycins. *Antimicrob. Agents Chemother.* **37**, 980–983 (1993).

81. Isono, F., Kodama, K. & Inukai, M. Susceptibility of Pseudomonas species to the novel antibiotics mureidomycins. *Antimicrob. Agents Chemother.* **36**, 1024–1027 (1992).

82. Xie, Y., Xu, H., Sun, C., Yu, Y. & Chen, R. Two novel nucleosidyl–peptide antibiotics: Sansanmycin F and G produced by Streptomyces sp SS. *J. Antibiot. (Tokyo)* **63**, 143–146 (2010).

83. Isono, F. *et al.* Mureidomycins E and F, minor components of mureidomycins. *J. Antibiot. (Tokyo)* **46**, (1993).

84. Li, Q. *et al.* SsaA, a member of a novel class of transcriptional regulators, controls sansanmycin production in Streptomyces sp. strain SS through a feedback mechanism. *J. Bacteriol.* **195**, 2232–2243 (2013).

85. Lam, W.-H., Rychli, K. & Bugg, T. D. H. Identification of a novel β-replacement reaction in the biosynthesis of 2,3-diaminobutyric acid in peptidylnucleoside mureidomycin A. *Org. Biomol. Chem.* **6**, 1912 (2008).

86. Ragab, A. E., Grüschow, S., Tromans, D. R. & Goss, R. J. M. Biogenesis of the unique 4',5'-dehydronucleoside of the uridyl peptide antibiotic pacidamycin. *J. Am. Chem. Soc.* **133**, 15288–15291 (2011).

87. Zhang, W., Ntai, I., Kelleher, N. L. & Walsh, C. T. tRNA-dependent peptide bond formation by the transferase PacB in biosynthesis of the pacidamycin group of pentapeptidyl nucleoside antibiotics. *Proc. Natl. Acad. Sci.* **108**, 12249–12253 (2011).

88. Zhang, W. *et al.* Nine Enzymes Are Required for Assembly of the Pacidamycin Group of Peptidyl Nucleoside Antibiotics. *J. Am. Chem. Soc.* **133**, 5240–5243 (2011).

89. Zhang, W., Heemstra, J. R., Walsh, C. T. & Imker, H. J. Activation of the Pacidamycin PacL Adenylation Domain by MbtH-like Proteins. *Biochemistry* **49**, 9946–9947 (2010).

90. Boojamra, C. G. *et al.* Stereochemical Elucidation and Total Synthesis of Dihydropacidamycin D, a Semisynthetic Pacidamycin. *J. Am. Chem. Soc.* **123**, 870–874 (2001).

91. Okamoto, K. *et al.* Total Synthesis of Pacidamycin D by Cu(I)-Catalyzed Oxy Enamide Formation. *Org. Lett.* **13**, 5240–5243 (2011).

92. Pubill-Ulldemolins, C. *et al.* Heck Diversification of Indole-Based Substrates under Aqueous Conditions: From Indoles to Unprotected Halo-tryptophans and Halo-tryptophans in Natural Product Derivatives. *Chem. – Eur. J.* **25**, 10866–10875 (2019).

93. Mueller, E. A. & Levin, P. A. Bacterial Cell Wall Quality Control during Environmental Stress. *mBio* **11**, 10.1128/mbio.02456-20 (2020).

94. Silhavy, T. J., Kahne, D. & Walker, S. The Bacterial Cell Envelope. *Cold Spring Harb. Perspect. Biol.* **2**, a000414 (2010).

95. Kimura, K. & Bugg, T. D. H. Recent advances in antimicrobial nucleoside antibiotics targeting cell wall biosynthesis. *Nat. Prod. Rep.* **20**, 252–273 (2003).

96. Vollmer, W. Structural variation in the glycan strands of bacterial peptidoglycan. *FEMS Microbiol. Rev.* **32**, 287–306 (2008).

97. Garde, S., Chodisetti, P. K. & Reddy, M. Peptidoglycan: Structure, Synthesis, and Regulation. *EcoSal Plus* **9**, (2021).

98. Sham, L.-T. *et al.* Bacterial cell wall. MurJ is the flippase of lipid-linked precursors for peptidoglycan biogenesis. *Science* **345**, 220–222 (2014).

99. Spratt, B. G. Distinct penicillin binding proteins involved in the division, elongation, and shape of Escherichia coli K12. *Proc. Natl. Acad. Sci. U. S. A.* **72**, 2999–3003 (1975).

100. Emami, K. *et al.* Corrigendum: RodA as the missing glycosyltransferase in Bacillus subtilis and antibiotic discovery for the peptidoglycan polymerase pathway. *Nat. Microbiol.* **2**, 17019 (2017).

101. Ikeda, M., Wachi, M., Jung, H. K., Ishino, F. & Matsuhashi, M. The Escherichia coli mraY gene encoding UDP-N-acetylmuramoyl-pentapeptide: undecaprenyl-phosphate phospho-N-acetylmuramoyl-pentapeptide transferase. *J. Bacteriol.* **173**, 1021–1026 (1991).

102. Egan, A. J. F., Errington, J. & Vollmer, W. Regulation of peptidoglycan synthesis and remodelling. *Nat. Rev. Microbiol.* **18**, 446–460 (2020).

103. Kim, S. J., Matsuoka, S., Patti, G. J. & Schaefer, J. Vancomycin derivative with damaged D-Ala-D-Ala binding cleft binds to cross-linked peptidoglycan in the cell wall of Staphylococcus aureus. *Biochemistry* **47**, 3822–3831 (2008).

104. Stone, K. J. & Strominger, J. L. Mechanism of Action of Bacitracin: Complexation with Metal Ion and C55-Isoprenyl Pyrophosphate. *Proc. Natl. Acad. Sci. U. S. A.* **68**, 3223–3227 (1971).

105. Boyle, D. S. & Donachie, W. D. mraY Is an Essential Gene for Cell Growth in Escherichia coli. *J. Bacteriol.* **180**, 6429–6432 (1998).

106. Chung, B. C. *et al.* Crystal structure of MraY, an essential membrane enzyme for bacterial cell wall synthesis. *Science* **341**, 1012–1016 (2013).

107. Lloyd, A. J., Brandish, P. E., Gilbey, A. M. & Bugg, T. D. H. Phospho-N-Acetyl-Muramyl-Pentapeptide Translocase from Escherichia coli: Catalytic Role of Conserved Aspartic Acid Residues. *J. Bacteriol.* **186**, 1747–1757 (2004).

108. Brandish, P. E. *et al.* Slow Binding Inhibition of Phospho-N-acetylmuramyl-pentapeptide-translocase (Escherichia coli) by Mureidomycin A (∗). *J. Biol. Chem.* **271**, 7609–7614 (1996).

109. Li, Y. *et al.* Effects of combined treatment with sansanmycin and macrolides on Pseudomonas aeruginosa and formation of biofilm. *Biomed. Environ. Sci. BES* **22**, 170–177 (2009).

110. Bernhardt, T. G., Struck, D. K. & Young, R. The lysis protein E of phi X174 is a specific inhibitor of the MraY-catalyzed step in peptidoglycan synthesis. *J. Biol. Chem.* **276**, 6093–6097 (2001).

111. Mendel, S., Holbourn, J. M., Schouten, J. A. & Bugg, T. D. H. Interaction of the transmembrane domain of lysis protein E from bacteriophage phiX174 with bacterial translocase MraY and peptidyl-prolyl isomerase SlyD. *Microbiol. Read. Engl.* **152**, 2959–2967 (2006).

112. Rodolis, M. T. *et al.* Identification of a novel inhibition site in translocase MraY based upon the site of interaction with lysis protein E from bacteriophage φX174. *Chembiochem Eur. J. Chem. Biol.* **15**, 1300–1308 (2014).

113. Boojamra, C. G. *et al.* Synthetic dihydropacidamycin antibiotics: A modified spectrum of activity for the pacidamycin class. *Bioorg. Med. Chem. Lett.* **13**, 3305–3309 (2003).

114. Howard, N. I. & Bugg, T. D. H. Synthesis and activity of 5'-uridinyl dipeptide analogues mimicking the amino terminal peptide chain of nucleoside antibiotic mureidomycin A. *Bioorg. Med. Chem.* **11**, 3083–3099 (2003).

115. Gentle, C. A., Harrison, S. A., Inukai, M. & Bugg, T. D. H. Structure–function studies on nucleoside antibiotic mureidomycin A: synthesis of 5J-functionalised uridine models. (1999).

116. Okamoto, K. *et al.* Synthesis of pacidamycin analogues via an Ugi-multicomponent reaction. *Bioorg. Med. Chem. Lett.* **22**, 4810–4815 (2012).

117. Mashalidis, E. H. *et al.* Chemical logic of MraY inhibition by antibacterial nucleoside natural products. *Nat. Commun.* **10**, 2917 (2019).

118. Terasawa, Y. *et al.* Elucidating the Structural Requirement of Uridylpeptide Antibiotics for Antibacterial Activity. *J. Med. Chem.* **63**, 9803–9827 (2020).

119. Pletzer, D. *et al.* The Pseudomonas aeruginosa PA14 ABC Transporter NppA1A2BCD Is Required for Uptake of Peptidyl Nucleoside Antibiotics. *J. Bacteriol.* **197**, 2217–2228 (2015).

120. Grüschow, S., Rackham, E. J. & Goss, R. J. M. Diversity in natural product families is governed by more than enzyme promiscuity alone: establishing control of the pacidamycin portfolio. *Chem. Sci.* **2**, 2182 (2011).

121. Rackham, E. J., Grüschow, S., Ragab, A. E., Dickens, S. & Goss, R. J. M. Pacidamycin biosynthesis: identification and heterologous expression of the first uridyl peptide antibiotic gene cluster. *Chembiochem Eur. J. Chem. Biol.* **11**, 1700–1709 (2010).

122. Gust, B., Challis, G. L., Fowler, K., Kieser, T. & Chater, K. F. PCR-targeted Streptomyces gene replacement identifies a protein domain needed for biosynthesis of the sesquiterpene soil odor geosmin. *Proc. Natl. Acad. Sci. U. S. A.* **100**, 1541–1546 (2003).

123. Eustáquio, A. S. *et al.* Heterologous Expression of Novobiocin and Clorobiocin Biosynthetic Gene Clusters. *Appl. Environ. Microbiol.* **71**, 2452–2459 (2005).

124. Flett, F., Mersinias, V. & Smith, C. P. High efficiency intergeneric conjugal transfer of plasmid DNA from Escherichia coli to methyl DNA-restricting streptomycetes. *FEMS Microbiol. Lett.* **155**, 223–229 (1997).

125. Paget, M. S. B., Chamberlin, L., Atrih, A., Foster, S. J. & Buttner, M. J. Evidence that the Extracytoplasmic Function Sigma Factor σE Is Required for Normal Cell Wall Structure in Streptomyces coelicolor A3(2). *J BACTERIOL* **181**, (1999).

126. Sambrook, J. & Russell, D. W. *Molecular cloning: a laboratory manual*. (Cold Spring Harbor Laboratory Press, 2001).

127. Kieser, T. *Practical Streptomyces Genetics*. (John Innes Foundation, 2000).

128. Fronko, R., Lee, M., Lee, V. J. & Leger, R. Pacidamycins produced by Streptomyces coeruleorubidus. (2001).

129. Cherepanov, P. P. & Wackernagel, W. Gene disruption in Escherichia coli: TcR and KmR cassettes with the option of Flp-catalyzed excision of the antibiotic-resistance determinant. *Gene* **158**, 9–14 (1995).

130. Datsenko, K. A. & Wanner, B. L. One-step inactivation of chromosomal genes in Escherichia coli K-12 using PCR products. *Proc. Natl. Acad. Sci. U. S. A.* **97**, 6640–6645 (2000).

131. MacNeil, D. J. *et al.* Analysis of Streptomyces avermitilis genes required for avermectin biosynthesis utilizing a novel integration vector. *Gene* **111**, (1992).

132. Chater, K. F. & Wilde, L. C. Restriction of a bacteriophage of Streptomyces albus G involving endonuclease SalI. *J. Bacteriol.* **128**, (1976).

133. Myronovskyi, M. *et al.* Generation of a cluster-free Streptomyces albus chassis strains for improved heterologous expression of secondary metabolite clusters. *Metab. Eng.* **49**, 316–324 (2018).

134. Malmierca, M. G. *et al.* Searching for Glycosylated Natural Products in Actinomycetes and Identification of Novel Macrolactams and Angucyclines. *Front. Microbiol.* **9**, 39 (2018).

135. Engler, C., Kandzia, R. & Marillonnet, S. A One Pot, One Step, Precision Cloning Method with High Throughput Capability. *PLoS ONE* **3**, e3647 (2008).

136. Montiel, D., Hs, K., Fy, C., Z, C.-P. & Sf, B. Yeast homologous recombination-based promoter engineering for the activation of silent natural product biosynthetic gene clusters. *Proc. Natl. Acad. Sci. U. S. A.* **112**, (2015).

137. Wiker, F. S. Identification of novel α-pyrones serving as sulfate shuttles from Conexibacter woesei. (Eberhard Karls Universitaet Tuebingen, 2018).

138. Fernández-Martínez, L. T. & Bibb, M. J. Use of the Meganuclease I-SceI of Saccharomycescerevisiae to select for gene deletions in actinomycetes. *Sci. Rep.* **4**, 7100 (2014).

139. Bai, C. *et al.* Exploiting a precise design of universal synthetic modular regulatory elements to unlock the microbial natural products in Streptomyces. *Proc. Natl. Acad. Sci.* **112**, 12181–12186 (2015).

140. Wang, W. *et al.* An Engineered Strong Promoter for Streptomycetes. *Appl. Environ. Microbiol.* **79**, 4484–4492 (2013).

141. Myronovskyi, M. & Luzhetskyy, A. Native and engineered promoters in natural product discovery. *Nat. Prod. Rep.* **33**, 1006–1019 (2016).

142. O'Neil, D., Glowatz, H. & Schlumpberger, M. Ribosomal RNA Depletion for Efficient Use of RNA-Seq Capacity. *Curr. Protoc. Mol. Biol.* **103**, 4.19.1-4.19.8 (2013).

143. Prado-Alonso, L. *et al.* Colibrimycins, Novel Halogenated Hybrid Polyketide Synthase-Nonribosomal Peptide Synthetase (PKS-NRPS) Compounds Produced by Streptomyces sp. Strain CS147. *Appl. Environ. Microbiol.* **88**, e01839-21.

144. Botas, A. *et al.* Genetic Engineering in Combination with Semi-Synthesis Leads to a New Route for Gram-Scale Production of the Immunosuppressive Natural Product Brasilicardin A. *Angew. Chem. Int. Ed.* **60**, (2021).

145. Tang, X., Gross, M., Xie, Y., Kulik, A. & Gust, B. Identification of Mureidomycin Analogues and Functional Analysis of an N-Acetyltransferase in Napsamycin Biosynthesis. *ChemBioChem* **14**, 2248–2255 (2013).

146. Watve, M. G., Tickoo, R., Jog, M. M. & Bhole, B. D. How many antibiotics are produced by the genus Streptomyces? *Arch. Microbiol.* **176**, 386–390 (2001).

147. Bentley, S. D. *et al.* Complete genome sequence of the model actinomycete Streptomyces coelicolor A3(2). **417**, (2002).

148. Challis, G. L. Mining microbial genomes for new natural products and biosynthetic pathways. *Microbiology* **154**, 1555–1569 (2008).

149. Aigle, B. *et al.* Genome mining of *Streptomyces ambofaciens*. *J. Ind. Microbiol. Biotechnol.* **41**, 251–263 (2014).

150. Rutledge, P. J. & Challis, G. L. Discovery of microbial natural products by activation of silent biosynthetic gene clusters. *Nat. Rev. Microbiol.* **13**, 509–523 (2015).

151. Mo, S., Lee, S.-K., Jin, Y.-Y., Oh, C.-H. & Suh, J.-W. Application of a combined approach involving classical random mutagenesis and metabolic engineering to enhance FK506 production in Streptomyces sp. RM7011. *Appl. Microbiol. Biotechnol.* **97**, 3053–3062 (2013).

152. Wang, X. *et al.* Enhanced doxorubicin production by Streptomyces peucetius using a combination of classical strain mutation and medium optimization. *Prep. Biochem. Biotechnol.* **48**, 514–521 (2018).

153. Zettler, J. *et al.* New Aminocoumarins from the Rare Actinomycete Catenulispora acidiphila DSM 44928: Identification, Structure Elucidation, and Heterologous Production. *ChemBioChem* **15**, 612–621 (2014).

154. Armin, R., Zühlke, S., Grunewaldt-Stöcker, G., Mahnkopp-Dirks, F. & Kusari, S. Production of Siderophores by an Apple Root-Associated Streptomyces ciscaucasicus Strain GS2 Using Chemical and Biological OSMAC Approaches. *Molecules* **26**, 3517 (2021).

155. Fang, Y. *et al.* Geninthiocins E and F, two new cyclic thiopeptides with antiviral activities from soil-derived Streptomyces sp. CPCC 200267 using OSMAC strategy. *J. Antibiot. (Tokyo)* **76**, 101–104 (2023).

156. Tang, Z. *et al.* Improved oxytetracycline production in Streptomyces rimosus M4018 by metabolic engineering of the G6PDH gene in the pentose phosphate pathway. *Enzyme Microb. Technol.* **49**, 17–24 (2011).

157. Song, E. *et al.* Proteomic approach to enhance doxorubicin production in panK-integrated Streptomyces peucetius ATCC 27952. *J. Ind. Microbiol. Biotechnol.* **38**, 1245–1253 (2011).

158. Hosoya, Y., Okamoto, S., Muramatsu, H. & Ochi, K. Acquisition of Certain Streptomycin-Resistant (str) Mutations Enhances Antibiotic Production in Bacteria. *Antimicrob. Agents Chemother.* **42**, 2041–2047 (1998).

159. Tanaka, Y. *et al.* Activation and Products of the Cryptic Secondary Metabolite Biosynthetic Gene Clusters by Rifampin Resistance (rpoB) Mutations in Actinomycetes. *J. Bacteriol.* **195**, 2959–2970 (2013).

160. Liao, G. *et al.* Cloning, reassembling and integration of the entire nikkomycin biosynthetic gene cluster into Streptomyces ansochromogenes lead to an improved nikkomycin production. *Microb. Cell Factories* **9**, 6 (2010).

161. Zhang, Y.-X., Perry, K., Vinci, V. A., Powell, K. & Stemmer, W. P. C. Genome shuffling leads to rapid phenotypic improvement in bacteria. **415**, (2002).

162. Castro-Melchor, M., Charaniya, S., Karypis, G., Takano, E. & Hu, W.-S. Genome-wide inference of regulatory networks in Streptomyces coelicolor. *BMC Genomics* **11**, 578 (2010).

163. Mingyar, E. *et al.* A Regulator Based “Semi-Targeted” Approach to Activate Silent Biosynthetic Gene Clusters. *Int. J. Mol. Sci.* **22**, 7567 (2021).

164. Xu, J. *et al.* Activation and mechanism of a cryptic oviedomycin gene cluster via the disruption of a global regulatory gene, adpA, in Streptomyces ansochromogenes. *J. Biol. Chem.* **292**, 19708–19720 (2017).

165. Smanski, M. J., Peterson, R. M., Rajski, S. R. & Shen, B. Engineered *Streptomyces platensis* Strains That Overproduce Antibiotics Platensimycin and Platencin. *Antimicrob. Agents Chemother.* **53**, 1299–1304 (2009).

166. Xu, J. *et al.* ToyA, a positive pathway-specific regulator for toyocamycin biosynthesis in Streptomyces diastatochromogenes 1628. *Appl. Microbiol. Biotechnol.* **103**, 7071–7084 (2019).

167. Jiang, M. *et al.* GdmRIII, a TetR Family Transcriptional Regulator, Controls Geldanamycin and Elaiophylin Biosynthesis in Streptomyces autolyticus CGMCC0516. *Sci. Rep.* **7**, 4803 (2017).

168. Rawle, R. *et al.* Introducing the ArsR-Regulated Arsenic Stimulon. *Front. Microbiol.* **12**, (2021).

169. Shao, Z. *et al.* Refactoring the silent spectinabilin gene cluster using a plug-and-play scaffold. *ACS Synth. Biol.* **2**, 662–669 (2013).

170. Basitta, P. *et al.* AGOS: A Plug-and-Play Method for the Assembly of Artificial Gene Operons into Functional Biosynthetic Gene Clusters. *ACS Synth. Biol.* **6**, 817–825 (2017).

171. Tian, W. *et al.* Biosynthesis of Tetronates by a Nonribosomal Peptide Synthetase–Polyketide Synthase System. *Org. Lett.* **25**, 1628–1632 (2023).

172. Luo, Y., Zhang, L., Barton, K. W. & Zhao, H. Systematic Identification of a Panel of Strong Constitutive Promoters from Streptomyces albus. *ACS Synth. Biol.* **4**, 1001–1010 (2015).

173. Bauman, K. D. *et al.* Refactoring the Cryptic Streptophenazine Biosynthetic Gene Cluster Unites Phenazine, Polyketide, and Nonribosomal Peptide Biochemistry. *Cell Chem. Biol.* **26**, 724-736.e7 (2019).

174. Du, D. *et al.* Improvement of gougerotin and nikkomycin production by engineering their biosynthetic gene clusters. *Appl. Microbiol. Biotechnol.* **97**, 6383–6396 (2013).

175. Zhang, M. M. *et al.* CRISPR–Cas9 strategy for activation of silent Streptomyces biosynthetic gene clusters. *Nat. Chem. Biol.* **13**, 607–609 (2017).

176. Ji, C.-H. *et al.* Top-down synthetic biology approach for titer improvement of clinically important antibiotic daptomycin in Streptomyces roseosporus. *Metab. Eng.* **69**, 40–49 (2022).

177. Bibb, M. J., Janssen, G. R. & Ward, J. M. Cloning and analysis of the promoter region of the erythromycin resistance gene (ermE) of Streptomyces erythraeus. *Gene* **38**, 215–226 (1985).

178. Bibb, M. J., White, J., Ward, J. M. & Janssen, G. R. The mRNA for the 23S rRNA methylase encoded by the ermE gene of Saccharopolyspora erythraea is translated in the absence of a conventional ribosome-binding site. *Mol. Microbiol.* **14**, 533–545 (1994).

179. Olano, C. *et al.* Activation and identification of five clusters for secondary metabolites in *Streptomyces albus* J 1074. *Microb. Biotechnol.* **7**, 242–256 (2014).

180. Zheng, J., Li, Y., Guan, H., Zhang, J. & Tan, H. Enhancement of neomycin production by engineering the entire biosynthetic gene cluster and feeding key precursors in Streptomyces fradiae CGMCC 4.576. *Appl. Microbiol. Biotechnol.* **103**, 2263–2275 (2019).

181. Malla, S., Niraula, N. P., Liou, K. & Sohng, J. K. Self-resistance mechanism in Streptomyces peucetius: Overexpression of drrA, drrB and drrC for doxorubicin enhancement. *Microbiol. Res.* **165**, 259–267 (2010).

182. Cundliffe, E. How Antibiotic-Producing Organisms Avoid Suicide. *Annu. Rev. Microbiol.* **43**, 207–233 (1989).

183. Peterson, E. & Kaur, P. Antibiotic Resistance Mechanisms in Bacteria: Relationships Between Resistance Determinants of Antibiotic Producers, Environmental Bacteria, and Clinical Pathogens. *Front. Microbiol.* **9**, (2018).

184. Wright, G. D. Bacterial resistance to antibiotics: Enzymatic degradation and modification. *Adv. Drug Deliv. Rev.* **57**, 1451–1470 (2005).

185. Benveniste, R. & Davies, J. Aminoglycoside Antibiotic-Inactivating Enzymes in Actinomycetes Similar to Those Present in Clinical Isolates of Antibiotic-Resistant Bacteria. *Proc. Natl. Acad. Sci. U. S. A.* **70**, 2276–2280 (1973).

186. Murray, I. A., Gil, J. A., Hopwood, D. A. & Shaw, W. V. Nucleotide sequence of the chloramphenicol acetyltransferase gene of Streptomyces acrimycini. *Gene* **85**, 283–291 (1989).

187. Allignet, J., Loncle, V., Simenel, C., Delepierre, M. & El Solh, N. Sequence of a staphylococcal gene, vat, encoding an acetyltransferase inactivating the A-type compounds of virginiamycin-like antibiotics. *Gene* **130**, 91–98 (1993).

188. Galm, U. & Shen, B. Expression of biosynthetic gene clusters in heterologous hosts for natural product production and combinatorial biosynthesis. *Expert Opin. Drug Discov.* **1**, 409–437 (2006).

189. Nett, M., Ikeda, H. & Moore, B. S. Genomic basis for natural product biosynthetic diversity in the actinomycetes. *Nat. Prod. Rep.* **26**, 1362–1384 (2009).

190. Floriano, B. & Bibb, M. *afsR* is a pleiotropic but conditionally required regulatory gene for antibiotic production in *Streptomyces coelicolor* A3(2). *Mol. Microbiol.* **21**, 385–396 (1996).

191. Gomez-Escribano, J. P. & Bibb, M. J. Engineering Streptomyces coelicolor for heterologous expression of secondary metabolite gene clusters. *Microb. Biotechnol.* **4**, 207–215 (2011).

192. Pawlik, K., Kotowska, M., Chater, K. F., Kuczek, K. & Takano, E. A cryptic type I polyketide synthase (cpk) gene cluster in Streptomyces coelicolor A3(2). *Arch. Microbiol.* **187**, 87–99 (2007).

193. Zhou, M. *et al.* Sequential deletion of all the polyketide synthase and nonribosomal peptide synthetase biosynthetic gene clusters and a 900-kb subtelomeric sequence of the linear chromosome of Streptomyces coelicolor. *FEMS Microbiol. Lett.* **333**, 169–179 (2012).

194. Thanapipatsiri, A., Claesen, J., Gomez-Escribano, J.-P., Bibb, M. & Thamchaipenet, A. A Streptomyces coelicolor host for the heterologous expression of Type III polyketide synthase genes. *Microb. Cell Factories* **14**, 145 (2015).

195. Ikeda, H. *et al.* Complete genome sequence and comparative analysis of the industrial microorganism Streptomyces avermitilis. *Nat. Biotechnol.* **21**, 526–531 (2003).

196. Ikeda, H., Kazuo, S. & Omura, S. Genome mining of the Streptomyces avermitilis genome and development of genome-minimized hosts for heterologous expression of biosynthetic gene clusters. *J. Ind. Microbiol. Biotechnol.* **41**, 233–250 (2014).

197. Komatsu, M., Uchiyama, T., Ōmura, S., Cane, D. E. & Ikeda, H. Genome-minimized Streptomyces host for the heterologous expression of secondary metabolism. *Proc. Natl. Acad. Sci.* **107**, 2646–2651 (2010).

198. Komatsu, M. *et al.* Engineered Streptomyces avermitilis Host for Heterologous Expression of Biosynthetic Gene Cluster for Secondary Metabolites. *ACS Synth. Biol.* **2**, 384–396 (2013).

199. Rodríguez, A. M., Olano, C., Vilches, C., Méndez, C. & Salas, J. A. Streptomyces antibioticus contains at least three oleandomycin-resistance determinants, one of which shows similarity with proteins of the ABC-transporter superfamily. *Mol. Microbiol.* **8**, 571–582 (1993).

200. Yanai, K., Murakami, T. & Bibb, M. Amplification of the entire kanamycin biosynthetic gene cluster during empirical strain improvement of Streptomyces kanamyceticus. *Proc. Natl. Acad. Sci.* **103**, 9661–9666 (2006).

201. Li, H., Pan, Y. & Liu, G. Multiplying the heterologous production of spinosad through tandem amplification of its biosynthetic gene cluster in Streptomyces coelicolor. *Microb. Biotechnol.* **15**, 1550–1560 (2022).

6. List of Tables

Table 1: Structures of representative uridyl peptide antibiotics 4
Table 2: Orthologous genes of the pacidamycin and napsamycin gene clusters and deduced roles, generated by BLAST analysis [13,17] 7
Table 3: Devices used in this study 18
Table 4: Equipment and consumables used in this study 19
Table 5: Chemicals used in this study 20
Table 6: Enzymes and kits used in this study 23
Table 7: Gel electrophoresis supplies used in this study 24
Table 8: Antibiotics used in this study 24
Table 9: Primers designed in this study 24
Table 10: gBlocks® designed in this study 29
Table 11: Plasmids and cosmids used and designed in this study 29
Table 12: *E. coli* strains 37
Table 13: *Streptomyces* strains 38
Table 14: Software used in this study 44
Table 15: Composition of Taq/Pfu PCR reactions 48
Table 16: Temperature program for Taq/Pfu PCR reactions 48
Table 17: Composition of Q5 PCR reactions 49
Table 18: Temperature program for Q5 PCR reactions 49
Table 19: Temperature program for PCR-targeting 51
Table 20: Thermocycling program GGA 53
Table 21: Pipetting scheme Cre recombinase 55
Table 22: LC-MS solvent program 60
Table 23: Organization and sequences (5' → 3') of promoter cassettes 63
Table 24: RNA-Seq samples and respective amount of total isolated RNA 85
Table 25: Percentage of reads in RNA-Seq samples aligned to *S. albus* J1074 DNA, *E. coli* DNA and *S. albus* J1074 rRNA 86
Table 26: Mutant strains constructed in this study displaying a positive effect on compound production 109
Table 27: UPAs produced by the napsamycin/mureidomycin gene cluster with an overview over the amino acid sequence in their scaffold. Postulated effect of knockouts on different compounds are indicated. 118
Table 28: Mutant strains, harboring the napsamycin BGC, constructed in this study displaying a positive effect on compound production 128
Table 29: Compounds detected in study by Jiang *et al.* (2015)[15], mureidomycins A and B included as a reference. For UPA scaffold see Fig. 1. 143
Table 30: Consecutive secondary metabolite gene cluster deletions in optimized *S. albus* J1074 derivatives, adapted from Myronovskyi *et al.* (2018)[133] 147

7. List of Figures

Fig. 1: Uridyl peptide antibiotic structure scaffold 4

Fig. 2: Pacidamycin and napsamycin biosynthetic gene clusters, the orthologous genes have been connected .. 6

Fig. 3: Schematic representation of peptidoglycan biosynthesis, adapted from Egan *et al.* (2020)[102] 10

Fig. 4: Data from crystal structure of *A. aeolicus* MraY, figure adapted from Chung *et al.* (2013)[106] 11

Fig. 5: SARs of UPAs, adapted from Terasawa *et al.* (2020)[118]. 14

Fig. 6: Integrative plasmids harboring genes beneficial for mureidomycin biosynthesis 15

Fig. 7: Genetic organization of the modified pacidamycin BGC on cosmid pacRS01, sites harboring uni - or bidirectional promoters are displayed by thin arrows 61

Fig. 8: Schematic representation of the annotations of the pacidamycin biosynthetic gene cluster by Zhang *et al*. (2010) and by Rackham *et al.* (2010) 62

Fig. 9: Schematic representation of promoter cassettes 1 and 2, constructed by Franziska Wiker[137]. 63

Fig. 10: Schematic representation of the conducted promoter replacements on pacRS01 and resulting BGCs pacHK01 - pacHK05 64

Fig. 11: LC-MS analysis of knock-ins of PC1 on pacRS01 based on annotation by Zhang *et al.* (2010) (UV-chromatograms) 65

Fig. 12: LC-MS analysis of knock-ins of PC1 on pacRS01 based on annotation by Zhang *et al.* (2010) (mureidomycin A) 66

Fig. 13: LC-MS analysis of knock-ins of PC1 on pacRS01 based on annotation by Zhang *et al.* (2010) (EIC met-pacidamycin 4) 67

Fig. 14: LC-MS analysis of knock-ins of PC1 on pacRS01 based on annotation by Rackham *et al.* (2010) 68

Fig. 15: LC-MS analysis of knock-in of PC1 in between *pac3* and *pac4* on pacRS01 based on annotation by Rackham *et al.* (2010) 69

Fig. 16: LC-MS analysis of knock-in of PC2 in between *npsP4* and *npsP8* on pacRS01 70

Fig. 17: LC-MS analysis of knock-ins of PC2 on pacRS01 between *npsP4* and *npsP8* 71

Fig. 18: Schematic representation of further knock-ins on pacRS01 and resulting BGCs pacHK06 and pacHK08 72

Fig. 19: LC-MS analysis of knock-ins of PC1 into pacRS01 between *npsP4* and *npsP8* 73

Fig. 20: Schematic representation of the strategy designed to construct pacHK08 74

Fig. 21: LC-MS analysis of knock-ins of PC1 into pacHK03 between *npsP4* and *npsP8* 75

Fig. 22: LC-MS analysis of feeding studies of *S. albus* J1074/pRS02/pacHK03 76

Fig. 23: Schematic representation of the novel modified pacidamycin BGC on pacRS03 containing PC1 77

Fig. 24: LC-MS analysis of knock-in of PC1 in between *pac3* and *pac4* on pacRS03 (statistical analysis) 78

Fig. 25: LC-MS analysis of knock-in of PC1 in between *pac3* and *pac4* on pacRS03 (EICs of mureidomycin A and met-pacidamycin 5) 78

Fig. 26: Schematic representation of promoter cassettes 3 and 4 79

Fig. 27: Schematic representation of the strategy designed to construct bidirectional promoter cassettes PC3 and PC4 by Golden Gate Assembly 80

Fig. 28: Schematic representation of the promoter replacements conducted with PC3 and PC4 and the resulting BGCs encoded on pacHK12, pacHK09 and pacHK10 80
Fig. 29: LC-MS analysis of knock-in of PC3 between *npsP4* and *npsP8* on pacHK03 81
Fig. 30: LC-MS analysis of knock-in of PC4 in between *pac3* and *pac4* on pacRS03 82
Fig. 31: LC-MS analysis of knock-in of PC3 in between *pac3* and *pac4* on pacRS03 83
Fig. 32: LC-MS analysis of further promoter swaps on pacRS03 84
Fig. 33: RNA sequencing results regarding the pacidamycin BGC of strain *S. albus* J1074/pacNH01 89
Fig. 34: RNA sequencing results regarding the pacidamycin BGC of strain *S. albus* J1074/pacRS01 90
Fig. 35: RNA sequencing results regarding the pacidamycin BGC of strain *S. albus* J1074/pRS02/pacRS01 91
Fig. 36: RNA sequencing results regarding the plasmid pRS02 of strain *S. albus* J1074/pRS02/pacRS01 92
Fig. 37: RNA sequencing results regarding the pacidamycin BGC of strain *S. albus* J1074/pRS02/pacHK03 (2 days) 94
Fig. 38: RNA sequencing results regarding the plasmid pRS02 of strain *S. albus* J1074/pRS02/pacHK03 (2 days) 95
Fig. 39: RNA sequencing results regarding the pacidamycin BGC of strain *S. albus* J1074/pRS02/pacHK03 (4 days) 96
Fig. 40: RNA sequencing results regarding the plasmid pRS02 of strain *S. albus* J1074/pRS02/pacHK03 (4 days) 97
Fig. 41: RNA sequencing results regarding the pacidamycin BGC of strain *S. albus* J1074/pRS04/pacHK03 (2 days) 98
Fig. 42: RNA sequencing results regarding the plasmid pRS04 of strain *S. albus* J1074/pRS04/pacHK03 (2 days) 99
Fig. 43: RNA sequencing results regarding the pacidamycin BGC of strain *S. albus* J1074/pRS04/pacHK03 (4 days) 100
Fig. 44: RNA sequencing results regarding the plasmid pRS04 of strain *S. albus* J1074/pRS04/pacHK03 (4 days) 101
Fig. 45: LC-MS analysis of extracts of optimized heterologous hosts harboring the modified pacidamycin BGC pacHK11 103
Fig. 46: LC-MS measurements of extracts of different heterologous hosts carrying the pacidamycin gene cluster harboring the first promoter swap 104
Fig. 47: Genetic organization of pacHK11 and pacHK14, areas modified in the inversion strategy were highlighted. 105
Fig. 48: A) Schematic representation of the strategy designed to construct pacHK13 106
Fig. 49: A) Schematic representation of the strategy designed to construct pacHK14 107
Fig. 50: LC-MS analysis of mutant strain extracts, which harbor the inverted pacidamycin BGC pacHK11 or pacHK14 108
Fig. 51: Genetic organization of the napsamycin biosynthetic gene cluster 110
Fig. 52: Genetic organization of the napsamycin biosynthetic gene cluster, modifications conducted by Philipp Konrad are highlighted on the constructed cosmids npsPK01, npsPK02 and npsPK03. 111

Fig. 53: LC-MS analysis of heterologous expression of the napsamycin BGC on cosmid npsXT01 114
Fig. 54: LC-MS analysis of mutant strain extracts, which harbor the napsamycin gene cluster carrying promoter cassette 1 between *npsL* and *npsM* 115
Fig. 55: LC-MS analysis of mutant strain extracts, which harbor the napsamycin gene cluster carrying promoter cassette 1 between *npsO* and *npsP7* 115
Fig. 56: LC-MS analysis of mutant strain extracts, which harbor the napsamycin gene cluster carrying promoter cassette 1 between *npsL* and *npsM* and between *npsO* and *npsP7* 116
Fig. 57: LC-MS measurements of extracts of mutant strains carrying the napsamycin gene cluster harboring npsPK01, npsPK02 or npsPK03 117
Fig. 58: LC-MS analysis of Δ*npsE* mutant strain extracts, in comparison with the original napsamycin gene cluster (UV-chromatogram and EICs of mureidomycin B and napsamycin C) 119
Fig. 59: LC-MS analysis of Δ*npsE* mutant strain extracts, in comparison with the original napsamycin gene cluster 120
Fig. 60: LC-MS measurements of extracts of Δ*npsE* knockout strains 121
Fig. 61: LC-MS analysis of Δ*npsU* mutant strain extracts, in comparison with the original napsamycin gene cluster (UV-chromatogram and EICs of mureidomycin A and mureidomycin E/napsamycin A) 122
Fig. 62: LC-MS analysis of Δ*npsU* mutant strain extracts 123
Fig. 63: LC-MS analysis of Δ*npsU* mutant strain extracts in comparison with the original napsamycin gene cluster (mureidomycin B und napsamycin C) 124
Fig. 64: LC-MS measurements of extracts of Δ*npsU* knock-out strains (total statistical analysis) 124
Fig. 65: LC-MS measurements of extracts of Δ*npsU* knock-out strains, comparison of the heterologous hosts *S. albus* J1074 and *S. albus* Del14 125
Fig. 66: LC-MS analysis of extracts of Δ*npsU* and Δ*npsE* double knockout mutant strain, compared with Δ*npsU* mutants 126
Fig. 67: LC-MS measurements of extracts of *S. albus* J1074/npsHK02 (Δ*npsU*) and *S. albus* Del14/npsHK03 (Δ*npsU*, PC1) 127
Fig. 68: LC-MS analysis of final mutant strains *S. albus* Del14/npsHK02 and *S. albus* Del14/pRS04/pacHK11 (UV- and base peak chromatograms) 130
Fig. 69: LC-MS analysis of final mutant strains *S. albus* Del14/npsHK02 and *S. albus* Del14/pRS04/pacHK11 (EICs) 131

Appendix

Fig. S1: LC-MS analysis of knock-ins of PC1 between *pac3* and *pac4* on pacRS01 based on annotation by Rackham *et al.* (2010) 174
Fig. S2: LC-MS analysis of feeding studies of *S. albus* J1074/pRS02/pacHK03 (met-pacidamycin S and D) 174
Fig. S3: LC-MS analysis of feeding studies of *S. albus* J1074/pRS02/pacHK03 (met-pacidamycin 5) 175
Fig. S4: LC-MS analysis of knock-in of PC3 between *npsP4* and *npsP8* on pacHK03 175

Fig. S5: LC-MS analysis of mutant strain extracts, which harbor the inverted pacidamycin BGC 176
Fig. S6: LC-MS analysis of mutant strain extracts, which harbor the napsamycin gene cluster carrying promoter cassette 1 between *npsL* and *npsM* (with and without pRS02) 176
Fig. S7: LC-MS analysis of mutant strain extracts, which harbor the napsamycin gene cluster carrying promoter cassette 1 between *npsL* and *npsM* (with pRS04) 177
Fig. S8: LC-MS analysis of mutant strain extracts, which harbor the napsamycin gene cluster carrying promoter cassette 1 between *npsO* and *npsP7* 177
Fig. S9: LC-MS analysis of mutant strain extracts, which harbor the napsamycin gene cluster carrying promoter cassette 1 between *npsL* and *npsM* and between *npsO* and *npsP7* (with and without pRS02) 178
Fig. S10: LC-MS analysis of mutant strain extracts, which harbor the napsamycin gene cluster carrying promoter cassette 1 between *npsL* and *npsM* and between *npsO* and *npsP7* (with pRS04) 178
Fig. S11: LC-MS analysis of mutant strain extracts, which harbor the napsamycin gene clusters npsPK01, npsPK02 or npsPK03 179
Fig. S12: LC-MS analysis of extracts of Δ*npsU* knock-out strains, comparison of the heterologous hosts *S. albus* J1074 and *S. albus* Del14 179
Fig. S13: LC-MS analysis of Δ*npsU* mutant strain extracts of *S. albus* J1074 and *S. albus* Del14 180
Fig. S14: LC-MS analysis of *npsU* and *npsE* double knockout mutant strain extracts 180
Fig. S15: RNA sequencing results regarding the pacidamycin BGC of strain *S. albus* J1074/pacNH01 (exconjugant II) 181
Fig. S16: RNA sequencing results regarding the pacidamycin BGC of strain *S. albus* J1074/pacNH01 (exconjugant III) 182
Fig. S17: RNA sequencing results regarding the pacidamycin BGC of strain *S. albus* J1074/pacRS01 183
Fig. S18: RNA sequencing results regarding the pacidamycin BGC of strain *S. albus* J1074/pRS02/pacHK03 184
Fig. S19: RNA sequencing results regarding the plasmid pRS02 of strain *S. albus* J1074/pRS02/pacHK03 185
Fig. S20: RNA sequencing results regarding the pacidamycin BGC of strain S. albus J1074/pRS04/pacHK03 186
Fig. S21: RNA sequencing results regarding the plasmid pRS04 of strain *S. albus* J1074/pRS04/pacHK03 187

8. Appendix

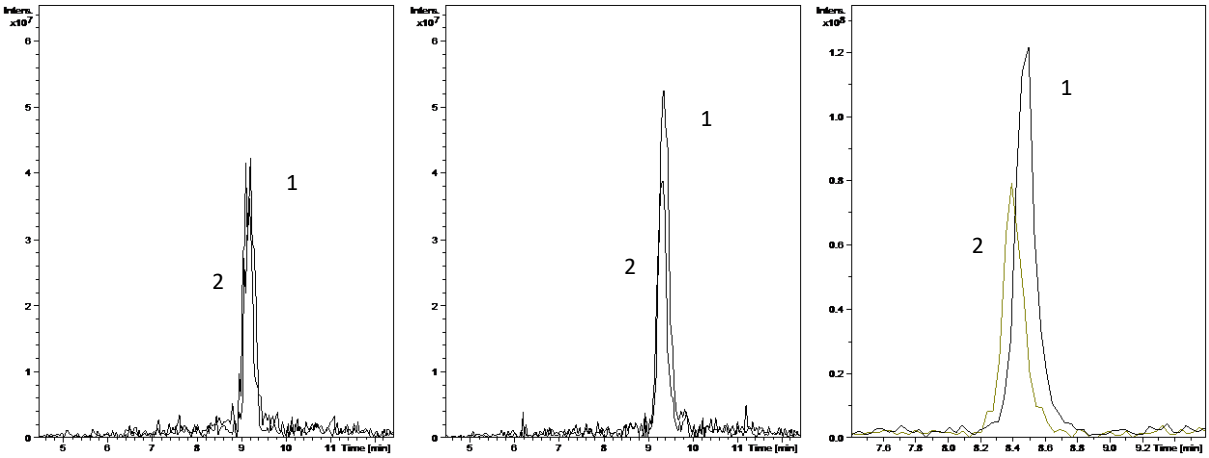


Fig. S1: LC-MS analysis of knock-ins of PC1 between *pac3* and *pac4* on pacRS01 based on annotation by Rackham *et al.* (2010) (Left to right): Extracted ion chromatograms of met-pacidamycin 5 (*m/z* 825.3 $[M+H]^+$), met-pacidamycin 4 (*m/z* 864.3 $[M+H]^+$) and met-pacidamycin D (*m/z* 772.3 $[M+H]^+$) are displayed for: 1) *S. albus* J1074/pRS02/pacHK03 and 2) *S. albus* J1074/pRS02/pacRS01.

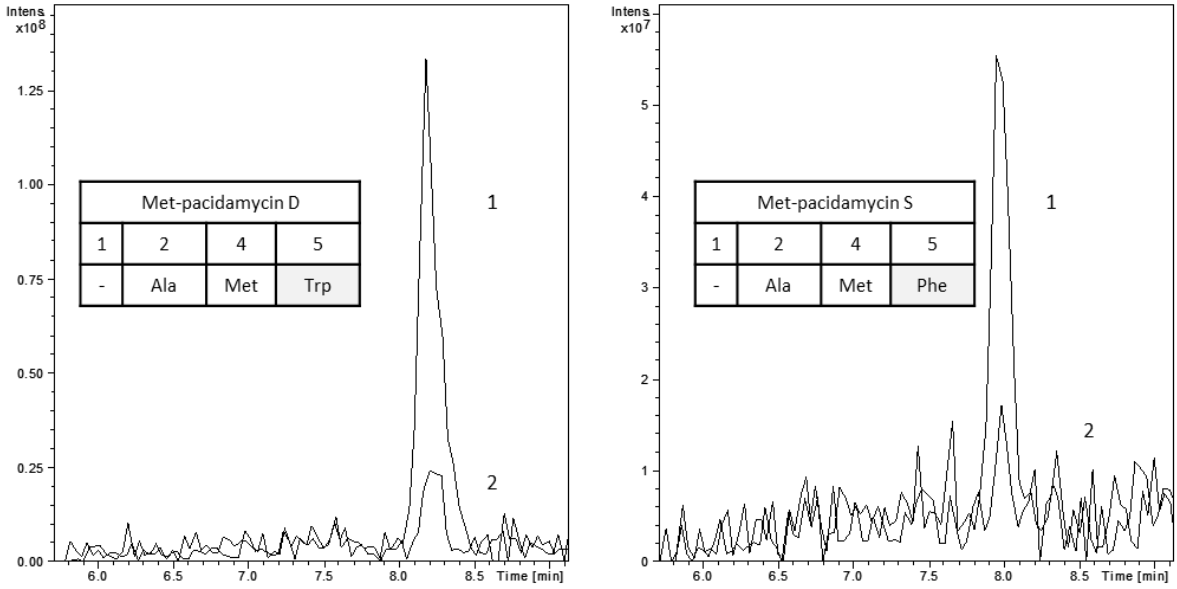
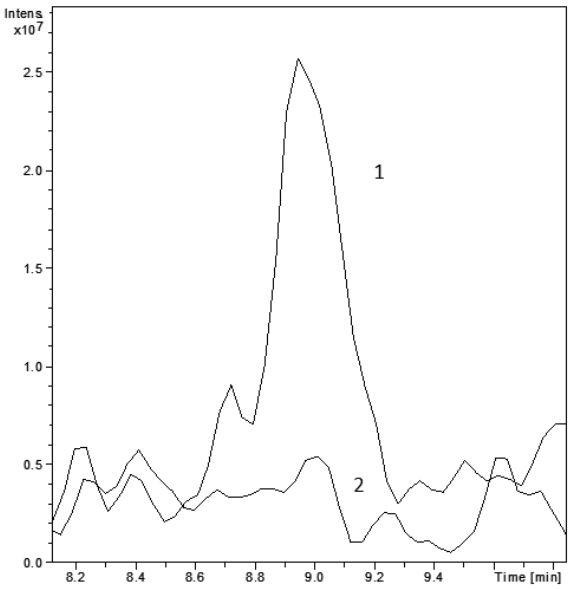


Fig. S2: LC-MS analysis of feeding studies of *S. albus* J1074/pRS02/pacHK03, 1) No feeding, 2) Feeding of *m*-tyrosine (5 mM) and glycine (5 mM). Left side: Extracted ion chromatograms of met-pacidamycin D (*m/z* 772.3 $[M+H]^+$); Right side: Extracted ion chromatograms of met-pacidamycin S (*m/z* 732.3 $[M+H]^+$); The respective amino acid composition has been noted.



Met-pacidamycin 5			
1	2	4	5
-	*m*-Tyr	Met	Trp

Fig. S3: LC-MS analysis of feeding studies of *S. albus* J1074/pRS02/pacHK03, 1) No feeding, 2) Feeding of *m*-tyrosine (5 mM) and glycine (5 mM). Extracted ion chromatograms of met-pacidamycin 5 (*m/z* 825.3 $[M+H]^+$), the respective amino acid composition has been noted; EICs of met-pacidamycin 5 have been processed by Gaussian smoothing (2.24,1).

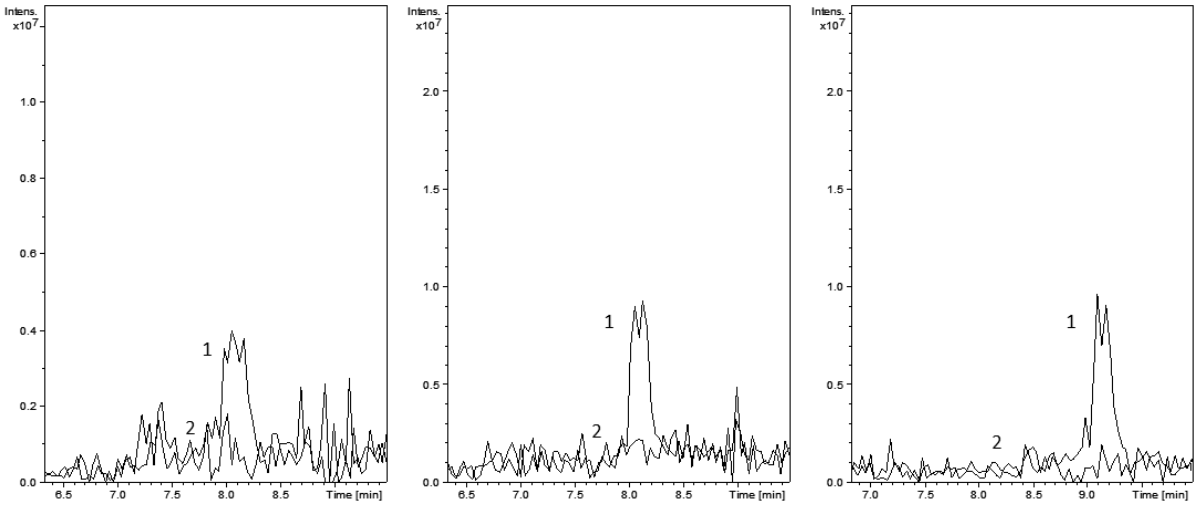


Fig. S4: LC-MS analysis of knock-in of PC3 between *npsP4* and *npsP8* on pacHK03 (Left to right): Extracted ion chromatograms of mureidomycin A (*m/z* 841.3 $[M+H]^+$), met-pacidamycin S (*m/z* 733.3 $[M+H]^+$) and met-pacidamycin 5 (*m/z* 825.3 $[M+H]^+$) are displayed for: 1) *S. albus* J1074/pRS02/pacHK03 and 2) *S. albus* J1074/pRS02/pacHK12.

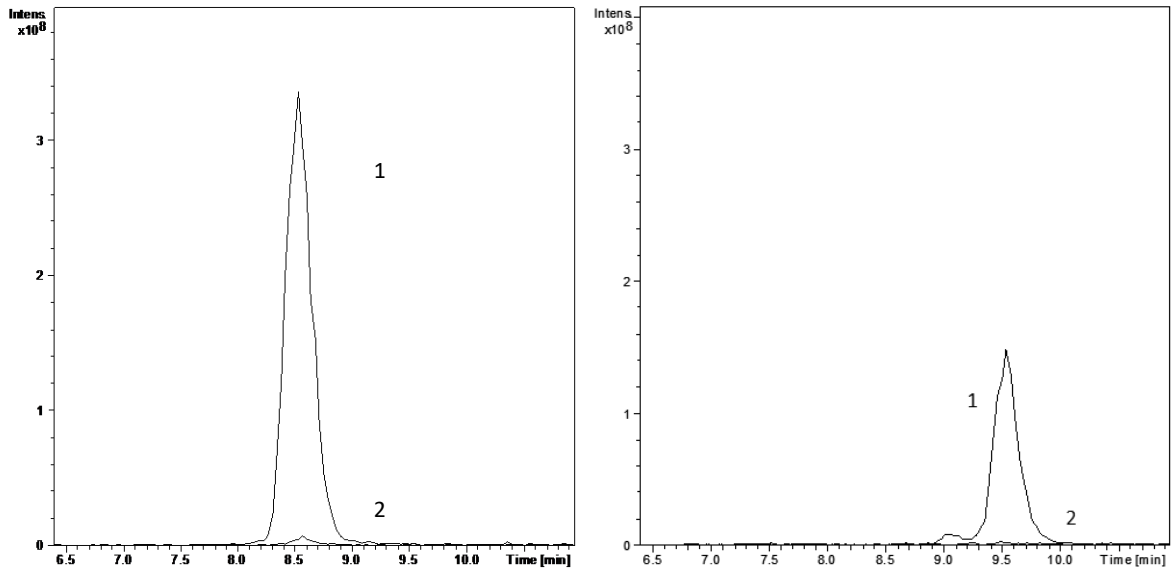


Fig. S5: LC-MS analysis of mutant strain extracts, which harbor the inverted pacidamycin BGC: Extracted ion chromatograms of mureidomycin A (*m/z* 841.3 $[M+H]^+$, left side) and met-pacidamycin 5 (*m/z* 825.3 $[M+H]^+$, right side) are displayed for: 1) *S. albus* Del14/pRS04/pacHK11 and 2) *S. albus* Del14/pRS04/pacHK14.

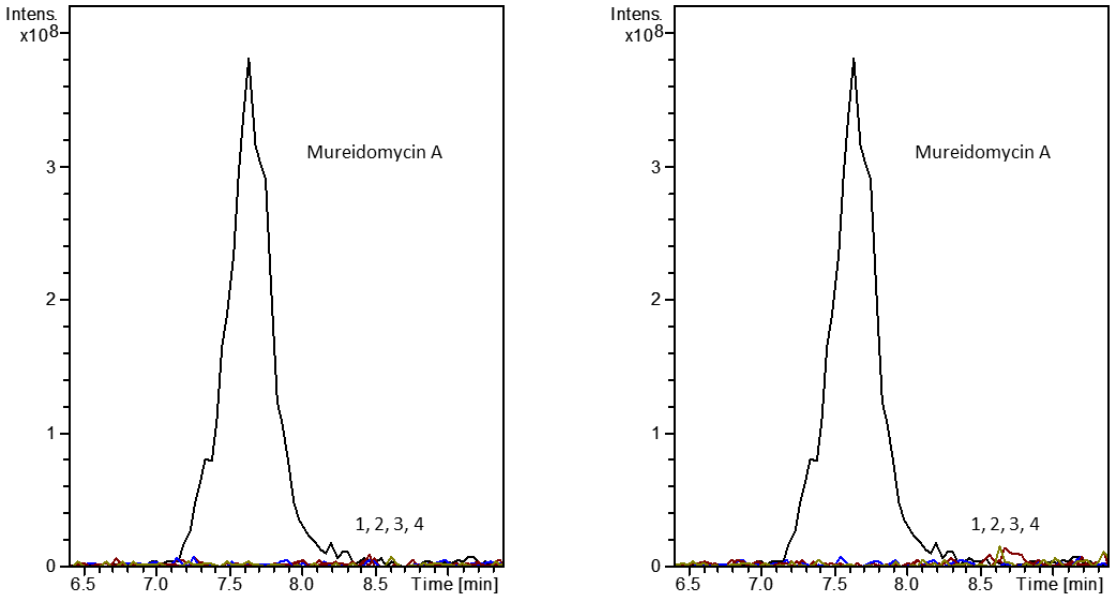


Fig. S6: LC-MS analysis of mutant strain extracts, which harbor the napsamycin gene cluster carrying promoter cassette 1 between *npsL* and *npsM*. Extracted ion chromatograms of 1) mureidomycin A (*m/z* 841.3 $[M+H]^+$), 2) mureidomycin B (*m/z* 843.3 $[M+H]^+$), 3) mureidomycin E/napsamycin A (*m/z* 853.3 $[M+H]^+$) and 4) napsamycin C (*m/z* 855.3 $[M+H]^+$) are displayed for *S. albus* J1074/npsPK01 (left side) and *S. albus* J1074/pRS02/npsPK01 (right side). A reference peak of mureidomycin A of *S. albus* J1074/npsXT01 is depicted in each graph.

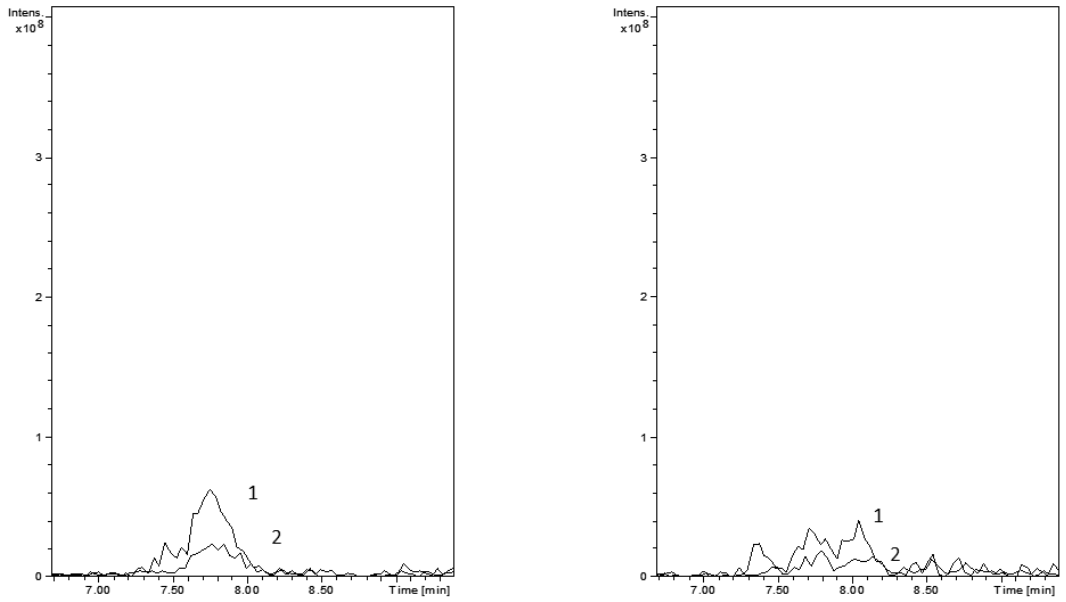


Fig. S7: LC-MS analysis of mutant strain extracts, which harbor the napsamycin gene cluster carrying promoter cassette 1 between *npsL* and *npsM*. Extracted ion chromatograms of mureidomycin A (*m/z* 841.3 $[M+H]^+$, left side) and mureidomycin E/napsamycin A (*m/z* 853.3 $[M+H]^+$, right side) are displayed for: 1) *S. albus* J1074/npsXT01 and 2) *S. albus* J1074/pRS04/npsPK01.

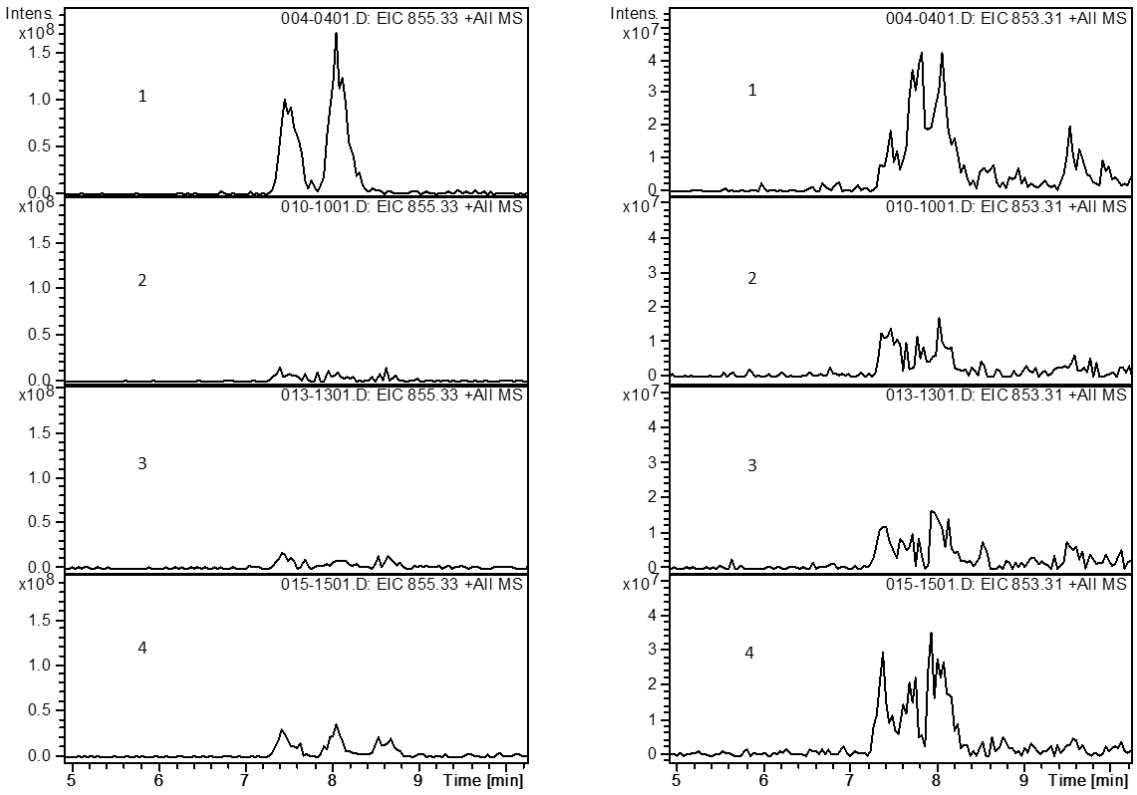


Fig. S8: LC-MS analysis of mutant strain extracts, which harbor the napsamycin gene cluster carrying promoter cassette 1 between *npsO* and *npsP7*. Extracted ion chromatograms of napsamycin C (*m/z* 855.3 $[M+H]^+$, left side) and mureidomycin E/napsamycin A (*m/z* 853.3 $[M+H]^+$, right side) are displayed for: 1) *S. albus* J1074/npsXT01, 2) *S. albus* J1074/npsPK02, 3) *S. albus* J1074/pRS02/npsPK02 and 4) *S. albus* J1074/pRS04/npsPK02.

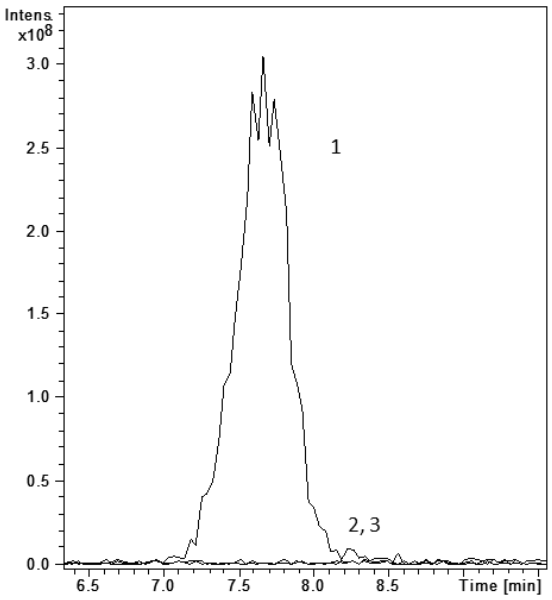


Fig. S9: LC-MS analysis of mutant strain extracts, which harbor the napsamycin gene cluster carrying promoter cassette 1 between *npsL* and *npsM* and between *npsO* and *npsP7*; *npsP6* was knocked out. Extracted ion chromatograms of mureidomycin B (*m/z* 843.3 $[M+H]^+$) are displayed for: 1) *S. albus* J1074/npsXT01, 2) *S. albus* J1074/npsPK03 and 3) *S. albus* J1074/pRS02/npsPK03.

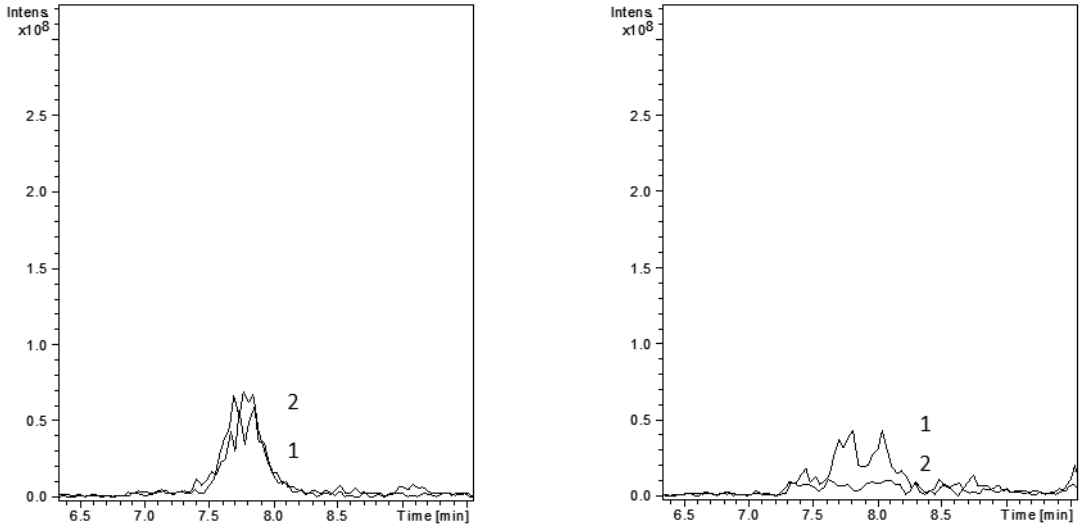


Fig. S10: LC-MS analysis of mutant strain extracts, which harbor the napsamycin gene cluster carrying promoter cassette 1 between *npsL* and *npsM* and between *npsO* and *npsP7*; *npsP6* was knocked out. Extracted ion chromatograms of mureidomycin A (*m/z* 841.3 $[M+H]^+$, left side) and mureidomycin E/napsamycin A (*m/z* 853.3 $[M+H]^+$, right side) are displayed for: 1) *S. albus* J1074/npsXT01 and 2) *S. albus* J1074/pRS04/npsPK03.

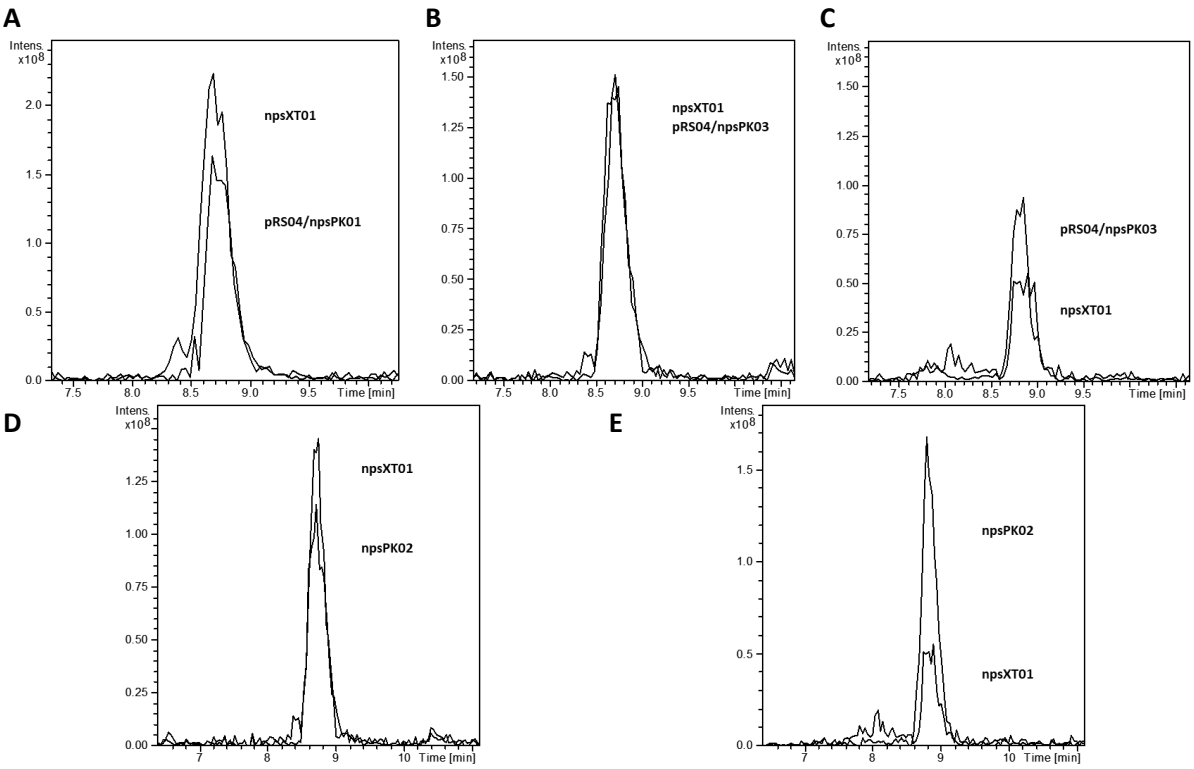


Fig. S11: LC-MS analysis of mutant strain extracts, which harbor the napsamycin gene clusters npsPK01, npsPK02 or npsPK03. Extracted ion chromatograms of compounds with *m/z* values of 883.4 $[M+H]^+$ (C and E) or 885.4 $[M+H]^+$ (A, B and D) are displayed for *S. albus* J1074/npsXT01, *S. albus* J1074/pRS04/npsPK01 (A), *S. albus* J1074/pRS04/npsPK03 (B and C) and *S. albus* J1074/npsPK02 (D and E).

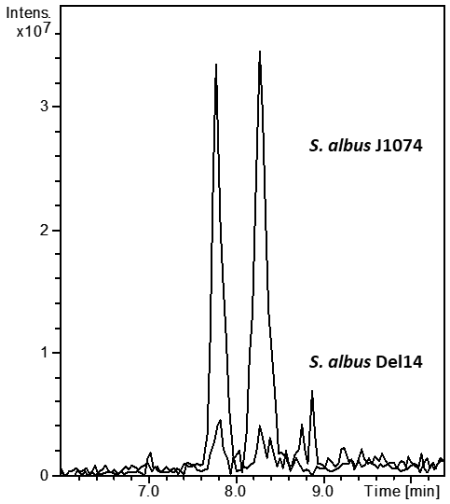


Fig. S12: LC-MS analysis of extracts of Δ*npsU* knock-out strains, comparison of the heterologous hosts *S. albus* J1074 and *S. albus* Del14; Extracted ion chromatograms of mureidomycin E/napsamycin A (*m/z* 853.3 $[M+H]^+$) are depicted from mutant strains *S. albus* J1074/npsHK02 and *S. albus* Del14/npsHK02.

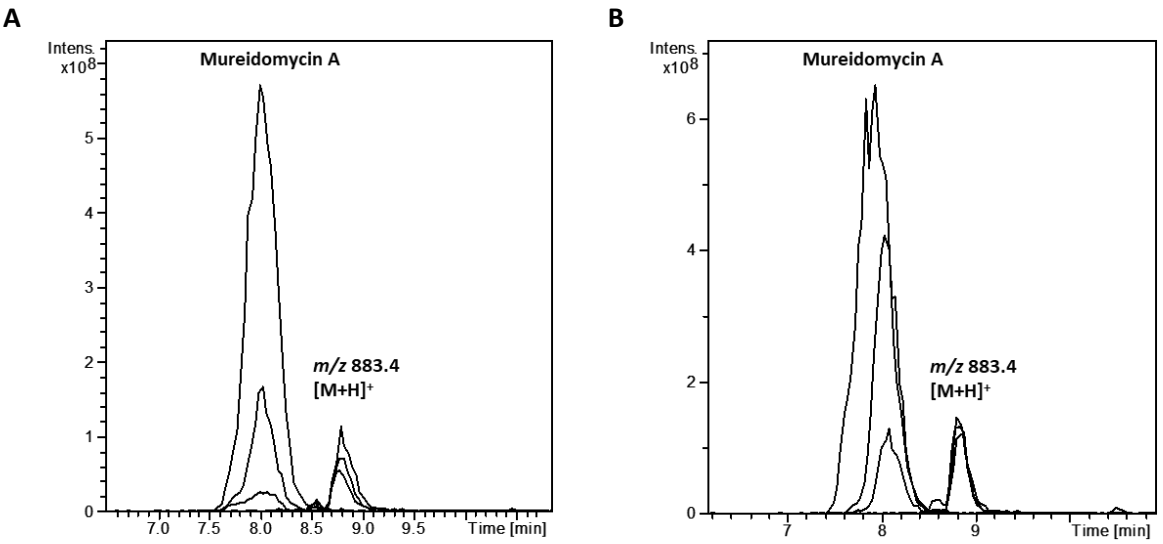


Fig. S13: LC-MS analysis of Δ*npsU* mutant strain extracts of *S. albus* J1074 and *S. albus* Del14. A) Extracted ion chromatograms of mureidomycin A (*m/z* 841.3 $[M+H]^+$) and the compound with an *m/z* value of 883.4 $[M+H]^+$ from *S. albus* J1074/npsHK02, B) Extracted ion chromatograms of mureidomycin A (*m/z* 841.3 $[M+H]^+$) and the compound with an *m/z* value of 883.4 $[M+H]^+$ from *S. albus* Del14/npsHK02.

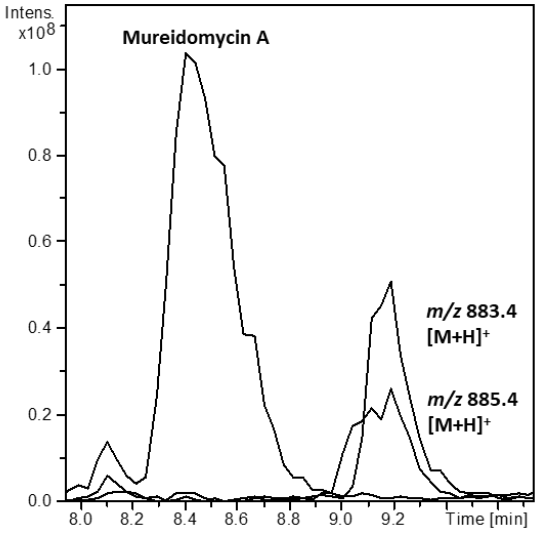


Fig. S14: LC-MS analysis of *npsU* and *npsE* double knockout mutant strain extracts. A) Extracted ion chromatograms of mureidomycin A (*m/z* 841.3 $[M+H]^+$) and the compounds with an *m/z* value of 883.4 $[M+H]^+$ and 885.4 $[M+H]^+$.

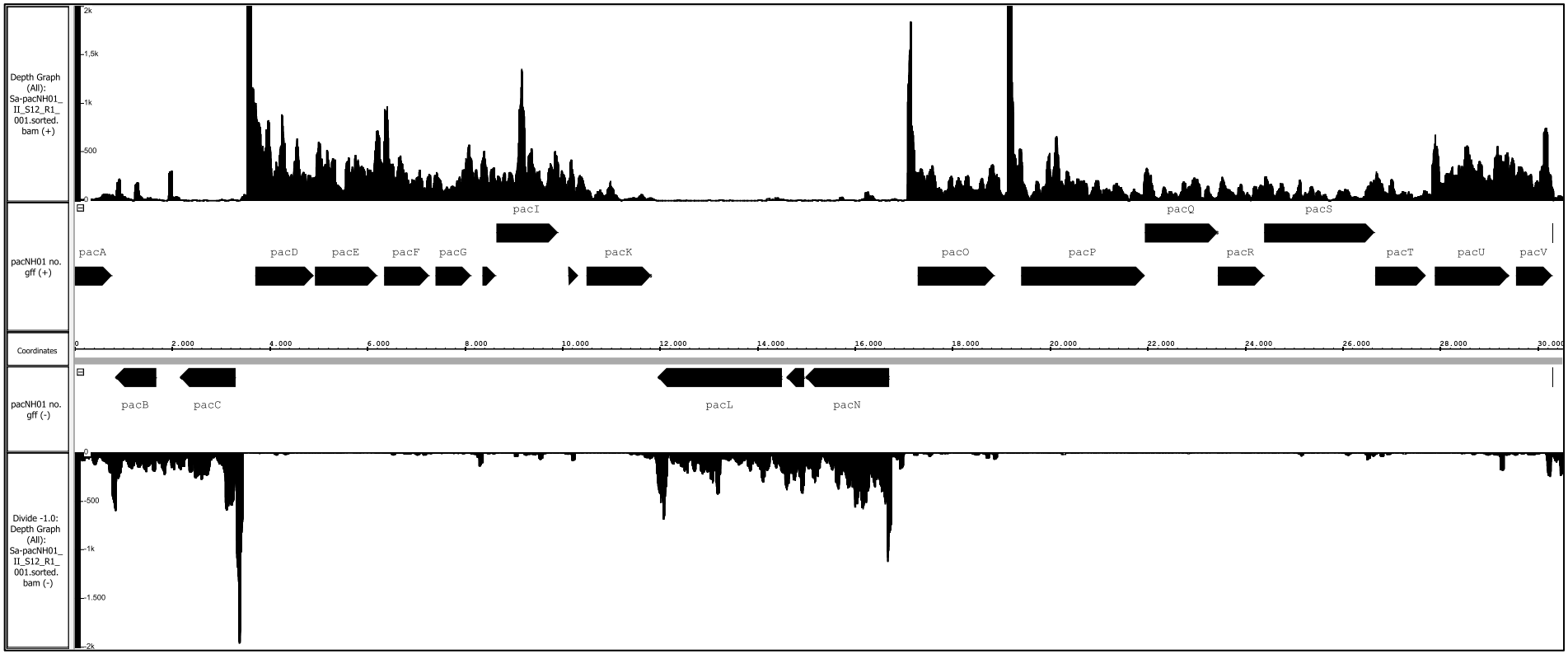


Fig. S15: RNA sequencing results regarding the pacidamycin BGC of strain *S. albus* J1074/pacNH01; exconjugant II (native pacidamycin biosynthetic gene cluster) after 4 days of cultivation. While the annotation of the BGC is depicted with arrows on the x-axis in the middle of the graph and separated into sense and antisense strands, the y-axis displays the coverage plots for the respective strands. In this case, the annotation of Zhang *et al.* (2010)[17] was utilized, by which the genes were labeled *pacA* - *pacV* (see 1.2).

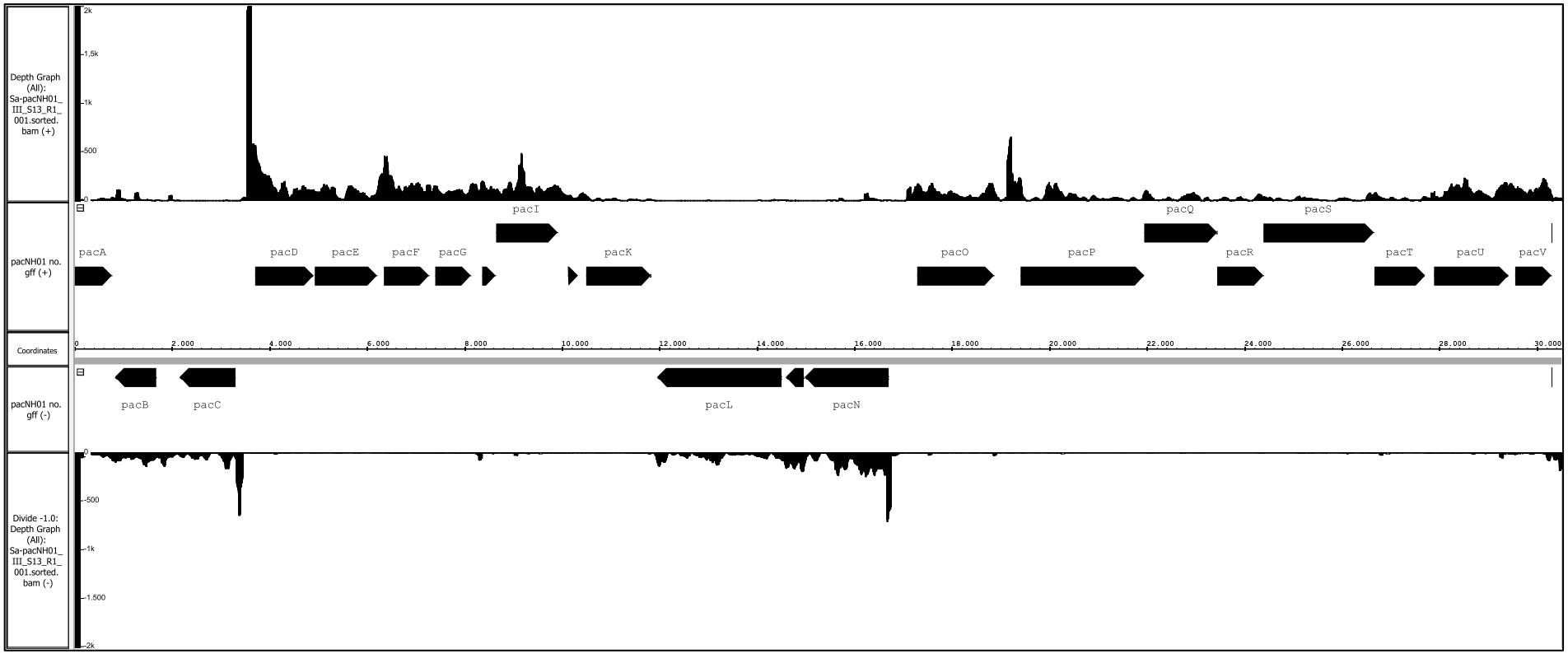


Fig. S16: RNA sequencing results regarding the pacidamycin BGC of strain *S. albus* J1074/pacNH01; exconjugant III (native pacidamycin biosynthetic gene cluster) after 4 days of cultivation. While the annotation of the BGC is depicted with arrows on the x-axis in the middle of the graph and separated into sense and antisense strands, the y-axis displays the coverage plots for the respective strands. In this case, the annotation of Zhang *et al.* (2010)[17] was utilized, by which the genes were labeled *pacA* - *pacV* (see 1.2).

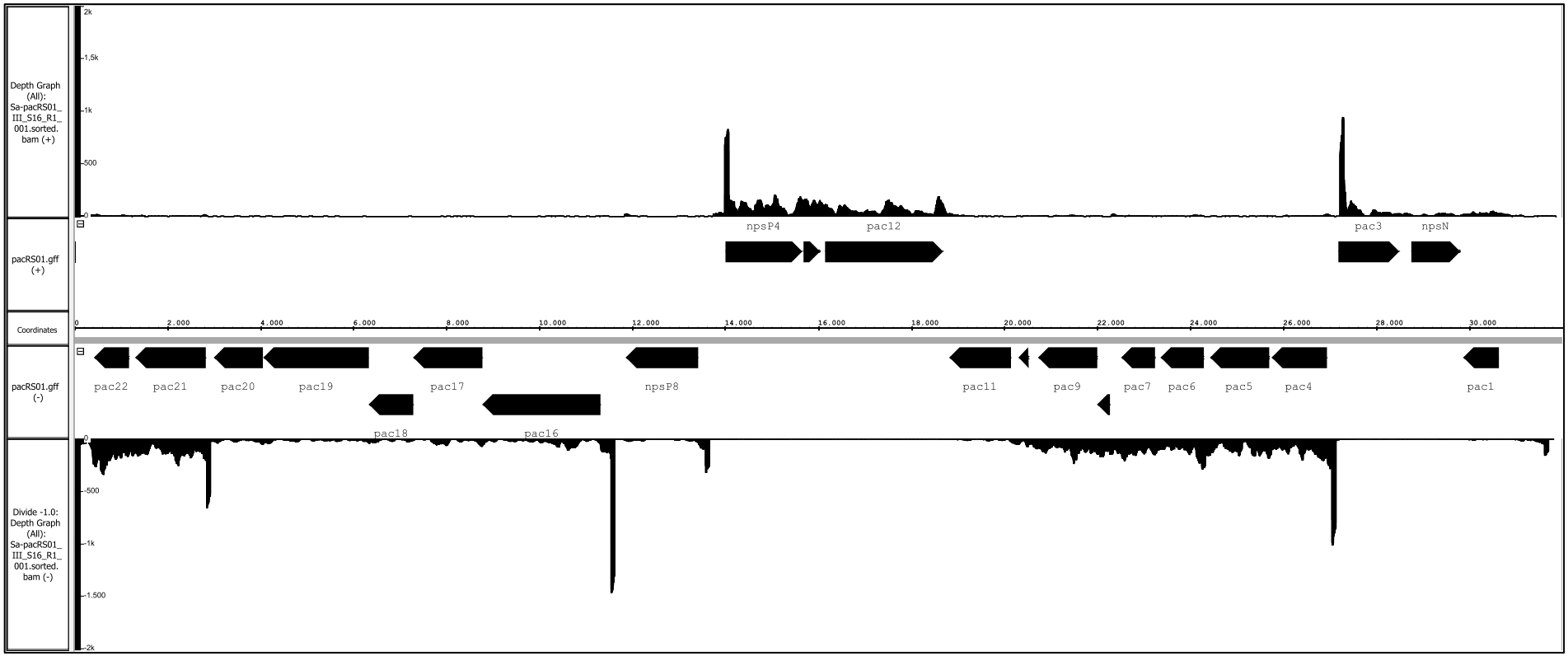


Fig. S17: RNA sequencing results regarding the pacidamycin BGC of strain *S. albus* J1074/pacRS01; exconjugant III (modified pacidamycin biosynthetic gene cluster) after 4 days of cultivation. While the annotation of the BGC is depicted with arrows on the x-axis in the middle of the graph and separated into sense and antisense strands, the y-axis displays the coverage plots for the respective strands. In this and all following cases, the annotation of Rackham *et al.* (2010)[121] was utilized, by which the genes were labeled *pac1* - *pac22* (see 1.2).

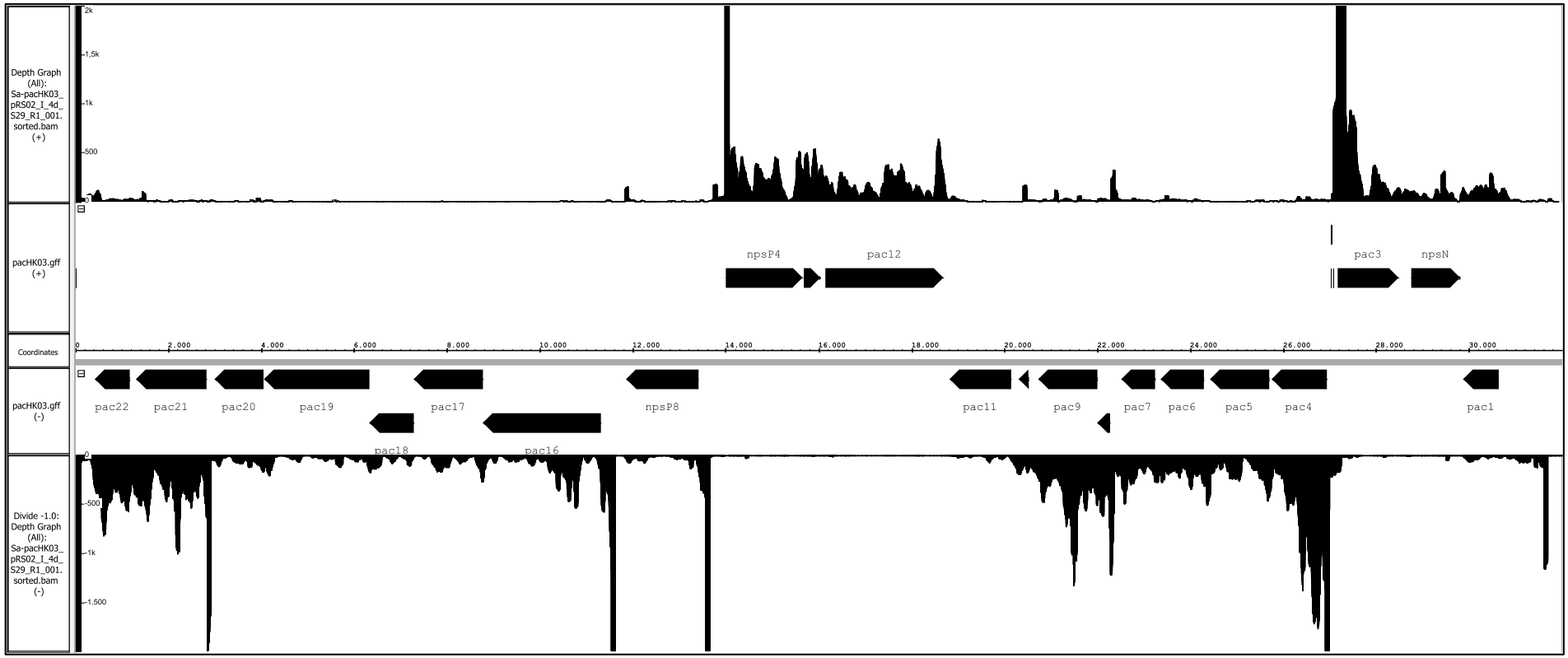


Fig. S18: RNA sequencing results regarding the pacidamycin BGC of strain *S. albus* J1074/pRS02/pacHK03; exconjugant I (modified pacidamycin biosynthetic gene cluster with bidirectional promoter cassette 1 between *pac3* and *pac4* in combination with plasmid pRS02 harboring genes for *m*-tyrosine incorporation and biosynthesis) after 4 days of cultivation. While the annotation of the BGC is depicted with arrows on the x-axis in the middle of the graph and separated into sense and antisense strands, the y-axis displays the coverage plots for the respective strands.

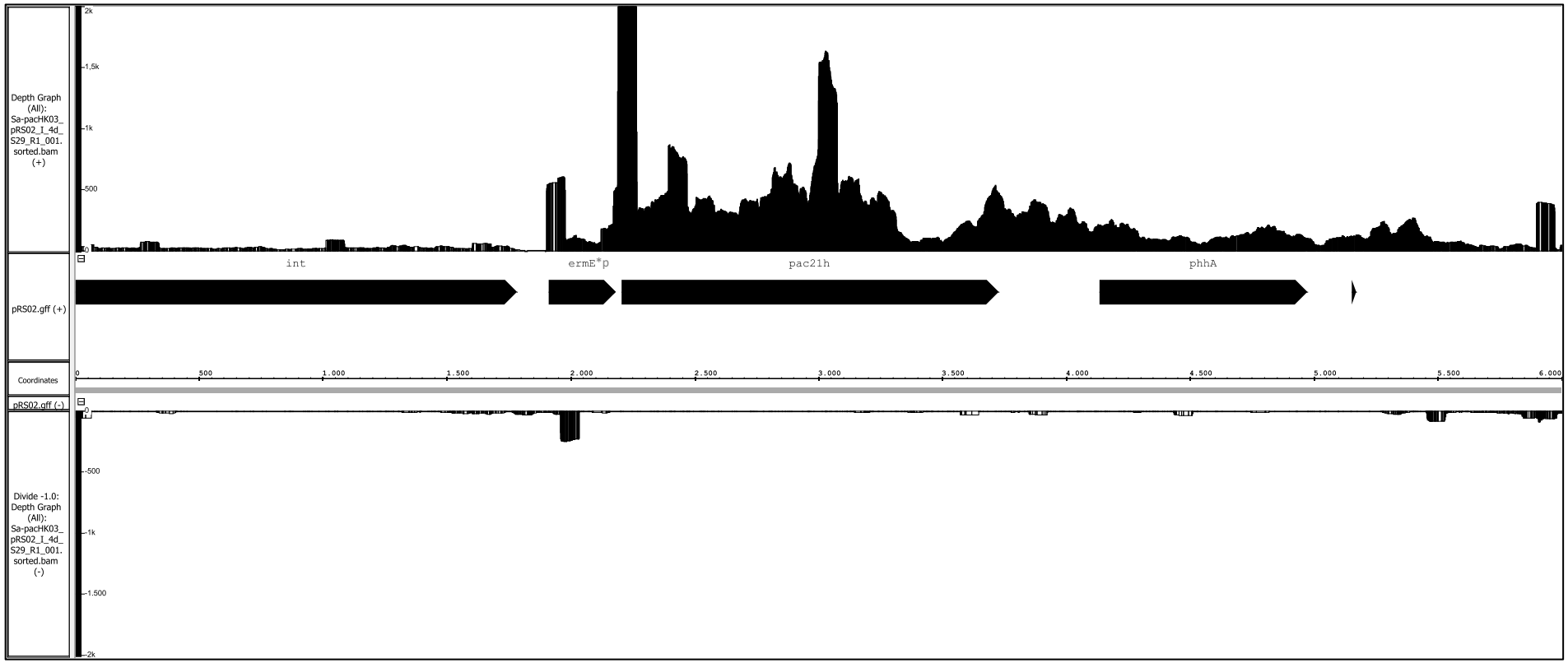


Fig. S19: RNA sequencing results regarding the plasmid pRS02 of strain *S. albus* J1074/pRS02/pacHK03; exconjugant I (modified pacidamycin biosynthetic gene cluster with bidirectional promoter cassette 1 between *pac3* and *pac4* in combination with plasmid pRS02 harboring genes for *m*-tyrosine incorporation and biosynthesis) after 4 days of cultivation. While part of the annotation of the plasmid is depicted with arrows on the x-axis in the middle of the graph and separated into sense and antisense strands, the y-axis displays the coverage plots for the respective strands.

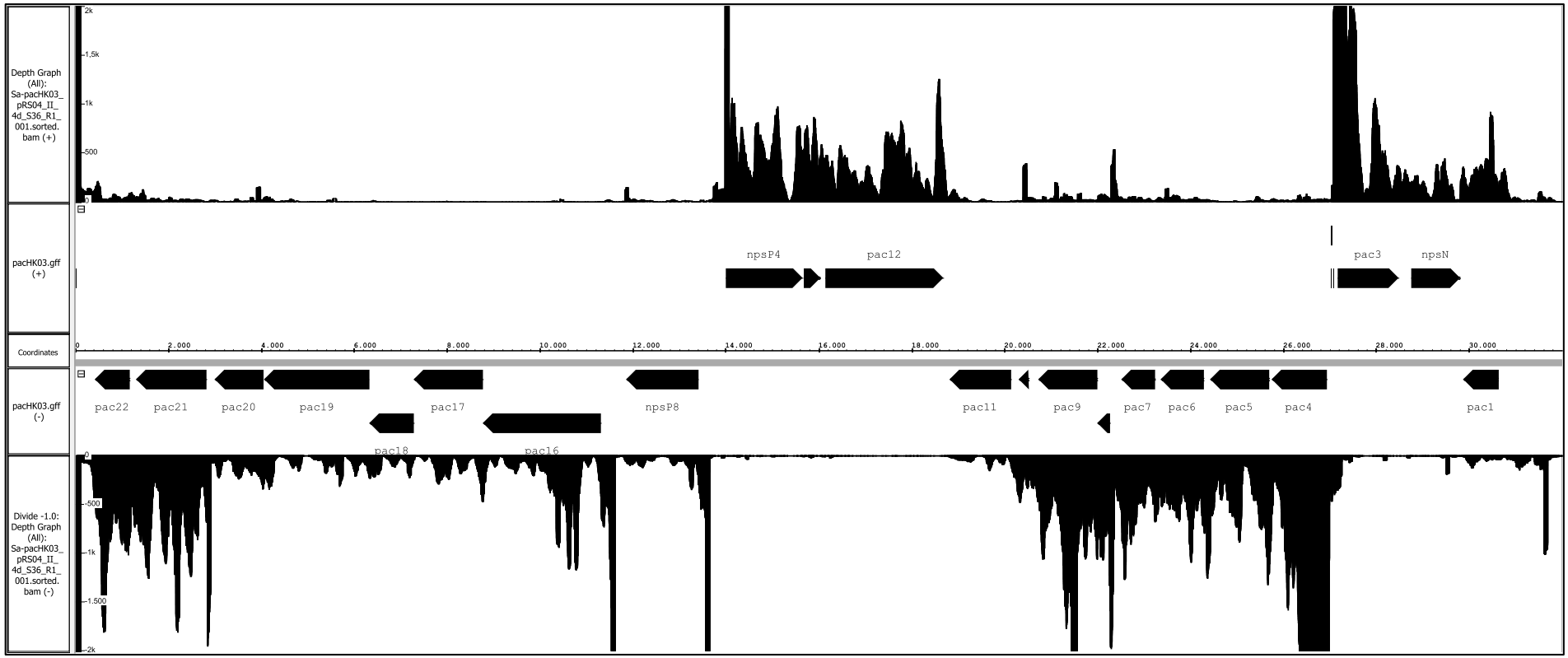


Fig. S20: RNA sequencing results regarding the pacidamycin BGC of strain S. albus J1074/pRS04/pacHK03; exconjugant II (modified pacidamycin biosynthetic gene cluster with bidirectional promoter cassette 1 between pac3 and pac4 in combination with plasmid pRS04 harboring genes for m-tyrosine incorporation and biosynthesis and the cluster-specific positive regulator of the napsamycin BGC npsM) after 4 days of cultivation. While the annotation of the BGC is depicted with arrows on the x-axis in the middle of the graph and separated into sense and antisense strands, the y-axis displays the coverage plots for the respective strands.

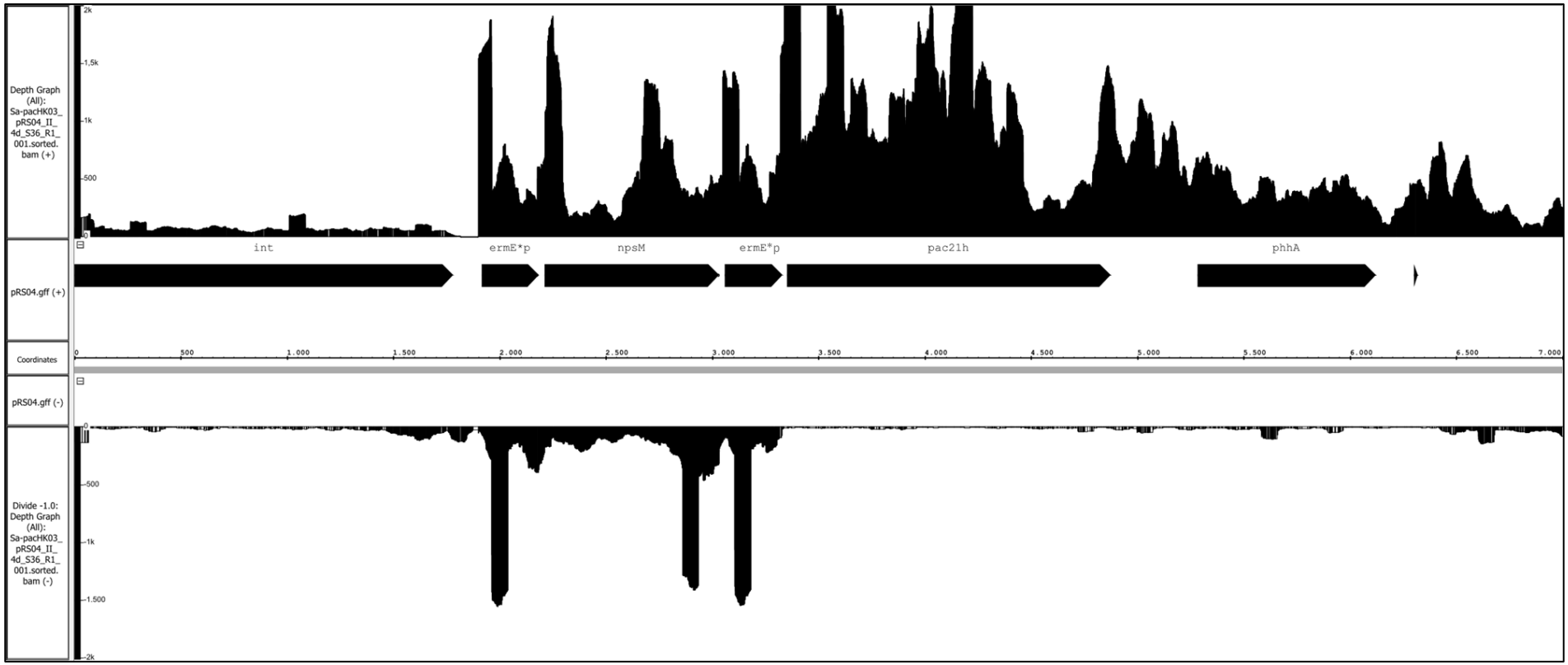


Fig. S21: RNA sequencing results regarding the plasmid pRS04 of strain *S. albus* J1074/pRS04/pacHK03; exconjugant II (modified pacidamycin biosynthetic gene cluster with bidirectional promoter cassette 1 between *pac3* and *pac4* in combination with plasmid pRS04 harboring genes for *m*-tyrosine incorporation and biosynthesis and the cluster-specific positive regulator of the napsamycin BGC *npsM*) after 4 days of cultivation. While part of the annotation of the plasmid is depicted with arrows on the x-axis in the middle of the graph and separated into sense and antisense strands, the y-axis displays the coverage plots for the respective strands.